SH
11
.A2
FS3

FISH

U.S. Department
of Commerce

Volume 111
Number 4
October 2013

Fishery Bulletin

LIBRARIES

U.S. Department of Commerce
Penelope S. Pritzker
Secretary of Commerce

National Oceanic and Atmospheric Administration
Kathryn D. Sullivan
Acting Administrator

National Marine Fisheries Service
Samuel D. Rauch III
Acting Assistant Administrator for Fisheries

Fishery Bulletin

Scientific Editor
Bruce C. Mundy

Associate Editor
Kathryn Dennis

National Marine Fisheries Service
Pacific Islands Fisheries Science Center
Aiea Heights Research Facility
99-193 Aiea Heights Drive, Suite 417
Aiea, Hawaii 96701-3911

Managing Editor
Sharyn Matriotti

National Marine Fisheries Service
Scientific Publications Office
7600 Sand Point Way NE
Seattle, Washington 98115-0070

Editorial Committee

Richard Brodeur	National Marine Fisheries Service, Newport, Oregon
John Carlson	National Marine Fisheries Service, Panama City, Florida
Kevin Craig	National Marine Fisheries Service, Beaufort, North Carolina
Jeff Leis	Australian Museum, Sydney, New South Wales, Australia
Rich McBride	National Marine Fisheries Service, Woods Hole, Massachusetts
Rick Methot	National Marine Fisheries Service, Seattle, Washington
Adam Moles	National Marine Fisheries Service, Auke Bay, Alaska
Frank Parrish	National Marine Fisheries Service, Honolulu, Hawaii
Dave Somerton	National Marine Fisheries Service, Seattle, Washington
Ed Trippel	Department of Fisheries and Oceans, St. Andrews, New Brunswick, Canada
Mary Yoklavich	National Marine Fisheries Service, Santa Cruz, California

***Fishery Bulletin* web site: www.fisherybulletin.noaa.gov**

The *Fishery Bulletin* (ISSN 0090-0656) is published quarterly by the Scientific Publications Office, National Marine Fisheries Service, NOAA, 7600 Sand Point Way NE, Seattle, WA 98115-0070.

Although the contents of this publication have not been copyrighted and may be reprinted entirely, reference to source is appreciated.

The Secretary of Commerce has determined that the publication of this periodical is necessary according to law for the transaction of public business of this Department. Use of funds for printing of this periodical has been approved by the Director of the Office of Management and Budget.

For sale by the Superintendent of Documents, U.S. Government Printing Office, Washington, DC 20402. Subscription price per year: $32.00 domestic and $44.80 foreign. Cost per single issue: $19.00 domestic and $26.60 foreign. **See back for order form.**

The *Fishery Bulletin* carries original research reports and technical notes on investigations in fishery science, engineering, and economics. It began as the Bulletin of the United States Fish Commission in 1881; it became the Bulletin of the Bureau of Fisheries in 1904 and the *Fishery Bulletin* of the Fish and Wildlife Service in 1941. Separates were issued as documents through volume 46; the last document was No. 1103. Beginning with volume 47 in 1931 and continuing through volume 62 in 1963, each separate appeared as a numbered bulletin. A new system began in 1963 with volume 63 in which papers are bound together in a single issue of the bulletin. Beginning with volume 70, number 1, January 1972, the *Fishery Bulletin* became a periodical, issued quarterly. In this form, it is available by subscription from the Superintendent of Documents, U.S. Government Printing Office, Washington, DC 20402. It is also available free in limited numbers to libraries, research institutions, State and Federal agencies, and in exchange for other scientific publications.

U.S. Department of Commerce
Seattle, Washington

Volume 111
Number 4
October 2013

Fishery Bulletin

Contents

Articles

293–308 Misa, William F. X. E., Jeffrey C. Drazen, Christopher D. Kelley, and Virginia N. Moriwake
Establishing species–habitat associations for 4 eteline snappers with the use of a baited stereo-video camera system

309–324 Cappo, Mike, Ross J. Marriott, and Stephen J. Newman
James's rule and causes and consequences of a latitudinal cline in the demography of John's Snapper (*Lutjanus johnii*) in coastal waters of Australia

325–336 Macchi, Gustavo J., Ezequiel Leonarduzzi, Marina V. Diaz, Marta Renzi, and Karina Rodrigues
Maternal effects on fecundity and egg quality of the Patagonian stock of Argentine Hake (*Merluccius hubbsi*)

337–351 Porter, Steven M., and Kevin M. Bailey
Using measurements of muscle cell nuclear RNA with flow cytometry to improve assessment of larval condition of Walleye Pollock (*Gadus chalcogrammus*)

352–369 Wuenschel, Mark J., Kenneth W. Able, James M. Vasslides, and Donald M. Byrne
Habitat and diet overlap of 4 piscivorous fishes: variation on the inner continental shelf off New Jersey

370–380 Drymon, J. Marcus, Laure Carassou, Sean P. Powers, Mark Grace, John Dindo, and Brian Dzwonkowski
Multiscale analysis of factors that affect the distribution of sharks throughout the northern Gulf of Mexico

The National Marine Fisheries Service (NMFS) does not approve, recommend, or endorse any proprietary product or proprietary material mentioned in this publication. No reference shall be made to NMFS, or to this publication furnished by NMFS, in any advertising or sales promotion which would indicate or imply that NMFS approves, recommends, or endorses any proprietary product or proprietary material mentioned herein, or which has as its purpose an intent to cause directly or indirectly the advertised product to be used or purchased because of this NMFS publication.

The NMFS Scientific Publications Office is not responsible for the contents of the articles or for the standard of English used in them.

381–389 Wenzel, Frederick W., Pamela T. Polloni, James E. Craddock, Damon P. Gannon, John R. Nicolas, Andrew J. Read, and Patricia E. Rosel
Food habits of Sowerby's beaked whales (*Mesoplodon bidens*) taken in the pelagic drift gillnet fishery of the western North Atlantic

390–401 Colmenero, Ana I., Víctor M. Tuset, Laura Recasens, and Pilar Sánchez
Reproductive biology of Black Anglerfish (*Lophius budegassa*) in the northwestern Mediterranean Sea

402 Errata

403 Acknowledgment of reviewers

404–406 Guidelines for authors

Establishing species–habitat associations for 4 eteline snappers with the use of a baited stereo-video camera system

William F. X. E. Misa (contact author)[1]
Jeffrey C. Drazen[1]
Christopher D. Kelley[2]
Virginia N. Moriwake[1]

Email address for contact author: wfmisa@hawaii.edu

[1] Department of Oceanography
School of Ocean and Earth Science and Technology
University of Hawaii at Manoa
1000 Pope Rd., MSB 205
Honolulu, Hawaii 96822
Present address for contact author: Fisheries Research and Monitoring Division
Pacific Islands Fisheries Science Center
National Marine Fisheries Service, NOAA
2570 Dole St.
Honolulu, HI 96822

[2] Hawaii Undersea Research Laboratory
School of Ocean and Earth Science and Technology
University of Hawaii at Manoa
1000 Pope Rd., MSB 303
Honolulu, Hawaii 96822

Abstract—With the use of a baited stereo-video camera system, this study semiquantitatively defined the habitat associations of 4 species of Lutjanidae: Opakapaka (*Pristipomoides filamentosus*), Kalekale (*P. sieboldii*), Onaga (*Etelis coruscans*), and Ehu (*E. carbunculus*). Fish abundance and length data from 6 locations in the main Hawaiian Islands were evaluated for species-specific and size-specific differences between regions and habitat types. Multibeam bathymetry and backscatter were used to classify habitats into 4 types on the basis of substrate (hard or soft) and slope (high or low). Depth was a major influence on bottomfish distributions. Opakapaka occurred at depths shallower than the depths at which other species were observed, and this species showed an ontogenetic shift to deeper water with increasing size. Opakapaka and Ehu had an overall preference for hard substrate with low slope (hard-low), and Onaga was found over both hard-low and hard-high habitats. No significant habitat preferences were recorded for Kalekale. Opakapaka, Kalekale, and Onaga exhibited size-related shifts with habitat type. A move into hard-high environments with increasing size was evident for Opakapaka and Kalekale. Onaga was seen predominantly in hard-low habitats at smaller sizes and in either hard-low or hard-high at larger sizes. These ontogenetic habitat shifts could be driven by reproductive triggers because they roughly coincided with the length at sexual maturity of each species. However, further studies are required to determine causality. No ontogenetic shifts were seen for Ehu, but only a limited number of juveniles were observed. Regional variations in abundance and length were also found and could be related to fishing pressure or large-scale habitat features.

Manuscript submitted 11 August 2012.
Manuscript accepted 9 July 2013.
Fish. Bull. 111:293–308 (2013).
doi: 10.7755/FB.111.4.1

The views and opinions expressed or implied in this article are those of the author (or authors) and do not necesarily reflect the position of the National Marine Fisheries Service, NOAA.

The catch of deepwater fisheries comprises a multitude of species that live on continental slopes and deep topographic oceanic structures, such as seamounts, ridges, and banks to depths below 2000 m. In the Indo-Pacific region, deepwater snappers (Lutjanidae), groupers (Serranidae), and jacks (Carangidae) that inhabit deep slopes and seamounts at depths of 100–400 m make up a major component of this fishery. The deepwater handline or "bottomfish" fishery of Hawaii also targets these groups of fishes (Haight et al., 1993a). Some of the commercially important bottomfish species can live in excess of 35 years (Andrews et al., 2011; Andrews et al., 2012)—a longevity that indicates low rates of natural mortality and susceptibility to overfishing (Haight et al., 1993a). Four of these key bottomfish species are the focus of this study: Crimson Jobfish (*Pristipomoides filamentosus*), Lavender Jobfish (*Pristipomoides sieboldii*), Flame Snapper (*Etelis coruscans*), and Ruby Snapper (*Etelis carbunculus*). In Hawaii, these species are known by a different set of common names, and these names will be used for simplicity throughout this article. *Pristipomoides filamentosus* is commonly called Opakapaka, *P. sieboldii* is called Kalekale, *E. coruscans* is called Onaga, and *E. carbunculus* is called Ehu. Opakapaka and Onaga rank first and second in total landed weight and value in the Hawaiian Archipelago, and the smaller species, Ehu and Kalekale, are abundant but lower in value and landings (WPRFMC[1]).

From the late 1980s to early 2000s, the Division of Aquatic Resources (DAR) of the Hawaii Department of Land and Natural Resources (DLNR) and the Western Pacific Re-

[1] WPRFMC (Western Pacific Regional Fishery Management Council). 2006. Bottomfish and seamount groundfish fisheries of the western Pacific region, 2005 annual report, 113 p. [Available from Western Pacific Regional Fishery Management Council, 1164 Bishop Street, Suite 1400, Honolulu, HI 96813.]

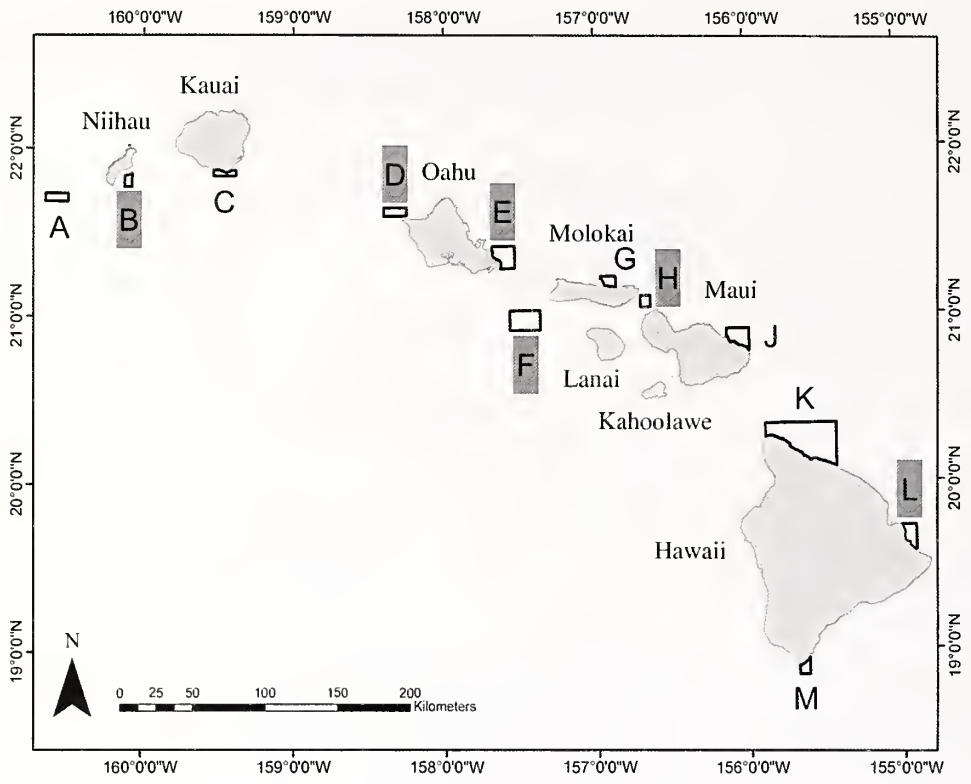

Figure 1

Map of the current bottomfish restricted fishing areas (BRFAs) in the main Hawaiian Islands. Highlighted letters indicate the 6 BRFAs—(B) Niihau, (D) Kaena, (E) Makapuu, (F) Penguin Bank, (H) Pailolo Channel, and (L) Hilo—that were sampled from May 2007 to June 2009 with the use of a baited stereo-video camera system for the study of the habitat associations of 4 snapper species.

gional Fishery Management Council (WPRFMC) assessed bottomfish stocks in the main Hawaiian Islands (MHI) by calculating their estimated spawning potential ratios (SPRs) from annual commercial catch data and established the critical threshold for designation of a stock in a state of recruitment overfishing at a SPR of 20%. Two bottomfish species, the Onaga and Ehu, had SPRs well below 20% for most of this period (DAR[2]) and were, therefore, considered to be in a state of recruitment overfishing.

In 1996, the Magnuson-Stevens Fishery Conservation and Management Act imposed a mandate on regional fishery councils to restore the stocks of overfished species to healthy levels (i.e., SPR >20%) within a 10-year time period. To address this problem, the WPRFMC turned to the DAR, which created 19 bottomfish restricted fishing areas (BRFAs) and prohibited bottomfishing in them (Div. Aquatic Resources, Department of Land and Natural Resources, Chapter 13-94, Bottomfish Management, Hawaii Administrative Rules). These BRFAs, which took effect on June 1, 1998, were designed to protect 20% of deepwater areas in the depth range of 100–400 m, where most Onaga and Ehu are found (Parke, 2007). However, identification of suitable geographic areas for closure was difficult at that time because of a lack of adequate habitat data—a common problem for most deepwater fisheries given the logistical challenges involved in sampling the deep sea.

In 2007, the DAR revised the BRFA system with data from surveys conducted with a multibeam sonar system, fishing surveys, and analysis of video collected during surveys with a submersible—all of which provided a great deal of new information on bottomfish habitats. The original BRFAs established in 1998 were retained, expanded, relocated, or opened to fishing, and the 12 BRFAs established in 2007 (Fig. 1) contained significantly more of the hard, steep habitat believed to be preferred by most bottomfish species (Parke, 2007). This belief was formed on the basis of results from submersible and fishing surveys that found some species in the water column adjacent to areas of high relief, such as underwater headlands, ledges, outcrops, and pinnacles

[2] DAR (Division of Aquatic Resources). 2006. Hawaii's bottomfish fishery, Land Board briefing paper, 17 p. [Available from Division of Aquatic Resources, Hawaii Department of Land and Natural Resources, 1151 Punchbowl St., Rm. 330, Honolulu, HI 96813.]

(Ralston et al., 1986; Haight et al., 1993a). More recent submersible surveys have supported those studies and have indicated that substrate type may be an important factor that influences distributions of adult bottomfishes (Kelley et al., 2006). However, information on species-specific and age-specific habitat associations for bottomfishes remains limited. Although the preferred habitat of juvenile Opakapaka has been observed to be soft substrates with little to no relief (Moffitt and Parrish, 1996; Parrish et al., 1997), variations in habitats between adults and juveniles, if any, have yet to be identified for other species of deepwater bottomfishes.

Information that can identify fish–habitat associations is fundamental to fisheries science. In addition to the requirement to improve overfished stocks, the Magnuson-Stevens Act required federal fishery management plans to identify the essential fish habitat (EFH) for their managed species (Rosenberg et al., 2000). The EFH for the bottomfish fishery in Hawaii currently is designated as depths from 0 to 400 m without species-specific habitat requirements, despite the notion that habitat requirements probably differ between bottomfish species and ontogenetic stage of these species. To guide management decisions on the protection and sustainable use of bottomfish resources in Hawaii, this EFH designation should be as complete and as specific as possible (Kelley et al., 2006).

New data are needed to obtain a greater understanding of the habitat associations of bottomfish species. Common shallow-water sampling techniques, such as diver transects, however, are not logistically feasible at depths below 100 m, and fishing surveys can be destructive to local populations. The need for a different survey method has led to the emergence of baited camera systems as cost-effective, nonextractive tools for the estimation of relative abundances of fish species at depths >100 m (Merritt et al., 2011; Moore et al., 2013).

With the use of a baited stereo-video camera system, we aimed to improve our understanding of the habitat associations of 4 species of bottomfishes, within different size classes, in the MHI. Data specific to each species can be used to assess the amount of suitable habitat present in management areas and to relate catch per unit of effort (CPUE) to habitat type. Most important, through expansion of our understanding of the ecology of bottomfishes, more specific and refined EFH designations can be forged and ecosystem-based management strategies can be further developed.

Materials and methods

The Bottom Camera Bait Station (BotCam) developed by the Coral Reef Ecosystem Division of the NOAA Pacific Islands Fisheries Science Center is a remote, fully automated, baited system with stereo-video cameras; it was designed specifically for nonextractive, fishery-independent sampling of deepwater bottomfish species in their habitat and depth range (Merritt, 2005; Merritt et al., 2011). The method for sampling fish populations with a baited stereo-video camera system has been found to generate more consistent data than have comparable unbaited systems (Harvey et al., 2007), has the ability to detect mobile fish species (Harvey et al., 2007; Watson et al., 2010), and has been determined to be effective in sampling bottomfishes in Hawaii (Ellis and DeMartini, 1995; Merritt et al., 2011). The BotCam is a means by which bottomfish abundance estimates can be made within actual bottomfish habitats and fish lengths can be accurately measured.

Upon deployment, the BotCam sits about 3 m off the bottom of the seafloor, and, depending on the depth of deployment, amount of light, and water clarity, the field of view may expand or contract. Moore et al. (2013) estimated that the visual area sampled by the BotCam was between 4 and 400 m^2. The BotCam makes use of ambient light, which allows for an operating depth of up to 300 m and is operational on multiple bottom types, including steep slopes and high relief. In our study, the BotCam recorded 30 to 45 min of continuous video at each of the 6 deployment locations. Depth data were taken from a conductivity, temperature, and depth profiler attached to the system. The bait canister attached to the BotCam was filled with ~800 g of ground anchovy and squid, a mix that is similar to the bait used by bottomfish fishermen (Merritt et al., 2011).

Bottomfish habitat types in the MHI were characterized with multibeam bathymetry and backscatter data that originated from a variety of mapping surveys conducted with multibeam sonar systems in and around the MHI since the late 1990s. The U.S. Geological Survey in collaboration with the Monterey Bay Aquarium Research Institute carried out the first survey in the MHI in 1998 (U.S. Geological Survey Digital Data Series DDS-55, http://pubs.usgs.gov/dds/dds-55/index.html; MBARI Hawaii Multibeam Survey, http://www.mbari.org/data/mapping/hawaii/index.htm) with a 30-kHz Simrad[3] EM 300 multibeam sonar system (Kongsberg Maritime AS, Kongsberg, Norway). Both the bathymetry and backscatter data from this survey were processed at a grid resolution of 20 m. The majority of the remaining data came from subsequent surveys conducted from 2002 to 2006 by researchers at the Hawaii Undersea Research Laboratory, University of Hawaii at Manoa, with a 95-kHz Simrad EM 1002 multibeam sonar system. The editing and processing of raw data were carried out by the Hawaii Mapping Research Group of the University of Hawaii at Manoa using the SABER multibeam editing program (SAIC, Inc., McLean, VA) and other proprietary software. Bathymetry data were processed at a 20-m grid resolution, and backscatter data were processed at either a 10-m resolution or a 20-m resolution, depending on the survey. The processed

[3] Mention of trade names or commercial companies is for identification purposes only and does not imply endorsement by the National Marine Fisheries Service, NOAA

data from these cruises have not been made publicly available, with the exception of the bathymetry data that have been incorporated into a 50-m-resolution synthesis of the entire MHI that is available from the Hawaii Mapping Research Group (http://www.soest.hawaii.edu/hmrg/multibeam/index.php).

Multibeam backscatter data in grids with a 20-m resolution cannot be used effectively to identify specific substrate types, such as mud, sand, pebbles, cobbles, boulders, and bedrock, because more than one of these substrate types often can be found on the seafloor in an area of 20×20 m. Similarly, more than one type of slope can be found in areas of that size because of the presence of small carbonate ledges, large boulders and blocks, sand dunes, and other small-scale topographic features common to seafloors in the Hawaiian Archipelago. Multibeam data values for each grid cell (20×20 m) are typically derived through calculation of either the Gaussian weighted means (bathymetry) or the medians (backscatter) of the sonar footprints within each cell. For these reasons, only 4 general habitat types were derived from these multibeam data: hard substrate with high slope (hard-high), hard substrate with low slope (hard-low), soft substrate with high slope (soft-high), and soft substrate with low slope (soft-low). Bathymetry data from the different sonar systems generally were consistent.

After a number of slope analyses were conducted in ArcGIS 9.1 (Esri, Redlands, CA), a value of 20° was determined to be a reasonable boundary between the high and low slopes that appeared in the bathymetry images. Backscatter data, however, are often inconsistent between systems with different frequencies. Furthermore, the backscatter data used in this study were processed in different ways by different technicians. As a result, boundary values between hard and soft substrates had to be determined on a basis of per system and per cruise. A value of 187 was used as the boundary between hard and soft substrates for the EM 300 data and was validated through examination of video from submersible surveys. Boundary values for the EM 1002 data ranged from –41 to 150 and were established through comparison of areas of overlap with EM 300 data and analysis of video from submersible surveys.

Habitat was classified at a resolution of 200×200 m for areas in and around BRFAs. Polygons for high and low slopes and hard and soft substrates were generated with the Raster calculator in ArcGIS 9.1. Intersects of slope and hardness resulted in polygons for the 4 habitat types. A grid cell (200×200 m) was superimposed over these polygons, and the areas of the habitat types within each grid cell were calculated. Each grid cell was assigned a habitat type on the basis of which habitat type was observed in the greatest proportion in that area.

A stratified-random sampling approach was used to select locations for BotCam sampling. Although the purpose of our study was to evaluate species–habitat associations, another goal of this project was to evaluate population changes inside and outside of BRFAs. This objective affected our sampling design. We used data from 625 deployments of the BotCam conducted inside and outside of 6 of the 12 current BRFAs (Fig. 1) between May 2007 and June 2009. The 6 BRFAs that were sampled are located off Niihau (BRFA B), Kaena (BRFA D), Makapuu (BRFA E), and Penguin Bank (BRFA F), in Pailolo Channel (BRFA H), and outside of Hilo (BRFA L). The Niihau and Hilo BRFAs were areas of continued closure from the initial implementation of BRFAs in 1998. The Makapuu and Penguin Bank BRFAs were expanded versions of smaller preexisting BRFAs from 1998, and the BRFAs off Kaena and in Pailolo Channel were areas newly closed in 2007.

The BotCam was lowered to depths of 100–300 m. Although the EFH for deep bottomfishes in Hawaii extends to 400 m, the video cameras work under ambient light to only 300 m, thus limiting the depth range of our sampling. Sampling effort was weighted toward known preferred bottomfish habitats to ensure greater replication where fish densities were expected to be higher. Because previous studies have found bottomfishes associated with hard substrates, high slopes, or a combination of both (Polovina et al., 1985; Ralston et al., 1986; Haight et al., 1993a; Parke, 2007), for our study, hard-high habitats were considered the most suitable and soft-low habitats the least suitable. To sample a BRFA, 32 BotCam deployments inside and 32 outside but adjacent to a BRFA were completed over grids of each habitat type with the following replication: 12 hard-high, 8 hard-low, 8 soft-high, and 4 soft-low. BotCam deployments targeted centroids of randomly selected grid cells (200×200 m) and were kept a minimum of 400 m apart to reduce the likelihood of sampling overlap. In regions where a given habitat type was not present, sampling intensity was increased in the next most suitable habitat. This approach led to skewed sampling across habitat types in Pailolo Channel because only low-slope habitats were identified at a resolution of 200×200 m. When BotCam deployments did not yield usable video (e.g., no recordings or extremely dark imagery), the BotCam was redeployed at that location on another day. As often happens during sampling efforts in the field, not all targeted grids were sampled because of weather and equipment issues. In the 2-year sampling period covered by this study (2007–09), 4 of the 6 BRFAs (Niihau, Makapuu, Penguin Bank, and Pailolo Channel) were sampled twice and the Kaena and Hilo BRFAs were sampled only once.

BotCam video footage was reviewed in the laboratory to estimate the relative abundance, recorded as the maximum number of a particular species observed in a single frame of video (MaxNo), of Opakapaka, Kalekale, Onaga, and Ehu with VF Deep Portal (Deep Development Corp., Sumas, WA) and Adobe Premiere Pro CS4 (Adobe Systems, Inc., San Jose, CA) software programs. Fishes were identified to the most specific taxonomic classification possible with a species identification reference (Randall, 2007). MaxNo is a conservative abun-

dance estimate that avoids the potential problem of counting the same fish multiple times as it re-enters a camera's field of view. Many studies have determined that MaxNo is positively correlated with fish density (Ellis and DeMartini, 1995; Priede and Merrett, 1996; Willis et al., 2000; Willis and Babcock, 2000; Yau et al., 2001; Cappo et al., 2003). This parameter also has been found to be highly correlated with the traditional parameter of CPUE used in fishing surveys (Ellis and DeMartini, 1995). MaxNo was recorded for all fishes present in the BotCam video footage, but only data for the 4 species of interest were analyzed.

Permutational analysis of variance (PERMANOVA) of the data was performed in Primer 6 (PRIMER-E Ltd., Ivybridge, UK) with PERMANOVA+ (Anderson et al., 2008). With PERMANOVA, the data are not assumed to be normally distributed; therefore, this technique was deemed appropriate for analysis of our data, which included a highly skewed (overdispersed) relative abundance distribution due to an unbalanced experimental design and frequent zero counts. The 4 species considered in our study do not all occupy the entire depth range sampled (Polovina et al., 1985; Haight, 1989; Everson et al., 1989; Merritt et al., 2011). To constrain the data to an appropriate range for each species, the depths at which each species had its greatest MaxNo had to be identified. For the initial analysis, depth was divided into 30-m bins from 90 to 300 m. Relative abundance values were square-root transformed to compensate for numerous zero counts and occasional large numbers. A Euclidean distance matrix was used in the statistical test with a type-III sum of squares. If a significant difference ($P<0.05$) was observed across depth bins, a subsequent pair-wise PERMANOVA was performed to determine the preferred depths of each species. Subsequent analyses (MaxNo and fork length [FL]) were then constrained to the depth preferences identified for each of the 4 species studied.

Through identification of habitat preferences, the influence of BRFA location (i.e., combined area inside and outside a BRFA) and protection (i.e., area inside versus outside a BRFA) could not be overlooked. PERMANOVA in a 3-way crossed design was used to determine how BRFA location (BR, 6 levels, fixed), protection (PR, 2 levels, fixed), habitat type (HA, 4 levels, fixed), and the interaction of these factors affected the relative distribution of each species. MaxNo values were square-root transformed, and the PERMANOVA was run on a Euclidean distance matrix with type-III sum of squares. Where significant results ($P<0.05$) occurred, pair-wise testing was performed to identify specific differences.

For individual fish visible in both BotCam cameras, FL was measured with stereo-photogrammetric measurement software: Visual Measurement System 7.5 (Geometric Software Pty. Ltd., Coburg, Victoria,

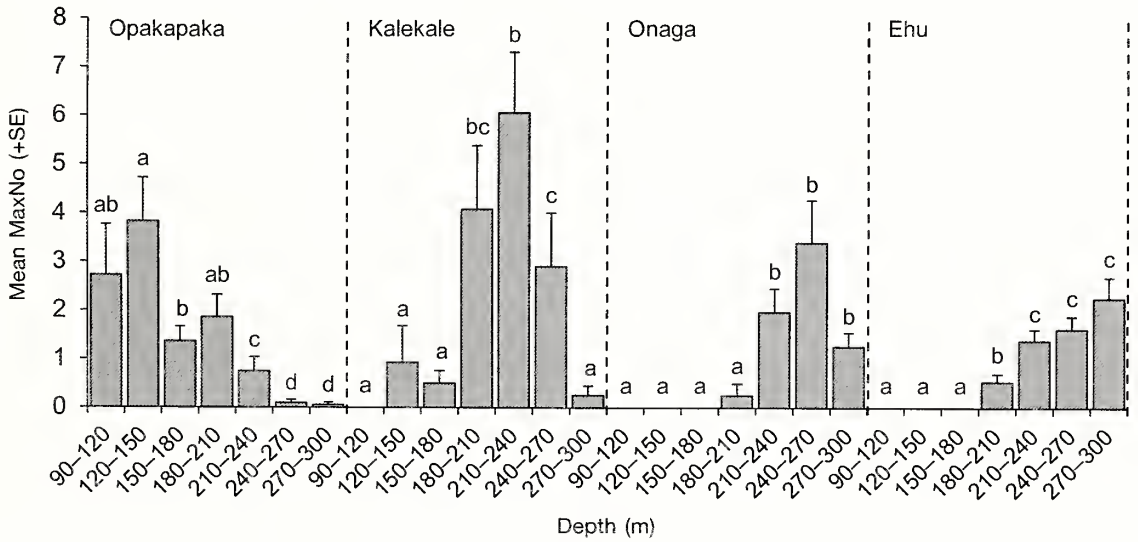

Figure 2

Mean relative abundance (MaxNo) with standard error (SE) across 7 depth bins for Opakapaka (*Pristipomoides filamentosus*), Kalekale (*P. sieboldii*), Onaga (*Etelis coruscans*), and Ehu (*E. carbunculus*) from surveys of these species conducted in the main Hawaiian Islands from May 2007 to June 2009 with the use of a baited stereo-video camera system. Columns with the same letter are not significantly different from each other ($P>0.05$, post hoc permutational analysis of variance [PERMANOVA] testing). Error bars indicate ±1 SE of the mean.

Table 1

Results of permutational analysis of variance (PERMANOVA) with relative abundance (MaxNo) data from our surveys of 4 species—Opakapaka (*Pristipomoides filamentosus*), Kalekale (*P. sieboldii*), Onaga (*Etelis coruscans*), and Ehu (*E. carbunculus*)—in the main Hawaiian Islands between May 2007 and June 2009. The following factors were tested within the preferred depths of each species: bottomfish restricted fishing area location (BR), protection (PR), and habitat type (HA). Preferred depths are noted in the column head for each species. df=degrees of freedom; *F*=PERMANOVA *F*-statistic; *P*=PERMANOVA *P*-value. Asterisks indicate statistical significance at $P<0.05$.

	Opakapaka (90–210 m)			Kalekale (180–270 m)			Onaga (210–300 m)			Ehu (210–300 m)		
Factor	df	*F*	*P*	df	*F*	*P*	df	*F*	*P*	df	*F*	*P*
BR	5	2.86	0.02*	5	2.07	0.09	5	1.54	0.17	5	4.78	0.00*
PR	1	0.00	1.00	1	0.07	0.79	1	0.07	0.78	1	0.31	0.58
HA	3	8.28	0.00*	3	1.68	0.18	3	3.87	0.02*	3	2.83	0.04*
BR×PR	5	0.63	0.66	5	0.55	0.72	5	0.56	0.70	5	0.81	0.54
BR×HA	13	0.64	0.80	12	1.89	0.06	13	0.69	0.71	13	2.33	0.01*
PR×HA	3	0.62	0.59	3	0.87	0.45	3	0.56	0.62	3	0.93	0.42
BR×PR×HA	12	1.02	0.42	10	0.44	0.91	9	0.59	0.76	9	0.58	0.79
Residual	247			282			295			295		

Australia) and PhotoMeasure 1.74 (SeaGIS Pty. Ltd., Bacchus Marsh, Victoria, Australia). Measurements of individual fish were taken at the point of MaxNo or at the point in the video where the most fish could be measured to ensure that individuals were not repeatedly measured at various times during video analysis. Replicate measurements were taken for individual fish to increase the accuracy of the measurement. An LED device was used to ensure synchronicity of the video footage from the left and right cameras. A root-mean-square error or residual parallax >10 mm and a precision-to-FL ratio >10% were indicative of inaccurate measurements. To ensure the quality of fish length data, these measurements were removed from the analyses in this study. The same 3-way crossed design from the PERMANOVA of relative abundance (BR, PR, HA) was used to test FLs for each species. Transformation of FLs, however, was not necessary because these data typically were normally distributed.

Because only variations in mean length were evaluated with the previously described approach, additional analyses were undertaken to investigate size-related changes in habitat association. A linear regression was used to evaluate the relationship between depth and FL for each of the 4 species studied to identify ontogenetic shifts with depth. As part of our examination of ontogenetic shifts across habitat types, a contingency table (tested with Pearson's chi-square test) was used to determine whether the size-class distribution of each species was independent of habitat type. Fork lengths were grouped into 10-cm bins. This size interval was chosen to maximize the number of observations in each size bin. Merritt et al. (2011) tested and found measurements from BotCam video to be accurate to within 0.3–0.9 cm, making such a grouping very robust.

Results

For all 4 species studied, significant differences in relative abundance were found across depth bins (PERMANOVA, $P<0.05$). Pair-wise comparisons of MaxNo from the 7 depth bins highlighted the depth preference of each species (Fig. 2). MaxNo was highest from 90 to 210 m for Opakapaka (post hoc PERMANOVA, $P<0.05$). The preferred depths of Kalekale were 180–270 m, and both Onaga and Ehu had the deepest range among species at 210–300 m (post hoc PERMANOVA, $P<0.05$).

Within the preferred depths of a species, either BRFA location, habitat type, or the interaction of these 2 factors had an effect on the relative abundance of 3 of the 4 species studied (Table 1). Protection and the interaction of all other factors with protection, however, did not have an effect (PERMANOVA, $P>0.05$). BRFA location and habitat type were each significant factors for Opakapaka. Hilo had the highest relative abundance of this species among sampled locations, and hard-low habitats yielded greater abundance estimates for Opakapaka than other habitat types (Fig. 3; post hoc PERMANOVA, $P<0.05$). Although no significant location or habitat effects were observed for Kalekale, the interaction of BRFA location and habitat type was marginal ($P=0.06$; Table 1); 2 of the largest counts of this species (100 and 85 individuals) occurred on hard-high habitats at Niihau and led to a high mean MaxNo (Fig. 3).

Habitat type was the only factor that affected the relative abundance of Onaga. Hard substrate habitats, with either high or low slope, had greater mean MaxNo for Onaga than soft substrate habitats (Fig. 3; post hoc PERMANOVA, $P<0.05$). BRFA location, habitat type, and the interaction of these 2 factors were significant

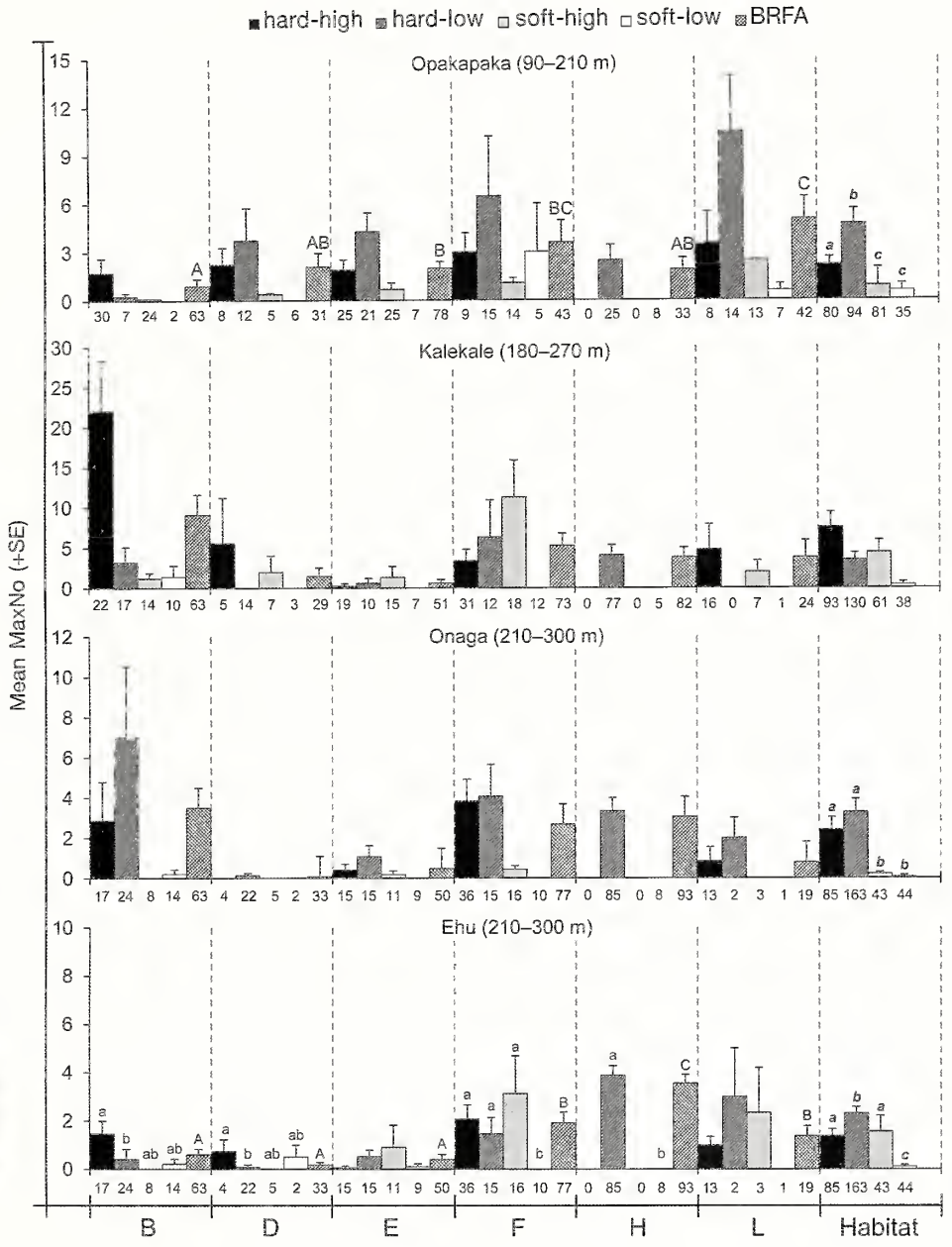

Figure 3

Mean relative abundance (MaxNo) with standard error (SE) by location of bottomfish restricted fishing area (BRFA; i.e., combined area inside and outside a BRFA), by habitat type combined for all BRFA locations (habitat), and by habitat type in each BRFA location (BRFA×habitat) for Opakapaka (*Pristipomoides filamentosus*), Kalekale (*P. sieboldii*), Onaga (*Etelis coruscans*), and Ehu (*E. carbunculus*) within the preferred depths of each species in the main Hawaiian Islands. A baited stereo-video camera system (BotCam) was used to collect data from May 2007 to June 2009. Columns with the same letter (uppercase type for BRFA; lowercase, bold, italic type for habitat; lowercase type for BFRA×habitat) are not significantly different from each other ($P>0.05$, post hoc permutational analysis of variance [PERMANOVA]). The number below each column is the number of BotCam deployments. The 4 habitat classifications used in our study were derived from data collected with multibeam sonar systems: hard substrate with high slope (hard-high), hard substrate with low slope (hard-low), soft substrate with high slope (soft-high), and soft substrate with low slope (soft-low). The 6 sampled BRFAs were (B) Niihau, (D) Kaena, (E) Makapuu, (F) Penguin Bank, (H) Pailolo Channel, and (L) Hilo. Error bars indicate ±1 SE of the mean.

Table 2

Results of permutational analysis of variance (PERMANOVA) with fork length data from our surveys of 4 species—Opakapaka (*Pristipomoides filamentosus*), Kalekale (*P. sieboldii*), Onaga (*Etelis coruscans*), and Ehu (*E. carbunculus*)—in the main Hawaiian Islands between May 2007 and June 2009. The following factors were tested within the preferred depths of each species: bottomfish restricted fishing area location (BR), protection (PR), and habitat type (HA). Preferred depths are noted in the column head for each species. df=degrees of freedom; *F*=PERMANOVA *F*-statistic; *P*=PERMANOVA *P*-value. Asterisks indicate statistical significance at $P<0.05$.

	Opakapaka (90–210 m)			Kalekale (180–270 m)			Onaga (210–300 m)			Ehu (210–300 m)		
Factor	df	*F*	*P*	df	*F*	*P*	df	*F*	*P*	df	*F*	*P*
BR	5	36.04	0.00*	5	28.20	0.00*	4	11.05	0.00*	4	4.90	0.00*
PR	1	14.24	0.00*	1	1.43	0.23	0	No test		0	No test	
HA	3	11.39	0.00*	3	18.38	0.00*	1	0.48	0.49	2	1.77	0.17
BR×PR	5	2.02	0.08	3	16.57	0.00*	3	4.82	0.00*	4	0.84	0.52
BR×HA	9	7.66	0.00*	4	1.16	0.33	1	23.69	0.00*	5	1.62	0.16
PR×HA	2	0.45	0.64	2	0.21	0.82	2	0.48	0.61	2	1.31	0.27
BR×PR×HA	5	3.42	0.01*	2	0.21	0.81	1	13.26	0.00*	0	No test	
Residual	419			446			242			274		

for Ehu. The highest relative abundance for this species was in Pailolo Channel, and the lowest levels were seen at Niihau, Kaena, and Makapuu (Fig. 3; post hoc PERMANOVA, $P<0.05$). Overall, hard-low habitats had significantly greater numbers of Ehu than did other habitat types. By BRFA location and habitat type, the mean MaxNo of Ehu in Pailolo Channel was higher for hard-low than for soft-low habitats, and similar abundance estimates were found for hard-high, hard-low, and soft-high habitats on Penguin Bank. Niihau and Kaena differed from the other sampled locations in that hard-high habitats had a greater relative abundance of Ehu than did hard-low habitats.

In our evaluation of mean lengths, BRFA location, protection, and habitat type were all important factors, and the interactions between them were sometimes significant (Table 2). BRFA location, protection, habitat type, the interaction of BRFA location and habitat type, and the interaction of all 3 factors were significant for Opakapaka. Niihau had the largest Opakapaka on average (65.29 cm FL) among sampled locations, and the smallest Opakapaka (28.35 cm FL; Fig. 4; post hoc PERMANOVA, $P<0.05$) were seen at Hilo. The smallest individual at Hilo measured ~16 cm FL, and the largest individual at Niihau was ~79 cm FL. Opakapaka from outside protected areas had a mean length of 42.89 cm FL and were larger than those fish observed inside the sampled BRFAs (40.53 cm FL; PERMANOVA, $P<0.05$). The smallest mean lengths of this species were found over hard-low habitats compared with other habitat types overall, other habitats at each BRFA location, and other habitats either inside or outside a particular BRFA (Fig. 4; Table 3; post hoc PERMANOVA, $P<0.05$).

BRFA location, habitat type, and the interaction of BRFA location and protection were significant for Kalekale. Pair-wise comparisons showed that this species had its smallest mean length (23.64 cm FL) at Kaena, was largest in hard-high habitats (31.46 cm FL) and smallest in soft-low habitats (8.64 cm FL, $n=2$), and was larger inside the Penguin Bank and Pailolo Channel BRFAs and outside the Hilo BRFA than in other sampled areas (Fig. 4; Table 3; post hoc PERMANOVA, $P<0.05$). The smallest individual Kalekale, however, measured 7.63 cm FL at Niihau. BRFA location, the interaction of BRFA location with protection, the interaction of BRFA location with habitat type, and the interaction of all 3 of these factors were significant for Onaga. Mean length for Onaga was smallest in Pailolo Channel (42.80 cm FL) than at other locations (Fig. 4) but larger inside the Pailolo Channel BRFA than outside this protected area (Table 3; post hoc PERMANOVA, $P<0.05$). The smallest individual Onaga measured 15.05 cm FL. Although the interaction of BRFA location and habitat type and the interaction of BRFA location, protection, and habitat type had significant results for Onaga, no clear trends were seen. BRFA location was the only factor that had an influence on mean length for Ehu (Table 2; PERMANOVA, $P<0.05$). Overall, mean sizes were very similar for this species but were smallest at Makapuu and Hilo (Fig. 4).

For all sampled locations combined, size-related shifts in species–habitat associations were evident. The linear regressions of FL against depth for each species showed that size increased with depth for Opakapaka (coefficient of determination $[r^2] = 0.438$, $P<0.01$) but did not for the other 3 species (Fig. 5). In our evaluation of the proportion of fish measured in each habitat type by size class, habitat associations clearly varied by size for Opakapaka, Kalekale, and Onaga (Fig. 6). Ehu had very similar habitat associa-

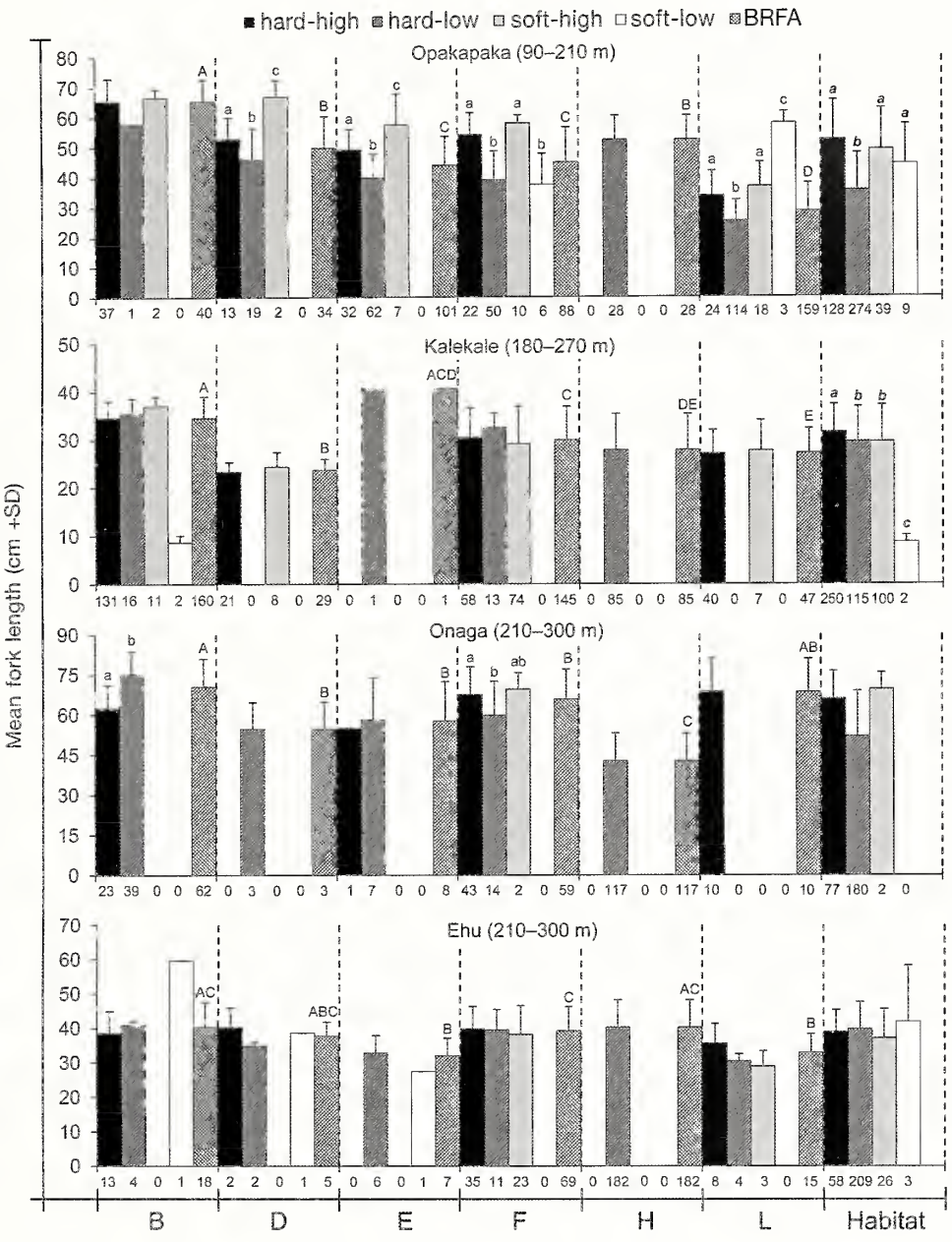
hard-high hard-low soft-high soft-low BRFA
Opakapaka (90–210 m)
Kalekale (180–270 m)
Onaga (210–300 m)
Ehu (210–300 m)
Mean fork length (cm +SD)
B D E F H L Habitat

Figure 4

Mean fork length with standard deviation (SD) by location of bottomfish restricted fishing area (BRFA; i.e., combined area inside and outside a BRFA), by habitat type combined for all BRFA locations (habitat), and by habitat type in each BRFA location (BRFA×habitat) for Opakapaka (*Pristipomoides filamentosus*), Kalekale (*P. sieboldii*), Onaga (*Etelis coruscans*), and Ehu (*E. carbunculus*) within the preferred depths of each species in the main Hawaiian Islands. A baited stereo-video camera system (BotCam) was used to collect data from May 2007 to June 2009. Columns that have the same letter (uppercase type for BRFA; lowercase, bold, italic type for habitat; lowercase type for BRFA×habitat) are not significantly different from each other (P>0.05, post hoc permutational analysis of variance [PERMANOVA] testing). Number below each column is the number of fish measured. For protection effects, refer to Table 3. The 4 habitat classifications used in our study were hard substrate with high slope (hard-high), hard substrate with low slope (hard-low), soft substrate with high slope (soft-high), and soft substrate with low slope (soft-low). The 6 sampled BRFAs were (B) Niihau, (D) Kaena, (E) Makapuu, (F) Penguin Bank, (H) Pailolo Channel, and (L) Hilo. Error bars indicate ±1 SD of the mean.

Table 3

Summary of significant comparisons from post hoc permutational analysis of variance (PERMANOVA) of fork lengths for bottomfish restricted fishing area location (BR), protection (PR), habitat type (HA), and the interaction of these factors for Opakapaka (*Pristipomoides filamentosus*), Kalekale (*P. sieboldii*), Onaga (*Etelis coruscans*), and Ehu (*E. carbunculus*) within the preferred depths of each species from our study of these species in the main Hawaiian Islands between May 2007 and June 2009. Locations of the 6 BRFAs where sampling was conducted are the following: Niihau (B), Kaena (D), Makapuu (E), Penguin Bank (F), Pailolo Channel (H), and Hilo (L). Protection is designated as inside (in) or outside (out) a BRFA. Habitat types are hard-high (HH), hard-low (HL), soft-high (SH), soft-low (SL). NS=nonsignificant comparisons. Preferred depths are noted under the species name in the first column.

	BR	PR	HA	BR×PR	BR×HA	PR×HA	BR×PR×HA
Opakapaka (90–210 m)	Largest in B Smallest in L	Larger outside	Smallest in HL	NS	(D) largest in SH, smallest in HL (E) largest in SH, smallest in HL (F) largest in high slope, smallest in low slope (L) largest in SL, smallest in HL	NS	(D in) SH>HL (E in) HH,SH>HL (E out) SH>HH>HL (F in) HH,SH>HL (F out) HH,SH>SL (L in) HH>HL (L out) SL>HH>SH>HL
Kalekale (180–270 m)	Smallest in D	NS	Largest in HH	(F) larger inside (H) larger inside (L) larger outside	NS	NS	NS
Onaga (210–300 m)	Smallest in H	No test	NS	(H) larger inside	(B) larger in HL than HH (F) similar mean size	NS	(B in) HL>HH (F in) HH>HL
Ehu (210–300 m)	Similar mean size	No test	NS	NS	NS	NS	No test

tions in all size classes and did not show any habitat shifts with size (Pearson's chi-square, $P>0.05$). Opakapaka had a shift from hard-low habitats to hard-high habitats with an increase in size. There was a greater proportion of sexually mature individuals (≥43 cm FL; Kikkawa, 1984) for this species over hard-high habitats, and individuals <43 cm FL were seen mostly in hard-low habitats. Although less evident than the habitat shift by Opakapaka, a habitat shift by Kalekale to hard-high from other habitat types was observed within the size class of 25–35 cm. Onaga and Ehu were recorded mostly in hard-low habitats in all size classes. For Onaga, however, the smallest individuals (<55 cm FL) were found only in hard-low habitats, and, as size increased, hard-high habitats were equally dominant for this species.

Discussion

Depth has a significant influence on the distribution of bottomfishes in Hawaii. Two distinct depth groupings were seen within the sampling range of this study. Opakapaka was dominant in the shallower end of the sampling depths (<200 m), and Kalekale, Onaga, and Ehu were observed more frequently toward the deeper end (>200 m). This finding is consistent with that of previous studies in Hawaii (Haight, 1989; Everson et al., 1989; Merritt et al., 2011) and in the Mariana Archipelago (Polovina et al., 1985). When establishing species-specific differences in distribution, depth must be the first factor evaluated.

Although the limitations of our sampling methods have been discussed in previous studies (e.g., Merritt et al., 2011; Moore et al., 2013), it is important to review them here before further discussion of our results. The absence of a quantifiable sampling area, variability in the field of view of the BotCam, and the scale at which habitats were classified are confounding factors that limit the interpretation of the results of this study to a semiquantitative nature. Because the BotCam makes use of ambient light and because environmental conditions, such as water clarity can differ from site to site, variability in the visual area sampled was unavoidable. However, unlike other visual survey methods, where quadrats or transect lines are used, this approach reduces, but does not eliminate, the effect of visual area because it relies on attracting fishes close to the cameras. What may be more important is the effect of the attracting bait-odor plume.

It was our working assumption that any fish seen on BotCam video was from the targeted grid area

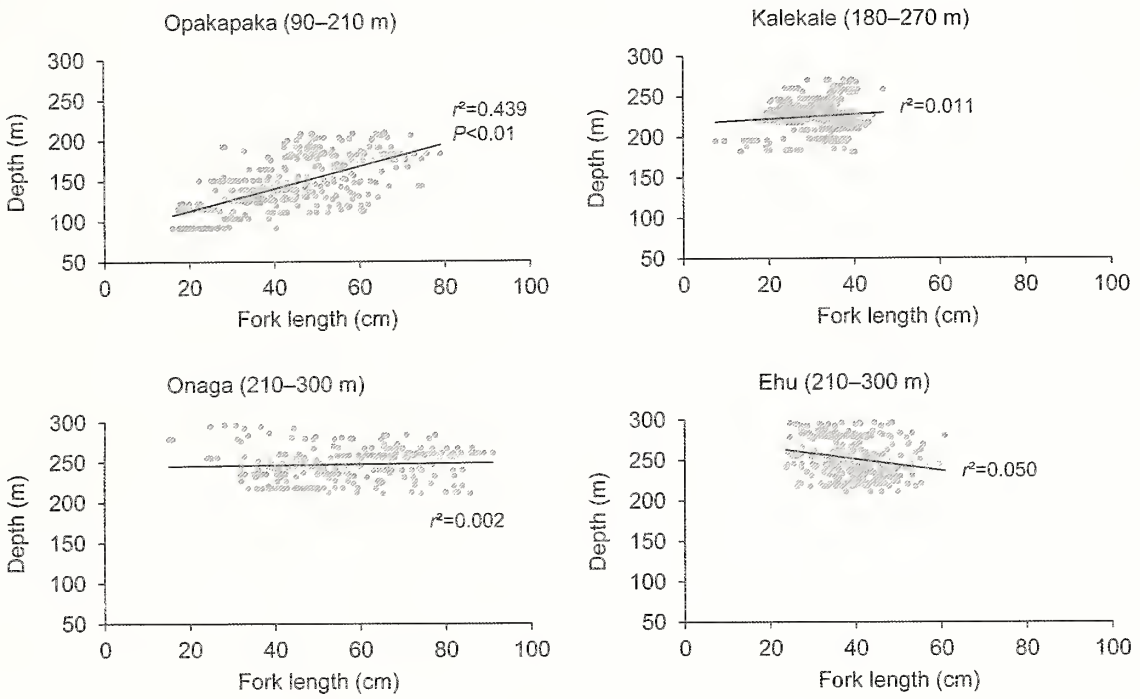

Figure 5

Comparison of fork length with depth for Opakapaka (*Pristipomoides filamentosus*), Kalekale (*P. sieboldii*), Onaga (*Etelis coruscans*), and Ehu (*E. carbunculus*) within the preferred depths of each species for our study of habitat associations of these species in the main Hawaiian Islands from May 2007 to June 2009. The coefficient of determination (r^2) is given for each species.

(200×200 m) regardless of the visual area observed in the video. This assumption was made on the basis of the limited information available on the distance of bottomfish attraction to bait stations. Ellis and DeMartini (1995) estimated that the greatest distance of attraction for juvenile Opakapaka to their baited cameras was between 48 and 90 m. Merritt et al. (2011), in their baited camera survey of Penguin Bank, used a 200-m distance between deployment locations to avoid a cross influence of bait.

The area of fish attraction (sampling area) has been quantified at abyssal depths by Priede and Merrett (1996) through the use of current velocity, fish swimming speed, and a bait dispersal model. Their determination of the area of attraction, however, relied on assumptions (i.e., fish are evenly dispersed) that do not apply to the fish species and shallower depth ranges in this study. Furthermore, bottom current variability, habitat variability, and small-scale bathymetric features at mesophotic depths around Hawaii make the quantification of the area of attraction to bait extremely challenging. In a comparison of baited and unbaited underwater video stations, Harvey et al. (2007) acknowledged that fish behavior and life history also may affect attraction to bait. All the species in this study are regularly attracted to bait and are taken on baited hooks, but other behavioral traits (e.g., mobility, schooling, and reproductive cycles) could affect species-specific responses to a bait-odor plume. Given the difficulty involved in the determination of the actual area of bait influence, the appropriateness of the habitat-classification scale chosen for use in this study cannot be evaluated. Until an effective scale of attraction can be verified for deepwater snappers and other bottomfishes, a fully quantitative assessment of species–habitat associations is not yet possible.

Although previous studies have indicated that habitats with hard substrates and high slopes, such as headlands and promontories, are preferred by many bottomfish species (Ralston and Polovina, 1982; Ralston et al., 1986; Parrish, 1987; Kelley et al., 2006; Parke, 2007), we determined that other habitat types, such as hard-low habitats, are important to eteline snappers and that species-specific differences in habitat preference exist. On the basis of relative abundance, we found that the overall habitat preference of Opakapaka was for low-sloping hard substrates. Onaga was associated with hard-high and hard-low habitats, and Ehu was seen mostly on hard-low habitats. The observed association of juvenile Opakapaka and Onaga with hard-low habitats may be driving their preference for this habitat type. In contrast, the finding for Ehu could

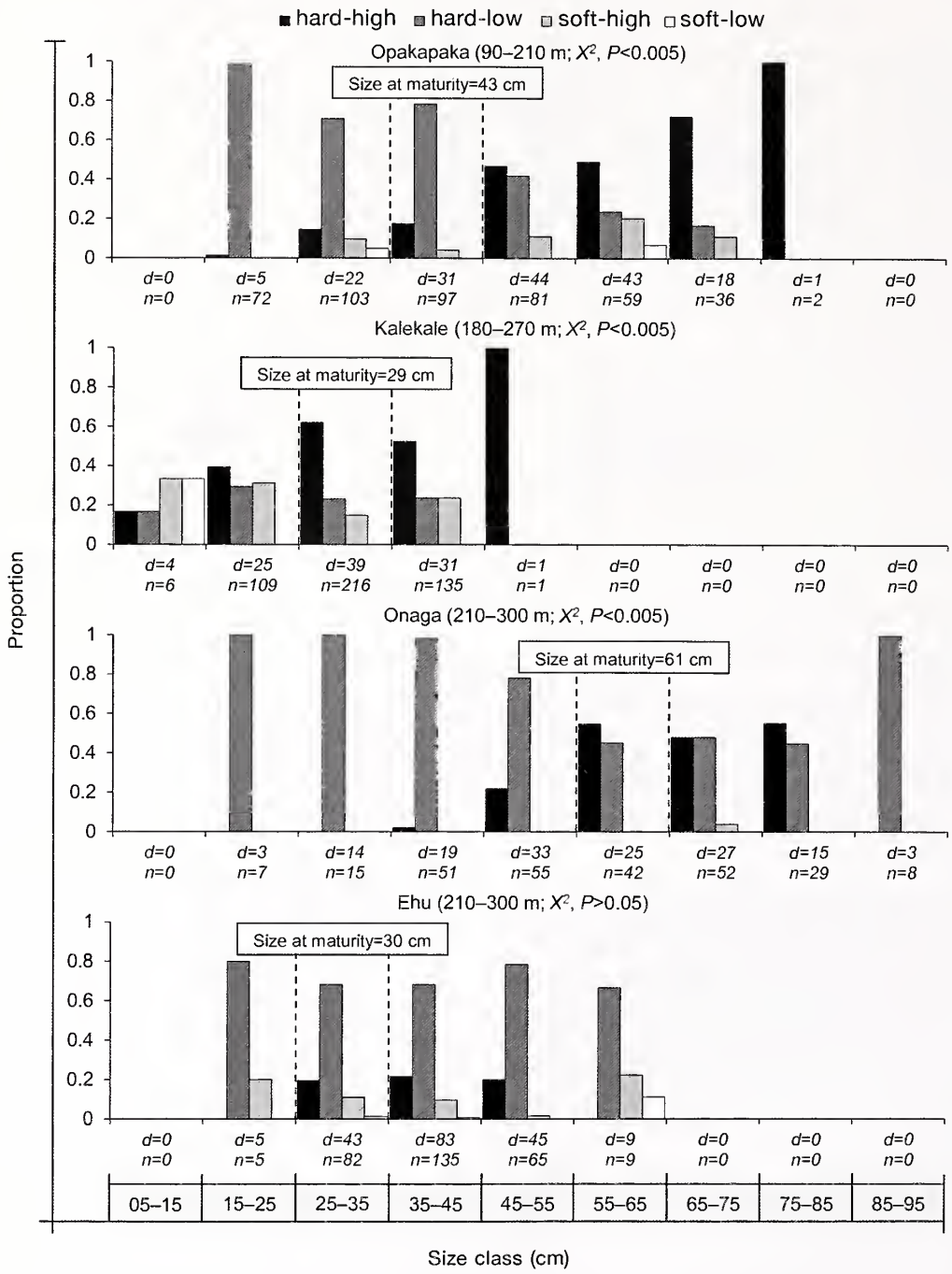

Figure 6

Proportion of fish found in each habitat type by size class tested with Pearson's chi-square (χ^2) test for Opakapaka (*Pristipomoides filamentosus*), Kalekale (*P. sieboldii*), Onaga (*Etelis coruscans*), and Ehu (*E. carbunculus*) within the preferred depths of each species in the main Hawaiian Islands. A baited stereo-video camera system (BotCam) was used to collect data from May 2007 to June 2009. The 4 habitat classifications used in our study were hard substrate with high slope (hard-high), hard substrate with low slope (hard-low), soft substrate with high slope (soft-high), and soft substrate with low slope (soft-low). d=number of BotCam deployments; n=number of fish measured. References for size at maturity: Kikkawa, 1984 (Opakapaka); DeMartini and Lau, 1999 (Kalekale); Everson et al., 1989 (Onaga); Everson, 1986 (Ehu).

have been the result of a sampling artifact caused by the lack of habitat types other than the hard-low environments in Pailolo Channel, where many observations of this species were made. Regardless, the results of this study clearly show the importance of this habitat type for Ehu. Kalekale were observed often in large schools in our video footage. For defense against predators, this species may rely on its schooling behavior instead of associating with the bottom habitat. The lack of a significant habitat preference for Kalekale could, consequently, be driven by this defense mechanism. Assessment of species–habitat associations, therefore, requires an understanding of species behaviors and the changes in habitat use by life stage.

Clear ontogenetic shifts in habitat associations were evident for 3 of the 4 species studied. For Opakapaka, there was a distinct ontogenetic progression in habitat association that expands what is known for this species. The known habitat for juveniles of this species at 7–25 cm FL is shallow, low-sloping, soft substrates (Moffitt and Parrish, 1996). Juvenile Opakapaka have been observed at depths of 65–100 m offshore of Kaneohe Bay (Parrish, 1989; Moffitt and Parrish, 1996) and more recently off Waikiki, Oahu, at depths of 37–42 m (J. Drazen, unpubl. data). These juveniles move out of their nursery grounds and presumably merge with the adult schools in deeper waters after about 1 year (Parrish et al., 1997). Within the preferred depth range identified in our study for Opakapaka (90–210 m), the smallest mean lengths were found over hard-low habitats at 4 of the 6 sampled locations. We recorded Opakapaka as small as 16 cm FL within our sampling depths over hard-low habitats. On the basis of growth curves from DeMartini et al. (1994), the juvenile Opakapaka in our study were just under 1 year old and could be recent migrants from a surrounding nursery area. The results of this study show that these fish continue to stay in hard-low habitats until they reach 45 cm FL or about 5 years of age and, thereafter, increasingly use hard-high habitats. It is possible that this species uses hard substrates with low slopes as a transitional habitat before a move into hard-high habitats. Opakapaka reaches sexual maturity at ~43 cm FL (Kikkawa, 1984). The shift in habitat from hard-low to hard-high could be a response to reproductive maturity, which is discussed later.

Size-related habitat shifts also were evident for Kalekale and Onaga but were observed without a change in their depth of occurrence. Previous studies also showed a lack of depth change with size for these species (Kelley et al[4]; Ikehara, 2006). The move into hard-high habitats with increasing size coincided roughly with the onset of sexual maturity in both species. The size (25–35 cm FL) at which Kalekale shifted to hard-high habitats from other types includes the size (29 cm FL) at which this species reaches sexual maturity (DeMartini and Lau, 1999). The onset of sexual maturity for Onaga occurs at 61 cm FL (Everson et al., 1989)—a size larger than the size (55 cm FL) at which a shift in habitat use was observed in our study. On the basis of size-at-age curves, the onset of sexual maturity occurs between the ages of 3 and 6 years for Kalekale (Williams and Lowe, 1997) and 5 to 6 years for Onaga (Everson et al., 1989).

In contrast to the other 3 species, no size-related habitat shifts were observed for Ehu, but very few juveniles of this species were measured (Fig. 6; n=37). Juvenile Ehu, along with other smaller bottomfishes, are highly vulnerable to predation by demersal carnivores, such as the Greater Amberjack (*Seriola dumerili*) (Humphreys and Kramer, 1984). A few instances where Greater Amberjack seemed to scare away Kalekale and Ehu were observed in the BotCam video collected during our study. No aggressive behavior toward the target species by other predators was seen, but it is possible that carnivorous species could have affected our ability to sample certain size ranges of bottomfishes, particularly Ehu. Smaller snappers may have moved out of the BotCam's field of view before predators entered. Even if they were possibly in the vicinity of the BotCam, juveniles may have remained close to the bottom of the seafloor for protection and out of the unit's field of view. Until very small Ehu (i.e., 5–15 cm FL) can be observed regularly, a complete ontogenetic assessment of habitat for this species will not be possible. However, it is important to note that the size range of Ehu harvested by the fishery is represented in this study.

The ontogenetic habitat shifts observed for Opakapaka, Kalekale, and Onaga could be related to shifts in diet, increases in reproductive output, and predator avoidance at smaller sizes. Szedlmayer and Lee (2004) reported a shift in the diet of the shallow-water juvenile Red Snapper (*Lutjanus campechanus*) from crustaceans to fishes and cephalopods with increasing size. This change in diet was associated with the migration from nursery habitats to coral reefs. For deepwater snappers, diet shifts have yet to be documented. DeMartini et al. (1996) examined the diet of juvenile Opakapaka from the nursery in Kaneohe Bay and discovered that it was composed of crustaceans (shrimps and stomatopods), gelatinous organisms (salps and heteropods), nekton (fishes and squids), and benthic organisms (demersal octopods, echinoids, and microgastropods). With the exception of benthic prey, a similar diet was found for Opakapaka caught at depths of 100–300 m in Penguin Bank by Haight et al. (1993b). It is possible that smaller individuals (<43 cm FL) of this species associate with low-sloping, hardbottom habitats to feed on the benthos and then shift to a pelagic diet when they move into hard-high habitats where the postulated increase in water flow increases prey availability (Ralston et al., 1986; Haight et al., 1993a; Kelley et al., 2006).

[4] Kelley, C. D., B. C. Mundy, and E. G. Grau. 1997. The use of the Pisces V submersible to locate nursery grounds of commercially important deepwater snappers, family Lutjanidae, in Hawaii, 62 p. Paper presented at the 5th Indo-Pacific Fish Conference; Nouméa, New Caledonia, 10–16 November.

With the hypothesis that the levels of bottomfish prey and current speed are greater over hard-high habitats than over other environments (Ralston et al., 1986; Haight et al., 1993a; Kelley et al., 2006), it could be inferred that Opakapaka, Kalekale, and Onaga move into this habitat type upon reaching sexual maturity to increase their foraging rates and maximize reproductive output and gamete dispersal. On coral reefs in Hawaii, the Yellow Tang (*Zebrasoma flavescens*) has been found to shift into habitats with increased food resources when it reaches reproductive size to possibly improve its reproductive ability (Claisse et al., 2009). No actual bottomfish spawning events were recorded during our study. Opakapaka and Onaga are known to spawn at night (C. Kelley, unpubl. data), and camera deployments were restricted to daytime hours. Other than seasonality, habitat and environmental parameters of bottomfish spawning have yet to be determined. It remains possible, however, that the observed ontogenetic habitat shifts occurred as a result of a reproductive cue—given that the change in habitat roughly coincided with sexual maturity.

Another factor that may influence ontogenetic habitat shifts is habitat complexity. Laidig et al. (2009) found that juvenile rockfishes on the continental shelf off central California were associated with boulder and cobble habitats before they moved into the slope habitats used by adults. It is plausible that juveniles and smaller species of bottomfishes use more complex habitats in a similar manner for protection and predator avoidance. However, because habitats were classified at a 200-m scale, our study did not take into account habitat heterogeneity within grid cells and smaller-scale habitat characteristics, such as complexity or rugosity. Structural complexity and the combination of habitat types in a given area are likely to influence fish distributions at their respective scales. Future work is needed to investigate the role of habitat complexity and heterogeneity on size distributions of bottomfishes and to look more closely into how specific habitat types are used. Such an approach could provide more information about the cause of the ontogenetic habitat shifts observed in this study.

The regional variations in relative abundance and mean length could be related to differential fishing pressure or large-scale habitat features. It can be expected that remote locations, such as Niihau, would have less fishing pressure than locations closer to major ports and, thereby, would have greater relative abundances and lengths of target species. Contrary to this expectation, the highest levels of relative abundance were found at Hilo for Opakapaka and in Pailolo Channel for Ehu. Both areas are easily accessible to fishing; therefore, other factors may have driven the observed distributions. Protection did not have an influence on the relative abundance of any of the 4 species studied, a finding that is consistent with the results of Moore et al. (2013). In terms of mean length, the largest Opakapaka may have been found at Niihau because of the remote location and longevity of the protection of this small island. The Niihau BRFA has been closed to fishing since 1998. The opposite may be true for Hilo, where the smallest Opakapaka were observed. Before the implementation of the revised system of BRFAs, fishing in the depth range of Opakapaka was permitted because the BRFA boundary began at 200 m. How protection and fishing pressure affect abundance and size distributions of bottomfishes should be investigated further because these factors may confound any trends attributed to habitat or other environmental variables.

Mega-scale habitat features (scale from Greene et al., 1999: macro=1–10 m; meso=10–1000 m; mega=1–10 km), such as pinnacles, banks, terraces, and even featureless carbonate flats, also could be influencing bottomfish distributions. In this study, juvenile Opakapaka and Onaga were found to associate with hard-low habitats. There is a large terrace at Hilo, where most juvenile Opakapaka were observed, and flat, hardbottom habitats predominate in Pailolo Channel, where most Onaga juveniles were present. These large-scale features predominantly have low slopes and hard bottoms and match the observed habitat preference of these species at the meso-scale. However, because of the difference between the habitat classification scale (200×200 m) used in our study and the size of mega-scale features, further investigation is required to establish a conclusive connection between the bottomfish distributions observed in this study and mega-scale features. In the case of Pailolo Channel, for example, with its large, flat areas of hardbottom habitat, our results agreed with a finding of another survey effort. Previous fishing surveys have indicated that this area possibly was a nursery ground for Onaga (C. Kelley, unpubl. data). Because the smallest mean length (42.80 cm FL) and about 75% of all juveniles of this species measured (<61 cm FL) in this study came from Pailolo Channel, it is highly likely that a nursery ground for Onaga exists in this area.

Conclusions

This study has improved our understanding of the species-specific ecology of 4 bottomfish species in the MHI. Analyses of habitat preferences on the basis of relative abundance and length-frequency distributions showed that habitat types other than hard-high environments are important to each of the species studied, often as a result of ontogenetic shifts in habitat use. Given that these bottomfishes are found throughout the Indo-Pacific region, these findings may provide the framework for the prediction of species distributions outside of Hawaii. Because juveniles of Opakapaka and Onaga were associated mostly with hard-low habitats, it is imperative that future definitions of the bottomfish EFH take into account habitat associations by life stage. Although some species share similar preferences,

it also is clear that bottomfish distributions are species-specific and cannot be generalized for all members of the bottomfish fishery in Hawaii. Because it has increased our knowledge of the ecology of individual species, the results of this study can aid in the improvement of ecosystem-based management strategies and definitions of species-specific EFHs. Moving forward, to further improve our understanding of the habitat requirements of bottomfish species in Hawaii, research on bottomfish habitat should focus on development of models to determine the dispersal range of bait-odor plumes, identification of the effective scale of attraction to bait stations, standardization of sampling areas, and inclusion of habitat heterogeneity and macroscale habitat characteristics in future analyses of bottomfish distributions.

Acknowledgments

We would like to thank C. Moore, D. Sackett, and F. DeLeo for input on statistical design and testing; C. Demarke, B. Alexander, J. Yeh, J. Friedman, and B. Schumacher for many hours of field operations and video analysis; D. Merritt, K. Wong, and the Coral Reef Ecosystem Division of the NOAA Pacific Islands Fisheries Science Center for giving us access to BotCam units; J. Ault, S. Smith, M. Parke, G. DiNardo, and J. Brodziak for assistance with the experimental design; and captains R. Cates (*Wailoa*) and G. Jones (*Red Raven*; *Huki Pono*). This project was funded by the State of Hawaii DLNR-DAR and in part by the Federal Aid in Sport Fish Restoration Program.

Literature cited

Anderson, M. J., R. N. Gorley, and K. R. Clarke.
2008. PERMANOVA+ for PRIMER: Guide to software and statistical methods. PRIMER-E Ltd, Plymouth, UK.

Andrews, A. H., J. M. Kalish, S. J. Newman, and J. M. Johnston.
2011. Bomb radiocarbon dating of three important reef-fish species using Indo-Pacific $\Delta^{14}C$ chronologies. Mar. Freshw. Res. 62:1259–1269.

Andrews, A. H., E. E. DeMartini, J. Brodziak, R. S. Nichols, and R. L. Humphreys.
2012. A long-lived life history for a tropical, deepwater snapper (*Pristipomoides filamentosus*): bomb radiocarbon and lead-radium dating as extensions of daily increment analyses in otoliths. Can. J. Fish. Aquat. Sci. 69:1–20.

Cappo, M. C., E. S. Harvey, H. A. Malcolm, and P. J. Speare.
2003. Potential of video techniques to design and monitor diversity, abundance and size of fish in studies of marine protected areas. *In* Aquatic protected areas—what works best and how do we know? World congress on aquatic protected areas; Cairns, Australia, 14–17 August 2002 (J. P. Beumer, A. Grant, and D. C. Smith, eds.), p. 455–464. Austr. Soc. Fish Biol., North Beach, Western Australia, Australia.

Claisse, J. T., M. Kienzle, M. E. Bushnell, D. J. Shafer, and J. D. Parrish.
2009. Habitat- and sex-specific life history patterns of yellow tang *Zebrasoma flavescens* in Hawaii, USA. Mar. Ecol. Prog. Ser. 389:245–255.

DeMartini, E. E., K. Landgraf, and S. Ralston.
1994. A recharacterization of the age-length and growth relationships of the Hawaiian snapper, *Pristipomoides filamentosus*. NOAA Tech. Memo. NMFS-SWFSC-199, 15 p.

DeMartini, E. E., and B. B. Lau.
1999. Morphometric criteria for estimating sexual maturity in two snappers, *Etelis carbunculus* and *Pristipomoides sieboldii*. Fish. Bull. 97:449–458.

DeMartini, E. E., F. A. Parrish, and D. M. Ellis.
1996. Barotrauma-associated regurgitation of food: implications for diet studies of Hawaiian pink snapper, *Pristipomoides filamentosus* (family Lutjanidae). Fish. Bull. 94:250–256.

Ellis, D. M., and E. E. DeMartini.
1995. Evaluation of a video camera technique for indexing abundances of juvenile pink snapper, *Pristipomoides filamentosus*, and other Hawaiian insular shelf fishes. Fish. Bull. 93:67–77.

Everson, A. R.
1986. Ehu. *In* Fishery atlas of the Northwestern Hawaiian Islands (R. Uchida and J. H. Uchiyama, eds.), p. 106–107. NOAA Tech. Rep. NMFS 38, 142 p.

Everson, A. R., H. A. Williams, and B. M. Ito.
1989. Maturation and reproduction in two Hawaiian eteline snappers, uku, *Aprion virescens*, and onaga, *Etelis coruscans*. Fish. Bull. 87:877–888.

Greene, H. G., M. M. Yoklavich, R. M. Starr, V. M. O'Connell, W. W. Wakefield, D. E. Sullivan, J. E. McRea Jr., and G. M. Cailliet.
1999. A classification scheme for deep seafloor habitats. Oceanol. Acta 22:663–678.

Haight, W. R.
1989. Trophic relationships, density and habitat associations of deepwater snappers (Lutjanidae) from Penguin Bank, Hawaii. M.S. thesis., 86 p. Univ. Hawaii, Honolulu, HI.

Haight, W. R., D. R. Kobayashi, and K. E. Kawamoto.
1993a. Biology and management of deepwater snappers of the Hawaiian Archipelago. Mar. Fish. Rev. 55(2):20–27.

Haight, W. R., J. D. Parrish, and T. A. Hayes.
1993b. Feeding ecology of deepwater lutjanid snappers at Penguin Bank, Hawaii. Trans. Am. Fish. Soc. 122:328–347.

Harvey, E. S., M. Cappo, J. J. Butler, N. Hall, and G. A. Kendrick.
2007. Bait attraction affects the performance of remote underwater video stations in assessment of demersal fish community structure. Mar. Ecol. Prog. Ser. 350:245–254.

Humphreys, R. L., and S. H. Kramer.
1984. Ciguatera and the feeding habits of the greater amberjack, *Seriola dumerili*, in the Hawaiian Archipelago. *In* Proceedings of the second symposium on resource investigations in the Northwestern Hawaiian Islands, vol. 2; Honolulu, 25–27 May 1983 (R. W. Grigg and K. Y. Tanoue, eds.), p. 237–264. Univ. Hawaii Sea Grant College Program, Honolulu, HI.

Ikehara, W.
2006. Bottomfish management and monitoring in the main Hawaiian Islands. *In* Deep sea 2003: conference on the governance and management of deep-sea fisheries. Part 2: conference poster papers and workshop papers; Queenstown, New Zealand, 1–5 December 2003, Dunedin, New Zealand, 27–29 November 2003 (R. Shotton, ed.), p. 289–300. FAO Fisheries Proceedings 3/2. FAO, Rome.

Kelley, C., R. Moffitt, and J. R. Smith.
2006. Mega- to micro-scale classification and description of bottomfish essential fish habitat on four banks in the Northwestern Hawaiian Islands. Atoll Res. Bull. 543:319–332.

Kikkawa, B. S.
1984. Maturation, spawning, and fecundity of opakapaka, *Pristipomoides filamentosus*, in the Northwestern Hawaiian Islands. *In* Proceedings of the second symposium on resource investigations in the Northwestern Hawaiian Islands, vol. 2; Honolulu, 25–27 May 1983 (R. W. Grigg and K. Y. Tanoue, eds.), p. 149–160. Univ. Hawaii Sea Grant College Program, Honolulu, HI.

Laidig, T. E., D. L. Watters, and M. M. Yoklavich.
2009. Demersal fish and habitat associations from visual surveys on the central California shelf. Estuar. Coast. Shelf Sci. 83:629–637.

Merritt, D. W.
2005. BotCam: Design, testing and development of a fully automated stereo-video bottom camera bait station for ecosystem monitoring of bottom fish species. M.S. thesis, 174 p. Univ. Hawaii, Honolulu, HI.

Merritt, D. W., M. K. Donovan, C. Kelley, L. Waterhouse, M. Parke, K. Wong, and J. C. Drazen.
2011. BotCam: a baited camera system for nonextractive monitoring of bottomfish species. Fish. Bull. 109:56–67.

Moffitt R. B., and F. A. Parrish.
1996. Habitat and life history of juvenile Hawaiian pink snapper, *Pristipomoides filamentosus*. Pac. Sci. 50:371–381.

Moore, C. H., J. C. Drazen, C. D. Kelley, and W. F. X. E. Misa.
2013. Deepwater marine protected areas of the main Hawaiian Islands: establishing baselines for commercially valuable bottomfish populations. Mar. Ecol. Prog. Ser. 476:167–183.

Parke, M.
2007. Linking Hawaii fishermen reported commercial bottomfish catch data to potential bottomfish habitat and proposed restricted fishing areas using GIS and spatial analysis. NOAA Tech. Memo. NMFS-PIFSC-11, 37 p.

Parrish, F. A.
1989. Identification of habitat of juvenile snappers in Hawaii. Fish. Bull. 87:1001–1005.

Parrish, F. A., E. E. DeMartini, and D. M. Ellis.
1997. Nursery habitat in relation to production of juvenile pink snapper, *Pristipomoides filamentosus,* in the Hawaiian Archipelago. Fish. Bull. 95:137–148.

Parrish, J. D.
1987. The trophic biology of snappers and groupers. *In* Tropical snappers and groupers: biology and fisheries management (J. J. Polovina and S. Ralston, eds.), p. 405–463. Westview Press, Boulder, CO.

Priede, I. G., and N. R. Merrett.
1996. Estimation of abundance of abyssal demersal fishes; a comparison of data from trawls and baited cameras. J. Fish Biol. 49(suppl. A):207–216.

Polovina, J. R., R. B. Moffitt, S. Ralston, P. M. Shiota, and H. A. Williams.
1985. Fisheries resource assessment of the Mariana Archipelago, 1982–85. Mar. Fish. Rev. 47(4):19–25.

Ralston, S., R. M. Gooding, and G. M. Ludwig.
1986. An ecological survey and comparison of bottom fish resource assessments (submersible versus handline fishing) at Johnston Atoll. Fish. Bull. 84:141–155.

Ralston, S., and J. R. Polovina.
1982. A multispecies analysis of the commercial deep-sea handline fishery in Hawaii. Fish. Bull. 80:435–448.

Randall, J. E.
2007. Reef and shore fishes of the Hawaiian Islands, 546 p. Univ. Hawaii Sea Grant College Program, Honolulu, HI.

Rosenberg, A., T. E. Bigford, S. Leathery, R. L. Hill, and K. Bickers.
2000. Ecosystem approaches to fishery management through essential fish habitat. Bull. Mar. Sci. 66:535–542.

Szedlmayer, S. T., and J. D. Lee.
2004. Diet shifts of juvenile red snapper (*Lutjanus campechanus*) with changes in habitat and fish size. Fish. Bull. 102:366–375.

Watson D. L., E. S. Harvey, B. M. Fitzpatrick, T. J. Langlois, and G. Shedrawi.
2010. Assessing reef fish assemblage structure: how do different stereo-video techniques compare? Mar. Biol. 157:1237–1250

Williams, H. A., and M. K. Lowe.
1997. Growth rates of four Hawaiian deep slope fishes: a comparison of methods for estimating age and growth from otolith micro-increment widths. Can. J. Fish. Aquat. Sci. 54:126–136.

Willis, T. J., and R. C. Babcock.
2000. A baited underwater video system for the determination of relative density of carnivorous reef fish. Mar. Freshw. Res. 51:755–763.

Willis, T. J., R. B. Millar, and R. C. Babcock.
2000. Detection of spatial variability in relative density of fishes: comparison of visual census, angling, and baited underwater video. Mar. Ecol. Prog. Ser. 198:249–260.

Yau, C., M. A. Collins, P. M. Bagley, I. Everson, C. P. Nolan, and I. G. Priede.
2001 Estimating the abundance of Patagonian toothfish, *Dissostichus eleginoides,* using baited cameras: a preliminary study. Fish. Res. 51:403–412.

James's rule and causes and consequences of a latitudinal cline in the demography of John's Snapper (*Lutjanus johnii*) in coastal waters of Australia

Mike Cappo (contact author)[1]
Ross J. Marriott[2]
Stephen J. Newman[2]

Email address for contact author: mcappo@aims.gov.au

[1] Australian Institute of Marine Science
PMB 3, Townsville MC
Townsville 4810
Queensland, Australia

[2] Western Australian Fisheries and Marine Research Laboratories
Department of Fisheries
Government of Western Australia
P.O. Box 20
North Beach 6920
Western Australia, Australia

Abstract—Demographic parameters were derived from sectioned otoliths of John's Snapper (*Lutjanus johnii*) from 4 regions across 9° of latitude and 23° of longitude in northern Australia. Latitudinal variation in size and growth rates of this species greatly exceeded longitudinal variation. Populations of John's Snapper farthest from the equator had the largest body sizes, in line with James's rule, and the fastest growth rates, contrary to the temperature-size rule for ectotherms. A maximum age of 28.6 years, nearly 3 times previous estimates, was recorded and the largest individual was 990 mm in fork length. Females grew to a larger mean asymptotic fork length (L_∞) than did males, a finding consistent with functional gonochorism. Otolith weight at age and gonad weight at length followed the same latitudinal trends seen in length at age. Length at maturity was ~72–87% of L_∞ and varied by ~23% across the full latitudinal gradient, but age at first maturity was consistently in the range of 6–10 years, indicating that basic growth trajectories were similar across vastly different environments. We discuss both the need for complementary reproductive data in age-based studies and the insights gained from experiments where the concept of oxygen- and capacity-limited thermal tolerance is applied to explain the mechanistic causes of James's rule in tropical fish species.

Manuscript submitted 29 June 2012.
Manuscript accepted 10 July 2013.
Fish Bull. 111:309–324.
doi: 10.7755/FB.111.4.2

The views and opinions expressed or implied in this article are those of the author (or authors) and do not necesarily reflect the position of the National Marine Fisheries Service, NOAA.

Body sizes generally increase across a range of taxa with increasing distance from the equator, a principle known as Bergmann's rule; another theory about variation of size by latitude, James's rule, applies this phenomenon within species (for review, see Blackburn et al., 1999). The potential existence of such an underlying latitudinal cline raises major ecological questions about 1) the mortality and lifetime reproductive contribution of adults throughout their geographic range, 2) the implications for recruitment rates at marginal latitudes, and 3) the implications for fishery harvests. James's rule has been well demonstrated in both cold temperate and tropical fish species (e.g., Choat and Robertson, 2002; Choat et al., 2003; Robertson et al., 2005a; Pörtner et al., 2008; Trip et al., 2008; Berumen et al., 2012), and the advent of warming oceans has caused an upsurge in interest in the underlying physiological mechanisms of this rule (Pörtner and Peck, 2010; Clark et al., 2012).

However, major equatorial gaps still remain in such descriptive knowledge of demographic processes for the large, economically important lutjanid snappers, lethrinid emperors, and serranid groupers, especially in the Indo-West Pacific, where most studies have been done south of 15°S. Ecosystem "mass balance" models (sensu Pauly et al., 1993) and life history classifications used for estimating resilience (King and MacFarlane, 2003) are sensitive to estimates of maximum size, growth rate, and longevity. In data-poor tropical fisheries, these estimates are often derived from only one part of a species' distribution (e.g., Binohlan and Froese, 2009) or from a mix of parameters derived from different studies in separate regions (e.g., Pauly et al., 1993). Consequently, there is a need to investigate regional differences to determine whether growth trajectories and reaction norms (i.e., the pattern of phenotypic expression of a single genotype across a range of environments) such as age at maturity are conserved in populations along latitudinal gradients (see Arendt, 2011).

John's Snapper (*Lutjanus johnii*), is widely distributed in the Indo-

West Pacific, extending from East Africa to Fiji, north to the Ryukyu Islands and south to Australia (Allen, 1985). In Southeast Asia, this species is called *jenahak* or *ang cho* and is important in both wild-harvest fisheries and sea-cage mariculture (Tanaka et al., 2011). In Australia, this species is known as "Golden Snapper" or "Fingermark" and is a dominant, large lutjanid of the nearshore community of reef fishes from the Kimberley region (~124° E) in northwestern Australia, across northern Australia, and down the Queensland coast to at least 23° S (Travers et al., 2009). Juvenile and younger adult John's Snapper generally are associated with the lower reaches of mangrove-lined estuaries (Kiso and Mahyam, 2003) and eventually move offshore toward fringing and coastal reefs (Tanaka et al., 2011). Large adults in Australia are found schooling in turbid waters around hard substrata and complex topography in muddy coastal areas and occasionally on deeper, sandier trawl grounds offshore (Marriott and Cappo, 2000).

Australia's northern coastline is mostly uninhabited by humans or sparsely populated and remote from domestic markets. The Northern Territory is the only state that reports landings of John's Snapper. The coastal hook-and-line fishery of the Northern Territory reported landings of only 8.64 metric tons (t) in 2009, 5.34 t in 2010, and 4.38 t in 2011 (Northern Territory Government[1]). John's Snapper is a prized sportfish in Australia and Malaysia, but skilled fishing techniques and approaches, such as night fishing and live squid baits, often are required to catch one. Sportfishing and spearfishing interest in John's Snapper is expanding in northern Australia with both the development of charter operations in remote locations and the rapid development of marine electronics for use on small boats to echolocate fish. Most charter boat operators and many top anglers practice catch and release for this species.

Longevities of <10 years have been published for John's Snapper from the reading of scales (Andaman Sea; Druzhinin, 1970) and from a single length-frequency composition (Bay of Bengal; Khan, 1986). The growth parameters from these studies still compose the major information source for John's Snapper (FishBase, http://www.fishbase.org/search.php; Froese, 2011). Both techniques are well known to have serious bias where size is uncoupled from age and where under-aging can lead to a three-fold overestimation of natural mortality for lutjanids (Newman et al., 2000), thus inflating estimates of potential fishery yield.

The primary objectives of this study were, therefore, 1) to describe the age composition, growth, and mortality of John's Snapper on the basis of age estimates from sectioned otoliths; 2) to quantify spatial variability in the length, otolith weight at age, and gonad weight at length of populations of John's Snapper along a latitudinal gradient, and 3) to examine catch records for other large lutjanids for signs of latitudinal variation in maximum size in the Indo-West Pacific.

Materials and methods

Sampling methods and locality

Filleted fish frames or whole specimens (identified using Allen, 1985) were collected during the period of February 1989–April 2002 from fish processing facilities, research surveys, sportfishing charter operators, anglers, and spearfishing individuals in 4 regions: the coast of the Kimberley (Western Australia); the Arafura Sea (Northern Territory); coast of Cape York (Queensland); and the coast from Townsville to Cairns (Queensland) (Fig. 1). The fork lengths (FL) were recorded in millimeters, and, where whole fish were available (n=129), whole weights (W_W) were measured in grams. Sagittae (hereafter, referred to as "otoliths") were removed from under the gill covers, washed, dried, weighed, and measured. Notable gaps in full information occurred because volunteers contributed mainly eviscerated fish frames. Of the 948 fish that were aged, 863 had reliable FL and 928 had reliable otolith weights. Sex was determined by macroscopic examination for 786 fish, but whole gonad weights (W_G) were measured, in grams, for only 277 of them.

Estimation of fish age

Three transverse sections were cut from otoliths embedded in resin with a low speed circular saw and diamond wafering blade in the vicinity of the primordium. The sections were 0.25–0.50 mm thick, depending on width of the otolith, and were lightly polished on wet ebony paper (1000 grade) and lapping film (9 and 3 μm). The sections were mounted in resin on microscope slides under cover slips. Opaque zones—annuli or annual growth rings—were counted along the ventral margin of the sulcus acousticus under reflected light against a dark background (see Newman et al., 2000). These zones are deposited annually from spring to early summer (Cappo et al., 2000). Categorization of otolith margins indicated that deposition of opaque zones occurred over a period of 9 months, with a low peak in October for the eastern regions (Cape York and north Queensland).

The index of average percent error (IAPE) (Beamish and Fournier, 1981) among readers and readings (eastern regions: IAPE=4.18 ±1.01%, n=55; Kimberley: IAPE=3.96 ±0.92%, n=55), was below a benchmark IAPE of 5% acceptable for long-lived species (Allman et al., 2005), and there was no significant drift in increment counts in age bias plots (see Campana et al., 1995).

A preliminary analysis of monthly mean gonadosomatic index (GSI) values (percentages) was made to

[1] Northern Territory Government. 2012. Fishery Status Reports 2011, 162 p. Northern Territory Government, Department of Primary Industry and Fisheries, Darwin, NT, Australia. Fishery Report No. 111. [Available from http://www.nt.gov.au/d/Content/File/p/Fish_Rep/FR111.pdf.]

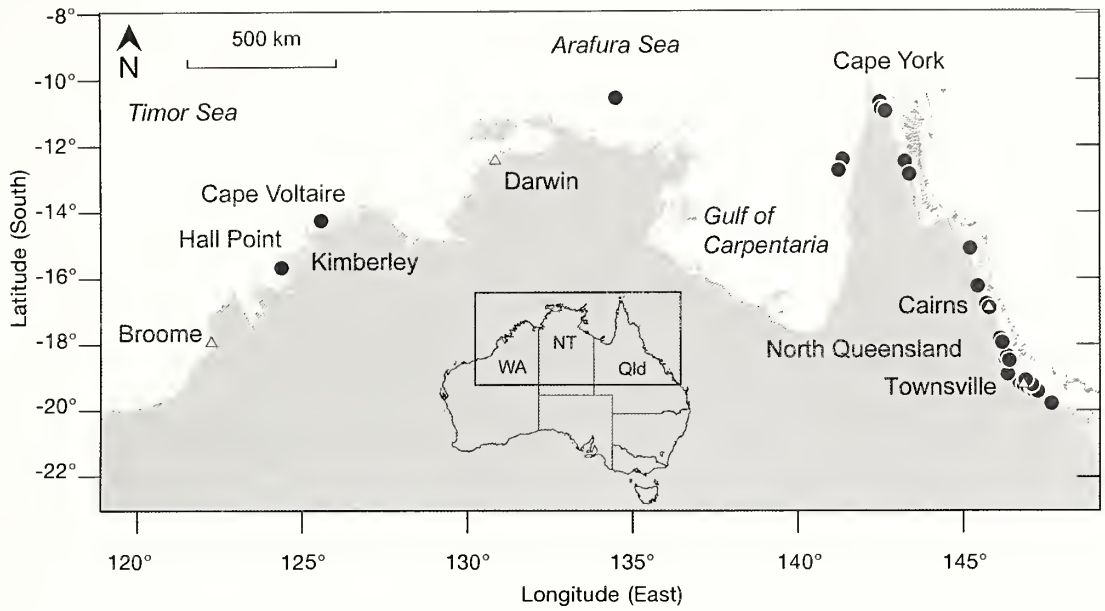

Figure 1

Map of sampling locations (circles) for an examination of a latitudinal cline in the demography of John's Snapper (*Lutjanus johnii*) collected over the period of February 1989–April 2002 in 4 regions in northern Australia: Kimberley, Arafura Sea, Cape York, and north Queensland. Triangles indicate major centers of human inhabitation.

estimate birth months with measurements of gonad weight available for 176 eastern fish. First, W_W estimates were calculated from FL (L_F) measurements using this equation:

$$W_W = a \times L_F{}^b, \quad (1),$$

with a nonlinear regression: $a=7.701\times10^{-5} \pm 2.046\times10^{-5}$, $b=2.741 \pm 0.0401$, coefficient of multiple determination ($R^2=0.987$, $n=77$). Equation 1 was applied to predict whole weight for all fish in the pooled subsample ($W_{w(pred)}$), and GSI values were calculated with the following equation:

$$GSI = (W_G / (W_{w(pred)} - W_G)) \times 100. \quad (2)$$

Equation 2 showed higher *GSI* values in the austral summer after October; therefore, the nominal birth date for John's Snapper in this study was chosen to be Oct. 1. Individual fish ages (in years) were the number of opaque increments (years) plus fractions of a year elapsed between sampling and Oct. 1.

Estimation of mortality

The instantaneous rate of total mortality (Z) was derived with the maximum age in years (t_{max}) from the equation of Hoenig (1983):

$$\log_e Z = 1.46 - 1.01 \log_e t_{max}. \quad (3)$$

This estimate of Z is from a lightly exploited population; therefore, the estimate of natural mortality (M) should be similar to Z. It has been applied as a reasonable approximation for unfished or lightly fished tropical demersal fishes in the absence of enough samples for catch curve analysis (Newman et al., 2000).

Growth parameters

The von Bertalanffy growth function *(VBGF)* was fitted to estimates of length at age through the use of nonlinear least squares estimation. The VBGF is defined by the equation

$$L_t = L_\infty \{1 - e^{-K(t - t_0)}\}, \quad (4)$$

where L_t = mean FL (in millimeters) of fish of age t (in years);
L_∞ = asymptotic mean length;
K = is a rate constant that determines the rate at which L_t approaches L_∞;
t = age of a fish; and
t_0 = the hypothetical age at which the mean length is zero.

The fit of the VBGF to different data sets was compared by using the likelihood ratio test for coincident curves (Cerrato, 1990) across comparable age ranges (Haddon, 2001) and analysis of covariance (ANCOVA) with type-III sums of squares and with $\log_e$-transformed age (year) as the linear covariate. This ANCOVA allowed for testing of an interaction of *sex×region* and accounted for type-I errors.

Otolith weight at age and gonad weight at length

Nonlinear least squares estimation also was used to fit second-order polynomial functions to regional estimates of otolith weight at age t (in years) and an exponential function to gonad weight (W_G) at FL (L_F in millimeters).

The functions were defined with relevant starting parameters (a,b,c) by the following equations:

$$Otolith\ weight = a + b\ (t) + c\ (t^2); \quad (5)$$

$$Gonad\ weight = e^{(a + b\ (L_F))}. \quad (6)$$

Quantile-quantile normal plots and Cook's Distance were used to identify outliers for exclusion, and plots of residuals were used to test for lack of homogeneity in variances. Comparisons in the 2 responses by sex or region were restricted to the range of explanatory data (sizes or ages) common to each level in the comparison with likelihood ratio tests for coincident curves and ANCOVA with type-III sums of squares. Log_e transformations were used to linearize the gonad weight and otolith weight covariates for the ANCOVA. Data from the Arafura Sea were too few for use in these tests and were compared visually with the other regions.

Australian and international fishing records

An Internet search for record sizes of John's Snapper and other large lutjanids landed by line and spearfishing was conducted for countries in the Indo-West Pacific, but only world and Australian records were available. The 2011 records maintained by the International Game Fishing Association (IGFA), Australian National Sportfishing Association (ANSA), Australian Angler's Association (AAA), and Australian Underwater Federation (AUF), were used

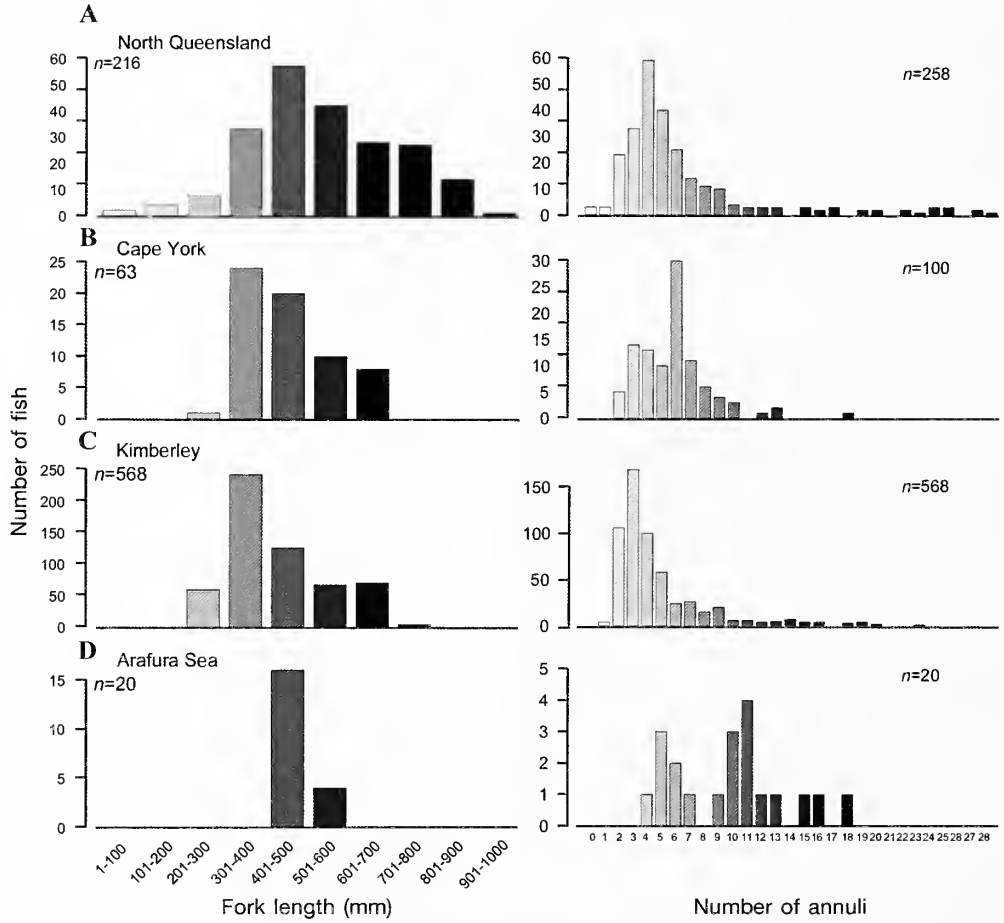

Figure 2

The length- and age-frequency distributions of John's Snapper (*Lutjanus johnii*) sampled during the period of February 1989–April 2002 in 4 regions of Australia: (**A**) north Queensland, (**B**) Cape York, (**C**) Kimberley, and (**D**) Arafura Sea. The y-axes represent the numbers of fish. Lengths are fork lengths measured in millimeters, and age is measured as the number of annuli (annual growth rings) observed in sectioned otoliths. n=sample size.

Table 1

Fitted parameter estimates for the von Bertalanffy growth models for males (M), females (F), and all John's Snapper (*Lutjanus johnii*) sampled from the Kimberley, north Queensland, and Cape York regions in Australia during the period of February 1989–April 2002 (see Fig. 3, for graphs of growth curves by sex and region). L_t=mean fork length (mm) of fish of age t (years), L_∞=asymptotic mean length (mm), t_0=the hypothetical age at which the mean length is zero, K is the growth coefficient at which L_t approaches L_∞. Standard errors of fitted parameter estimates are reported in parentheses, and the coefficient of multiple determination (R^2) and sample size (n) are also given.

Region	n	L_∞	K	t_0	R^2
Kimberley (M)	255	677.1 (20.53)	0.17 (0.02)	−0.81 (0.33)	0.76
Kimberley (F)	294	739.6 (27.05)	0.16 (0.02)	−0.62 (0.29)	0.79
North Queensland (M)	80	819.7 (25.27)	0.18 (0.02)	−0.32 (0.36)	0.85
North Queensland (F)	74	851.4 (37.37)	0.21 (0.03)	0.34 (0.29)	0.83
Kimberley	568	698.0 (14.48)	0.18 (0.01)	−0.51 (0.20)	0.79
North Queensland	216	843.5 (15.66)	0.19 (0.01)	0.02 (0.16)	0.87
Cape York	63	685.1 (50.04)	0.18 (0.05)	−0.82 (0.80)	0.74

to plot the maximum weights of John's Snapper and 6 other large lutjanids with latitude. These other species were Mangrove Jack (*Lutjanus argentimaculatus*), Twospot Snapper (*L. bohar*), Malabar Snapper (*L. malabaricus*), Emperor Snapper (*L. sebae*), Chinaman Fish (*Symphorus nematophorus*), and Green Jobfish (*Aprion virescens*).

Results

Length and age distributions

Samples from north Queensland had the smallest (55 mm FL) and largest (990 mm FL) fish, a higher modal FL (401–500 mm) than the samples from the Kimberley and Cape York regions (301–400 mm FL), and a much higher proportion of very large John's Snapper than samples from the other 3 regions (Fig. 2). The overall proportion of samples that were older than 8 years in the Kimberley region (11.6%) was smaller than the proportion of such samples in the north Queensland region (18.2%) but similar to the proportion in the Cape York region (11%). The modal age (4 years) for fish from north Queensland was higher than the modal age of fish from Kimberley (3 years), and the 6-year age class was most prevalent in the samples from Cape York. The oldest year classes were from north Queensland (28 year), Kimberley (23 year), and Cape York (18 year).

Mortality

The maximum observed age (t_{max}) of 28.6 years (a male) was used to produce an estimate of Z=0.146 year^{-1} with the Hoenig (1983) equation for the north Queensland region. Estimates of Z were not calculated for the other regions because of concerns that the t_{max} values might be skewed by a lack of older year classes that represented undersampling and not truncation of the true age distribution.

Growth

The von Bertalanffy growth curves fitted to length-at-age data revealed a relatively moderate growth trend (Fig. 3). This trend was reflected in estimates for the K curvature parameter, which ranged from 0.17 to 0.21 year^{-1} (Table 1). Relatively rapid growth from 0.5 year to 5–7 years was followed by a slower phase after approximately 7–10 years. Asymptotic growth began at approximately 18–20 years (Fig. 3).

Females were estimated to grow to a larger average asymptotic length (L_∞) in the Kimberley and north Queensland regions (Fig. 3; Table 1). However, sex-specific differences in growth curvature, K, were inconsistent between regions; a higher K value was evident for males than for females in the Kimberley region and a lower K value for males than for females in north Queensland (Table 2). The north Queensland L_∞ was 17.3% (145.5 mm FL) and 18.8% (158.4 mm FL) higher than the L_∞ for samples from the Kimberley and Cape York regions (Table 1; Fig. 3).

Apparent differences in growth trends between sexes and regions were observed to be statistically significant in both the likelihood ratio and ANCOVA tests (Table 2). Significant differences between sex-specific curves were detected within each of the Kimberley and north Queensland regions (Table 2). The lack of significant interaction for *sex* × *region* indicates that the larger L_∞ for females than for males was consistent among regions.

Likelihood ratio tests revealed significant differences in growth curves between samples from the

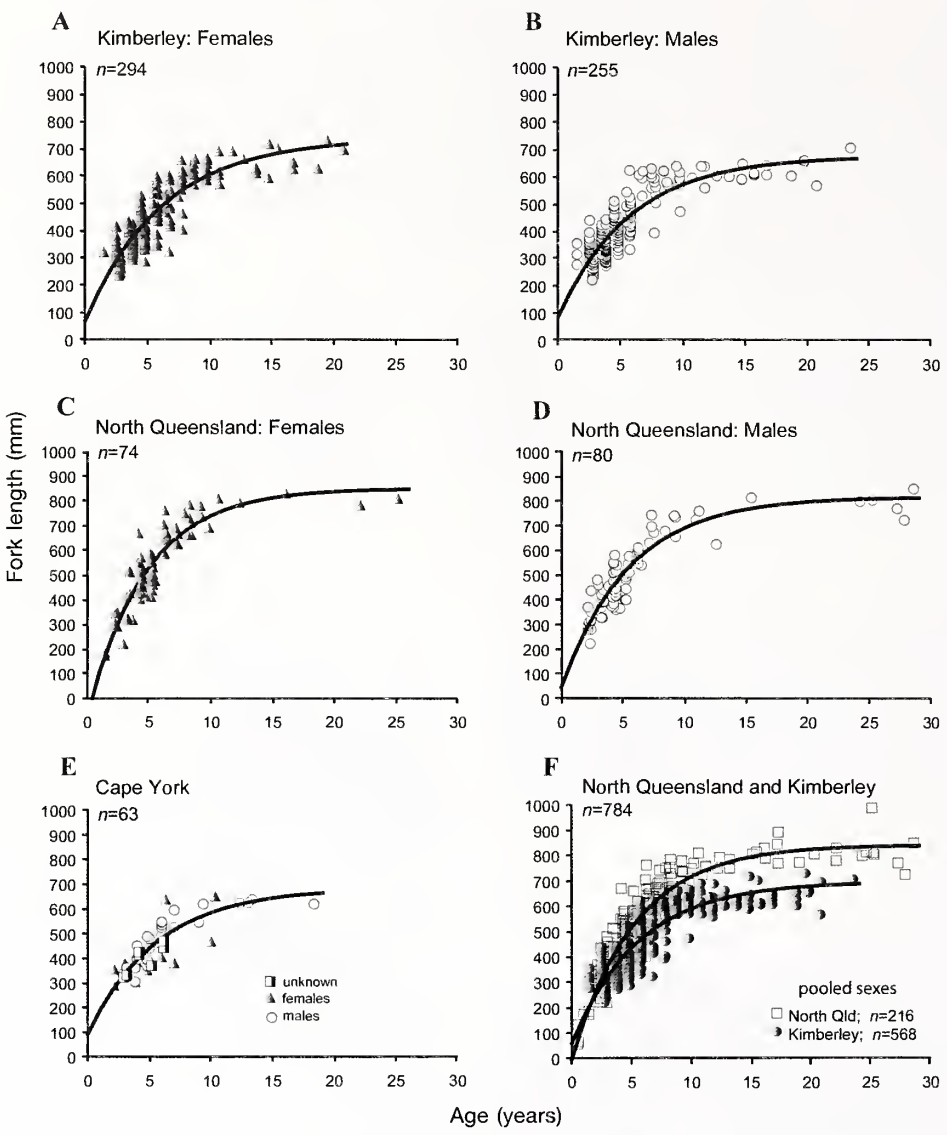

Figure 3

Fits of the von Bertalanffy growth function by sex and region for John's Snapper (*Lutjanus johnii*) sampled during the period of February 1989–April 2002 in northern Australia. Females (gray triangles) and males (open circles) are distinguished in separate curves for the (**A**, **B**) Kimberley and (**C**, **D**) north Queensland regions. A single curve describes the small sample size (n) for (**E**) Cape York, where a large proportion of fish were of unknown sex (shaded squares). Significantly different growth curves describe eastern and western fish (**F**) when sexes were pooled. For more information on growth estimates and comparisons from these models, see Tables 1 and 2.

Kimberley and north Queensland regions for each sex, and a significant main effect of region on the slope of transformed length at age (Table 2). The larger L_∞ and K for samples from north Queensland, therefore, were significantly different from those values for samples from the Kimberley and Cape York regions, but there was no significant difference between values for Cape York and Kimberley fish.

Otolith weight at age

The sagittae of John's Snapper are exceptionally large, and the largest otolith weighed in this study exceeded 5 g. Second-order polynomials provided the best fits for otolith weight at age with R^2 values of 0.77–0.95 (Table 3; Fig. 4). Very small values for the slope parameter c indicate that these relationships were close to linear

Table 2

Comparison of regional growth data for John's Snapper (*Lutjanus johnii*) from our study of a latitudinal cline in the demography of this species in Australia. Likelihood ratio tests, each with 3 degrees of freedom (df), were performed for coincidence of curves (Curves). Tests of the probability (*P*) of differences among slopes (β) and intercepts (α) were made for sex and region with 2-way analysis of covariance (ANCOVA) of fork length (mm) against $\log_e$ (age) for samples from the Kimberley and north Queensland regions (df numerator:df denominator=1:672). Tests of slopes and intercepts were made only for region for Cape York and Kimberley with 1-way ANCOVA (df=1:616) and for Cape York and north Queensland (df=1:256). *P*=probability of null hypothesis being true. If the chi-squared goodness of fit statistic (χ^2) is large, the null model is a poor fit to the curve. The *F* statistic is the ratio of between-group mean square values to the within-group mean square values for slopes and intercepts.

	Factor	Parameter	Test statistic	*P*
Excluding Cape York data				
Kimberley	Sex	Curves	χ^2=14.42	0.00
North Queensland	Sex	Curves	χ^2=8.70	0.03
Males	Region	Curves	χ^2=80.68	<0.00
Females	Region	Curves	χ^2=99.58	<0.00
Kimberley, north Queensland	Sex	β	*F*=9.47	0.00
Kimberley, north Queensland	Region	β	*F*=35.89	<0.00
Kimberley, north Queensland	Sex×Region	β	*F*=1.07	0.30
Kimberley, north Queensland	Sex	α	*F*=4.51	0.03
Kimberley, north Queensland	Region	α	*F*=3.00	0.08
Kimberley, north Queensland	Sex×Region	α	*F*=0.67	0.41
Including Cape York data: sexes pooled				
Cape York, Kimberley	Region	Curves	χ^2=2.06	0.56
Cape York, Kimberley	Region	β	*F*=1.45	0.23
Cape York, Kimberley	Region	α	*F*=1.95	0.16
Cape York, north Queensland	Region	Curves	χ^2=83.44	<0.00
Cape York, north Queensland	Region	β	*F*=19.43	<0.00
Cape York, north Queensland	Region	α	*F*=3.98	0.05

(Table 3). Departures from a linear relationship were evident for older fish (>10 years), where the rate of otolith weight accretion appeared to decline with age (Fig. 4).

Tests that spanned the widest age range, for the north Queensland region, showed no significant effects of sex on accretion rate, but there were significant differences in the coincidence of curves, slopes, and intercepts for pairwise comparisons of age ranges common between north Queensland and other regions (Table 4). Evidence of a difference in otolith weight at age between results for Kimberley and Cape York fish was equivocal because the fitted curves were not coincident, but the slopes and intercepts were not significantly different (Table 4). Cape York and Kimberley curves were intermediate between those from the north Queensland and Arafura Sea regions, showing a cline for an increasing rate of accretion of otolith weight with age and distance from the equator by about 0.2 g per degree of latitude for the oldest fish. Visual comparison of the regional fits with data from the Arafura Sea region showed an approximate two-fold difference in otolith weight at age beyond 10 years for north Queensland fish (Fig. 5).

Gonad weight at length and maturity

Exponential models provided the best fits for gonad weight at length (Table 5; Fig. 4), but the lack of data on gonad weights elsewhere severely restricted the tests in pairwise comparisons. There were no significant effects of sex for samples from north Queensland (Table 6), a finding that is not coincident with the Kimberley and Cape York fits. The tests on slopes and intercepts, however, were not significant.

For fish with gonads that weighed ≥20 g, maturity was evident from macroscopic classification (Fig. 4). Minimum lengths and ages for the females of these mature fish were 690 mm FL and 9.83 years for north Queensland, 549 mm FL and 7.75 years for Kimberley, and 640 mm FL and 6.3 years for Cape York. Minimum lengths and ages for males that had gonads that weighed ≥20 g were 590 mm FL and 6.16 years for north Queensland, 590 mm FL and 9.75 years for Kimberley, and 620 mm FL and 9.33 years for Cape York (Fig. 4). In contrast, the Arafura Sea fish appeared to develop earlier. Fish sampled in that region

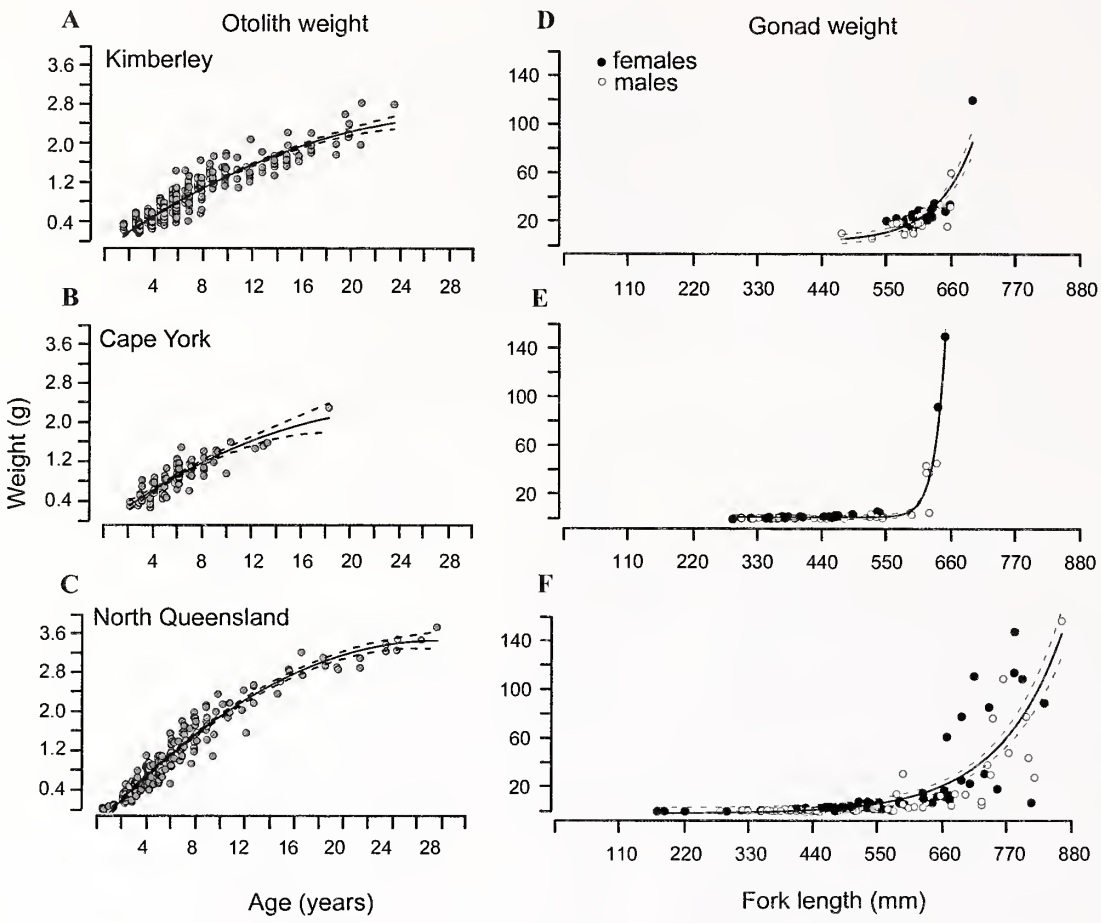

Figure 4

Fitted relationships that relate weights of otoliths to age (years) and weights of gonads to fork length for John's Snapper (*Lutjanus johnii*) sampled during the period of February 1989–April 2002 in the (**A**, **D**) Kimberley, (**B**, **E**) Cape York, and (**C**, **F**) North Queensland regions in northern Australia. Dashed lines show the 95% confidence intervals around each fit. For the graphs of gonad weights, black circles indicate females and open circles indicate males. For details on parameters, see Tables 3 and 4.

had ovaries ≥20 g at 448 mm FL (5.0 years) and testes ≥20 g at 472 mm FL (10.91 years) (Fig. 5).

These preliminary data indicate the difference in length at maturity may be up to 24% between the northernmost and southernmost samples, but age at maturity (6–10 years) may be similar among regions, depending on sex. The north Queensland females and males matured at ~81% and ~72% of L_∞, respectively, and for samples from the Kimberley region they matured at ~74% and ~87%, respectively.

Latitudinal spread of catch records

Catch records for Indo-West Pacific lutjanids indicate that the latitudes farthest from the equator produced the largest individuals for 7 species, in a steeply concave, "U-shaped" relationship, but we could not locate any records for other equatorial countries to fit statistical relationships (Fig. 6). Most records were obtained from landings in the southern hemisphere, but several world records came from Japan. The largest records for John's Snapper show a steep rise over about 8°S from 7.2 kg in Darwin (Australian all-tackle [AAA] record) to weights of 10.5 kg (97 cm total length, world all-tackle [IGFA] record), 12.420 kg (6-kg line-class [ANSA] record), and 12.0 kg (spearfishing [AUF] record) near Cairns. The maximum published weight from scientific samples is 4.7 kg for a 71-cm John's Snapper from the Andaman Sea (Druzhinin and Hlaing, 1972).

Discussion

Our detection of latitudinal clines in L_∞ of John's Snapper with distance from the equator is explained

Table 3

Parameters of the functions that relate otolith weight (grams) to age (t years) for males (M), females (F), and all John's Snapper (*Lutjanus johnii*) sampled in northern Australia over the period of February 1989–April 2002. Data were pooled from 3 regions with nonlinear least-squares estimation of *otolith weight* = a + b (t) + c (t^2). Standard errors of parameters are shown in parentheses, and the range in ages (years), sample size (n), and coefficient of multiple determination (R^2) are also given.

	t range (years)	n	a	b	c	R^2
North Queensland (M)	2.16–28.58	84	–0.31 (0.06)	0.25 (0.02)	–0.00 (0.00)	0.95
North Queensland (F)	1.41–25.16	80	–0.34 (0.08)	0.27 (0.02)	–0.01 (0.00)	0.90
North Queensland	1.41–28.58	244	–0.34 (0.05)	0.26 (0.01)	–0.00	0.91
Kimberley	1.5–23.5	563	–0.16 (0.02)	0.18 (0.01)	–0.00	0.89
Cape York	2.16–18.33	99	–0.07 (0.09)	0.18 (0.02)	–0.00 (0.00)	0.77

in theories of variation in body size of ectotherms in relation to geography (James's rule; Blackburn et al., 1999) and temperature (temperature-size rule; Atkinson, 1994). However, our estimation of faster growth rates in cooler water farther from the equator contradicts the temperature-size rule. Here, we discuss the major explanations for the patterns we observed through the use of prevailing ecological theories, and we consider the effects of our revised estimates of parameters for the VBGF on studies of life history.

Explanations of James's rule for tropical fishes

Similar clines in maximum size and growth have been documented for some sedentary coral reef species at much larger and smaller latitudinal scales, but, in the case of some lutjanids, the same trends have always been interpreted as an effect of fishing, regional differences in productivity of habitats, or the evolution of separate stocks. For example, Allman and Goetz (2009) and Burton (2001) reported that mean size at age in Gray Snapper (*Lutjanus griseus*) in Florida in-

Table 4

Summary of regional comparisons of otolith weight at age for John's Snapper (*Lutjanus johnii*) from this study of a latitudinal cline in the demography of this species in Australia. Likelihood ratio tests, each with 3 degrees of freedom, were performed for coincidence of curves (Curves). Tests of differences among slopes (β) and intercepts (α) were made by using 1-way analysis of covariance of otolith weight against $\log_e$ (age). All tests were conducted over age ranges present at both levels of the pairwise comparisons. The number of samples (n, otolith weights) is shown in parentheses for each member of the pairs, with the common age range in years (yr). P=probability of null hypothesis being true. If the chi-squared goodness of fit statistic (χ^2) is large, then the null model is a poor fit to the curve. The F statistic is the ratio of between-group mean square values to the within-group mean square values for slopes and intercepts. Inf=infinity.

Region; age range	Parameter	Test statistic	P
North Queensland			
Male (80), Female (77); 2.16–25.16 yr	Curves	χ^2=Inf	1
	β	F=0.59	0.44
	α	F=0.33	0.57
North Queensland (227), Kimberley (563); 1.5–23.5 yr	Curves	χ^2=349.19	<0.00
	β	F=168.48	<0.00
	α	F=69.30	<0.00
North Queensland (221), Cape York (98); 2.16–18.3 yr	Curves	χ^2=86.19	<0.00
	β	F=168.48	<0.00
	α	F=69.30	<0.00
Cape York (96), Kimberley (550); 2.16–18.3 yr	Curves	χ^2=23.21	<0.00
	β	F=0.31	0.58
	α	F=1.59	0.21

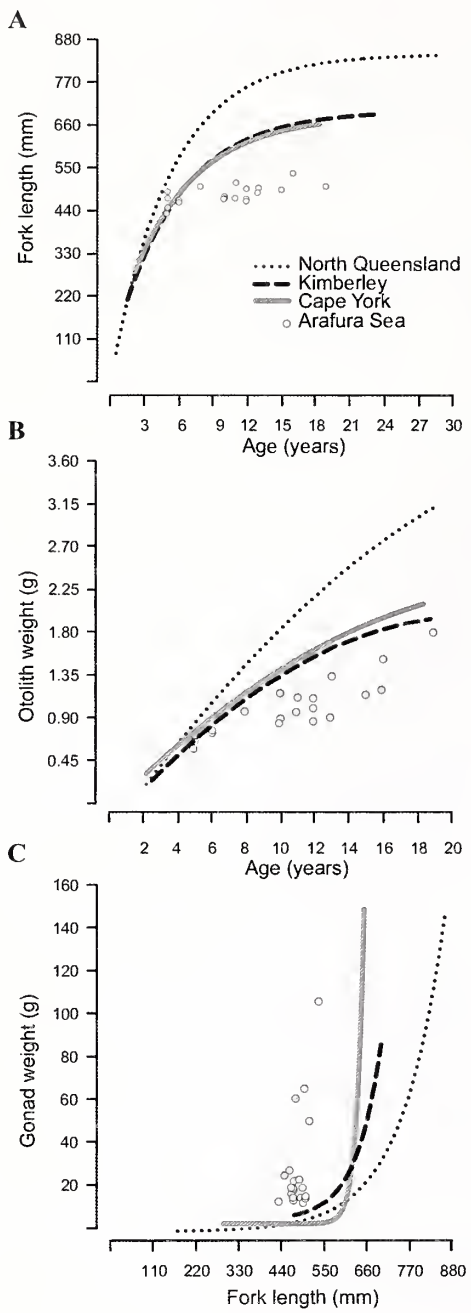

Figure 5

Comparisons of parameters by region, and fits of Arafura Sea data points, for John's Snapper (*Lutjanus johnii*) sampled during the period of February 1989–April 2002 in 4 regions of Australia—north Queensland, Kimberley, Cape York, and Arafura Sea: (**A**) fork length (mm) at age (years) with von Bertalanffy growth function (sexes pooled; see Table 2); (**B**) otolith weight at age with first-order polynomials (see Table 3); and (**C**) gonad weight at fork length with exponential relationships (see Table 5).

creased with distance from the equator, but they invoked major regional differences in exploitation rate as an explanation. At a smaller latitudinal scale, Saari (2011) concluded that Red Snapper (*L. campechanus*) from northern Texas and Alabama reach significantly larger L_∞ than do Red Snapper from southern Texas and northwestern Florida. Saari (2011) discussed severe overfishing as the primary cause of the difference, as well as differences in environmental factors, fishing behavior between sectors, habitat-preference, and management regimes. In eastern Indonesia, the Crimson Snapper (*L. erythropterus*) and Malabar Snapper grow faster than their conspecifics in northern Australia, but Fry and Milton (2009) interpreted this pattern in relation to the genetic evidence for separate stocks. Mangrove Jack at the southern end of their Australian range have faster juvenile growth and are larger at a given age, but Russell et al.[2] were concerned that sample sizes were too small for any inferences to be made from such observations.

There is no doubt that heavy fishing can affect body sizes of fishes across latitudes. Throughout the 1970s, there was a ten-fold increase in mean body size of 326 fish species from low to high latitudes in the North Atlantic. However, this trend began to weaken under heavy fishing pressure in the early 1980s, and, by 1991, mean body sizes had declined steeply to the extent that a gradient was no longer detectable (Fisher et al., 2010). This homogenization of community size structures was a breakdown of Bergmann's rule that Fisher et al. (2010) predicted will lead to declining stability in populations, communities, and ecosystems.

The earliest explanations for James's rule concerned a quandary posed by the temperature-size rule (Atkinson, 1994): for most ectotherms, decreased nutrition and decreased temperature both reduce growth rates, but each affects maturity differently. Decreased nutrition results in delayed maturity at a *smaller* size, yet decreased temperature usually results in delayed maturity at a *larger* size. This puzzle led Berrigan and Charnov (1994) to propose that the effects of temperature on maturity are associated with the existence of a negative correlation between L_∞ and the growth coefficient, K, in the VBGF.

In contrast, the latitudinal studies of tropical fish growth at the largest scales, over 56° of latitude for Ocean Surgeon (*Acanthurus bahianus*) and 14° of latitude for Stoplight Parrotfish (*Sparisoma viride*), have shown that growth rate is *faster* in cooler waters (22.6–28.1°C), not slower. Maximum age, adult survivorship, terminal size, and absolute growth rate are inversely related to temperature in populations of Ocean Sur-

[2] Russell, D. J., A. J. McDougall, A. S. Reicher, J. R. Ovenden, and R. Street. 2003. Biology, management and genetic stock structure of mangrove jack (*Lutjanus argentimaculatus*) in Australia, 198 p. Queensland Department of Primary Industries, Brisbane, Australia. [Available from http://era.deedi.qld.gov.au/3119/1/BiologyManGeneticStock_report_final%5B1%5D-sec.pdf.]

Table 5

Parameters of the functions relating gonad weight (grams) to fork length (FL) for John's Snapper (*Lutjanus johnii*) sampled in 3 regions of Australia over the period of February 1989–April 2002. Nonlinear least-squares estimation was calculated with the following equation: $gonad\ weight = e^{(a + b\ (L_F))}$. Standard errors of parameters are shown in parentheses, and the range in FL (L_F), sample size (n), and coefficient of multiple determination (R^2) are also given.

Region; sex	L_F range (mm)	n	a	b	R^2
North Queensland (Male)	222–860	67	−5.24 (0.99)	0.01 (0.00)	0.75
North Queensland (Female)	173–830	60	−2.27 (1.08)	0.01 (0.00)	0.57
North Queensland	173–860	127	−2.98 (0.75)	0.01 (0.00)	0.60
Kimberley	473–696	60	−6.49 (0.69)	0.02 (0.00)	0.68
Cape York	290–652	56	−31.64 (2.19)	0.06 (0.00)	0.96

geon (Robertson et al., 2005a) and there are no indications of consistent effects of fishing on longevity or adult survivorship (Robertson et al., 2005b). In relation to Berrigan and Charnov's (1994) commentary, it is important to note that there was no sign of a negative relationship between locality-specific L_∞ and K in fig. 5 of Robertson et al. (2005a) for Ocean Surgeon, but such a negative relationship was noted for Stoplight Parrotfish in fig. 4 of Choat et al. (2003).

Counter-gradient variation in growth rates has been proposed to explain this contradiction of the temperature-size rule. This counter-gradient variation occurs where genetic and environmental influences on phenotypes oppose one another to produce metabolic compensation (Conover et al., 1997). Various physiological rates and processes are now known to be elevated to counteract the dampening effect of reduced temperature and diminished length of the optimal season for

Table 6

Comparison of regional summaries of gonad weight at length for John's Snapper (*Lutjanus johnii*) from our study of a latitudinal cline in the demography of this species in Australia. Likelihood ratio tests, each with 2 degrees of freedom (df) were performed for coincidence of curves. Tests of differences among slopes (β) and intercepts (α) were made by using 1-way analysis of covariance of gonad weight against $\log_e$ (age). All tests were conducted over age ranges in fork length (FL) present in both levels of the pairwise comparisons. The number of samples (n, shown in parentheses) and gonad weights is shown for each member of a pair, and the common length range in millimetres is also given. P=probability of null hypothesis being true. If the chi-squared goodness-of-fit statistic (χ^2) is large, the null model is a poor fit to the curve. The F statistic is the ratio of between-group mean square values to the within-group mean square values for slopes and intercepts. Inf=infinity.

Region; fork length range	Parameter	Test statistic	P
North Queensland			
Male (66), Female (57); 222–830 mm	Curves	χ^2=Inf	1
	β	F=0.08	0.77
	α	F=0.60	0.44
Regions			
North Queensland (60), Kimberley (60); 473–696 mm	Curves	χ^2=74.17	<0.00
	β	F=1.05	0.31
	α	F=3.24	0.07
North Queensland (89), Cape York (56); 290–652 mm	Curves	χ^2=281.74	<0.00
	β	F=2.24	0.14
	α	F=0.55	0.46
Kimberley (55), Cape York (22); 473–652 mm	Curves	χ^2=157.12	<0.00
	β	F=25.74	<0.00
	α	F=28.25	<0.00

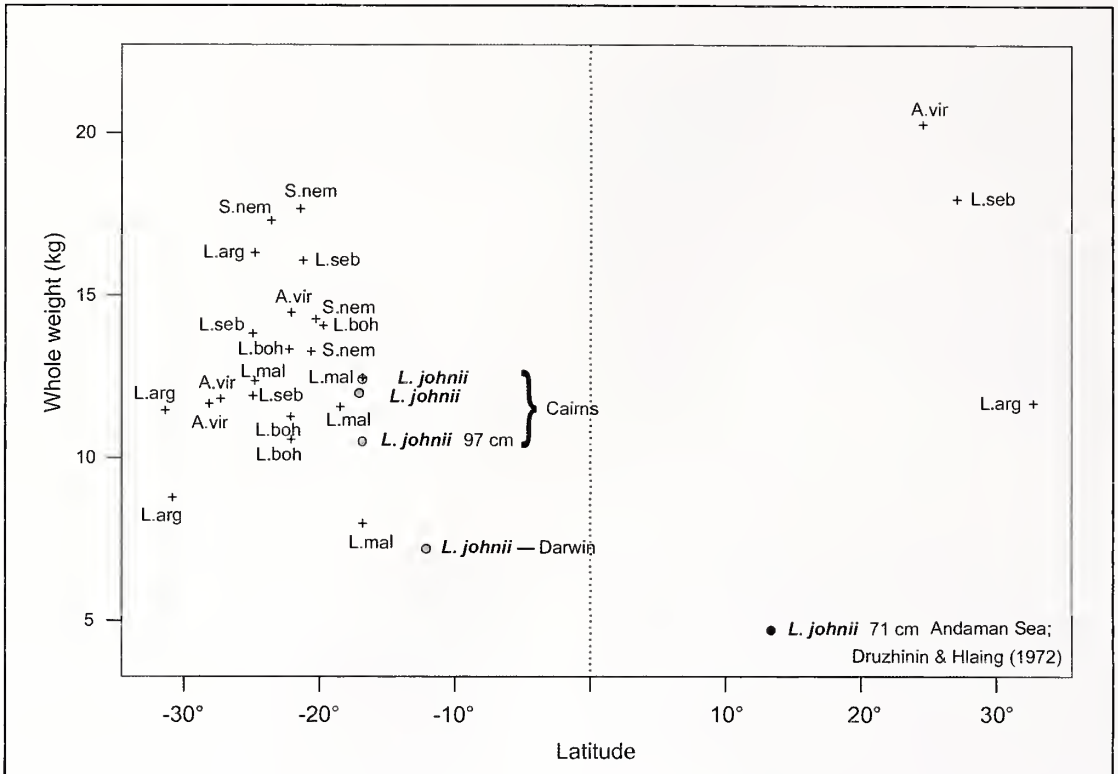

Figure 6

Records of maximum weight of John's Snapper (*Lutjanus johnii*) and 6 other large lutjanids landed until 2011, shown by latitude. The data (whole weight in kilograms) for each species was provided by the following sources: the International Game Fishing Association, Australian National Sportfishing Association, Australian Angler's Association, and Australian Underwater Federation. The cluster of data for John's Snapper is bracketed for comparison with the data from Darwin and the largest weight reported in the scientific literature, by Druzhinin and Hlaing (1972) (bottom right). The other 6 lutjanids were Mangrove Jack (*L. argentimaculatus*: L.arg), Twospot Snapper (*L. bohar*: L.boh), Malabar Snapper (*L. malabaricus*: L.mal), Emperor Snapper (*L. sebae*: L.seb), Chinaman Fish (*Symphorus nematophorus*: S.nem), and Green Jobfish (*Aprion virescens*: A.vir).

feeding and growth at increasing distance from the equator (see Conover et al., 2009, for review). In fact, the crisper clarity of opaque and translucent zones in otoliths of tropical fishes from latitudes where water temperatures are 5–10° Celsius cooler may be a physiological product of this counter-gradient variation in growth (see photomicrographs in Choat et al., 2003, 2009; Marriott and Mapstone, 2006; Robertson et al., 2005a).

Pörtner and Knust (2007) proposed a "thermal limitation hypothesis" that natural selection favors individuals that maximize growth and energy efficiency at the expense of ranges of thermal tolerance (see also Pörtner et al., 2008). The underlying concept of oxygen- and capacity-limited thermal tolerance (OCLT) implies that oxygen supply to tissues is optimal between lower and upper temperature limits. Between these limits (termed *pejus* temperatures), oxygen supply also can be increased to exceed maintenance demand and fuel aerobic metabolism for the performance of growth, foraging, migration, and reproduction.

These "performances" support the fitness of species, and the excess in oxygen availability that supports them is reflected in a species-specific aerobic scope. The aerobic scope is the difference between the lowest and highest rates of aerobic respiration, with an optimum close to the upper pejus temperature. Beyond upper pejus limits, oxygen supply decreases, maintenance demand rises, and aerobic scope begins to decrease (for review, see Pörtner 2012). At suboptimal high temperatures, fish cannot consume enough food to meet increasing metabolic needs because aerobic scope is insufficient to satisfy the increase in oxygen demand from exercise and digestion (Pörtner and Peck, 2010).

Populations of Atlantic Cod (*Gadus morhua*) also follow James's rule in the Atlantic, where the growth, spawning, and recruitment of this species are well

known along a latitudinal cline (Pörtner et al., 2008). Permanent physiological differences induced by temperature and climate have been identified in Atlantic Cod populations along that cline, resulting in population-specific patterns of OCLT. The Hb-I(1/1) allele displays an increasing frequency toward the (warmer) south, leading to a higher oxygen affinity at higher temperatures, and this feature is considered to be a microevolutionary adaptation to optimize oxygen transport (Pörtner et al., 2008).

The OCLT concept does not imply strict positive or negative correlations between longevity, maximum size, or growth rate along latitudinal clines. It offers a promising new way forward to use physiological challenges under controlled conditions (see Clark et al., 2012) to disentangle true mechanistic causes (and contradictions) of the temperature-size rule from effects of fishing and unknown environmental differences between regions. This approach may explain why responses in growth rate and maximum size along long latitudinal gradients are inconsistent in statistical correlations used in intensive field studies of tropical fishes. For example, Robertson et al. (2005a) concluded that variation in growth and terminal size is related strongly to both habitat and temperature, yet Trip et al. (2008) proposed that growth and adult size are most responsive to local environmental features unrelated to latitudinal (temperature) effects.

Growth trajectories and length at maturity

Despite vast differences in the local environments sampled, the basic patterns in the growth curves of John's Snapper are conserved. This snapper species has a relatively gradual growth trajectory through early life, maturing at 6–10 years and at 70–80% of L_∞, and reaching an asymptotic length at ~18–20 years. The consistent, sex-specific differences in growth rates are consistent with functional gonochorism for John's Snapper, for which there is a higher selective pressure for females to grow to a larger size and have a higher fecundity (Roff, 1983). Longevities >20 years are known for many small and large lutjanids (e.g., Heupel et al., 2010; Martinez-Andrade, 2003) and are considered to be beneficial by ensuring a long reproductive life. This life history minimizes the risk that unfavorable events at large scales will result in the loss of a metapopulation. In life history terms, John's Snapper is an "intermediate strategist" falling in the center of a continuum between large species that mature at later ages and have large eggs and those that are long-lived, slow-growing, and highly fecund species (King and MacFarlane, 2003).

Our demonstration of a longevity that is nearly 3 times that reported from early studies is not surprising, or novel, but it is nonetheless very important to improve meta-analyses, such as analyses with Ecopath and stock reduction models. Compared with the parameters derived by Khan (1986), which appear in the online database FishBase (Froese, 2011), the parameters we have shown for John's Snapper give evidence of a higher longevity (28.6 versus 10 years derived by Khan), lower K (0.16–0.21 versus 0.28), about 4% of the total instantaneous mortality Z (0.146 versus 2.700), and, consequently, about 25% of the rate of natural mortality M (≤0.146 versus ≤0.590).

The estimates of length at maturity of John's Snapper are coarse and preliminary but indicate differences as high as 24% between the latitudinal limits sampled. Therefore, it is interesting to note that the minimum estimates exceeded predictions from regressions on the basis of L_∞ and L_{max} from published meta-analyses. With our L_{max} of 990 mm FL and L_∞ of 843.5 mm FL for the north Queensland region, we calculated an estimated L_m of 495 ±10 mm FL using the Binohlan and Froese (2009) method and estimated L_m of 448 ±10 mm FL in the Froese and Binohlan (2000) equation. Martinez-Andrade (2003) generalized that L_m occurred at a length about half (0.52) of the L_∞ for lutjanids, producing an even smaller estimate (L_m=438 mm FL) for John's Snapper. Our estimates were considerably larger at 590 mm FL for males and 690 mm FL for females in north Queensland, representing from 59.6% (males) to 69.7% (females) of L_{max} and from 69.9% to 81.8% of L_∞. The legal limits to fish size at first capture of John's Snapper in Western Australia (300 mm total length) and Queensland (350 mm total length) do not approach any of the estimates discussed above. The Northern Territory has no size limit.

The northernmost (Arafura Sea) samples were at the smallest extremes of length and otolith weight at age and of gonad weight at length, when compared with samples from the other regions. However, the fishery on the coastal reefs of the Northern Territory, inshore of the Arafura Sea trawl grounds, recorded John's Snapper up to 820 mm FL and 23 years of age (Hay et al.[3]). Of these coastal females, 50% reached sexual maturity (L_{m50}) at a much larger size of 630 mm FL (8–10 years) than did Arafura Sea females, although males reached maturity at a similar size (L_{m50}=470 mm FL). There is clearly a need to accurately measure regional length at maturity and establish fecundity-size curves to fully understand the nested hierarchy within growth curves. In general terms, larger adults of tropical fish populations farther from the equator might be expected to have much larger ovaries (and hence batch fecundity) and a longer spawning life in comparison with their smaller counterparts close to the equator. However, there is no evidence that recruitment rates are higher for populations at these margins. Instead, Pörtner et al. (2008) proposed that recruitment rates should show a dome-shaped distribution about an optimal temperature range.

[3] Hay T., I. Knuckey, C. Calogeras, and C. Errity. 2005. NT coastal reef fish: population and biology of the golden snapper. Fishnote No: 21 Department of Primary Industry, Fisheries and Mines, Darwin, Northern Territory, Australia, 4 p. [Available from http://www.nt.gov.au/d/Content/File/p/Fishnote/FN21.pdf.]

The appearance of a U-shaped relationship between record sizes of lutjanids and latitude among 3 genera highlights the chronic lack of basic length and weight information on equatorial and Asian populations of lutjanids in the Indo-West Pacific. These records also suggest that James's rule may apply in age-based studies when such studies are eventually undertaken in those countries.

Conclusions

As with some studies of site-attached coral reef fishes, our findings of larger terminal size, faster growth, and larger size at maturity for John's Snapper farthest from the equator agree with James's rule but do not agree with the presumption of "slower growth in colder water" of the temperature-size rule for ectotherms. Further, age-based studies alone cannot resolve the variability in the growth response reported in some tropical studies. More powerful insights can be obtained through the use of the concept of OCLT and measurement of physiological response to exercise and thermal challenges in populations along latitudinal clines.

The existence of older, larger John's Snapper in the southern portion of the range of this species has raised some compelling questions concerning the lifetime reproductive output and subsequent recruitment rates of tropical fish populations at the warmer core and cooler limits of their ranges. If recruitment also is marginal at thermal limits, then is the development of larger gonads each year over a longer life in cooler waters a wasted investment for John's Snapper or is it an adaptation to episodic recruitment success? Such questions can be investigated only if age-based studies of fish demography are accompanied by information on size-fecundity curves and egg size and quality, along with some relative indices of recruitment.

Acknowledgments

We wish to thank all the tackle store proprietors, numerous anglers, and spearfishing individuals who provided specimens for use in this study or assisted with fieldwork. From the fishing community, we would like to thank, in particular, A. J. McDougall, D. Donald, A. Mead, E. Riddle, M. Kenway, S. Boyle, and P. Hazard. Archived otoliths and fish frames were supplied also by D. Milton, G. McPherson, M. Sheaves, and A. Coleman. Field and laboratory support was provided by R. Steckis, J. Jenke, C. Skepper, and B. Robertson. We especially appreciate the critical and constructive advice of 3 reviewers including J. H. Choat and A. J. McDougall.

Literature cited

Allen, G. R.
1985. FAO species catalogue. Vol. 6. Snappers of the world. An annotated and illustrated catalogue of lutjanid species known to date. FAO Fish. Synop. 125, 208 p. FAO, Rome.

Allman, R. J., and L. A. Goetz.
2009. Regional variation in the population structure of gray snapper, *Lutjanus griseus*, along the west Florida shelf. Bull. Mar. Sci. 84:315–330.

Allman, R. J., G. R. Fitzhugh, K. J. Starzinger, and R. A. Farsky.
2005. Precision of age estimation in red snapper (*Lutjanus campechanus*). Fish. Res. 73:123–133.

Arendt, J. D.
2011. Size-fecundity relationships, growth trajectories, and the temperature-size rule for ectotherms. Evolution 65:43–51.

Atkinson, D.
1994. Temperature and organism size—a biological law for ectotherms. Adv. Ecol. Res. 25:1–58.

Beamish, R. J., and D. A. Fournier.
1981. A method for comparing the precision of a set of age determinations. Can. J. Fish. Aquat. Sci. 38:982–983.

Berrigan, D., and E. L. Charnov.
1994. Reaction norms for age and size at maturity in response to temperature: a puzzle for life historians. Oikos 70:474–478.

Berumen, M. L., E. D. L. Trip, M. S. Pratchett, and J. H. Choat.
2012. Differences in demographic traits of four butterflyfish species between two reefs of the Great Barrier Reef separated by 1,200 km. Coral Reefs 31:169–177.

Binohlan, C., and R. Froese.
2009. Empirical equations for estimating maximum length from length at first maturity. J. Appl. Ichthyol. 25:611–613.

Blackburn, T. M., K. J. Gaston, and N. Loder.
1999. Geographic gradients in body size: a clarification of Bergmann's rule. Divers. Distrib. 5:165–174.

Burton, M. L.
2001. Age, growth, and mortality of gray snapper, *Lutjanus griseus*, from the east coast of Florida. Fish. Bull. 99:254–265.

Campana, S. E., M. C. Annand, and J. I. McMillan.
1995. Graphical and statistical methods for determining the consistency of age determinations. Trans. Am. Fish. Soc. 124:131–138.

Cappo, M., P. Eden, S. J. Newman, and S. Robertson.
2000. A new approach to tetracycline validation of the periodicity and timing of opaque zone formation in the otoliths of 11 species of *Lutjanus* from the central Great Barrier Reef. Fish. Bull. 98:474–488.

Cerrato, R. M.
1990. Interpretable statistical tests for growth comparisons using parameters in the von Bertalanffy equation. Can. J. Fish. Aquat. Sci. 47:1416–1426.

Choat, J. H., and D. R. Robertson.
2002. Age-based studies. *In* Coral reef fishes: dynamics and diversity in a complex ecosystem (P. F. Sale, ed.), p. 57–80. Academic Press, San Diego, CA.

Choat, J. H., D. R. Robertson, J. L. Ackerman, and J. M. Posada.
2003. An age-based demographic analysis of the Caribbean stoplight parrotfish *Sparisoma viride*. Mar. Ecol. Prog. Ser. 246:265–277.

Choat, J. H., J. P. Kritzer, and D. R. Robertson.
2009. Ageing in coral reef fishes: do we need to validate the periodicity of increment formation for every species of fish for which we collect age-based demographic data? *In* Tropical fish otoliths: information for assessment, management and ecology (B. S. Green, B. D. Mapstone, G. Carlos, and G. A. Begg, eds.), p. 23–45. Springer, New York.

Clark, T. D., M. R. Donaldson, S. Pieperhoff, S. M. Drenner, A. Lotto, S. J. Cooke, S. G. Hinch, D. A. Patterson, and A. P. Farrell.
2012. Physiological benefits of being small in a changing world: responses of coho salmon (*Oncorhynchus kisutch*) to an acute thermal challenge and a simulated capture event. PLoS ONE 7(6):e39079.

Conover, D. O., J. J. Brown, and A. Ehtisham.
1997. Countergradient variation in growth of young striped bass (*Morone saxatilis*) from different latitudes. Can. J. Fish. Aquat. Sci. 54:2401–2409.

Conover, D. O., T. A. Duffy, and L. A. Hice.
2009. The covariance between genetic and environmental influences across ecological gradients: reassessing the evolutionary significance of countergradient and cogradient variation. Ann. N.Y. Acad. Sci. 1168:100–129.

Druzhinin, A. D.
1970. The range and biology of snappers (Fam. Lutjanidae). J. Ichthyol. 10:717–736.

Druzhinin, A. D., and U. P. Hlaing.
1972. Observations on the trawl fishery of southern Burma. *In* Proc. Indo-Pac. Fish. Coun, Session 13, Sect. III Tech. Pap., Symposium on Demersal Fisheries; Brisbane, Australia, 14–25 October 1968, p. 151–209. IPFC (Indo-Pacific Fisheries Council) Secretariat, FAO Regional Office for Asia and the Far East, Bangkok, Thailand.

Fisher, J. A. D., K. T. Frank, and W. C. Leggett.
2010. Breaking Bergmann's rule: truncation of Northwest Atlantic marine fish body sizes. Ecology 91:2499–2505.

Froese, R.
2011. The science in FishBase. *In* Ecosystem approaches to fisheries: a global perspective (V. Christensen and J. Maclean, eds.), p. 47–54. Cambridge Univ. Press, Cambridge, UK.

Froese, R., and C. Binohlan.
2000. Empirical relationships to estimate asymptotic length, length at first maturity and length at maximum yield per recruit in fishes, with a simple method to evaluate length frequency data. J. Fish Biol. 56:758–773.

Fry, G. C., and D. A. Milton.
2009. Age, growth and mortality estimates for populations of red snappers *Lutjanus erythropterus* and *L. malabaricus* from northern Australia and eastern Indonesia. Fish. Sci. 75:1219–1229.

Haddon, M.
2001. Modelling and quantitative methods in fisheries, 424 p. Chapman and Hall/CRC Press, Boca Raton, FL.

Heupel, M. R., A. Penny, A. J. Williams, J. P. Kritzer, D. J. Welch, R. J. Marriott, C. R. Davies, and B. D. Mapstone.
2010. Demographic characteristics of exploited tropical lutjanids: a comparative analysis. Fish. Bull. 108:420–432.

Hoenig, J. M.
1983. Empirical use of longevity data to estimate mortality rates. Fish. Bull. 82: 898–902.

Khan, M. G.
1986. Age, growth and mortality rates of the red snapper (*Lutjanus johnii* Bloch) of the Bay of Bengal, Bangladesh. Bangladesh J. Agric. 11(2):49–61.

King, J. R., and G. A. McFarlane.
2003. Marine fish life history strategies: applications to fishery management. Fish. Manage. Ecol. 10:249–264.

Kiso, K., and M. I. Mahyam.
2003. Distribution and feeding habits of juvenile and young John's snapper *Lutjanus johnii* in the Matang mangrove estuary, west coast of Peninsular Malaysia. Fish. Sci. 69:563–568.

Marriott, R. J., and M. Cappo.
2000. Comparative precision and bias of five different ageing methods for the large tropical snapper *Lutjanus johnii*. Asian Fish. Sci. 13:149–160.

Marriott, R. J., and B. D. Mapstone.
2006. Geographic influences on and the accuracy and precision of age estimates for the red bass, *Lutjanus bohar* (Forsskal 1775): a large tropical reef fish. Fish. Res. 80:322–328.

Martinez-Andrade, F.
2003. A comparison of life histories and ecological aspects among snappers (Pisces: Lutjanidae). Ph.D. diss., 194 p. Louisiana State Univ., Baton Rouge, LA.

Newman, S., M. Cappo, and D. McB. Williams.
2000. Age, growth, mortality rates and corresponding yield estimates using otoliths of the tropical red snappers, *Lutjanus erythropterus, L. malabaricus* and *L. sebae*, from the central Great Barrier Reef. Fish. Res. 48:1–14.

Pauly, D., S. Samiblya Jr., and S. Opitz.
1993. Estimates of relative food consumption by fish and invertebrate populations, required for modelling the Bolinao Reef Ecosystem, Philippines. *In* Trophic models of aquatic ecosystems (V. Christensen and D. Pauly, eds.), p. 236–251. ICLARM Conference Proceedings 26, International Center for Living Aquatic Resources Management, Metro Manila, Philippines.

Pörtner, H. O.
2012. Integrating climate-related stressor effects on marine organisms: unifying principles linking molecule to ecosystem-level changes. Mar. Ecol. Prog. Ser. 470:273–290.

Pörtner, H. O., C. Bock, R. Knust, G. Lannig, M. Lucassen, F. C. Mark, and F. J. Sartoris.
2008. Cod and climate in a latitudinal cline: physiological analyses of climate effects in marine fishes. Clim. Res. 37:253–270.

Pörtner, H. O., and R. Knust.
2007. Climate change affects marine fishes through the oxygen limitation of thermal tolerance. Science 315:95–97.

Pörtner, H. O., and M. A. Peck.
2010. Climate change effects on fishes and fisheries: towards a cause-and-effect understanding. J. Fish Biol. 77:1745–1779.

Robertson, D. R., J. L. Ackerman, J. H. Choat, J. M. Posada, and J. Pitt.
2005a. Ocean surgeonfish *Acanthurus bahianus*. I. The geography of demography. Mar. Ecol. Prog. Ser. 295:229–244.

Robertson, D. R., J. H. Choat, J. M. Posada, J. Pitt, and J. L. Ackerman.
2005b. Ocean surgeonfish *Acanthurus bahianus*. II. Fishing effects on longevity, size and abundance? Mar. Ecol. Prog. Ser. 295:245–256.

Roff, D. A.
1983. An allocation model of growth and reproduction in fish. Can. J. Fish. Aquat. Sci. 40:1395–1404.

Saari, C. R.
2011. Comparison of the age and growth of red snapper (*Lutjanus campechanus*) amongst habitats and regions in the Gulf of Mexico. M.S. diss., 134 p. Louisiana State Univ., Baton Rouge, LA.

Tanaka, K., Y. Hanamura, V. C. Chong, S. Watanabe, A. Man, F. M. Kassim, M. Kodama, and T. Ichikawa.
2011. Stable isotope analysis reveals ontogenetic migration and the importance of a large mangrove estuary as a feeding ground for juvenile John's snapper *Lutjanus johnii*. Fish. Sci. 77:809–816.

Travers, M. J., I. C. Potter, K. R. Clarke, S. J. Newman, and J. B. Hutchins.
2009. The inshore fish faunas over soft substrates and reefs on the tropical west coast of Australia differ and change with latitude and bioregion. J. Biogeogr. 37:148–169.

Trip, E. L., J. H. Choat, , D. T. Wilson, and D. R. Robertson.
2008. Inter-oceanic analysis of demographic variation in a widely distributed Indo-Pacific coral reef fish. Mar. Ecol. Prog. Ser. 373:97–109.

Abstract—The influences of age, size, and condition of spawning females on fecundity and oocyte quality were analyzed for the Patagonian stock of Argentine Hake (*Merluccius hubbsi*). Samples of mature females were collected in the spawning area as part of 2 research surveys conducted in January 2010 and 2011, during the peak of the reproductive season. Batch fecundity (BF) ranged between 40,500 (29 cm total length [TL]) and 2,550,000 (95 cm TL) hydrated oocytes, and was positively correlated with TL, gutted weight, age, hepatosomatic index (HSI), and the relative condition factor (Kn). Relative fecundity ranged between 85 and 1040 hydrated oocytes g^{-1} and showed significant positive relationships with gutted weight, HSI, and Kn; however, coefficients of determination were low for all regressions. Dry weights of samples of 100 hydrated oocytes ranged between 1.8 and 3.95 mg and were positively correlated with all variables analyzed, including batch and relative fecundity. Multiple regression models created with data of the morphophysiological characteristics of females supported maternal influences on fecundity and egg weights. Within the studied size range (29–95 cm TL), larger individuals had better somatic and egg condition, mainly revealed by higher HSI and hydrated oocytes with larger oil droplets (275.71µm [standard error 1.49]). These results were associated with the higher feeding activity of larger females during the spawning season in comparison with the feeding activity of young individuals (<5 years old); the better nutritional state of larger females, assumed to result from more feeding, was conducive to greater production of high-quality eggs.

Manuscript submitted 11 January 2013.
Manuscript accepted 7 August 2013.
Fish. Bull. 111:325–336.
doi: 10.7755/FB.111.4.3

The views and opinions expressed or implied in this article are those of the author (or authors) and do not necesarily reflect the position of the National Marine Fisheries Service, NOAA.

Maternal effects on fecundity and egg quality of the Patagonian stock of Argentine Hake (*Merluccius hubbsi*)

Gustavo J. Macchi (contact author)[1, 2]
Ezequiel Leonarduzzi[2]
Marina V. Diaz[2]
Marta Renzi[2]
Karina Rodrigues[1, 2]

Email address for contact author: gmacchi@inidep.edu.ar

[1] Consejo Nacional de Investigaciones Científicas y Técnicas (CONICET)
Av. Rivadavia 1917
C1033AAJ Buenos Aires, Argentina

[2] Instituto Nacional de Investigación y Desarrollo Pesquero (INIDEP)
Paseo Victoria Ocampo Nro. 1
B7602HSA Mar del Plata, Argentina

The Argentine Hake (*Merluccius hubbsi*), with a biomass of around 700,000 metric tons (t) estimated from virtual population analysis in 2009, is one of the most important fish resources for the Argentine fleet (Irusta and Datri[1]; Villarino and Santos[2]). Two main stocks have been identified in the Argentine Sea: the northern group (between 34° and 41°S) and the southern group (between 41° and 55°S). The latter group, known also as the Patagonian stock, is the most abundant population of this species, accounting for about 85% of the total biomass estimated for this fish resource in Argentina (Aubone et al., 2000). This fishery historically has registered the most important commercial landings for Argentina, with annual catches between 170,000 and 370,000 t since 2000 (Sánchez et al., 2012). Nevertheless, during the 1990s, both stocks of Argentine Hake suffered overexploitation and their spawning biomass decreased drastically, and changes also were observed in the parent-stock structure (Aubone et al., 2000).

It has been shown that the reproductive potential of a fish stock is strongly influenced by the size and age of spawning females. During the reproductive season, older and larger individuals produce more oocytes than younger and smaller spawners because fecundity and spawning frequency are higher in larger females and, in general, their reproductive period is longer than the period of smaller spawners (Marshall et al., 1998; Marteinsdottir and Thorarinsson, 1998; Marteinsdottir and Begg, 2002; Macchi et al, 2004; Mehault et al., 2010). Therefore, variation in length composition of a fish stock caused by fishing activity or by other sources of mortality would affect the number of eggs spawned at

[1] Irusta, C. G., and L. D'Atri. 2010. Evaluación del estado del efectivo norte de 41° S de la merluza (*Merluccius hubbsi*) y estimación de la Captura Biológicamente Aceptable para el año 2011. INIDEP Informe Técnico Oficial No. 42, 28 p. [Available from INIDEP, Paseo Victoria Ocampo Nro. 1, B7602HSA Mar del Plata, Argentina.

[2] Villarino, M. F., and B. Santos. 2010. Evaluación del estado de explotación del efectivo sur de 41° S de la merluza (*Merluccius hubbsi*) y estimación de las capturas biológicamente aceptables correspondiente al año 2011. INIDEP Informe Técnico Oficial No. 43, 27 p. [Available from INIDEP, Paseo Victoria Ocampo Nro. 1, B7602HSA Mar del Plata, Argentina.]

a population level. In this sense, fecundity estimates by length class give information on the number of potential offspring that can be produced. Nevertheless, viability during the early life stages depends mainly on egg quality, which is associated with the quantity of nutrients stored in the oocytes (Brooks et al., 1997). Bromage et al. (1994) defined egg quality as "those characteristics of the egg that determine its capacity to survive." There are different methods and indices that can be used to estimate the quality of fish eggs. Some of them are very simple, such as those techniques where morphometrical attributes (e.g., egg diameter or weight and size of the oil droplet) are used, and others are more complex, such as those where the biochemical composition (e.g., lipid or protein concentration) of the oocytes are used (Nocillado et al., 2000).

Most studies have concluded that larger eggs are of better quality because they can produce larger larvae with higher survival rates (Hinckley, 1990; Rijnsdorp and Vingerhoed, 1994; Nissling et al., 1998; Trippel, 1998). It is a general assumption that larger larvae may have advantages in finding food and in actively swimming through the water column that increase their probability of survival (Brooks et al., 1997; Álvarez Colombo et al., 2011). In contrast, in some studies, no relationship between egg diameter and larval size was observed (Landaeta and Castro, 2012), or it was suggested that larger offspring could be more easily detected by predators, and, therefore, large larval size would increase the risk of mortality (Kjesbu et al., 1996). However, in general, it is assumed that increased egg size leads to higher larval survival.

Fish condition can be assessed through the use of different indices, on the basis of length:body-weight ratio (K) or liver-weight:body-weight ratio (hepatosomatic index [HSI]) or on the basis of the biochemical composition (e.g., lipids, proteins, or glycogen) of different tissues (Dominguez-Petit et al., 2010). It was observed that lipids play an important role as stored energy that can affect fecundity, oocyte quality, and larval viability (Wiegand, 1996; Lambert et al., 2003; Aristizabal, 2007). Therefore, because the liver is generally the organ with the highest levels of lipid storage for gadoids, the HSI may be considered a good descriptor of female condition, and a strong influence on reproduction (Marshall et al., 1999; Marteinsdottir and Begg, 2002; Alonso-Fernández, 2011).

Spawning of the Patagonian stock of the Argentine Hake occurs in waters off the province of Chubut in southern Argentina during spring and summer, and a main peak occurs between December and January (Macchi et al., 2007). This species is a batch spawner with indeterminate annual fecundity, meaning that unyolked oocytes continuously mature and are spawned throughout the reproductive season (Macchi et al., 2004). It has been reported that the size and age compositions of Argentine Hake females in Patagonian waters change during the spawning season, affecting egg production of this stock during this period (Macchi et al., 2004). Moreover, Macchi et al. (2006) found positive relationships between oocyte dry weight (DW) and maternal variables, such as total length (TL) and age, relationships that could indicate a possible effect of female size on egg quality.

Although different aspects of reproductive biology of Argentine Hake have been studied in recent years (Macchi et al., 2004, 2005, 2006, 2007), information about the nutritional condition of spawning females in relation to reproductive potential is scarce. This information is essential for understanding the strategy of energy allocation during reproduction and for estimating whether variations in size composition and feeding condition of spawning females could affect egg quality and, therefore, larval survival. Such information could improve the understanding of the recruitment variations that have been observed in the Argentine Hake fishing stocks.

The objective of this study was to determine which maternal features—length, weight, age, HSI, and condition—were correlated with which measures of egg quality and quantity—DW, oil globule size, and fecundity—in Argentine Hake from Patagonian waters. We also examined stomach fullness as a function of fish length to establish the relationship between feeding activity and the size of spawning females.

Materials and methods

Sample collection

Samples of Argentine Hake were obtained from bottom trawls during 2 research surveys carried out in the north Patagonian area during January 2010 and 2011 by the Instituto Nacional de Investigación y Desarrollo Pesquero (INIDEP) (Fig. 1). Argentine Hake specimens were captured at depths between 50 and 110 m through employment of a bottom trawl with a mouth width of about 20 m, a height of about 4 m, and with a 20-mm mesh size at the inner lining of the codend.

For histological analysis of ovaries, 192 mature females near spawning condition (with hydrated oocytes after germinal vesicle breakdown) were sampled; ovaries were removed and preserved (fixed) in 10% neutrally buffered formalin. From each specimen, the following measurements were recorded: TL in centimeters and total weight (TW), gutted weight (GW), and liver weight (LW) in grams. In addition, the sagittae otoliths were collected for age determination. Ages were obtained through the use of the methods of Renzi and Pérez (1992).

Female condition and fecundity estimation

Because fish weight may be greatly influenced by the stomach content and fullness of the gut, GW was used to estimate the condition of Argentine Hake females.

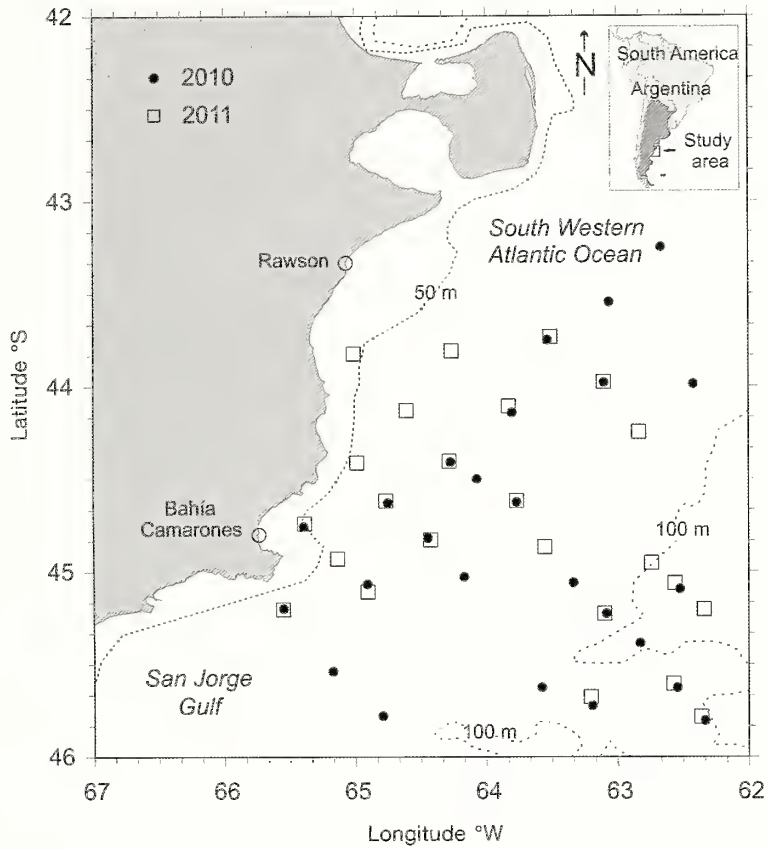

Figure 1

Map of locations where samples of Argentine Hake (*Merluccius hubbsi*) were collected during the peak spawning season (January) of 2010 (black dots) and 2011 (squares) in waters off the province of Chubut in Argentina to examine maternal effects on the fecundity and egg quality.

Nutritional status was determined by means of 2 indices:

1) the relative condition factor (Kn), expressed as a proportion between the observed GW and the GW determined by the relationship of TL versus GW, described by the following equation:

$$GW = 0.0148 \times TL^{2.7634} \quad (1)$$

(coefficient of determination [r^2]=0.98, n=181, P<0.01)

2) the HSI, which provides an indication of the status of energy reserves in the liver, defined by the following equation:

$$HSI = (LW / GW) * 100. \quad (2)$$

Ovaries collected were weighed to the nearest 0.1 g after fixation, and a portion of each sample (about 2.0 g) was removed from each gonad, dehydrated in ethanol, cleared in xylol, and embedded in paraffin. Sections of ovaries that were 5 µm thick were mounted and stained with Harris's hematoxylin followed by eosin counterstain. Histological diagnosis was used to discard ovaries with evidence of recent spawning.

Batch fecundity (BF), or the number of oocytes released per spawning, and relative fecundity (RF), or the number of hydrated oocytes per gram of body weight, were estimated with the hydrated oocyte method on fixed ovarian samples (Hunter et al., 1985). Only ovaries without evidence of recent spawning (no postovulatory follicles) were selected (102 ovaries from samples collected in 2010 and 79 ovaries from samples collected in 2011). Three pieces of ovary, approximately 0.1–0.2 g each, were removed from the anterior, middle, and posterior parts of one gonad and weighed to the nearest 0.1 mg, and hydrated oocytes were counted. Batch fecundity for each female was the product of the mean number of hydrated oocytes per unit of weight and the total weight of the ovaries. Relative fecundity was determined as the batch fecundity divided by female weight (without ovary).

The relationships of BF to TL obtained in 2010 and 2011 were compared on the basis of overlapping length ranges of the females (32–83 cm TL) with analysis of covariance on the log-transformed data (Draper and Smith, 1981). After comparison, the relationships of BF and RF to TL, gutted weight, age, HSI, and Kn obtained from samples and data collected in both years were described through the use of simple regression analysis.

Egg quality

A sample of 100 hydrated oocytes was removed from one ovary of each female selected for estimation of fecundity, rinsed in distilled water to remove formaldehyde remnants, dried for 24 h at 60°C, and weighed to the nearest 0.1 mg. The DW of each of these samples was considered an index of egg quality for the spawning females of Argentine Hake collected during the 2 research cruises because, in general, dry mass is associated with the quantity of yolk reserves stored in oocytes (Macchi et al., 2006; Mehault et al., 2010). The relationships between DW and the different morphophysiological variables (TL, GW, age, HSI, and Kn), on the basis of length, weight, or organ-body weight ratios, were evaluated with simple regression analysis as were the fecundity data. Moreover, the relationships between DW and the number of oocytes spawned by batch (BF) and by unit of female weight (RF) were analyzed.

To determine the effect of each maternal attribute on fecundity and egg quality and to establish which of these predictor variables had more influence on the number and quality of the oocytes, multiple regression analyses of BF and DW in relation to morphophysiological variables were carried out with the forward stepwise method. In the case of the regression model for BF, the data showed heteroscedasticity and were log-transformed. Colinearity between variables was analyzed to include in the model only those variables that were uncorrelated. All statistical analyses were conducted with R software (R Development Core Team, 2010).

Another variable possibly associated with egg quality is the size of the oil droplet in mature eggs, because it functions as an energy source for larvae (Wiegand, 1996; Nocillado et al., 2000; Rodgveller et al., 2012). For this reason, the diameters of oil droplets in hydrated oocytes were measured in samples of Argentine Hake females collected in January 2011. Samples collected in 2010 were not used, because hydrated oocytes from this year were in bad condition as a consequence of long-term preservation in formalin solution. To analyze possible differences between old and young females, 2 length groups were considered for this analysis: individuals <40 cm TL (n=12) and >70 cm TL (n=17). Most adult female Argentine Hake <40 cm TL are 2–3 years old and considered first-time spawners for the Patagonian stock of this species (Otero et al., 1986). First-time spawners are thought to produce eggs of lower quality than the eggs of older females, as Trippel (1998) found for Atlantic Cod (*Gadus morhua*). Hydrated oocytes from each of the 2 length groups of females (n=641 and 1000 oocytes) were sampled and the diameters of the oil droplets were measured to the nearest 0.01 µm with a Carl Zeiss[3] stereomicroscope equipped with AxioVision 4.6 software (Carl Zeiss Microscopy, Jena, Germany). The mean diameters obtained for each size group were compared with a t-test.

Because the size of hydrated oocytes in the ovaries may be influenced by the degree of hydration, we used spawned eggs to analyze the relationship between egg diameter and size of the oil droplet. Therefore, egg diameters and sizes of oil droplets were measured from Argentine Hake eggs collected in plankton samples, from oblique tows conducted with a bongo net (mesh sizes: 300 and 500 µm) in the research survey of January 2010. Samples were fixed in 5% formalin, and later Argentine Hake eggs in early developmental stages were sorted and rinsed in distilled water. Argentine Hake eggs were identified according to Ehrlich (1998). Egg diameter and size of the oil droplet (n=102) were measured to the nearest 0.01 µm, as was done for hydrated oocytes, and the relationship between them was evaluated with simple regression analysis.

Feeding activity during spawning

Stomach fullness of Argentine Hake females during spawning was analyzed to find a possible relationship between feeding activity and the size of spawners. Information on stomach content obtained from all adult females sampled in the reproductive area during the 2 research cruises in January 2010 and 2011 (n=2091) was considered in this study. Individuals with everted stomachs as a consequence of pressure changes during capture were not used in this analysis. A gross scale of 4 stages was employed to classify the degree of stomach fullness: 0=empty, 1=few contents (<25% full), 2=moderate contents (25–75% full) and 3=full stomach (Prenski and Angelescu[4]). The frequency distribution of each stomach stage by length class was considered in this analysis, but only stage 0 was employed to determine differences in feeding activity. The relationship between the proportion of empty stomachs and female size was described with simple regression analysis.

---

[3] Mention of trade names or commercial companies is for identification purposes only and does not imply endorsement by the National Marine Fisheries Service, NOAA.

[4] Prenski, L. B., and V. Angelescu. 1993. Ecología trófica de la merluza común (*Merluccius hubbsi*) del Mar Argentino. Parte 3. Consumo anual de alimento a nivel poblacional y su relación con la explotación de las pesquerías multiespecíficas. INIDEP Documento Científico No. 1, 118 p. [Available from INIDEP, Paseo Victoria Ocampo Nro. 1, B7602HSA Mar del Plata, Argentina.]

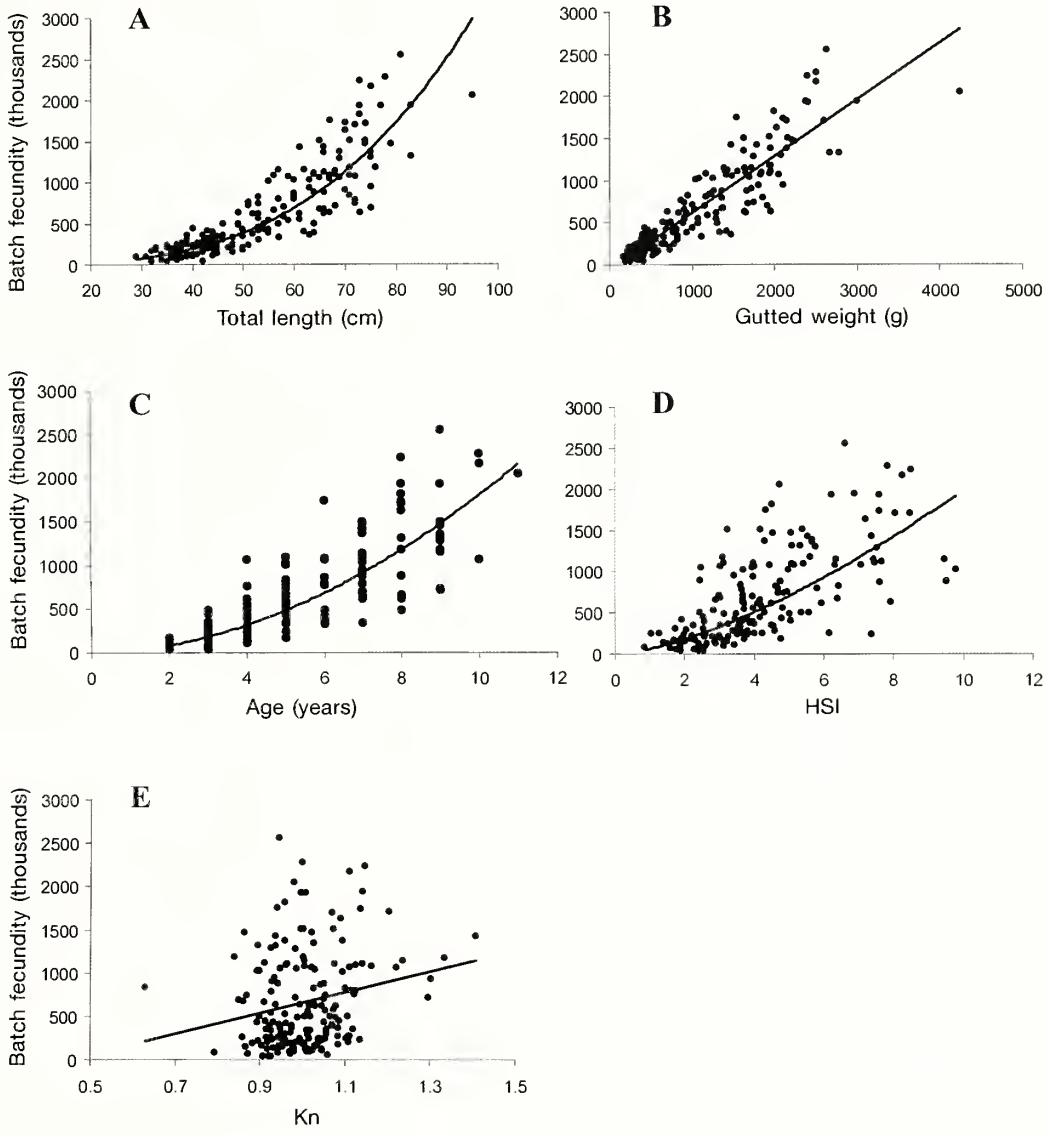

Figure 2

Batch fecundity as a function of (**A**) total length, (**B**) gutted weight, (**C**) age, (**D**) hepatosomatic index (HSI), and (**E**) relative condition factor (Kn) for the Patagonian stock of Argentine Hake (*Merluccius hubbsi*), which was sampled in waters off the province of Chubut in Argentina during the peak spawning season in 2010 and 2011.

Results

Female condition and fecundity estimation

Batch fecundity estimates obtained for Argentine Hake females collected during January 2010 and 2011 ranged between 40,500 hydrated oocytes (29 cm TL) and 2,550,000 hydrated oocytes (95 cm TL). The analysis of covariance applied to compare the coefficients of the relationship of BF to TL obtained for each year did not show statistical differences ($P>0.01$); therefore, data from 2010 and 2011 were pooled to estimate all the regression analyses. The relationship between BF and TL was curvilinear, fitting better to a power model (Fig. 2A, Table 1). The relationship of BF to GW was linear, and, in the case of BF to age, a power model was fitted (Figs. 2B and C, Table 1).

A positive power relationship was observed between BF and the HSI (Fig. 2D, Table 1). In the case of BF and Kn, the relationship was linear and significant ($P<0.01$), but a low r^2 was obtained (Fig. 2E, Table 1).

Table 1

Results of the regression analyses between batch fecundity (BF), relative fecundity (RF), and oocyte dry weight (DW) and the variables of total length (TL), gutted weight (GW), age (A), hepatosomatic index (HSI), and relative condition index (Kn) for female Argentine Hake (*Merluccius hubbsi*) of the Patagonian stock obtained from bottom trawls during research surveys in January 2010 and 2011. r^2=coefficient of determination; a and b=parameters of the equation, n=sample size, P=P-value of the relationship. The sample size for regressions with age (n=173) was smaller than the sample size for regressions with other variables (n=181) because some otoliths were broken or otherwise unusable for age determination.

		Relationship	r^2	a	b	n	P
BF	TL	Power	0.75	10.07	2.74	181	<0.01
	GW	Linear	0.81	−64235.60	675.48	181	<0.01
	A	Power	0.68	38103.41	1.67	173	<0.01
	HSI	Power	0.47	126319.30	1.17	181	<0.01
	Kn	Linear	0.04	−528543.19	1183337.78	181	<0.01
RF	TL	Linear	0.03	396.99	2.37	181	>0.01
	GW	Linear	0.04	471.76	0.05	181	<0.01
	A	Linear	0.03	448.49	15.12	173	>0.01
	HSI	Linear	0.11	388.49	33.56	181	<0.01
	Kn	Linear	0.07	21.68	500.84	181	<0.01
DW	TL	Logarithmic	0.18	2.62	0.0001	181	<0.01
	GW	Logarithmic	0.17	1.48	0.20	181	<0.01
	A	Logarithmic	0.14	2.31	0.34	173	<0.01
	HSI	Linear	0.18	2.49	0.08	181	<0.01
	Kn	Linear	0.05	2.01	0.82	181	<0.01

Relative fecundity ranged from 85 to 1040 hydrated oocytes g^{-1}(female weighed without ovaries), with a mean value of 526 hydrated oocytes g^{-1} (standard error [SE] 183). Positive linear significant relationships (P<0.01) between RF and the morphophysiological variables of GW, HSI, and Kn were observed, but r^2 values were low for all variables, explaining in some cases 3% or 4% of the variance (Fig. 3, Table 1). The strongest correlation, with an r^2 of 0.11, was obtained with the relationship of RF to the HSI (Table 1).

In the multiple regression analysis of the influence of maternal characteristics on BF, 87% of the variability in BF was explained by GW, DW, and the HSI, and described by the following equation:

$$BF = 5.08 + 0.96\mathrm{Ln}GW + 1.08\mathrm{Ln}DW + 0.27\mathrm{Ln}HSI \quad (3)$$

(r^2=0.87, n=178, [P<0.01])

Most of this variability was explained exclusively by GW (95%). The forward stepwise method gave evidence that inclusion of other variables did not improve BF predictions significantly.

Egg quality

For 100 hydrated oocytes, DW estimated from Argentine Hake females collected during the spawning peak in January 2010 and 2011 ranged from 1.8 to 3.95 mg, and had a mean value of 2.83 mg (SE 0.36). There were significant positive relationships between DW and all morphophysiological variables considered during this study: TL, GW, age, HSI, and Kn (Fig. 4, Table 1). Moreover, positive significant relationships (P<0.01) also were obtained between DW and fecundity (BF and RF), described by the following equations:

$$DW = 2.62 + 0.0003BF. \quad (4)$$

(r^2=0.25, n=181)

$$DW = 2.42 + 0.0008RF. \quad (5)$$

(r^2=0.16, n=181)

In general, r^2 values were low for all relationships estimated and BF was the variable best correlated with DW, although it is possible that size may have some influence on this relationship. Regardless, RF, which was uncorrelated with TL, also showed a significant positive relationship to DW.

In the multiple regression analysis carried out with DW as the dependent variable and morphophysiological variables, only the HSI and GW were included because the other variables did not improve DW predictions significantly. This model explained 20% of the total variability, and 90% of this percentage was contributed by the HSI:

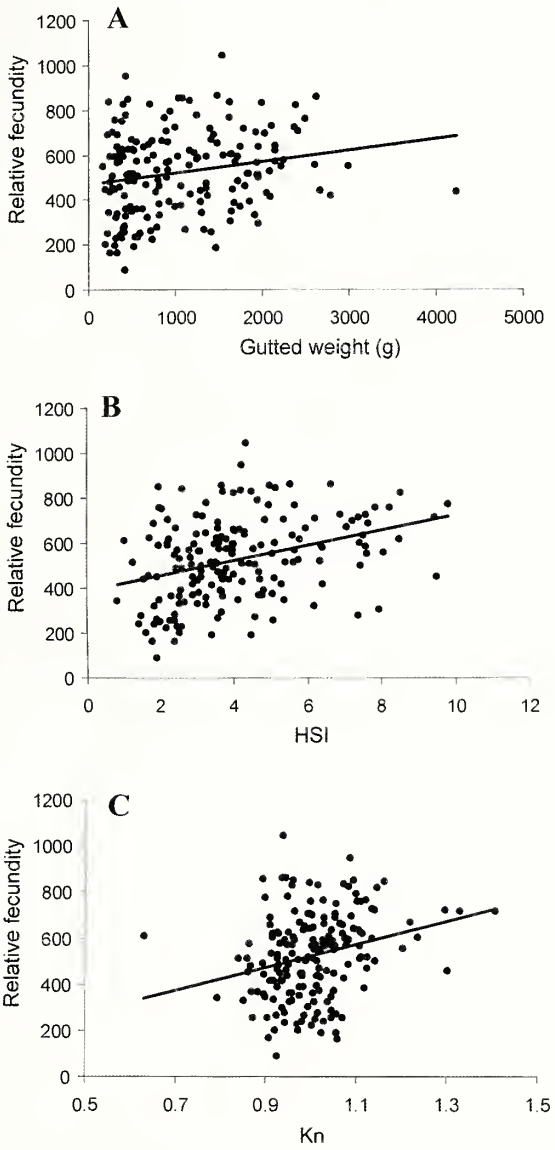

Figure 3

Relative fecundity as a function of (**A**) gutted weight, (**B**) hepatosomatic index (HSI), and (**C**) relative condition factor (Kn) for the Patagonian stock of Argentine Hake (*Merluccius hubbsi*), which was sampled in waters off the province of Chubut in Argentina during the peak spawning season in 2010 and 2011.

$$DW = 2.49 + 0.061HSI + 0.00009GW. \quad (6)$$

(r^2=0.20, n=178, [P<0.03])

The mean diameters of the oil droplets in hydrated oocytes that were estimated for young (<40 cm TL) and old (>70 cm TL) Argentine Hake females were 265.82 µm (SE 20.33) and 275.71 µm (SE 1.49), respectively. Comparison of this variable between both length groups showed highly significant differences (P<0.001), indicating more lipid accumulated in eggs from larger females than in eggs from first-time spawners.

The regression analysis between the sizes of the oil droplets (OD) and egg diameters (ED) of Argentine Hake eggs collected during plankton sampling showed a significant positive relationship (P<0.01), described by the following equation:

$$OD = 0.4168ED - 146.46. \quad (7)$$

(r^2=0.34, n=102)

This result corroborates the notion that larger eggs of Argentine Hake have more lipid reserves for larval growth and, therefore, have a higher probability that they will produce larger larvae.

Feeding activity during spawning

The regression analysis between the proportion of empty stomachs (PE) and TL for data obtained in January 2010 and 2011 showed a significant negative logarithmic relationship (P<0.01), indicating that intensity of feeding during spawning increases with female size. This tendency was more evident in Argentine Hake females <55 cm TL because individuals of this species in larger length classes showed high variability in feeding activity (Fig. 5). This relationship was described by the following equation:

$$PE = 1.6824 - 0.2937\mathrm{Ln}TL. \quad (8)$$

(r^2=0.39, n=45)

Discussion

Batch fecundity values for the Patagonian stock of Argentine Hake, estimated with samples collected in January 2010 and 2011, did not differ statistically and showed a positive relationship with size, weight, and age of the spawning females. The range of fecundity data (40,500–2,550,000 hydrated oocytes) was similar to estimated values from previous studies of Argentine Hake during the same month in other years (Macchi et al., 2004), but the range was much higher than values obtained for other species of *Merluccius*: Peruvian Hake (*M. gayi peruanus*) (see Canal, 1989), New Zealand Hake (*M. australis*) (see Balbontín and Bravo, 1993), European Hake (*M. merluccius*) (see Murua et al., 2006; Recasens et al., 2008; El Habouz et al., 2011), Cape Hake (*M. capensis*), and Deepwater Hake (*M. paradoxus*) (see Osborne et al., 1999). Batch fecundity was influenced also by female condition, expressed mainly by liver weight, as was evident from the positive relationship between the number of eggs produced by batch and the HSI. In addition, relative fecundity, a variable that did not show a significant relationship with female size in Argentine Hake (Macchi et al., 2004), also was influenced positively by the HSI.

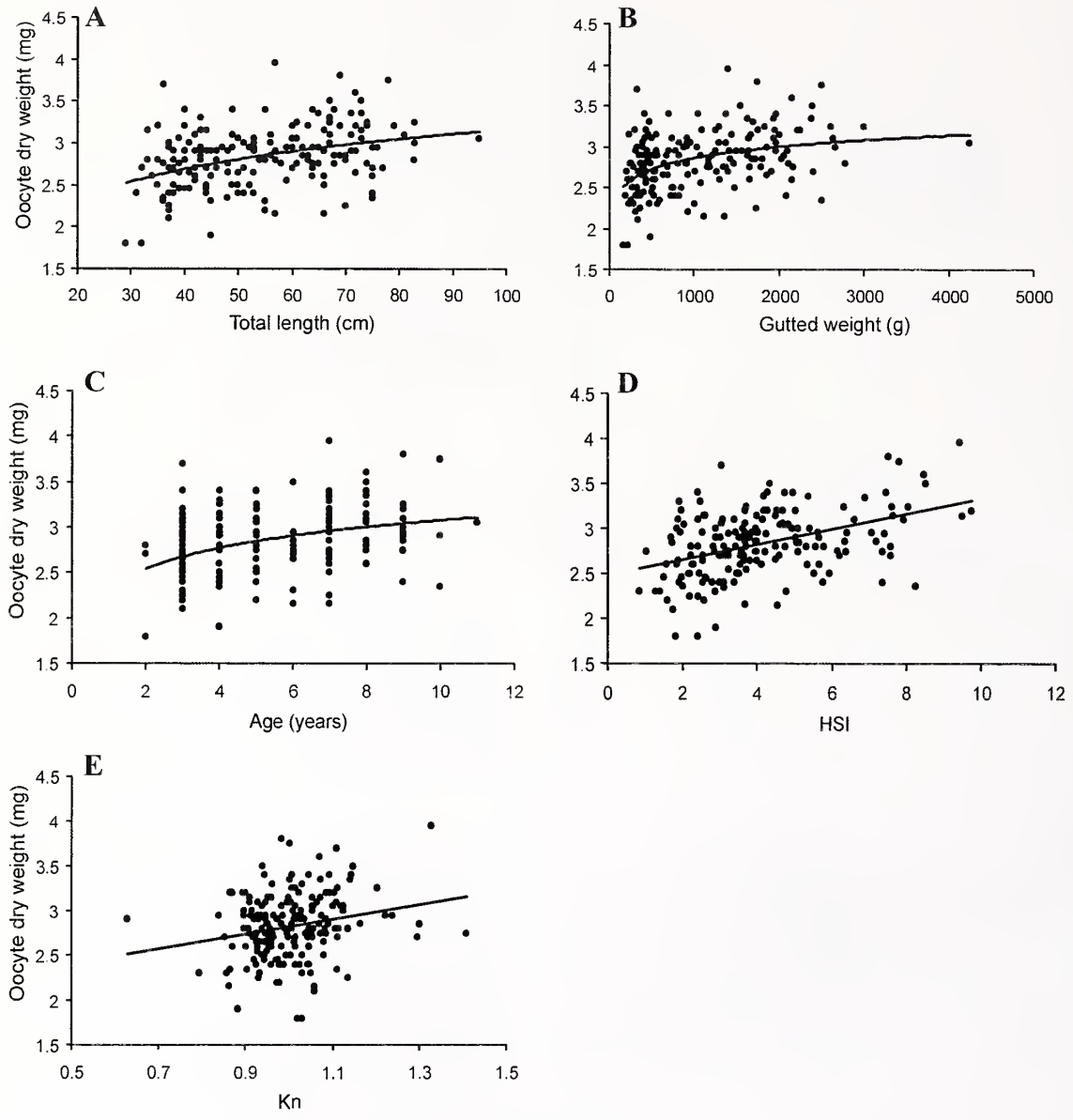

Figure 4

Dry weight of 100 hydrated oocytes as a function of (**A**) total length, (**B**) gutted weight, (**C**) age, (**D**) hepatosomatic index (HSI), and (**E**) relative condition factor (Kn) for the Patagonian stock of Argentine Hake (*Merluccius hubbsi*), which was sampled in waters off the province of Chubut in Argentina during the peak spawning season in 2010 and 2011.

The hepatosomatic index was the maternal condition measure that best correlated with fecundity in Argentine Hake in this study. Different authors have reported that the liver is the main deposit of lipids for gadoids and have considered this organ as the main source of energy for reproduction (Lambert and Dutil, 1997; Alonso-Fernández, 2011). In addition, certain egg constituents, such as yolk proteins and egg coat substances, are synthesized in the liver (Brooks et al., 1997). It has been suggested that lipids play a key role during the early life history of many species (Nocillado et al., 2000), serving as structural components of membranes and providing physical protection of organs, buoyancy, or nutrients for embryos (Wiegand, 1996). Lipids of oocytes are stored mainly as lipoproteins, which are the major components of oocyte yolk, or as oil droplets (Wiegand, 1996). In Atlantic Cod, it has been suggested that the HSI is a good index of repro-

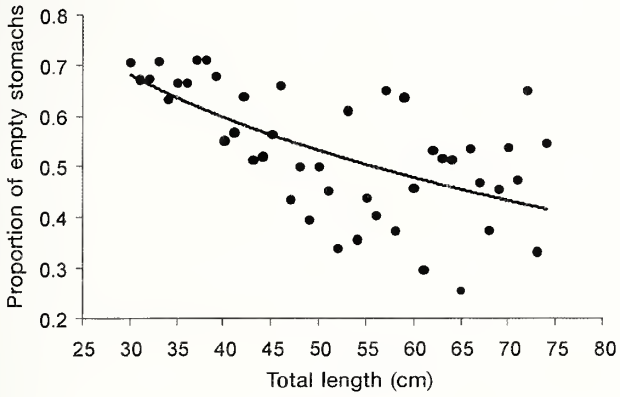

Figure 5

Relationship between proportion of females with empty stomachs and female size obtained for the Patagonian stock of Argentine Hake (*Merluccius hubbsi*), which was sampled in waters off the province of Chubut in Argentina during the peak spawning season in January 2010 and 2011.

ductive potential because of the role that lipids serve in reserving energy (Marshall et al., 1999). Supporting this idea, Leonarduzzi et al. (2012) analyzed the proximal composition of different tissues in Argentine Hake females and showed that the best morphological index for the somatic condition in Argentine Hake is the HSI—a finding that agrees with results obtained for other fish species (Alonso-Fernández, 2011). Therefore, it is reasonable to assume that reproductive potential of Argentine Hake may be affected by the liver condition of spawning females.

Positive relationships between DW and the variables of TL, GW, and age were observed for Argentine Hake—results that coincide with previous studies of this species (Macchi et al., 2006), and for European Hake (Mehault et al., 2010). Moreover, the positive relationship between DW and fecundity indicates that larger females of Argentine Hake invest energy in both the quantity and quality of the oocytes that they produce. The increases observed in oocyte mass with female size for Argentine Hake agrees with the hypothesis of a maternal effect on the spawning quality of this species. Argentine Hake also showed a positive relationship between DW and female condition, expressed by the HSI. This result supports the idea that the size and composition of oocytes depend on the maternal nutritional state and are particularly associated with liver weight (Marteinsdottir and Begg, 2002).

The difference observed between the size of the oil droplets in hydrated oocytes of first-time spawners (<40 cm TL) and old females (>70 cm TL) also reflected the maternal contribution to reproductive success. Oocytes of old individuals were characterized by oil globules that were larger than the oil globules of young spawners, indicating that more lipids were stored in the eggs of larger females. In other fish species that have been studied (e.g., *Sebastes* spp.), older females produced eggs with larger oil globules, which result in larvae with better chance of survival (Berkeley et al., 2004; Sogard et al., 2008). Similar conclusions indicating that fatty acids are essential for egg composition and reproductive success were drawn with species maintained in captivity and fed with different concentrations of lipids (Watanabe et al., 1984; Fernández-Palacios et al., 1995; Sewall and Rodgveller, 2009). Furthermore, the positive relationship observed in Argentine Hake in this study between the sizes of eggs from plankton samples and diameters of their oil droplets indicates that larger eggs contain a higher amount of lipids than do smaller eggs, supporting the idea that bigger oocytes are of better quality.

The decrease in frequency of empty stomachs with the size of the Argentine Hake females is evidence that feeding activity is higher in larger individuals. In addition, this result supports the hypothesis of continuous feeding during breeding season for other hake species (Dominguez-Petit and Saborido-Rey, 2010). The relationship between the percentage of individuals with empty stomachs and TL was more evident in females <55 cm TL; at this size range, the slope of the equation was more pronounced. This break in the regression model is similar to the break previously found for the relationship of oocyte weight to female size in Argentine Hake (Macchi et al., 2006). Those authors reported that differences between egg mass and female size can be observed mainly in young spawners (<55 cm TL) because, in females >55 cm TL, the slope of the model decreased, as a consequence of the high variability in oocyte weight.

Female condition and the quality of eggs produced by Argentine Hake may be associated with the feeding range of this species. It is possible that larger individuals would be capable of swimming longer distances as they search for food in deeper waters, where it is common to find great concentrations of squid (*Illex argentinus*) in the austral summer. This squid species is considered the most important prey for larger individuals of Argentine Hake in the Patagonian area (Angelescu and Prenski, 1987). A recent study described an offshore spawning group of Argentine Hake in Patagonian waters in January that was characterized by a high proportion of females >55 cm TL and older than 5 years (Macchi et al., 2010). The selection of squid for food by larger females may be advantageous for spawning, if the high concentration of fatty acids detected in this mollusk is taken into account (Watanabe et al., 1984). Therefore, studies on Argentine Hake diet and the effect of diet composition on egg quality are needed. In particular, further information is required about lipid, fatty acids, proteins, and ascorbic acid content, all rel-

evant components that affect egg and embryo survival (Brooks et al., 1997; Sewall and Rodgveller, 2009).

Conclusions

This study provides further evidence of maternal influence on the reproductive potential and spawning quality of the Patagonian stock of Argentine Hake. Within the analyzed size range (29–95 cm TL), larger females were characterized not only by higher fecundities but also by heavier eggs with larger oil droplets. Larger individuals were in better condition than smaller ones, as shown by higher HSI values, supporting the assumption that this index is a good predictor of reproductive potential. Moreover, feeding activity during the spawning peak in January was higher for larger females than for smaller and younger individuals, indicating that Argentine Hake may incorporate energy during the reproductive season. This strategy of energy allocation is typical of an income breeder and is similar to the strategy suggested for the European Hake by Dominguez-Petit and Saborido-Rey (2010). However, because Argentine Hake may be an opportunistic feeder during reproduction, it may be advantageous for spawning females to feed on higher quality food, such as squid, found offshore. This benefit may be restricted to larger individuals because they are more likely than smaller females to have the ability to find food offshore.

Acknowledgments

We wish to thank M. Estrada and H. Brachetta for preparation of the histological sections. Special thanks to M. Iorio and C. Dato for their help during sample collection and the technical staff of the Hake Assessment Group of the INIDEP for age determination. We also would like to thank the anonymous reviewers for making suggestions to improve this manuscript. This work was supported by the INIDEP and the CONICET (PIP 112 200801 00815). This is INIDEP contribution no. 1822.

Literature cited

Alonso-Fernández, A.
2011. Bioenergetics approach to fish reproductive potential: case of *Trisopterus luscus* (Teleostei) on the Galician Shelf (NW Iberian Peninsula). Ph.D. diss., 266 p. Univ. Vigo, Vigo, Spain.

Álvarez-Colombo, G., C. Dato, G. J. Macchi, E. Palma, L. Machinandiarena, H. E. Christiansen, P. Betti, P. Martos, F. Castro-Machado, D. Brown, M. Ehrlich, H. Mianzan, and M. Acha.
2011. Distribution and behavior of Argentine hake larvae: evidences of a biophysical mechanism for self-recruitment at the North Patagonian shelf waters. Cienc. Mar 37:633–657.

Angelescu, V., and L. B. Prenski.
1987. Ecología trófica de la merluza común del mar argentino (Merluccidae, *Merluccius hubbsi*). Parte 2. Dinámica de la alimentación analizada sobre la base de las condiciones ambientales, la estructura y las evaluaciones de los efectivos en su área de distribución. Contrib. Inst. Nac. Invest. Desarr. Pesq. 561:1–205.

Aristizabal, E. O.
2007. Energy investment in the annual reproductive cycle of red porgy (*Pagrus pagrus*). Mar. Biol. 152:713–724.

Aubone, A., S. Bezzi, R. Castrucci, C. Dato, P. Ibañez, G. Irusta, M. Pérez, M. Renzi, B. Santos, N. Scarlato, M. Simonazzi, L. Tringali, and F. Villarino.
2000. Merluza (*Merluccius hubbsi*). *In* Síntesis del estado de las pesquerías marítimas argentinas y de la Cuenca del Plata. Años 1997–1998, con una actualización de 1999 (S. Bezzi, R. Akselman, and E. Boschi, eds.), p. 29–40. Publicaciones Especiales INIDEP (Instituto Nacional de Investigación y Desarrollo Pesquero), Mar del Plata, Argentina.

Balbontín, F., and R. Bravo.
1993. Fecundidad, talla de la primera madurez sexual y datos biométricos en la merluza del sur *Merluccius australis*. Rev. Biol. Mar. 28:111–132.

Berkeley S. A, C. Chapman, and S. M. Sogard.
2004. Maternal age as a determinant of larval growth and survival in a marine fish, *Sebastes melanops*. Ecology 85:1258–1264.

Bromage, N., M. Bruce, N. Basavaraja, K. Rana, R. Shields, C. Young, J. Dye, P. Smith, M. Gillespie, and J. Gamble.
1994. Egg quality determinants in finfish: the role of overripening with special reference to the timing of stripping in the Atlantic halibut *Hippoglossus hippoglossus*. J. World Aquacult. Soc. 25:13–21.

Brooks, S., C. R. Tyler, and J. P. Sumpter.
1997. Egg quality in fish: what makes a good egg? Rev. Fish Biol. Fish. 7:387–416.

Canal, R. L.
1989. Evaluación de la capacidad y condición reproductiva de la merluza (*Merluccius gayi peruanus*). Bol. Inst. Mar Peru 13:40–70.

Domínguez-Petit, R., and F. Saborido-Rey.
2010. New bioenergetic perspective of European hake (*Merluccius merluccius* L.) reproductive ecology. Fish. Res. 104:83–88.

Domínguez-Petit, R., F. Saborido-Rey, and I. Medina.
2010. Changes of proximate composition, energy storage and condition of European hake (*Merluccius merluccius* L. 1758) through the spawning season. Fish. Res. 104:73–82.

Draper, N. R., and H. Smith.
1981. Applied regression analysis, 2nd ed., 709 p. Wiley, New York.

El Habouz, H., L. Recasens, S. Kifani, A. Moukrim, A. Bouhaimi, and S. El Ayoubi.
2011. Maturity and batch fecundity of the European hake (*Merluccius merluccius*, Linnaeus, 1758) in the eastern central Atlantic. Sci. Mar. 75:447–454.

Ehrlich, M. D.
1998. Los primeros estadios de vida de la merluza *Merluccius hubbsi* Marini 1933, como aporte al conocimiento de su reclutamiento y estructura poblacional. Ph.D. diss., 318 p. Facultad de Ciencias Exactas y Naturales, Univ. Buenos Aires, Buenos Aires, Argentina.

Fernández-Palacios, H., M. S. Izquierdo, L. Robaina, A. Valencia, M. Salhi, and J. M. Vergara.
1995. Effect of n-3 HUFA level in broodstock diets on egg quality of gilthead seabream (*Sparus aurata* L.). Aquaculture 132:325–337.

Hinckley, S.
1990. Variation of egg size of walleye pollack *Theragra chalcogramma* with a preliminary examination of the effect of egg size on larval size. Fish. Bull. 88:471–483.

Hunter, J. R., N. C. H. Lo, and R. J. H. Leong.
1985. Batch fecundity in multiple spawning fishes. *In* An egg production method for estimating spawning biomass of pelagic fish: application to the northern anchovy, *Engraulis mordax* (R. Lasker, ed.), p. 67–77. NOAA Tech. Rep. NMFS 36.

Kjesbu, O. S., P. Solemdal, P. Bratlan, and M. Fonn.
1996. Variation in annual egg production in individual captive Atlantic cod (*Gadus morhua*). Can. J. Fish. Aquat. Sci. 53:610–620.

Lambert, Y., and J. D. Dutil.
1997. Can simple condition indices be used to monitor and quantify seasonal changes in the energy reserves of Atlantic cod (*Gadus morhua*)? Can. J. Fish. Aquat. Sci. 54:104–112.

Lambert Y., N. A. Yagarina, G. Kraus, G. Marteinsdottir, and P. J. Wright.
2003. Using environmental and biological indices as proxies for egg and larval production of marine fish. J. Northwest Atl. Fish. Sci. 33:115–159.

Landaeta, M. F., and L. R. Castro.
2012. Seasonal and annual variation in Chilean hake *Merluccius gayi* spawning locations and egg size off Central Chile. Prog. Oceanogr. 92–95:166–177.

Leonarduzzi, E. , A. Massa, and E. Manca.
2012. Variación de la composición bioquímica en hembras de merluza común (*Merluccius hubbsi*) durante el ciclo reproductivo. Rev. Invest. Desarr. Pesq. 21:5–19.

Macchi, G. J., P. Martos, R. Reta, and C. Dato.
2010. Offshore spawning of the Argentine hake (*Merluccius hubbsi*) Patagonian stock. PanamJAS 5:22–35.

Macchi, G. J., M. Pájaro, and C. Dato.
2007. Spatial variations of the Argentine hake (*Merluccius hubbsi*) spawning shoals in the Patagonian area during a reproductive season. Rev. Biol. Mar. Oceanog. 42:345–356.

Macchi, G. J., M. Pájaro, and M. Ehrlich.
2004. Seasonal egg production pattern of the Patagonian stock of Argentine hake (*Merluccius hubbsi*). Fish. Res. 67:25–38.

Macchi, G. J., M. Pájaro, and A. Madirolas.
2005. Can a change in the spawning pattern of Argentine hake (*Merluccius hubbsi*) affect its recruitment? Fish. Bull. 103:445–452.

Macchi, G. J., M. Pájaro, M. I. Militelli, N. Radovani, and L. Rivas.
2006. I nfluence of size, age and maternal condition on the oocyte dry weight of Argentine hake (*Merluccius hubbsi*). Fish. Res. 80:345–349.

Marshall, T., O. S. Kjesbu, N. A. Yaragina, P. Solemdal, and O. Ulltang.
1998. Is spawner biomass a sensitive measure of the reproductive and recruitment potential of Northeast Arctic cod? Can. J. Fish. Aquat. Sci. 55:1766–1783.

Marshall, C. T., N. A. Yaragina, Y. Lambert, and O. S. Kjesbu.
1999. Total lipid energy as a proxy for total egg production by fish stocks. Nature 402:288–290.

Marteinsdottir, G., and G. A. Begg.
2002. Essential relationships incorporating the influence of age, size and condition on variables required for estimation of reproductive potential in Atlantic cod *Gadus morhua*. Mar. Ecol. Prog. Ser. 235:235–256.

Marteinsdottir G., and K. Thorarinsson.
1998. Improving the stock-recruitment relationship in Icelandic cod (*Gadus morhua* L.) by including age diversity of spawners. Can. J. Fish. Aquat. Sci. 55:1372–1377.

Mehault, S., R. Domínguez-Petit, S. Cerviño, and F. Saborido-Rey.
2010. Total egg production and implications for management of the Southern stock of European hake. Fish. Res. 104:111–122.

Murua, H., P. Lucio, M. Santurtun, and L. Motos.
2006. Seasonal variation in egg production and batch fecundity of European hake *Merluccius merluccius* (L.) in the Bay of Biscay. J. Fish Biol. 69:1304–1316.

Nissling, A., R. Larsson, L. Vallin, and K. Frohlund.
1998. Assesment of egg and larval viability in cod, *Gadus morhua*: methods and results from an experimental study. Fish. Res. 38:169–186.

Nocillado, J. N., V. D. Peñaflorida, and I. G. Borlonga.
2000. Measures of egg quality in induced spawns of the Asian sea bass, *Lates calcarifer* Bloch. Fish Physiol. Biochem. 22:1–9.

Osborne, R. F., Y. C. Melo, M. D. Hofmeyer, and D.W. Japp.
1999. Serial spawning and batch fecundity of *Merluccius capensis* and *M. paradoxus*. S. Afr. J. Mar. Sci. 21:211–216.

Otero, H. O., M. S. Giangiobe, and M. A. Renzi.
1986. Aspectos de la estructura de población de la merluza (*Merluccius hubbsi*). II Distribución de tallas y edades. Estadios sexuales. Variaciones estacionales. Publ. Com. Téc. Mix. Fr. Mar. 1(1):147–179.

R Development Core Team.
2010. R: a language and environment for statistical computing. R Foundation for Statistical Computing, Vienna, Austria. [Available from: http://R-project.org, accessed December 2010.]

Recasens, L., V. Chiericone, and P. Belcari.
2008. Spawning pattern and batch fecundity of the European hake (*Merluccius merluccius* (Linnaeus, 1758)) in the western Mediterranean. Sci. Mar. 72:721–732.

Renzi M. A., and M. A. Pérez.
1992. Un criterio para la determinación de la edad en juveniles de merluza (*Merluccius hubbsi*) mediante la lectura de otolitos. Frente Maritimo 11(A):15–31.

Rijnsdorp, A. D., and B. Vingerhoed.
1994. The ecological significance of geographical and seasonal differences in egg size in sole *Solea solea* (L.). Neth. J. Sea Res. 32:255–270.

Rodgveller, C. J., C. R. Lunsford., and J. T. Fujioka.
2012. Effects of maternal age and size on embryonic energy reserves, developmental timing, and fecundity in quillback rockfish (*Sebastes malliger*). Fish. Bull. 110:35–45.

Sánchez, R. P., G. Navarro, and V. Rozycki.
2012. Estadísticas de la Pesca Marina en la Argen-

tina. Evolución de los desembarques 1898–2010, 528 p. Ministerio de Agricultura, Ganadería y Pesca de la Nación, Buenos Aires, Argentina.

Sewall F., and C. J. Rodgveller.
2009. Changes in body composition and fatty acid profile during embryogenesis of quillback rockfish (*Sebastes maliger*). Fish. Bull. 107:207–220.

Sogard, S. M., S. A. Berkeley, and R. Fisher.
2008. Maternal effects in rockfishes *Sebastes* spp.: a comparison among species. Mar. Ecol. Prog. Ser. 360:227–236.

Trippel, E. A.
1998. Egg size and viability and seasonal offspring production of young Atlantic cod. Trans. Am. Fish. Soc. 127:339–359.

Watanabe, T., T. Arakawa, C. Kitajima, and S. Fujita.
1984. Effect of nutritional quality of broodstock diets on reproduction of Red Sea bream. Bull. Jap. Soc. Sci. Fish. 50:495–501.

Wiegand, M. D.
1996. Composition, accumulation and utilization of yolk lipids in teleost fish. Rev. Fish Biol. Fish. 6:259–286.

Abstract—Nuclear RNA and DNA in muscle cell nuclei of laboratory-reared larvae of Walleye Pollock (*Gadus chalcogrammus*) were simultaneously measured through the use of flow cytometry for cell-cycle analysis during 2009–11. The addition of nuclear RNA as a covariate increased by 4% the classification accuracy of a discriminant analysis model that used cell-cycle, temperature, and standard length to measure larval condition, compared with a model without it. The greatest improvement, a 7% increase in accuracy, was observed for small larvae (<6.00 mm). Nuclear RNA content varied with rearing temperature, increasing as temperature decreased. There was a loss of DNA when larvae were frozen and thawed because the percentage of cells in the DNA synthesis cell-cycle phase decreased, but DNA content was stable during storage of frozen tissue.

Using measurements of muscle cell nuclear RNA with flow cytometry to improve assessment of larval condition of Walleye Pollock (*Gadus chalcogrammus*)

Steven M. Porter (contact author)
Kevin M. Bailey

Email address for contact author: steve.porter@noaa.gov

Resource Assessment and Conservation Engineering Division
Alaska Fisheries Science Center
National Marine Fisheries Service, NOAA
7600 Sand Point Way, NE
Seattle, Washington 98115-6349

Manuscript submitted 30 November 2012.
Manuscript accepted 12 August 2013.
Fish. Bull. 111:337–351.
doi: 10.7755/FB.111.4.4

The views and opinions expressed or implied in this article are those of the author (or authors) and do not necesarily reflect the position of the National Marine Fisheries Service, NOAA.

Marine fish larvae are most vulnerable to starvation during the first few weeks after they begin to feed (O'Connell, 1980; Theilacker, 1986; Theilacker and Porter, 1995). Starvation may contribute directly to mortality, or it may do so indirectly by making larvae more vulnerable to predation (Bailey and Yen, 1983; Folkvord and Hunter, 1986). Many methods, such as the RNA–DNA ratio (Buckley et al., 1999), lipid composition (Lochmann et al., 1995), histological condition of tissues (Theilacker, 1978), morphological measurements (Theilacker, 1978), and flow cytometry (Theilacker and Shen, 1993a), have been developed to measure the physiological condition of fish larvae. Mortality rate has been shown to correlate with nutritional condition of fish larvae (Theilacker et al., 1996). Hence, accurate assessment of condition can improve understanding of environmental processes that affect early life survival and recruitment.

Previous studies have assessed the condition and growth of fish larvae with flow-cytometric cell-cycle analysis, which is a technique that measures the DNA content of individual cells in a population to determine the proportion of cells in different phases of the cell cycle (Theilacker and Shen, 1993b, 2001; Bromhead et al., 2000; González-Quirós et al., 2007; Porter and Bailey, 2011; Domingos et al., 2012). Cells that are in the process of dividing can have up to twice the amount of DNA as cells that are not dividing. The cell cycle consists of discrete phases: gap 1 (G1), DNA synthesis (S), gap 2 (G2), and mitosis (M) (Murray and Hunt, 1993). Cell growth occurs during the G1 phase before cell division begins, and cells may enter a G0 resting state from this phase in response to starvation or other unfavorable environmental conditions (Murray and Hunt, 1993). For cells to divide, they must first replicate their DNA (S phase) and then grow and produce the structures (G2 phase) necessary for mitosis. Cell division occurs during mitosis.

The proportion of cells in the S, and G2 and M (G2/M) phases are indicative of cells that may divide, and the use of flow-cytometric cell-cycle analysis to assess physiological condition is founded on the premise that cell proliferation is related to condition. Specific tissue types (e.g., Theilacker and Shen, 1993b; González-Quirós et al., 2007; Porter and Bailey, 2011) or individual whole larval homogenates (Domingos et al., 2012) have been used with this method,

and flow-cytometric cell-cycle analysis is as responsive to starvation as the RNA:DNA ratio in that it is able to detect starvation within a few days of no feeding (Porter and Bailey, 2011).

Flow cytometry has been used to measure the relative amount of cellular RNA and DNA in the brain cells of fish larvae (Theilacker and Shen, 1993b, 2001). Brain cells in the G0 and G1 phases were separated through the use of ribonuclease (RNAse): G0 were quiescent cells with low RNA content, and G1 were growing cells with high RNA content (Theilacker and Shen, 1993b). Theilacker and Shen (1993b) showed that the proportion of high-RNA-content G1 cells differed between fed and starved larvae, and it was suggested that those cells gave an indication of short-term changes in past feeding history. Nuclear RNA (nRNA) may react faster to metabolic changes than does cellular RNA, making it more sensitive to environmental change (Piwnicka et al., 1983) and potentially useful for assessment of the condition of fish larvae.

Most nRNA is contained in the nucleolus (Li et al., 2006), the site of ribosome biogenesis (Sirri et al., 2008), and ribosome production correlates with cellular growth (Caldarola et al., 2009). For many cell types grown in culture, nRNA content of G1 cells is highly variable, and a specific amount may be required for entry into the S phase (Darzynkiewicz et al., 1980; Piwnicka et al., 1983; Staiano-Coico et al., 1989). The threshold amount needed for G1 cells to progress into the S phase has been defined as the minimum nRNA content of S-phase nuclei determined from plots of nRNA and DNA fluorescence measured by flow cytometry (Darzynkiewicz et al., 1980).

In a previous study with flow cytometry (Porter and Bailey, 2011), cell-cycle information (fraction of nuclei in the S and G2/M phases), larval standard length (SL), and temperature were used as covariates in a laboratory-developed model for measurement of the condition of larvae of Walleye Pollock (*Gadus chalcogrammus*). In the study that we describe here, we found that an additional covariate based on nRNA improved the classification accuracy of a similar condition model by more clearly defining healthy (i.e., feeding, growing) and unhealthy (i.e., starving) larval conditions. We also examined the effect of rearing temperature on nRNA measurements and the effect of storage on frozen tissue used for measurements with flow cytometry.

Materials and methods

Larval rearing

Adult Walleye Pollock were collected by trawl in Shelikof Strait, Gulf of Alaska, during the spawning season in March 2009 and 2010 by the Alaska Fisheries Science Center (AFSC). For our experiments in 2009 and 2010, eggs from a single fish pairing (one female and one male) were fertilized and maintained aboard ship in the dark at 3°C before they were transported to the AFSC in Seattle, Washington. Eggs used for 2011 experiments came from a brood stock of adults kept at the AFSC laboratory at the Hatfield Marine Science Center in Newport, Oregon, and were also the result of a single fish pairing.

In 2009 and 2010, larvae were reared in 2 feeding treatments: an *always-fed* treatment, in which larvae were considered healthy, and an *unfed* (starved) treatment in which larvae were considered unhealthy. Only the always-fed treatment was used in 2011. Rearing methods are described in Porter and Bailey (2011). Two replicate tanks were used for each feeding treatment. The size of the tanks varied with each experiment: 120 L in 2009, 20 L in 2010, and 60 L in 2011. The diet of larvae in the always-fed treatment consisted of laboratory-cultured rotifers (*Brachionus plicatilis*) that were fed an algal diet (*Isochrysis galbana* and *Pavlova lutheri*) and a commercial rotifer supplement. Rotifers were maintained in the rearing tanks at a concentration of 10 mL^{-1}. Natural zooplankton, which included primarily copepod nauplii (*Acartia* spp.) and gastropod veligers, were collected from a local lagoon and screened through 202-µm mesh; they also were maintained in the always-fed rearing tanks, at a concentration of 3 mL^{-1}. A 16-h daylight cycle with a light level of 2.5 µmol photon m^{-2} s^{-1} from overhead, full-spectrum fluorescent lights was used, and larvae were sampled 4–6 h after the lights turned on at 0600 h. To avoid sampling larvae that were not actively feeding and possibly unhealthy, only larvae that had prey in their gut were sampled from the always-fed treatment. Rearing temperatures varied: 6.0°C in 2009, 2.9°C, 5.9°C, and 8.7°C in 2010, and 6.5°C in 2011.

2009 experiments: nRNA staining protocol and covariate

Three methods for preservation of larvae were tested to determine which of them was optimal for simultaneous staining of DNA and nRNA in muscle cell nuclei of larvae of Walleye Pollock: 1) storage at –80°C, 2) a methanol treatment, and 3) storage at –80°C followed by a methanol treatment for 15 min before tissue processing. To stain DNA for cell-cycle analysis with flow cytometry, 4′,6-diamidino-2-phenylindole (DAPI), a fluorescent DNA stain, was used at a concentration of 10 µg mL^{-1}, and nRNA was stained with Invitrogen Syto RNASelect[1] green fluorecent cell stain (S32703, Life Technologies Corp., Carlsbad, CA), hereafter referred to as Syto RNASelect stain.

Preservation of tissue by freezing works well for DAPI-DNA staining (Theilacker and Shen, 2001), and methanol-preserved tissue has been stained successfully with Syto RNASelect stain (Life Technolo-

[1] Mention of trade names or commercial companies is for identification purposes only and does not imply endorsement by the National Marine Fisheries Service, NOAA

gies Corp.[2]; Molecular Probes, Inc.[3]). Syto RNASelect stain is known to also bind to DNA and emit an extremely weak fluorescent signal; therefore, we examined through the use of a staining study the effect that varying concentrations of Syto RNASelect stain had on the DAPI-DNA interaction to confirm that the stain concentration we used did not interfere with DAPI staining. Three concentrations of Syto RNASelect stain were mixed in DAPI and tested: 500 nM (concentration recommended by Invitrogen), 1000 nM (maximum concentration recommended by Invitrogen), and 2000 nM. The optimal preservative and stain concentration was defined as that which provided the highest nRNA fluorescence that did not affect DNA fluorescence as measured by flow cytometry. Each preservative was tested with the 3 concentrations of RNA stain previously described and a DAPI-only negative control that was used to determine background RNA fluorescence.

For preservative and stain testing, larvae were removed from a rearing tank, anesthetized in a 1% solution of tricaine methanesulfonate (MS222), measured for their SL with an ocular micrometer, and placed in a 1.5-mL microcentrifuge tube that was either filled with methanol or inserted into a gel-filled microcentrifuge tube holder that was frozen at –80°C. Tubes were kept in the holder until they were transferred to a –80°C freezer. The nuclei of 29 always-fed larvae were pooled to have enough material to simultaneously test 3 stain concentrations and the control group for each type of preservative. Six replicate aliquots were taken for each stain concentration and control. A specific volume of Syto RNASelect stain was then added to each aliquot to equal the desired final concentration. Larvae were processed and analyzed as described in the section *Materials and methods, Flow cytometry.* To determine optimal RNA stain concentration, analysis of variance (ANOVA), Tukey's tests, and Dunnett's tests were used to compare nRNA and DNA fluorescence associated with each RNA stain concentration and the control. SYSTAT, vers. 13 (Systat Software, Inc., Chicago), was used for all statistical testing.

After the optimal preservation method and stain concentration were determined, nRNA staining was confirmed through comparison of untreated muscle cell nuclei to those nuclei treated with RNAse. Nuclei were treated in a mixture of DAPI and RNAse A (50 μg mL^{-1} RNAse A, Sigma R6513, DNAse free) at room temperature for 25 min before adding the Syto RNASelect stain. The nuclei of 12 always-fed larvae were pooled to have enough nuclei to simultaneously test 3 treatments: a positive control (DAPI+RNA stain), a negative control (DAPI only), and a treatment (RNAse A+DAPI+RNA stain). Four replicate aliquots were taken for each treatment, and ANOVA and Tukey's tests were used to compare RNAse A-treated nuclei to both the positive and negative controls.

After the staining protocol, an nRNA covariate to test in a larval condition model was determined with larvae from the always-fed and unfed treatments. Ten individuals were taken from each replicate tank of both treatments at first feeding (defined as the day when 50% of the larvae had prey in their gut) and then at 4, 8, 11, and 14 days after first feeding. Five potential nRNA covariates were investigated: geometric mean fluorescence of nuclei in the G0 and G1 (G0/G1), S, and G2/M phases of the cell cycle pooled, mean fluorescence of each cell-cycle phase (G0/G1, S, and G2/M) separately, and the ratio of the number of S-phase nuclei to the number of G1-phase nuclei with high RNA content (hereafter, this ratio will be referred to as RSG1; see *Materials and methods, Flow cytometry* section). RSG1 is a measure of potential cell division based on progression of nuclei from the G1 to S phase. An unhealthy larva would not be expected to grow or it would grow more slowly than a healthy individual. Therefore, an unhealthy larva would have fewer dividing cells and potentially less S-phase nuclei, and its ratio of S-phase nuclei to G1-phase nuclei with high RNA content would be smaller than the ratio for healthy individuals. Nuclear RNA fluorescence between treatments was compared with the 2-sample *t*-test. The Mann-Whitney *U* test was used to compare RSG1 between treatments.

2010 experiment: nRNA, temperature, and condition

Five larvae were sampled from each always-fed tank on 3 separate days after feeding began. A degree-day model (degree-day=temperature*fish age in days) was used so that larvae were sampled on the day of similar developmental stage after first feeding, not on the same calendar day after first feeding (Table 1). Eight larvae from the unfed treatment were sampled from each tank daily, beginning at first feeding and ending at yolk exhaustion. All larvae were frozen at –80°C. Geometric mean nRNA fluorescence for nuclei in the G0/G1, S, and G2/M phases of the cell cycle pooled, and RSG1 for each larva was determined (see *Materials and methods, Flow cytometry* section). ANOVA and Tukey's tests were used to examine differences in fluorescence and RSG1 between feeding treatments and among temperatures.

2011 experiment: effect of freezing and storage on nRNA and DNA

After 4 days of feeding, 20 control larvae (not frozen) were processed directly from the rearing tanks (10 from each replicate tank) and analyzed by flow cytome-

[2] Life Technologies Corp. 2013. Life Technologies: Syto RNASelect green fluorescent cell stain—5 mM solution in DMSO. Life Technologies Corp., Carlsbad CA. [Product information webpage; Available from http://products.invitrogen.com/ivgn/product/S32703, accessed August 2013.]

[3] Molecular Probes, Inc. 2004. Syto RNASelect green fluorescent cell stain (S32703). Molecular Probes, Inc., Eugene, OR. [Product information document; Available from http://tools.invitrogen.com/content/sfs/manuals/mp32703.pdf.]

Table 1

Days after first feeding when laboratory-reared larvae of Walleye Pollock (*Gadus chalcogrammus*) were sampled to determine the effect of temperature on nuclear RNA. Rearing tanks were maintained at 3 different temperatures. Because temperature can affect the growth rate of fishes, a "degree-day" model (degree-day=temperature*fish age in days) was used to ensure that that fish were taken at similar developmental stages.

Rearing temperature (°C)	Sampling days after first feeding (determined by degree-day model)	Sampling days (calendar days) after first feeding
2.9	17, 35, 61	6, 12, 21
5.9	18, 35, 65	3, 6, 11
8.7	17, 33, 58	2, 4, 7

try (see *Materials and methods, Flow cytometry* section). On the same day, 60 larvae were frozen at –80°C in individual tubes (30 from each tank) for flow-cytometric cell-cycle analysis at later dates. At 4 weeks after they were frozen and at additional intervals of 3, 6, and 10 months, 15 of these frozen larvae were randomly selected and analyzed with flow cytometry. Geometric mean nRNA fluorescence for nuclei in the G0/G1, S, and G2/M phases of the cell cycle pooled and RSG1 was determined for each larva (see *Materials and methods, Flow cytometry* section). The fraction of nuclei in the G0/G1, S, and G2/M phases of the cell cycle also was determined for each larva (see *Materials and methods, Flow cytometry* section). ANOVA, Dunnett's tests, and Tukey's tests were used to compare nRNA fluorescence, DNA fluorescence, and fractions of nuclei in the G0/G1, S, and G2/M phases between the control and frozen samples and among the frozen samples over time.

Flow cytometry

The tissue preparation protocol described in Porter and Bailey (2011), modified from Theilacker and Shen (2001), was followed. A frozen larva was placed on ice to thaw just before it was processed. A methanol-preserved larva was processed directly from the preservative. The larva was then placed on a glass depression slide into an approximately 100-µL mixture of DAPI and Syto RNASelect stains. The head and gut were dissected away from the trunk musculature, and the muscle tissue was sliced into 4 or 5 pieces with 2 scalpels.

Only the pieces of muscle tissue were transferred into a microcentrifuge tube that contained a 230-µL mixture of DAPI and Syto RNASelect stains and the mixture was triturated 6 times with a 1-mL syringe with a 25-gauge needle to release the nuclei from the muscle cells. The solution was filtered through a 48-µm filter into another microcentrifuge tube to separate the stained nuclei from large cellular debris. Prepared samples were kept on ice until they were analyzed with a BD Biosciences Influx flow cytometer (BD Biosciences, San Jose, CA) typically within 4–5 h of preparation. DAPI was excited with a 350-nm UV laser, and Syto RNASelect stain was excited with a 488-nm laser. The DAPI/DNA detector filter was 450/40, and the detector filter for Syto RNASelect stain/RNA was 525/30. Flourochrome compensation for overlapping emissions spectra of RNA and DNA stains is unnecessary when exciting DAPI and Syto RNASelect stain with the BD Biosciences Influx flow cytometer. The beams of the 350-nm and 488-nm lasers intercept the stream at spatially separate points. Each beam excites only the stain for DNA (350 nm) or RNA (488 nm). The emission light is focused on separate mirror pinholes and is detected in separate modular detection blocks. Chicken and trout erythrocyte nuclei (Biosure, Inc., Grass Valley, CA) stained with the same mixture of DAPI and Syto RNASelect stains used for the muscle cell nuclei were used as controls.

At the beginning of each flow cytometry session, each control type was run and necessary adjustments were made to the flow cytometer to keep control fluorescence values similar to previous sessions. DNA and RNA fluorescence values for larvae within the same experiment but measured during different flow cytometry sessions were made comparable by standardizing to a common control value. Samples that had <5000 nuclei analyzed or a coefficient of variation >9.00 for the cell-cycle phase of G0/G1 were not used in further analyses, and the use of this criteria resulted in rejection of about a third of all samples.

For each larva, the fraction of nuclei in the G0/G1, S, and G2/M phases was calculated with MultiCycle AV software, vers. 4.0 (Phoenix Flow Systems, San Diego, CA). FCS Express flow cytometry analysis software, vers. 3.0 (De Novo Software, Los Angeles, CA) was used to calculate RSG1 and geometric mean fluorescence values for nRNA and DNA. DAPI area (DNA content, linear scale) in relation to DAPI height (DNA content, linear scale) was plotted for each larva, and a gate (a boundary used to enclose specific data points) was made to exclude debris, doublets, triplets, and large aggregates from nuclei in the G0/G1, S, and G2/M phases (Fig. 1A). Nuclei in those phases were located within the gate (Fig. 1B).

To calculate geometric mean values of nRNA and DNA fluorescence for each larva, a scatter plot of nRNA fluorescence (log scale) values in relation to DNA fluorescence (linear scale) values was made from the data enclosed within the gate for nuclei in the G0/G1, S, and G2/M phases. Each phase was gated separately for mean fluorescence values (Fig. 2), and a single gate that enclosed nuclei of all phases was used for the pooled mean fluorescence value. RSG1 was calculated with the same nRNA and DNA fluorescence scatter plot.

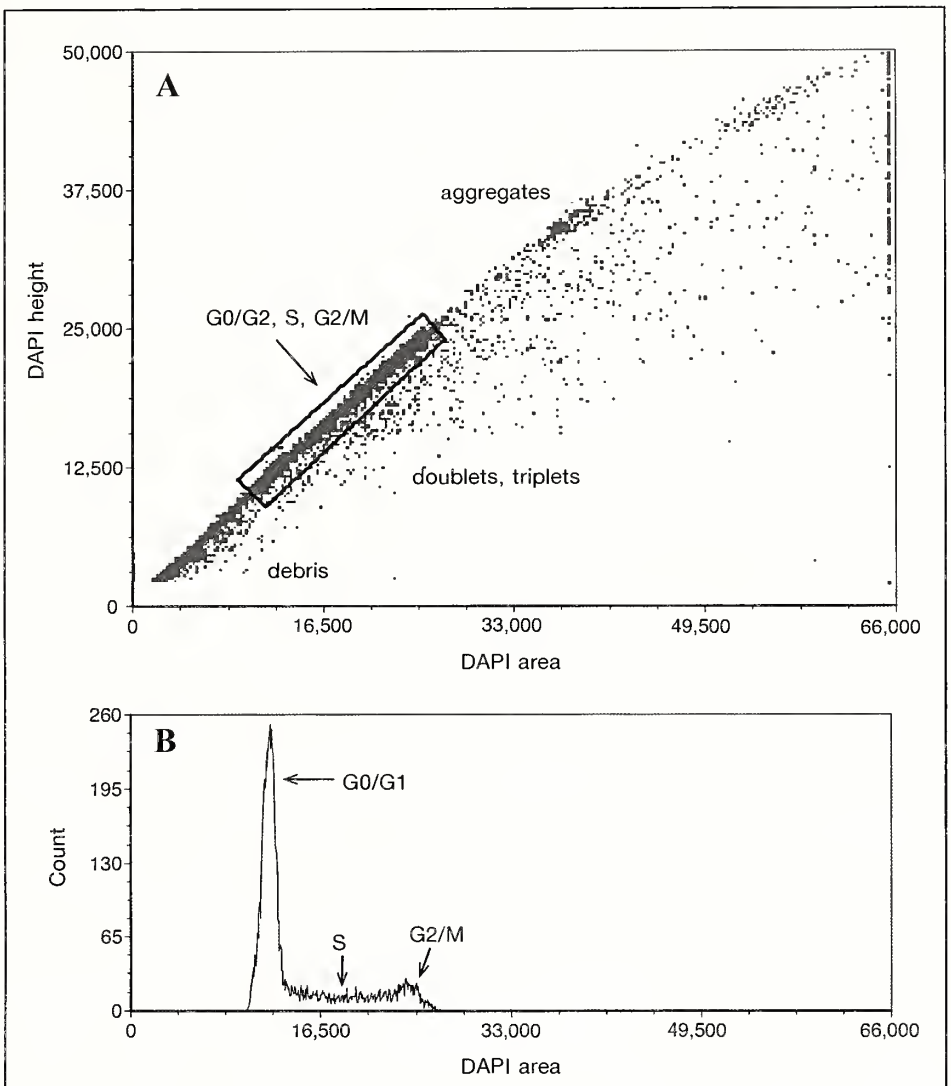

Figure 1

(**A**) Scatter plot of 4′,6-diamidino-2-phenylindole (DAPI) area (DNA content, linear scale) and DAPI height (DNA content, linear scale) for a laboratory-reared larva of Walleye Pollock (*Gadus chalcogrammus*) sampled in 2009, showing the gating strategy used to exclude debris, doublets, triplets, and large aggregates from muscle cell nuclei in the G0 and G1 (G0/G1), S, and G2 and M (G2/M) phases of the cell cycle. Those nuclei are enclosed within the gate, which is represented by a rectangle. (**B**) Histogram showing the distribution pattern of the nuclei within the gate. Phases of the cell cycle: G1=gap 1 or cell growth before cell division, G0=resting state from G1, S=DNA synthesis, G2=gap 2 or cell growth before mitosis, and M=mitosis.

A gate that divided G1-phase nuclei into fractions of low and high nRNA content on the basis of nRNA fluorescence of S-phase nuclei was made by following Staiano-Coico et al. (1989). The smallest value of S-phase nRNA fluorescence was the minimum nRNA content needed for G1 nuclei to enter the S phase, and it was assumed that any nuclei with greater fluorescence also could enter the S phase (Staiano-Coico et al., 1989). A gate that enclosed G1 nuclei was made, beginning at the smallest nRNA fluorescence value of the S-phase nuclei and extending to enclose the G1 nuclei with the highest nRNA fluorescence values (designated G1B; Fig. 3, A and B). The G1B group was defined as the number of nuclei with the potential to progress from the G1 to S phase. The number of S-phase nuclei was determined through the use of a gate that enclosed those nuclei (Fig. 3, A and B), and RSG1 was calculated by dividing that number by the number of G1B nuclei.

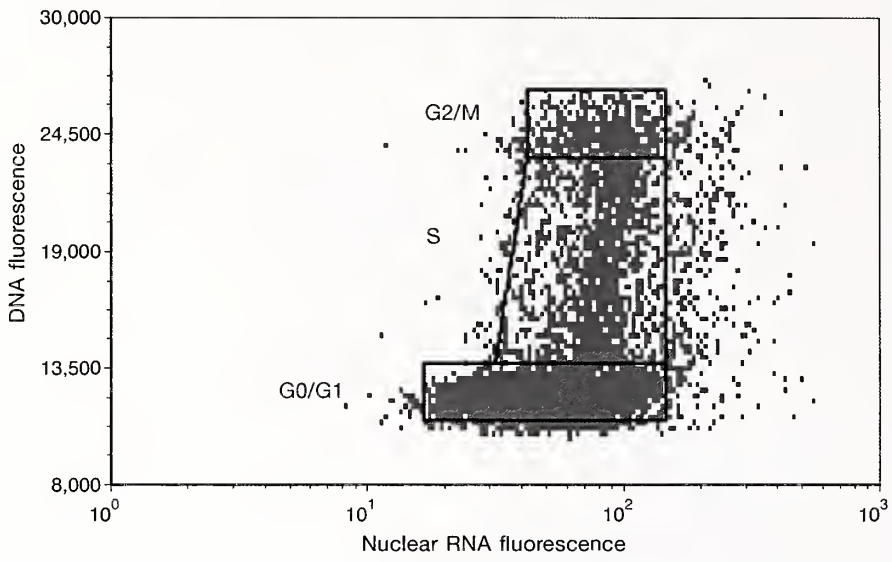

Figure 2

Scatter plot of nuclear RNA (log scale) and DNA fluorescence (linear scale) of muscle cell nuclei in the G0 and G1 (G0/G1), S, and G2 and M (G2/M) phases of the cell cycle for a laboratory-reared larva of Walleye Pollock (*Gadus chalcogrammus*) sampled in 2009. The rectangles outlined in black indicate the gates used to calculate geometric mean values of nuclear RNA and DNA fluorescence. Fluorescence values are arbitrary units. Phases of the cell cycle: G1=gap 1 or cell growth before cell division, G0=resting state from G1, S=DNA synthesis, G2=gap 2 or cell growth before mitosis, and M=mitosis.

Model testing

Data from all 3 years were pooled for model testing. One-third of the data were randomly removed from that data set and used for independent cross-validation testing. The remaining data were used to formulate discriminant analysis models similar to the model described in Porter and Bailey (2011) to classify larvae as healthy (feeding and growing) or unhealthy (starving). Models had SL, temperature, fraction of cells in the S phase, and fraction of cells in the G2/M phases as covariates, and were tested with and without the nRNA covariate included. The arcsin $\sqrt{x}$ transformation was used to normalize the fraction of cells in the S phase, fraction of cells in the G2/M phases, and RSG1. Models were compared on the basis of the accuracy of their classification of the cross-validation data set and Akaike's information criterion values (Burnham and Anderson, 2002).

Results

Nuclear RNA staining protocol

Flow-cytometric cell-cycle analysis showed that the tissue from frozen samples had a small amount of debris and distinct peaks in G0/G1 and G2/M phases. Fixing larvae in methanol for either a short period of time or long-term storage did not work as well; samples contained a large amount of cellular debris and aggregates, and the nuclei did not disassociate from the tissue easily. Samples from larvae preserved long term in methanol contained too much debris to be usable for further analysis. Debris was not as great in the samples that were frozen and then received a short-term methanol treatment as it was in the samples stored long term in methanol. The latter samples were usable, but they were not as clean as the samples that were frozen and not treated with methanol. Comparison of the RNA fluorescence between frozen tissues and tissues that were frozen and then treated with methanol indicated that short-term methanol preservation did not improve RNA staining; therefore, frozen tissue (stored at –80°C) worked best for preservation of muscle tissue from larvae of Walleye Pollock for nRNA and DNA staining and was used for all further tests and experiments.

Syto RNASelect stain concentration affected both nRNA and DNA fluorescence. The fluorescence of nRNA for all stain concentrations was significantly higher than the values observed for the DAPI–only control (ANOVA, $F_{(3,19)}$=165.94, P<0.001; Dunnett's test, P<0.001 for each concentration; Fig. 4A). The nRNA fluorescence values of the DAPI+1000-nM Syto

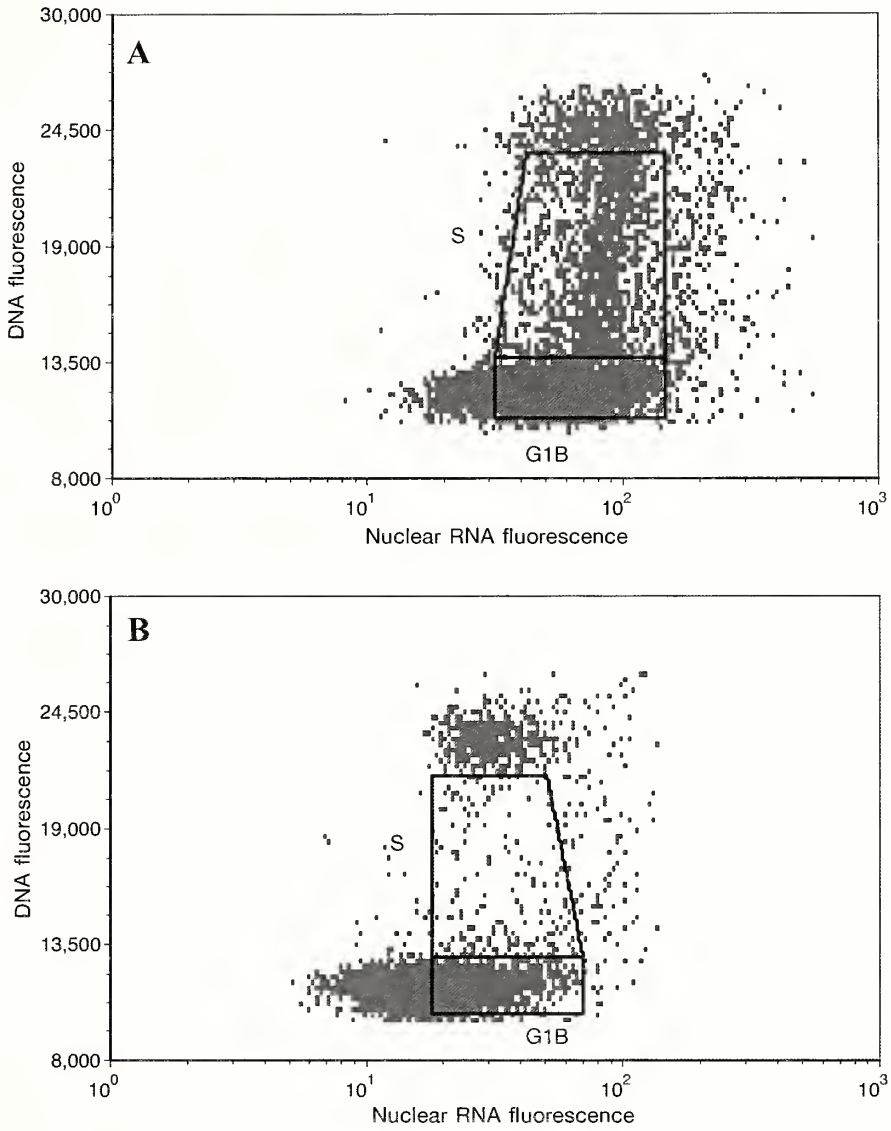

Figure 3

Scatter plots of cell-cycle analysis by flow cytometry of muscle cell nuclei of (**A**) an always-fed larva (fed 4 days) and (**B**) an unfed larva (starved 14 days) of Walleye Pollock (*Gadus chalcogrammus*) reared in 2009. The rectangles outlined in black indicate the gates used to determine the number of G1-phase nuclei with elevated nuclear RNA content needed to enter the S phase (G1B), and the total number of nuclei in the S phase of the cell cycle (S). The G1 phase of the cell cycle is when cell growth occurs before cell division, and the S phase is when DNA replicates. The always-fed larva had a distinct group of S-phase nuclei, and, for the unfed larva, S-phase nuclei were fewer and dispersed. Fluorescence values are arbitrary units.

RNASelect stain concentration and DAPI+2000-nM Syto RNASelect stain concentration were significantly higher than the values for the DAPI+500-nM Syto RNASelect stain concentration (ANOVA, $F_{(3,19)}$=165.94, P <0.001; Tukey's test, P<0.01 for both stain concentrations; Fig. 4A), but there was no significant difference in fluorescence between them (ANOVA, $F_{(3,19)}$=165.94, P<0.001; Tukey's test, P=0.44; Fig. 4A).

There was no significant difference in DNA fluorescence between the control and the 500-nM and 1000-nM Syto RNASelect stain concentrations (ANOVA, $F_{(3,19)}$=10.90, P<0.001; Dunnett's test, P=0.57 and

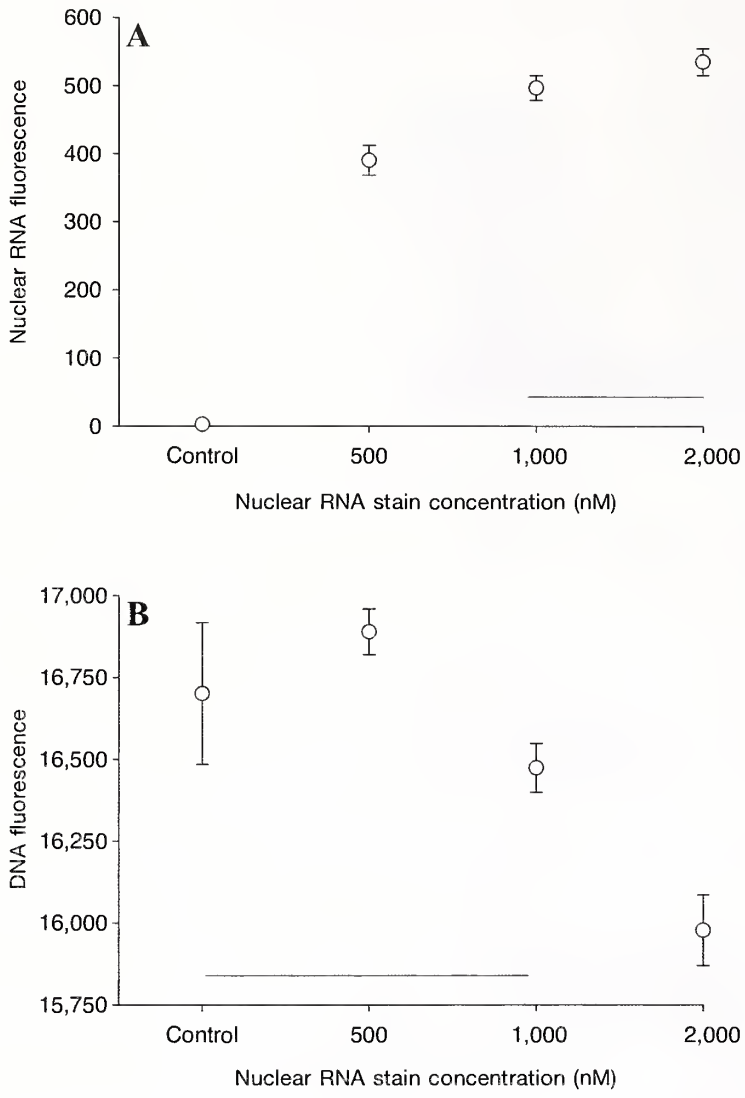

Figure 4

Mean fluorescence of (**A**) nuclear RNA and (**B**) DNA as a function of nuclear RNA stain concentration observed in muscle cell nuclei from larvae of Walleye Pollock (*Gadus chalcogrammus*) reared in 2009. The horizontal bar indicates fluorescence values that are not significantly different ($P>0.05$). Error bars indicate ±1 standard error of the geometric mean. Fluorescence values are arbitrary units.

0.44 respectively; Fig. 4B). The 2000-nM concentration caused a significant reduction of DNA fluorescence compared with the DNA fluorescence of the control (ANOVA, $F_{(3,19)}=10.90$, $P<0.001$; Dunnett's test, $P=0.002$; Fig. 4B), indicating that a Syto RNASelect stain concentration >1000 nM negatively affected DNA staining. Additionally, no significant difference was observed in DNA fluorescence between the 500-nM and 1000-nM concentrations (ANOVA, $F_{(3,19)}=10.90$, $P<0.001$; Tukey's test, $P=0.10$; Fig. 4B). Therefore, the 1000-nM concentration was optimal for nRNA staining because it produced the highest nRNA fluorescence and had no effect on DNA staining.

The nRNA fluorescence of the RNAse-treated nuclei was significantly less than the values seen for the positive control (DAPI+1000-nM Syto RNASelect stain), indicating that nRNA was being stained (ANOVA, $F_{(2,9)}=386.26$, $P<0.0001$; Tukey's test, $P<0.0001$; Fig. 5A); however, the treated nuclei had a higher fluorescence than the negative control (DAPI only; ANOVA, $F_{(2,9)}=386.26$, $P<0.0001$; Tukey's test, $P<0.0001$; Fig. 5A), indicating fluorescence signal from stained DNA or the incomplete removal of nRNA from the samples. There was no significant difference in DNA fluorescence among the 3 treatments (ANOVA, $F_{(2,9)}=0.009$, $P=0.99$; Fig. 5B); therefore, it is most likely that the treatment with RNAse A did not completely remove all of the nRNA. Additionally, this experiment independently confirmed that the 1000-nM concentration of the Syto RNASelect stain does not affect DNA staining because there was no significant difference in DNA fluorescence between the group stained with DAPI only and the group stained with DAPI+1000-nM Syto RNASelect stain.

Nuclear RNA covariate

For each treatment, larval SL was not significantly different between replicate tanks (always-fed treatment, 2-sample t-test, $t_{61}=0.196$, $P=0.85$; unfed treatment, 2-sample t-test, $t_{48}=0.45$, $P=0.65$), indicating that larvae in those tanks responded similarly to the same treatment. Therefore, replicate measurements of nRNA fluorescence from each tank for each treatment were pooled. The growth rate of larvae in the always-fed treatment from hatching to 19 days after hatching was 0.11 mm d^{-1}, a rate that is typical for larvae of Walleye Pollock reared in a 6°C laboratory (Porter and Theilacker, 1999). To formulate the nRNA covariate, we used 113 larvae, 63 always-fed (healthy) and 50 unfed (unhealthy). There was no significant difference in nRNA fluorescence between feeding treatments when all phases of the cell cycle were pooled or when phases were examined separately (Table 2), indicating that nRNA fluorescence was not a useful indicator of condition. Unlike nRNA fluorescence, RSG1 was responsive to feeding conditions; therefore, it was chosen as the nRNA covariate for model testing.

Plots of nRNA and DNA fluorescence showed that always-fed larvae had a distinct group of aggregated S-phase nuclei that joined the G0/G1 and G2/M phases, and S-phase nuclei were fewer and dispersed for unfed larvae (Fig. 3, A and B). Overall RSG1 was significantly larger for always-fed larvae than for unfed larvae (0.23 [standard error of the mean 0.01] for always-fed and 0.16 [SE 0.01] for unfed larvae; Mann-Whitney U test, U=2299.5, N_1=63, N_2=50, P<0.001), clearly distinguishing larvae between the 2 feeding treatments. For always-fed larvae, there was an initial increase in RSG1 and then a gradual decline to its initial value after 2 weeks of feeding (Fig. 6A). For unfed individuals, RSG1 declined throughout the time period to less than half its initial value after 2 weeks of feeding (Fig. 6A). Nuclear RNA fluorescence did not show a distinct difference between feeding treatments until after 2 weeks of feeding (Fig. 6B).

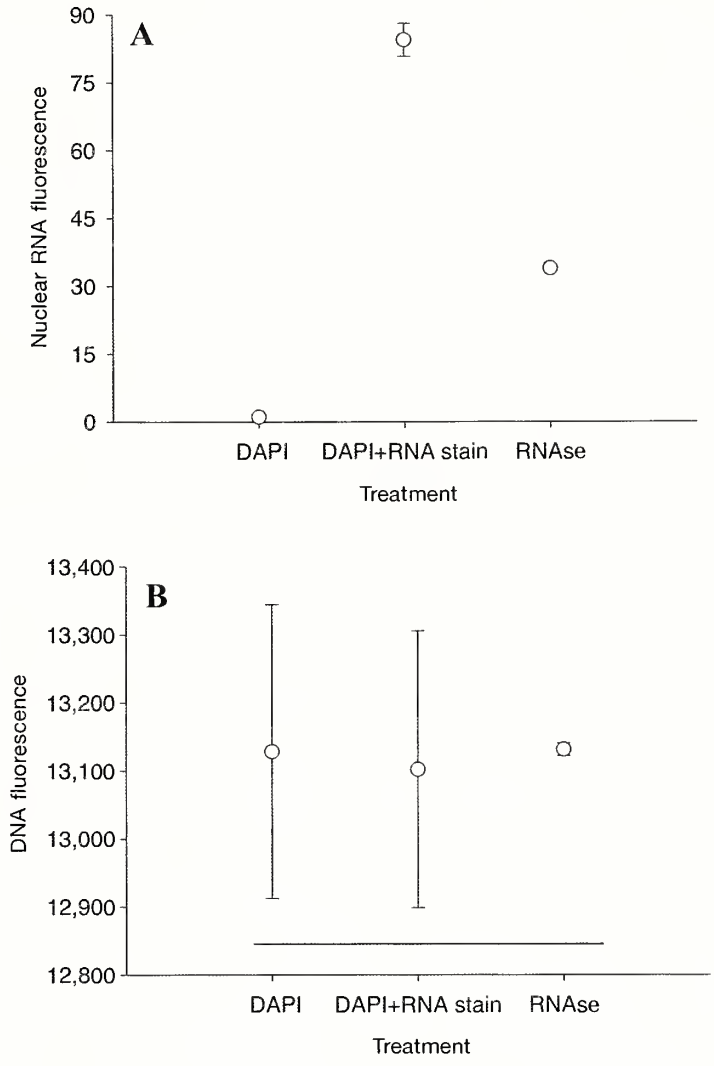

Figure 5

Mean fluorescence of (**A**) nuclear RNA and (**B**) DNA as a function of 3 treatments used to confirm nuclear RNA staining—4′,6-diamidino-2-phenylindole (DAPI) stain only (negative control), DAPI+nuclear RNA stain (positive control), and ribonuclease (RNAse) A—of muscle cell nuclei from larvae of Walleye Pollock (*Gadus chalcogrammus*) reared in 2009. The horizontal bar indicates fluorescence values that are not significantly different (P>0.05). Error bars indicate ±1 standard error of the geometric mean. Fluorescence values are arbitrary units.

Nuclear RNA, temperature, and condition

Growth in the always-fed treatment at the warmest temperature (8.7°C) was poor; therefore, larvae from this treatment were not used for further analyses. A growth rate of about 0.15 mm d^{-1} would be expected (senior author, unpubl. data), but larvae grew 0.08 mm d^{-1}. Both mean percentage of nuclei in the S-phase (8.90) and mean RSG1 (0.17) were small for a typical healthy, feeding larva, supporting the observation that those larvae were not growing well. Growth rates at the temperatures of 5.9°C (0.10 mm d^{-1}) and 2.9°C (0.06 mm d^{-1}) were typical for larvae reared at those temperatures.

There was no significant difference in overall nRNA fluorescence between the always-fed and unfed treatments (ANOVA, $F_{(1,61)}$=1.25, P=0.27; Table 3). Rearing temperature significantly affected overall nRNA fluorescence. Larvae reared at 2.9°C had a higher fluorescence than larvae reared at 5.9°C (ANOVA, $F_{(1,61)}$=4.47, P=0.04; Table 3), indicating more RNA in muscle nuclei from larvae reared at the colder temperature. RSG1 was significantly higher for the always-fed treatment than for the unfed treatment at both temperatures (ANOVA, $F_{(1,87)}$=59.65, P<0.01, Tukey's test, P<0.01; Table 3), similar to the result for the experiment conducted in 2009.

The effect of temperature on RSG1 was dependent on feeding treatment. RSG1 was smaller for always-fed larvae reared at 5.9°C compared with RSG1 of larvae reared at 2.9°C (ANOVA, $F_{(1,87)}$=18.56, P<0.001, Tukey's test, P<0.01; Table 3), and this result may indicate shorter duration for the cell cycle at warmer temperatures. RSG1 was not significantly different between unfed larvae reared at 8.7°C and at 2.9°C (ANOVA, $F_{(2,55)}$=3.61, P=0.03, Tukey's test, P=0.97; Table 3), indicating that temperature affected RSG1 only of

Table 2

Nuclear RNA fluorescence of muscle cell nuclei in various phases of the cell cycle from laboratory-reared larvae of Walleye Pollock (*Gadus chalcogrammus*). Larvae were sampled from the always-fed and unfed treatments used in experiments in 2009. Fluorescence values are arbitrary units and were adjusted on the basis of controls to make samples comparable among sessions of flow cytometry. Standard errors of geometric means are reported in parentheses. Cell-cycle phases: G1=gap 1 or cell growth before cell division, G0=resting state from G1 phase, S=DNA synthesis, G2=gap 2 or cell growth before mitosis, and M=mitosis. G0/G1=fluorescence of G0 and G1 phases combined, G2/M=fluorescence of G2 and M phases combined.

Treatment	RNA fluorescence	Mean	*n*	Statistical test	*P*
Always-fed	G0/G1, S, G2/M phases pooled	54.9 (1.9)	63	2-sample *t*-test, t_{111}=1.03	0.31
Unfed	G0/G1, S, G2/M phases pooled	52.1 (2.0)	50	–	–
Always-fed	G0/G1 phases	49.2 (1.6)	63	2-sample *t*-test, t_{111}=1.01	0.31
Unfed	G0/G1 phases	46.9 (1.6)	50	–	–
Always-fed	S phase	87.2 (2.7)	63	2-sample *t*-test, t_{111}=0.57	0.57
Unfed	S phase	90.5 (3.3)	50	–	–
Always-fed	G2/M phases	87.2 (2.7)	63	2-sample *t*-test, t_{111}=0.24	0.81
Unfed	G2/M phases	86.3 (3.1)	50	–	–

growing larvae. The data for unfed larvae were re-analyzed with the 8.7°C treatment removed to determine if the exclusion of the data from the 8.7°C always-fed treatment biased the conclusions from this study. The results were unchanged; there was no significant difference in RSG1 between unfed larvae at 2.9°C and 5.9°C (ANOVA, $F_{(1,87)}$=59.65, P<0.001, Tukey's test, P=0.05).

Model testing

Data from experiments in 2009, in 2010 (temperatures: 2.9°C and 5.9°C), and in 2011 were pooled for model testing (n=237). The 8.7°C experiment in 2010 was excluded because larvae grew poorly in the always-fed treatment. A control model used temperature, SL, arcsin $\sqrt{x}$ -transformed fraction of cells in the S phase, and arcsin $\sqrt{x}$ -transformed fraction of cells in the G2/M phases; and a test model added arcsin $\sqrt{x}$ -transformed RSG1 to the covariates used in the control model (n=158). For independent cross-validation testing, 49 always-fed larvae ranging from 5.36 to 8.64 mm SL and 30 unfed larvae from 5.20 to 5.92 mm SL were used (n=79). Both models significantly discriminated between the always-fed and unfed treatment groups (control model, Wilks's lambda=0.46, $F_{(4,153)}$=44.19, P<0.001; test model, Wilks's lambda=0.45, $F_{(5,152)}$=37.13, P<0.001).

The test model improved overall classification accuracy by 4%, and accuracy for both always-fed and unfed larvae increased (Table 4). The improvement in the always-fed treatment larvae was due to the correct classification of additional small, feeding larvae (<6.00 mm SL). The classification accuracy in the test model for those larvae improved 14%, increasing from 53% (8/15) to 67% (10/15) when RSG1 was used. Classification accuracy of unfed treatment larvae improved 3%, and the test model correctly classified all the unfed larvae tested (Table 4). For larvae <6.00 mm SL from both the always-fed and unfed treatments, classification accuracy improved 7% (an increase from 37/45 to 40/45). There was no difference in classification accuracy between models for larvae ≥6.00 mm SL, and both models correctly classified all of those larvae. Akaike's information criterion value for the test model was less than that value for the control model (–1130.53 and –1001.38, respectively), indicating that the addition of RSG1 improved model fit.

Effect of freezing and storage on nRNA and DNA

There was a loss of DNA when larvae were frozen and thawed, but that process did not affect nRNA measurements. The DNA fluorescence of fresh tissue was significantly greater than DNA fluorescence of frozen

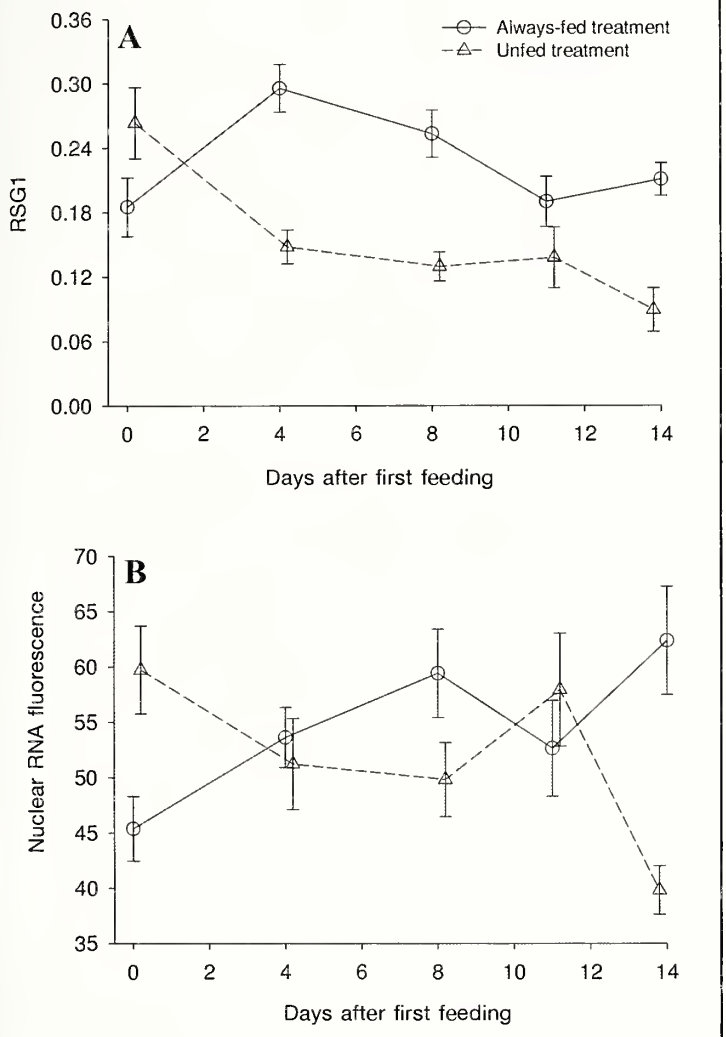

Figure 6

For always-fed and unfed treatments of larvae of Walleye Pollock (*Gadus chalcogrammus*) reared in 2009, (**A**) mean ratios of the number of S-phase nuclei to the number of G1-phase nuclei with high nuclear RNA content (RSG1) and (**B**) geometric mean fluorescence of nuclear RNA of all cell-cycle phases pooled. The G1 phase of the cell cycle is when cell growth occurs before cell division, and the S phase is when DNA replicates. Error bars indicate ±1 standard error of the mean. Fluorescence values are arbitrary units.

tissue (ANOVA, $F_{4,48}$=36.67, P<0.001, Dunnett's tests, P<0.05 for all frozen groups; Table 5), indicating that DNA was lost when tissue was frozen and thawed. The percentage of nuclei in the G2/M phases was not significantly different between the fresh and frozen tissue treatments (ANOVA, $F_{4,48}$= 2.00, P=0.11; Table 5), but freezing affected the percentage of nuclei in the G0/G1 and S phases. There was a significant increase in the percentage of nuclei in the G0/G1 phases between fresh and frozen tissue (ANOVA, $F_{4,48}$=19.90, P<0.001, Dunnett's tests, P<0.01; Table 5), and freezing had the opposite effect on S-phase nuclei, namely a decrease in the percentage of nuclei in that phase (ANOVA, $F_{4,48}$=19.14, P<0.001, Dunnett's tests, P<0.01; Table 5). The increase in the percentage of nuclei in the G0/G1 phases in the freezing treatment may be due to a loss of DNA from S-phase nuclei that caused them to be identified as nuclei in the G0/G1 phases on the basis of their fluorescence signal. There was no significant change in the percentage of G0/G1- or S-phase nuclei among the 4 frozen groups of larvae tested (Tukey's tests, P >0.35; Table 5), indicating that DNA was stable during storage of frozen tissue. This result indicates that DNA was lost by S-phase nuclei either during the freezing process or subsequent thawing. There was no significant difference in nRNA fluorescence between fresh and frozen tissues (ANOVA, $F_{4,48}$=2.38, P=0.06; Table 5), indicating no loss of nRNA. RSG1 showed results similar to those as DNA in that RSG1 of frozen tissue was significantly less than RSG1 of fresh tissue, and it was stable during the 10 months of storage of frozen tissue (ANOVA, $F_{4,48}$= 16.70, P<0.001, Dunnett's tests, P<0.01; Tukey's tests >0.90; Table 5).

Discussion

We developed a protocol for staining nRNA in muscle cell nuclei of larvae of Walleye Pollock for use in flow cytometry, and we showed that the inclusion of an nRNA covariate in a model resulted in more accurate measurement of physiological condition than did cell-cycle analysis alone. Accurate assessment of condition of fish larvae is essential because small changes in mortality rate over a long period of time can strongly influence future recruitment (Houde, 1987). RSG1, based on nRNA fluorescence, proved to be an indicator of potential growth that was responsive to feeding conditions, and it contributed meaningful improvement to the discriminant analysis model for assessment of larval condition, as shown by an increase in classification accuracy and a decrease in Akaike's information criterion value. Data from 3 years were used for model testing; therefore, results are not unique to a single group of larvae. The classification accuracy of small larvae (<6.00 mm SL) was most improved (7%). This result is important because that size class includes larvae that have just started to feed, and the S- and G2/M-phase fractions can be highly variable in first-feeding larvae and may not always distinctly indicate condition. Additionally,

Table 3

The ratio of the number of S-phase nuclei to the number of G1-phase nuclei with high nuclear RNA content (RSG1) and values of nuclear RNA (nRNA) fluorescence for larvae of Walleye Pollock (*Gadus chalcogrammus*) sampled from always-fed and unfed treatments reared at different temperatures in 2010. Fluorescence values are arbitrary units and were adjusted on the basis of controls to make samples comparable among sessions of flow cytometry. Standard errors of geometric means of nRNA fluorescence (all cell-cycle phases pooled) and of RSG1 means are reported in parentheses. Cell-cycle phases: G1=gap 1 or cell growth before cell division, G0=resting state from G1 phase, S=DNA synthesis, G2=gap 2 or cell growth before mitosis, and M=mitosis.

Rearing temperature (°C)	Treatment	*n*	RSG1	nRNA fluorescence
2.9	Unfed	28	0.14 (0.01)	32.3 (1.5)
2.9	Always-fed	26	0.26 (0.02)	32.5 (2.0)[1]
5.9	Unfed	13	0.09 (0.01)	26.7 (0.8)
5.9	Always-fed	24	0.19 (0.01)	30.5 (1.9)[2]
8.7	Unfed	17	0.13 (0.02)	26.5 (1.1)

[1] n=14.
[2] n=10.

the sizes of healthy and unhealthy larvae overlap in that size class.

Nuclear RNA varied with rearing temperature, increasing as temperature decreased, a result similar to the findings of other studies on the effect of temperature on RNA content of larval fishes (Canino, 1994; Malzahn et al., 2003). This result also indicates that our nRNA staining protocol worked as intended.

Temperature affected RSG1, and, therefore, it needs to be accounted for when our method is used to measure the condition of larvae sampled from the field. RSG1 for healthy larvae was smaller at warmer temperatures (5.9°C in our study), and this observation may indicate that nuclei were cycling faster through the cell cycle than nuclei at colder temperatures. Other studies have shown that increasing temperature decreases cell-cycle duration in other species, such as yeast (*Saccharomyces cerevisiae*) (Jagadish and Carter, 1978) and Magellan Plunderfish (*Harpagifer bispinis*) (Brodeur et al., 2003). There was no difference in the percentage of S-phase brain cells of fed larvae of Atlantic Cod (*Gadus morhua*) reared at 6°C and 10°C—a finding that was explained by an increased rate of progression by cells through the cell cycle at the higher temperature (González-Quirós et al., 2007). A similar result was also found for S-phase nuclei from muscle cells of larvae of Walleye Pollock reared at 3.2°C and 5.9°C, temperatures comparable to those used in our study (Porter and Bailey, 2011).

RSG1 of unhealthy larvae was not affected by temperature, probably as a result of the slow or ceased growth of these larvae. The brain cells of starved Atlantic Cod larvae reared at 10°C had a smaller percentage of S-phase cells than the brain cells of larvae starved at 6°C (González-Quirós et al., 2007), a difference that may be due to the length of time that the larvae were starved. Fish larvae in general starve faster at higher temperatures, and, for larvae of Walleye Pollock in a previous study, the percentage of S-phase nuclei decreased the longer larvae were starved (Porter and Bailey, 2011). Atlantic Cod larvae at both temperatures were starved for 5 days; therefore, the percentage of S-phase cells of the larvae starved at the higher temperature (10°C) would be expected to be less than the percentage for the larvae starved at the lower temperature.

The loss of DNA during freezing and thawing has been documented for human blood, where about 25% of the DNA was lost (Ross et al., 1990). Differences in nuclear membrane permeability among cell-cycle phases may account for the loss of DNA when larvae of Walleye Pollock were frozen and thawed, and they may explain why there was a decrease in the percentage of muscle cell nuclei in the S phase. S-phase nuclei may be more permeable than G2-phase nuclei (Coverly et al., 1993; Leno and Munshi, 1994), resulting in diffusion of DNA out of the nucleus, and they may rupture because they may be more fragile than nuclei at other phases—an outcome that also would contribute to loss of nuclei. Crytoprotectant has been used to stabilize DNA in brain cells of Walleye Pollock larvae during freezing (Theilacker and Shen, 1993a), and it could possibly be used to prevent the loss of DNA from muscle cell nuclei as well, but the use of cryptoprotectant needs further investigation, particularly for between-laboratory comparisons where standardized protocols are used (Caldarone et al., 2006). In our study, the loss of DNA was unchanged for up to 10 months when the

Table 4

Results of larval condition for laboratory-reared larvae of Walleye Pollock (*Gadus chalcogrammus*) sampled in 2009, 2010, and 2011. Independent cross-validation testing of models without (control) and with (test) the ratio of the number of S-phase nuclei to the number of G1-phase nuclei with high nuclear RNA content (RSG1) included as a covariate. The arcsin $\sqrt{x}$ transformation was used to normalize the fraction of cells in the S phase of the cell cycle, fraction of cells in the G2/M phases of the cell cycle, and RSG1. G2/M=fraction of nuclei in the G2 and M phases combined. Cell-cycle phases: S=DNA synthesis, G2=gap 2 or cell growth before mitosis, and M=mitosis.

Control model
Covariates: standard length, temperature, arcsin $\sqrt{\text{S-phase fraction}}$, arcsin $\sqrt{\text{G2/M-phase fraction}}$

	Classification		
Treatment	Healthy	Unhealthy	Percentage correct
Always-fed	42	7	86
Unfed	1	29	97
		Overall correct	90

Test model
Covariates: standard length, temperature, arcsin $\sqrt{\text{S-phase fraction}}$, arcsin $\sqrt{\text{G2/M-phase fraction}}$, arcsin $\sqrt{\text{RSG1}}$

	Classification		
Treatment	Healthy	Unhealthy	Percentage correct
Always-fed	44	5	90
Unfed	0	30	100
		Overall correct	94

Table 5

Percentages of nuclei in the G0/G1, S, and G2/M phases of the cell cycle, the ratio of the number of S-phase nuclei to the number of G1-phase nuclei with high nuclear RNA content (RSG1), nuclear RNA fluorescence, and DNA fluorescence for muscle cell nuclei from fresh and frozen larvae of Walleye Pollock (*Gadus chalcogrammus*) sampled in 2011. Fluorescence values are arbitrary units and were adjusted on the basis of controls to make samples comparable among sessions of flow cytometry. Standard errors of geometric means of nRNA and DNA fluorescence (all cell-cycle phases pooled), of means for RSG1 and percentages of nuclei in cell-cycle phases are reported in parentheses. G0/G1=percentage of nuclei in G0 and G1 phases combined, G2/M= percentage of nuclei in G2 and M phases combined. Cell-cycle phases: G1=gap 1 or cell growth before cell division, G0=resting state from G1 phase, S=DNA synthesis, G2=gap 2 or cell growth before mitosis, and M=mitosis.

Treatment	*n*	Percentage of nuclei in G0/G1	Percentage of nuclei in S phase	Percentage of nuclei in G2/M phases	RSG1	nRNA fluorescence	DNA fluorescence
Fresh tissue	18	76.7 (1.2)	20.64 (0.97)	2.63 (0.42)	0.37 (0.03)	22.22 (0.43)	14,691.03 (194.93)
Frozen 4 weeks	11	85.3 (0.8)	11.78 (1.27)	2.96 (0.73)	0.18 (0.01)	23.72 (0.68)	12,082.43 (137.11)
Frozen 3 months	10	87.4 (1.0)	8.22 (1.22)	4.36 (0.59)	0.18 (0.02)	21.30 (0.59)	12,866.44 (187.72)
Frozen 6 months	6	87.8 (1.4)	8.50 (1.85)	3.71 (1.05)	0.20 (0.02)	23.69 (0.68)	14,280.30 (144.20)
Frozen 10 months	8	88.2 (1.4)	10.01 (2.00)	1.79 (0.84)	0.19 (0.03)	22.83 (0.82)	14,104.69 (221.88)

tissue was frozen at –80°C, indicating that DNA was stable during that time and under that condition.

Neither freezing and thawing nor storage of frozen tissue affected RNA in muscle cell nuclei of larvae of Walleye Pollock in our study. For frozen human tissue, no significant RNA degradation (as measured by gene expression and electropherograms) was detected after 16 h on ice (Micke et al., 2006), and another study showed that significant RNA degradation did not begin until 30 min after thawing at room temperature (Botling et al., 2009). Although those studies did not measure the amount of RNA present, they do support our assertion that the protocol used in our study was adequate to preserve RNA because larvae were frozen quickly, thawed tissue was kept cool on ice, and the time from tissue thawing to analysis with flow cytometry was typically not longer than 5 h. Our results differ from the findings of Theilacker and Shen (1993b) in that their study indicated that a cryoprotectant and acid were needed before freezing to stabilize RNA in brain cells of larvae of Walleye Pollock. This difference in results may be due to the difference in type of tissue used (muscle cell nuclei versus whole brain cells) (Olivar et al., 2009) or in the method used for preparation of tissue for flow cytometry. In Theilacker and Shen (1993b), tissue dissection occurred before freezing and whole cells were analyzed; however, in our study, tissue preparation occurred after freezing, and only nuclei were used.

Our results indicate that only frozen tissue should be analyzed when condition is measured with the method described here. Results would be inaccurate if fresh tissue were used because of its higher fraction of S-phase nuclei. Cell-cycle measurements (fraction of S- and G2/M-phase nuclei pooled) of independent groups of larvae of Walleye Pollock reared under similar conditions were not significantly different (Porter and Bailey, 2011), indicating that the effect of freezing and thawing was consistent. Freezing and thawing of tissue was also part of the method used in another study where standardized protocols were used for spectrofluorometric analysis of RNA and DNA for assessing larval fish physiological condition (Caldarone et al., 2006).

Conclusions

An nRNA covariate improved larval condition measurements. For minimal cost (the cost of the Syto RNASelect stain), model accuracy increased, and the greatest improvement was for small larvae. The assay that we developed in our study quickly determines condition, and, therefore, many larvae can be analyzed in a short period of time. In addition, larvae can be kept frozen for at least 10 months without affecting condition measurements. There is no diel pattern in RNA content or measurements of the cell-cycle phases for larvae of Walleye Pollock (Bailey et al., 1995; Theilacker and Shen, 2001); therefore, our method can be applied in the field, where sampling can occur anytime during a 24-h period. Because we found that temperature affected RSG1, future studies should include measurements at additional temperatures to formulate a model for field-sampled larvae.

Acknowledgments

We would like to thank A. Dougherty for collection of Walleye Pollock eggs and her assistance in the laboratory. D. Prunkard at the University of Washington, Department of Pathology, Cytometry Core Facility assisted with flow cytometry. F. Morado, M. Paquin and 3 anonymous reviewers provided helpful comments on earlier drafts of the manuscript. This research was funded by the North Pacific Research Board (NPRB grant no. 926, publication 432) and the Alaska Fisheries Science Center. It is contribution EcoFOCI-0800 to NOAA's Ecosystems and Fisheries-Oceanography Coordinated Investigations.

Literature cited

Bailey, K. M., and J. Yen.
1983. Predation by a carnivorous marine copepod, *Euchaeta elongata* Esterly, on eggs and larvae of the Pacific hake, *Merluccius productus*. J. Plankton Res. 5:71–82.

Bailey, K. M., M. F. Canino, J. M. Napp, S. M. Spring, and A. L. Brown.
1995. Contrasting years of prey levels, feeding conditions and mortality of larval walleye pollock *Theragra chalcogramma* in the western Gulf of Alaska. Mar. Ecol. Prog. Ser. 119:11–23.

Botling, J., K. Edlund, U. Segersten, S. Tahmasebpoor, M. Engström, M. Sundström, P. Malmström, and P. Micke.
2009. Impact of thawing on RNA integrity and gene expression analysis in fresh frozen tissue. Diagn. Mol. Pathol. 18:44–52.

Brodeur, J. C., J. Calvo, A. Clarke, and I. A. Johnston.
2003. Myogenic cell cycle duration in *Harpagifer* species with sub-Antarctic and Antarctic distributions: evidence for cold compensation. J. Exp. Biol. 206:1011–1016.

Bromhead, D., J. Kalish, and P. Waring.
2000. Application of flow cytometric cell cycle analysis to the assessment of condition and growth in larvae of a freshwater teleost *Galaxias olidus*. Can. J. Fish. Aquat. Sci. 57:732–741.

Buckley, L., E. Caldarone, and T. L. Ong.
1999. RNA–DNA ratio and other nucleic acid-based indicators for growth and condition of marine fishes. Hydrobiologia 401:265–277.

Burnham, K. P., and D. R. Anderson.
2002. Model selection and multimodel inference: a practical information-theoretic approach, 2nd ed., 497 p. Springer-Verlag New York, Inc., New York.

Caldarola, S., M. C. De Stefano, F. Amaldi, and F. Loreni.
2009. Synthesis and function of ribosomal proteins—fading models and new perspectives. FEBS Journal 276:3199–3210.

Caldarone, E. M., C. M. Clemmesen, E. Berdalet, T. J. Miller, A. Folkvard, G. J. Holt, M. P. Olivar, and I. M. Suthers.
2006. Intercalibration of four spectroflourometric protocols for measuring RNA/DNA ratios in larval and juvenile fish. Limnol. Oceanogr. Methods 4:153–163.

Canino, M. F.
1994. Effects of temperature and food availability on growth and RNA/DNA ratios of walleye pollock *Theragra chalcogramma* (Pallas) eggs and larvae. J. Exp. Mar. Biol. Ecol. 175:1–16.

Coverly, D., C. S. Downes, P. Romanowski, and R. A. Laskey.
1993. Reversible effects of nuclear membrane permeabilization on DNA replication: evidence for a positive licensing factor. J. Cell Biol. 122:985–992.

Darzynkiewicz, Z., F. Traganos, and M. R. Melamed.
1980. New cell cycle compartments identified by multiparameter flow cytometry. Cytometry 1:98–108.

Domingos, J. A., P. Fromm, C. Smith-Keune, and D. R. Jerry.
2012. A robust flow-cytometric protocol for assessing growth rate of hatchery-reared barramundi *Lates calcarifer* larvae. J. Fish Biol. 80:2253–2266.

Folkvord, A., and J. R. Hunter.
1986. Size-specific vulnerability of northern anchovy, *Engraulis mordax*, larvae to predation by fishes. Fish. Bull. 84:859–869.

González-Quirós, R., I. Munuera, and A. Folkvord.
2007. Cell cycle analysis of brain cells as a growth index in larval cod at different feeding conditions and temperatures. Sci. Mar. 71:485–497.

Houde, E. D.
1987. Fish early life dynamics and recruitment variability. Am. Fish. Soc. Symp. 2:17–29.

Jagadish, M. N., and B. L. A. Carter.
1978. Effects of temperature and nutritional conditions on the mitotic cell cycle of *Saccharomyces cerevisiae*. J. Cell Sci. 31:71–78.

Leno, G. H., and R. Munshi.
1994. Initiation of DNA replication in nuclei from quiescent cells requires permeabilization of the nuclear membrane. J. Cell Biol. 127:5–14.

Li, Q., K. Yunkyung, J. Namm, A. Kulkarni, G. R. Rosania, Y-H. Ahn, and Y. T. Chang.
2006. RNA-selective, live cell imaging probes for studying nuclear structure and function. Chem. Biol. 13:615–623.

Lochmann, S. E., G. L. Maillet, K. T. Frank, and C. T. Taggart.
1995. Lipid class composition as a measure of nutritional condition in individual larval Atlantic cod (*Gadus morhua*). Can. J. Fish. Aquat. Sci. 52:1294–1306.

Malzahn, A. M., C. Clemmesen, and H. Rosenthal.
2003. Temperature effects on growth and nucleic acids in laboratory-reared larval coregonid fish. Mar. Ecol. Prog. Ser. 259:285–293.

Micke, P., M. Ohshima, S. Tahmasebpoor, Z.-P. Ren, A. Östman, F. Pontén, and J. Botling.
2006. Biobanking of fresh frozen tissue: RNA is stable in nonfixed surgical specimens. Lab. Invest. 86:202–211.

Murray, A., and T. Hunt.
1993. The cell cycle: an introduction, 251 p. Oxford Univ. Press, Inc., New York.

O'Connell, C. P.
1980. Percentage of starving northern anchovy, *Engraulis mordax*, larvae in the sea as estimated by histological methods. Fish. Bull. 78:475–489.

Olivar, M. P., M. V. Diaz, and M. A. Chícharo.
2009. Tissue effect on RNA:DNA ratios of marine fish larvae. Sci. Mar. 73S1:171–182.

Piwnicka, M., Z. Darzynkiewicz, and M. R. Melamed.
1983. RNA and DNA content of isolated cell nuclei measured by multiparameter flow cytometry. Cytometry 3:269–275.

Porter, S. M., and K. M. Bailey
2011. Assessing the condition of walleye pollock *Theragra chalcogramma* (Pallas) larvae using muscle-based flow cytometric cell cycle analysis. J. Exp. Mar. Biol. Ecol. 399:101–109.

Porter, S. M., and G. H. Theilacker.
1999. The development of the digestive tract and eye in larval walleye pollock, *Theragra chalcogramma*. Fish. Bull. 97:722–729.

Ross, K. S., N. E. Haites, and K. F Kelly.
1990. Repeated freezing and thawing of peripheral blood and DNA in suspension: effects on DNA yield and integrity. J. Med. Genet. 27:569–570.

Sirri, V., S. Urcuqui-Inchima, P. Roussel, and D. Hernandez-Verdun.
2008. Nucleolus: the fascinating body. Histochem. Cell Biol. 129:13–31.

Staiano-Coico, L., Z. Darzynkiewicz, and C. K. McMahon.
1989. Cultured human keratinocytes: discrimination of different cell cycle compartments based upon measurement of nuclear RNA or total cellular RNA content. Cell Tissue Kinet. 22:235–243.

Theilacker, G. H.
1978. Effect of starvation on the histological and morphological characteristics of jack mackerel, *Trachurus symmetricus*, larvae. Fish. Bull. 76:403–414.
1986. Starvation-induced mortality of young sea-caught jack mackerel, *Trachurus symmetricus*, determined with histological and morphological methods. Fish. Bull. 84:1–17.

Theilacker, G. H., and S. M. Porter.
1995. Condition of larval walleye pollock, *Theragra chalcogramma*, in the western Gulf of Alaska assessed with histological and shrinkage indices. Fish. Bull. 93:333–344.

Theilacker, G. H., and W. Shen.
1993a. Fish larval condition analyzed using flow cytometry. *In* Physiological and biochemical aspects of fish development (B. T. Walther, and H. J. Fyhn, eds.), p. 346–355. Univ. Bergen, Bergen, Norway.
1993b. Calibrating starvation-induced stress in larval fish using flow cytometry. Am. Fish. Soc. Symp. 14:85–94.
2001. Evaluating growth of larval walleye pollock, *Theragra chalcogramma*, using cell cycle analysis. Mar. Biol. 135:897–907.

Theilacker G. H., K. M. Bailey, M. F. Canino, and S. M. Porter.
1996. Variations in larval walleye pollock feeding and condition: a synthesis. Fish. Oceanogr. 5(suppl. 1):112–123.

Abstract—Piscivorous fishes, many of which are economically valuable, play an important role in marine ecosystems and have the potential to affect fish and invertebrate populations at lower trophic levels. Therefore, a quantitative understanding of the foraging ecology of piscivores is needed for ecosystem-based fishery management plans to be successful. Abundance and stomach contents of seasonally co-occurring piscivores were examined to determine overlap in resource use for Summer Flounder (*Paralichthys dentatus*; 206–670 mm total length [TL]), Weakfish (*Cynoscion regalis*; 80–565 mm TL), Bluefish (*Pomatomus saltatrix*; 55–732 mm fork length [FL]), and Striped Bass (*Morone saxatilis*; 422–920 mm FL). We collected samples from monthly, fishery-independent trawl surveys conducted on the inner continental shelf (5–27 m) off New Jersey from June to October 2005. Fish abundances and overlaps in diet and habitat varied over this study period. A wide range of fish and invertebrate prey was consumed by each species. Diet composition (determined from 1997 stomachs with identifiable contents) varied with ontogeny (size) and indicated limited overlap between most of the species size classes examined. Although many prey categories were shared by the piscivores examined, different temporal and spatial patterns in habitat use seemed to alleviate potential competition for prey. Nevertheless, the degree of overlap in both fish distributions and diets increased severalfold in the fall as species left estuaries and migrated across and along the study area. Therefore, the transitional period of fall migration, when fish densities are higher than at other times of the year, may be critical for unraveling resource overlap for these seasonally migrant predators.

Manuscript submitted 24 October 2012.
Manuscript accepted 26 August 2013.
Fish. Bull. 111:352–369.
doi: 10.7755/FB.111.4.5

The views and opinions expressed or implied in this article are those of the author (or authors) and do not necesarily reflect the position of the National Marine Fisheries Service, NOAA.

Habitat and diet overlap of 4 piscivorous fishes: variation on the inner continental shelf off New Jersey

Mark J. Wuenschel (contact author)[1]
Kenneth W. Able[1]
James M. Vasslides[1]
Donald M. Byrne[2*]

Email address for contact author: mark.wuenschel@noaa.gov

[1] Marine Field Station
Rutgers University
800 c/o 132 Great Bay Boulevard
Tuckerton, New Jersey 08087-2004
Present address for contact author: Northeast Fisheries Science Center
National Marine Fisheries Service, NOAA
166 Water St.
Woods Hole, Massachusetts 02543

[2] New Jersey Department of Environmental Protection
Nacote Creek Research Station
P.O. Box 418
Port Republic, New Jersey 08241

[*] Deceased

Predator species and their interactions with prey and other predator species play an important role in determination of the structure and function of ecosystems (Schmitz, 2007; Braga et al., 2012)—an especially important concern because populations of many predators have declined in abundance (Myers and Worm, 2003; Heithaus et al., 2008). In marine ecosystems, piscivorous fishes have the potential to affect fish and invertebrate populations at lower trophic levels. In some cases, direct removals of prey resources by piscivorous fishes have been shown to rival or even exceed the removals by commercial fisheries (Buckel et al., 1999c; Overholtz et al., 2000; Overholtz and Link, 2007). Therefore, fish trophic ecology is relevant to several aspects of fisheries management (Link, 2002). With the general move toward multispecies and ecosystem-based approaches to fisheries management, there is a need for more comprehensive information on food web structure, interspecific trophic interactions, and predator movements (Andrews and Harvey, 2013).

In temperate zones, many coastal marine fishes undergo large-scale seasonal and ontogenetic shifts in their spatial distribution. Examples from the east coast of the United States include species that migrate north to New England in summer and south to the Carolinas in winter (e.g., Striped Bass [*Morone saxatilis*] and Bluefish [*Pomatomus saltatrix*]) and species that move inshore in summer and offshore in winter (e.g., Summer Flounder [*Paralichthys dentatus*] and Weakfish [*Cynoscion regalis*]) (Able and Fahay, 2010). Further, many temperate, estuarine-dependent species in the Middle Atlantic Bight leave estuaries in the fall of their first year to avoid cold winter temperatures (Able and Fahay, 1998; 2010). Many of these young-of-the-year (YOY) fishes are piscivorous and their egress from estuaries to coastal waters acts to concentrate them in time and space with other

species or size classes, increasing the potential for both interspecific and intraspecific interactions. Interspecific competition and resource partitioning have been well documented for fish species in freshwater systems (Persson et al., 1999; Sutton and Ney, 2002; Bellgraph et al., 2008), where the potential for interactions may be greater than it is in marine systems given the closed nature of freshwater systems and fish populations. This interspecific competition and resource partitioning may apply to some degree in estuaries as well, as has been reviewed for European estuaries (Elliot and Hemingway, 2002). In contrast, because of the openness of marine populations and the ability of individuals to move great distances, interspecific competition in most marine systems likely is highly variable in time and space, making it more difficult to document and study interspecific competition in marine systems than in freshwater populations.

Summer Flounder, Weakfish, Bluefish, and Striped Bass are important commercial and recreational species in New Jersey and elsewhere on the east coast of the United States. These species co-occur seasonally and feed on similar prey, indicating potential for competitive interactions. However, studies of food habits for these species generally have focused on estuarine collections (Gartland et al., 2006; Latour et al., 2008) or have been limited to seasonal, offshore (at depths of 5–400 m) collections aggregated over multiple years (Buckel et al., 1999b, Garrison and Link, 2000a, 2000b; Link et al., 2002; Overton et al., 2008; Woodland et al., 2011). Further, most prior studies on these species typically have focused on a single (Gartland et al., 2006; Latour et al., 2008) or a pair of species (Buckel and McKown, 2002; Buckel et al., 2009). Because of the spatial and temporal variability in competitive interactions between migratory fishes, studies span-

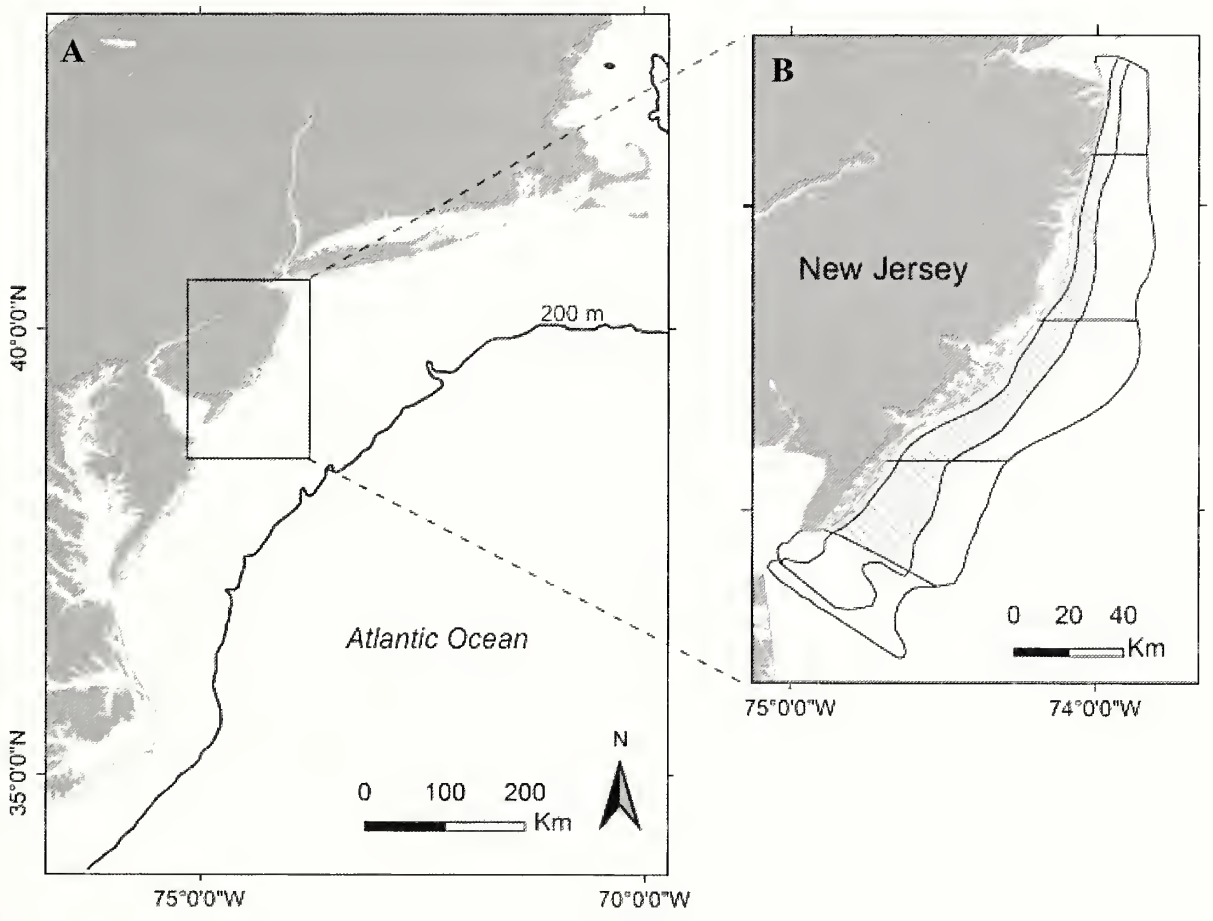

Figure 1

(**A**) Study area where Summer Flounder (*Paralichthys dentatus*), Weakfish (*Cynoscion regalis*), Bluefish (*Pomatomus saltatrix*), and Striped Bass (*Morone saxatilis*) were sampled in 2005 along the northeastern coast of the United States for a 5-month study of habitat and diet overlap of these 4 piscivorous fishes and (**B**) sample collection area off New Jersey with the 15 strata outlined (strata were defined on the basis of latitudinal boundaries and depth contours of 9, 18, and 27 m). In June, August, and October, all strata were sampled. In July and September, only strata indicated with diagonal lines were sampled.

ning multiple years, such as many of the ones listed above, potentially blur or miss finer-scale interactions that occur over shorter intervals. Therefore, to evaluate potential interactions between mobile, seasonally migratory species, information on spatial distributions and food habits is needed at finer spatial and temporal scales (Rudershausen et al., 2010). Although resource overlap among Summer Flounder, Weakfish, Bluefish, and Striped Bass has been indicated by or inferred in prior studies (Garrison and Link, 2000b), often over broad areas or time periods, a rigorous evaluation of these interactions at a more relevant ecological scale is lacking.

The objectives for this study were to compare habitat use and food habits of 4 common predators of the Middle Atlantic Bight over the course of a 5-month period of co-occurrence in nearshore (inner continental shelf) waters. The degree of overlap in both habitat and diet between different size classes of these 4 predators was quantified to determine resource overlap at a fine spatial and temporal scale.

Materials and methods

The distribution, abundance, and diet of Summer Flounder, Weakfish, Bluefish, and Striped Bass were evaluated from 20-min bottom trawls (30-m headrope, 6-mm codend liner [Byrne, 1994; Wuenschel et al., 2012]) conducted in inner continental shelf waters of New Jersey in collaboration with the Bureau of Marine Fisheries of the New Jersey Department of Environmental Protection. Through the use of a depth-stratified random sampling design, samples were taken during daylight hours at depths of 5 to 27 m along the New Jersey coast from the entrance of New York Harbor to the entrance of Delaware Bay (Fig. 1). The survey area was divided into 15 strata (Fig. 1) on the basis of latitudinal boundaries and depth contours (9, 18, and 27 m; Byrne, 1994). In June, August, and October 2005, all depths and strata were sampled with 2 tows per strata, plus 1 additional tow in each of the 9 largest strata (39 tows, Table 1; see Byrne 1994 for details). In the intervening months (July and September), sampling was undertaken with a bottom trawl net, bridles, and towing cables that were identical to the ones used in June, August, and October and were fished from the same vessel (RV *Seawolf*, SUNY Stonybrook) used during the other months, but because of constraints on vessel time, sampling was limited to 2 or 3 tows in nearshore and mid-shore depths for all but the northernmost and southernmost strata (18 tows, July; 12 tows, September; Table 1, Fig. 1). Representative subsamples, with a mean of 8.4 (9.6 standard deviation [SD]) per species per tow, of Summer Flounder, Weakfish, Bluefish, and Striped Bass were selected to cover the range of lengths of fish collected in a given tow for analysis of gut contents. Stomachs were re-

Table 1

Summary of samples collected in 2005 off the coast of New Jersey for this study of habitat and diet overlap of 4 piscivorous fishes. Collection month and sampling effort (numbers of tows in parentheses), numbers of fish collected, stomachs analyzed in the laboratory, and stomachs with prey in the gut for small, medium, and large Summer Flounder (*Paralichthys dentatus*), PdS, PdM, PdL; small, medium, and large Weakfish (*Cynoscion regalis*), CrS, CrM, CrL; small and large Bluefish (*Pomatomus saltatrix*), PsS, PsL; and Striped Bass (*Morone saxatilis*), Ms.

		PdS	PdM	PdL	CrS	CrM	CrL	PsS	PsL	Ms
June (39)	Fish collected	85	170	80	1	774	1	9	4	7
	Stomachs analyzed	47	63	35	0	46	1	0	6	0
	Stomachs with prey	30	42	26	0	42	1	0	4	0
July (18)	Fish collected	134	296	61	64	6319	0	48	3	0
	Stomachs analyzed	72	153	51	0	125	0	21	3	0
	Stomachs with prey	39	74	12	0	116	0	18	3	0
August (39)	Fish collected	302	950	148	2587	4232	31	890	23	214
	Stomachs analyzed	71	245	108	100	109	7	150	20	27
	Stomachs with prey	64	178	62	99	84	5	105	17	11
September (12)	Fish collected	29	783	116	17,836	11,752	189	2370	6	0
	Stomachs analyzed	4	117	22	134	58	5	185	5	0
	Stomachs with prey	3	74	8	96	45	5	147	2	0
October (39)	Fish collected	12	192	31	9746	10,275	1786	616	70	123
	Stomachs analyzed	6	134	26	172	93	86	156	67	89
	Stomachs with prey	3	79	13	130	75	66	130	52	37
All months (147)	Fish collected	562	2391	436	30,234	33,352	2007	3927	112	344
	Stomachs analyzed	200	712	242	406	431	99	512	101	116
	Stomachs with prey	139	447	121	325	362	77	400	78	48

moved immediately after capture and preserved in formalin for laboratory analysis. In some months, tagging and releasing Striped Bass was a higher priority than determining stomach contents; therefore, all fishes captured were not available for diet analysis.

To account for size-related changes in habitat use (Able and Fahay, 2010), diet composition within species (Garrison and Link, 2000b), and interactions across species (Buckel and McKown, 2002), species were split into multiple size classes when data permitted: small (Summer Flounder: 200–300 mm total length [TL]; Weakfish: 80–200 mm TL; Bluefish: 55–300 mm fork length [FL]), medium (Summer Flounder: 301–400 mm TL; Weakfish: 201–350 mm TL), and large (Summer Flounder: 401–670 mm TL; Weakfish: 351–565 mm TL; Bluefish: 301–732 mm FL). For Striped Bass, a single size class was used because of limited sample sizes, the absence of prior evidence for ontogenetic shifts beyond the YOY stage (Walter et al., 2003), and the relatively large sizes of our specimens (422–920 mm FL).

Diet analysis

In the laboratory, preserved stomachs were carefully opened and the contents transferred to a solution of rose bengal stain and 95% ethyl alcohol. Prey items were identified to the lowest practical taxonomic level by using available keys and guides for the Mid-Atlantic region (Weiss, 1995; Able and Fahay, 1998) and enumerated. For each stomach, abundant or large prey types were sorted and placed on preweighed filter papers or aluminum weighing pans and dried to a constant weight (±0.0001 g) in a drying oven (70°C). Dry weights were chosen because they are more representative of nutritional value and have less weighing error than wet weights (Hyslop, 1980), especially for small or partial prey (Carr and Adams, 1972). For small and, therefore, hard-to-separate prey items (e.g., copepods and mysids), an aggregate sample was dried and the percent contribution by volume of different prey types was recorded and later converted to weights. Through the use of this protocol, prey-specific dry weights were obtained directly for larger prey or estimated from aggregate samples of smaller, mixed prey items for each stomach analyzed.

Trawl collections yielded "clusters" of individuals within species and size classes per location; therefore, the percent contribution by weight of prey items was calculated with the following cluster sampling estimator (Buckel et al., 1999a; 1999b; Gartland et al., 2006). For a given size class of a predator, the percent contribution by weight of each prey type k ($\%W_k$) to the diet was calculated with the following equation:

$$\%W_k = \frac{\sum_{i=1}^{n} M_i q_{ik}}{\sum_{i=1}^{n} M_i} \cdot 100, \quad (1)$$

where $q_{ik} = \frac{W_{ik}}{W_i}$;

n = the number of trawls;

M_i = the number of species size class sampled per tow i;

w_i = the total dry weight of all prey in stomachs for that species size class in tow I; and w_{ik} = the total dry weight of prey type k in all stomachs for that species size class collected in tow i.

To facilitate analysis, prey items were grouped into the following general categories: squids (predominantly *Loligo* spp.), decapod crustaceans (including swimming crabs, sand crabs, rock crabs [*Cancer borealis* and *C. irroratus*], spider crabs, hermit crabs, decapod zoea, and shrimps [predominately *Crangon septemspinosa* and *Palaemonetes* sp.]), nondecapod crustaceans (including amphipods, isopods, cumaceans, mysids, and mantis shrimp), bivalves (clams and periwinkles), fishes (44 species identified), worms and wormlike organisms (nematodes, polychaetes, annelids, and leeches), and other unidentified (UID) items (inorganic matter, organic matter, eggs, and insects). In addition, prey items (species or higher taxa) that contributed on average >5% by weight to the overall mean diet of a species size class were included as additional prey categories. Therefore, if Bay Anchovy (*Anchoa mitchilli*) composed >5% of the diet for a given species size class in any month, it was included as a prey category and the category "fishes" represented all remaining fish prey that contributed <5% to the diet of that species size.

The cumulative trophic diversity was calculated for each species size class to determine whether the sample sizes that were analyzed were sufficient to describe the diet of a given species size class in each month (Ferry and Cailliet, 1996; Cortés, 1997; Braccini et al., 2005; Belleggia et al., 2008). The Shannon-Wiener index (H'), which describes entropy on the basis of information theory, was calculated as each stomach that contained prey was added to the analysis for 100 randomizations of the data for each species size class:

$$H' = -\sum_{i=1}^{S} (p_i) \cdot (\log_e p_i), \quad (2)$$

where S = the number of prey categories; and

p_i = the proportion of the cumulative (total) sample (gut contents) represented by the ith prey category.

Following Jost (2006), H' was converted to effective number of species ($\exp(H')$), a true diversity. Only groups (monthly species size classes) with mean trophic diversity curves that appeared asymptotic or with >40 sampled guts were included in the similarity analysis (described in the next paragraph).

To evaluate the degree of similarity in diets between species and size classes, nonmetric multidimensional scaling (nMDS) and hierarchical clustering were used

within each month and across all months (PRIMER-E, Ltd., Plymouth, UK[1]). The nMDS data were calculated as the percentage of diet by weight for each month and each species-size-class combination and were log-transformed before use in the Bray-Curtis index to construct the sample similarity matrix. Group-average hierarchical clustering was then used to identify those predators that had dietary similarities at the 60% level following Jaworski and Ragnarsson (2006) and Clarke and Warwick (2001).

Habitat and diet overlap

Habitat and diet overlap between pairs of species size classes were determined through the use of Schoener's index (Schoener 1970). This index was calculated with this equation:

$$\alpha = 1 - 0.5\left(\sum_{i=1}^{n} |pij - pik|\right), \quad (3)$$

which shows the overlap (α), where pij and pik are the proportions of the ith resource (trawl station or prey proportion) used by species j and k, respectively. Index values range from 0 to 1, with values >0.6 representing biologically important overlap in resource use (Wallace, 1981; Buckel and McKown, 2002; Bethea et al., 2004).

Results

Spatial distribution, abundance, and sizes

The spatial distribution, abundance, and size distribution for each of the 4 predators were variable over the course of our 5-month study (Table 1, Figs. 2 and 3). Summer Flounder were the most consistently collected species throughout this study. They were distributed throughout our study area, with a slight shift in abundance from offshore to inshore in summer followed by the reverse in fall. The size distribution of Summer Flounder was relatively constant, with individuals of 206–670 mm TL representing a broad range of age classes (YOY to 4+) collected from June to October. Weakfish (80–565 mm TL) also were collected consistently, with greater abundances occurring inshore. Catches of Weakfish in June and July were dominated by larger size classes (>200 mm TL), with smaller size classes (YOY or 1+, ≤200 mm TL) becoming abundant from August to October. Similarly, Bluefish (55–732 mm FL) were most abundant inshore. They were dominated by larger size classes (>300 mm FL) in June, with smaller size classes (≤300 mm FL) becoming abundant inshore from July to October.

Striped Bass, which were typically larger (422–920 mm FL) than the other 3 species (Fig. 3), were less abundant and highly variable in time and space. In June and August, collections of Striped Bass were limited to the northernmost strata of the sample area. No Striped Bass were collected in July and September, likely because the northern strata were not sampled during those months. In October, Striped Bass were distributed throughout our study area. In all months in which they were collected, they were typically inshore.

Diet analysis

Because of limited or zero abundance of some species size classes in some months (described previously), sampling limitations, and the occurrence of empty stomachs, adequate food habit information was not obtained over all species size classes or months. The relative contributions of prey types to the diets for species size classes in each month are summarized in Table 2 (species size classes with insufficient samples sizes to be included in subsequent analyses are presented). For the groups that were considered adequately sampled for diet description (Fig. 4) and, therefore, included in the cluster analysis, the cumulative trophic diversity curves indicated that sample sizes of 30–40 guts were sufficient to characterize the diet in most cases. However, for some monthly species size classes (e.g., medium Weakfish in August and medium Summer Flounder in October) trophic diversity continued to increase beyond 40 guts analyzed.

Size-specific patterns in trophic diversity differed across species, with Summer Flounder showing decreased diversity with size in June. In contrast, larger size classes of Weakfish in August and Bluefish in October had more diverse diets than did smaller size classes of these species. Overall, diversity of prey items increased throughout time in Summer Flounder and Striped Bass, and it remained low for small Bluefish. Weakfish diet diversity also was relatively stable through the 5-month period of this study, with the exception of the high trophic diversity of the medium size class of this species in August.

Cluster analysis separated the size classes for each of the 4 species into 3 groups in June at the 60% similarity level (Fig. 5). The first group consisted of large (>400 mm TL) Summer Flounder, which preyed predominantly on squids (88.1%) (Table 2). Small and medium Summer Flounder formed the second group, and medium (201–350 mm TL) Weakfish the third. Although the second and third groups consumed mostly fishes (0–73.3% sand lances [*Ammodytes* spp.] and 6.1–52.9% UID and other fishes), they were separated by the amounts of decapod crustaceans (2.1–20.9%) and squids (8.3–21.5%) in the former and mysids (33.4%) in the latter.

In July, the cluster analysis identified 3 groups at the 60% similarity level from among the 4 species size classes for which enough data were available. Small and medium Summer Flounder were grouped together, with diets consisting of both pelagic and benthic prey, including Butterfish (*Peprilus triacanthus*; 15.8–18.7%),

[1] Mention of trade names or commercial companies is for identification purposes only and does not imply endorsement by the National Marine Fisheries Service, NOAA.

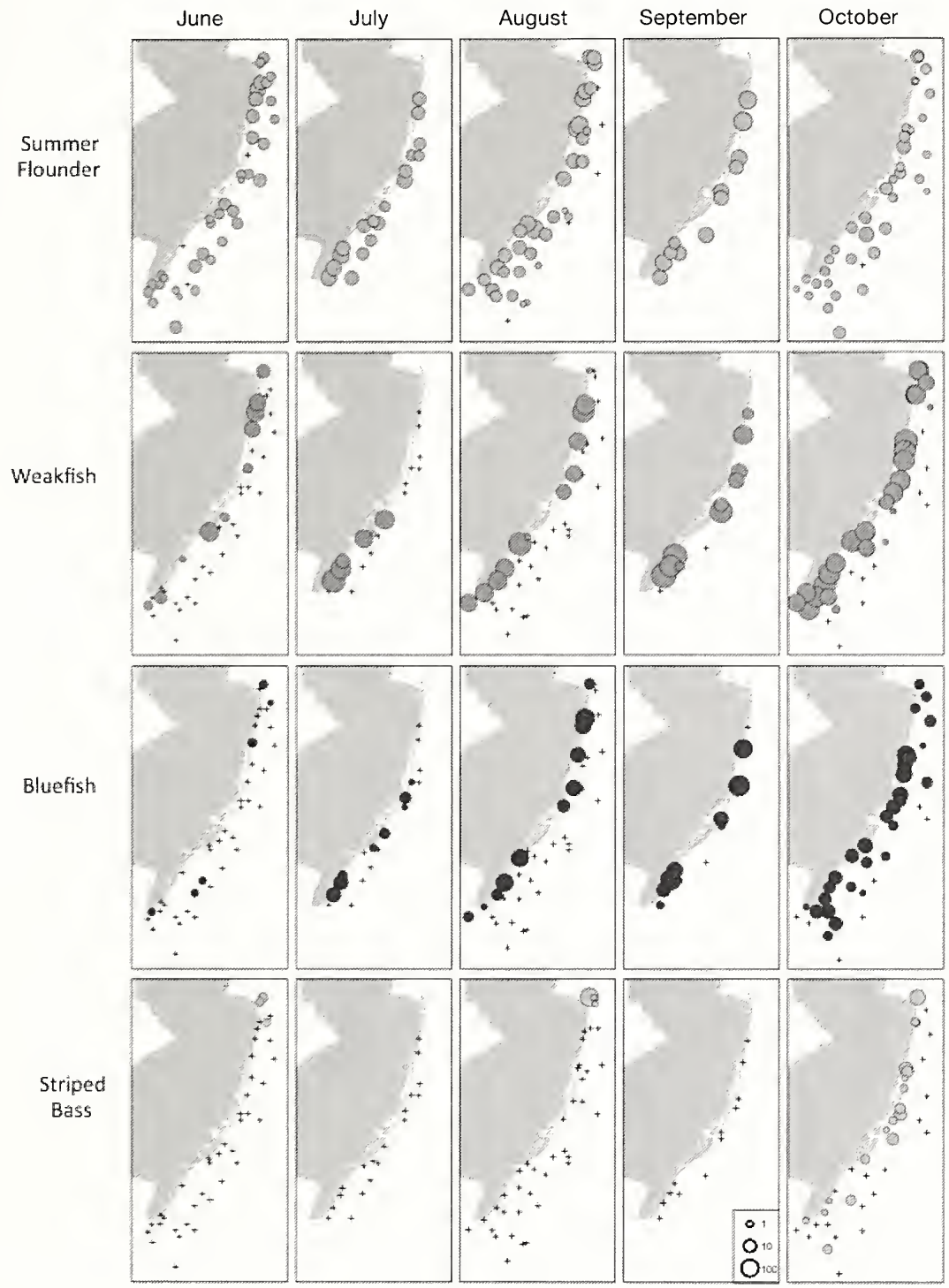

Figure 2

Distributions of Summer Flounder (*Paralichthys dentatus*), Weakfish (*Cynoscion regalis*), Bluefish (*Pomatomus saltatrix*), and Striped Bass (*Morone saxatilis*) sampled in June, July, August, September, and October of 2005 along the coast of New Jersey for this study. Circles are shaded by species and represent abundance (log transformed), with the same scale in all frames, and crosses indicate zero catches. See Table 1 for a summary of numbers caught for each species.

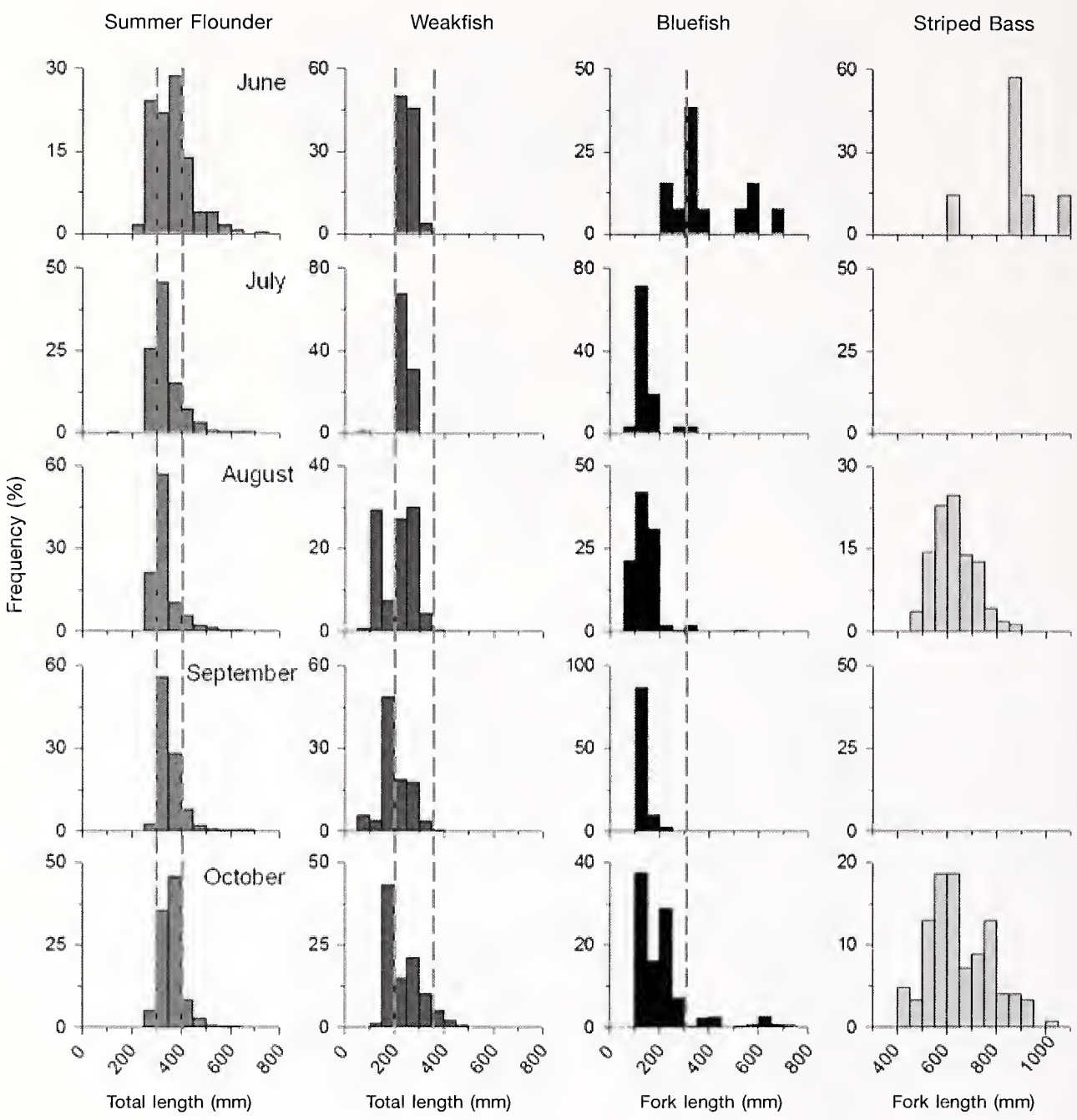

Figure 3

Length distributions (percent frequency) for Summer Flounder (*Paralichthys dentatus*), Weakfish (*Cynoscion regalis*), Bluefish (*Pomatomus saltatrix*), and Striped Bass (*Morone saxatilis*) collected from June (top row) to October (bottom row) in 2005 off the coast of New Jersey for this study. Bars are shaded by species (as in Fig. 2). Vertical, dashed gray lines indicate breakpoints between size classes. Note that the *x*-axis scales are different across species and the *y*-axis scales are different across months within species.

Table 2

Stomach contents of small, medium, and large Summer Flounder (*Paralichthys dentatus*), PdS, PdM, PdL; small, medium, and large Weakfish (*Cynoscion regalis*), CrS, CrM, CrL; small and large Bluefish (*Pomatomus saltatrix*), PsS, PsL; Striped Bass (*Morone saxatilis*), Ms, for this study of habitat and diet overlap of these 4 piscivorous fishes. All samples were collected in 2005 off the coast of New Jersey. Diet is summarized by month and for all months. $\%W_k$ is the proportion of identifiable prey to the diet by weight. Note that proportions from cluster estimators do not add up to 100% in all cases (see main text for calculation). An asterisk (*) indicates groups with insufficient sample sizes for inclusion in the analysis with nonmetric multidimensional scaling. UID=unidentified.

		n (no. of stomachs with prey)	*Anchoa mitchilli*	*Anchoa* spp.	*Brevoortia tyrannus*	*Ammodytes* spp.	*Cynoscion regalis*	*Etrumeus teres*	*Peprilus triacanthus*	*Sphoeroides maculatus*	UID and other fishes	Rock crabs	*Ovalipes ocellatus*	UID and other crabs	Mysids	Shrimps	Decapod crustaceans	Nondecapod crustaceans	Bivalves	Mollusks	Squids	Worms and wormlike prey	Other
Jun	CrM	42									52.9				33.4	0.7	9.4	0.7					2.9
	CrL*	1															21.2						78.8
	PdS	30				10.0					21.8	2.7			5.3		20.9	9.7	3.3		21.5		1.7
	PdM	42		1.5		73.3			0.8		6.1	4.9			<0.1	<0.1	2.1	0.1			8.3		2.8
	PdL	26		0.3		10.3					0.1						0.1				88.1		1.1
	PsL*	4				94.0																	6.0
Jul	CrM	116	15.6	1.5		0.9					4.2	0.1	1.7	1.6	62.4	1.5	5.1	3.4				0.5	1.3
	PdS	39				4.2	16.4		18.7		24.7	2.7	1.8	2.6	20.6	0.6	1.6	4.7					1.4
	PdM	74	2.9			0.9		9.8	15.8		35.3	23.8	0.3	3.0	4.8	0.4	0.6	<0.1	0.1		1.4	<0.1	0.7
	PdL*	12	1.4						61.6		24.3	9.5			1.9						1.1		0.1
	PsS	18	29.9	31.3							38.8					0.1							
	PsL*	3		19.1					52.6		28.2				0.1								
Aug	CrS	99	5.1	4.8							42.1			0.2	36.3	3.2	7.0	0.2				0.2	0.9
	CrM	84	7.6	10.0			23.5				28.5		1.2	1.6	16.3	8.0	0.8	0.2			0.2	2.0	0.2
	CrL*	5		10.9							54.2			10.1	0.7	0.1		0.1					24.0
	Ms	11							2.2		6.1		<0.1	0.2		<0.1	0.1	0.1	45.3		0.6	<0.1	0.1
	PdS	64		10.6					8.4		21.5	0.4	7.9	4.7	37.9	4.0	2.8		0.6				0.7
	PdM	178	2.5	0.8				7.6	1.2		41.0	11.8	6.2	4.3	19.7	0.1	0.3		0.4	0.1	3.5		0.3
	PdL	62	1.4	0.6				28.9	2.6		29.7	6.4	0.1	0.7	0.7		0.3		<0.1		28.0		0.5
	PsS	105	56.3	19.3			9.5		0.6		12.3			<0.1	0.5	<0.1	0.3				0.8		0.5
	PsL*	17	29.7	0.2					0.4		18.2		<0.1						23.5		4.2		0.2
Sep	CrS	96	20.5	8.7							33.4			<0.1	33.5	0.4	1.4	0.2			0.8		1.1
	CrM	45	33.1	2.3							25.3				34.5	0.1	4.1	<0.1				0.1	0.4
	CrL*	5	83.5								1.7				10.7		4.1						
	PdS*	3									23.0				77.0								
	PdM	74	17.8	10.4				12.8	1.3		13.4	13.7	2.3	1.6	13.2	0.4	2.5	7.2			1.7	0.2	1.7
	PdL*	8	5.0	11.5				19.7			14.6	3.9									45.3		
	PsS	147	13.2	16.7							64.2				<0.1						5.6	0.1	0.2
	PsL*	2	100.0																				
Oct	CrS	130	10.2	2.9			<0.1				51.7			0.4	23.2	0.3	9.4	1.0				0.2	0.7
	CrM	75	3.8	0.5		13.3					71.7		<0.1	0.1	2.8	3.7	1.0	0.6			2.0	0.1	0.3
	CrL	66	0.5	0.2	20.7						70.3			0.2	<0.1	0.7	0.5	0.2			6.2		0.4
	Ms	37	16.0	0.3	10.1	0.5	6.9			19.2	29.0	2.7	8.2	1.0		0.3	1.8	2.6	0.1		0.9		0.2
	PdS*	3									23.6		6.2	2.2	34.9		30.9						2.2
	PdM	79	13.3	4.7		2.3	9.5		1.3		43.1	1.7	0.4	0.3	13.2	0.9	0.3	1.1			6.6	<0.1	1.3
	PdL*	13	1.9				26.7				26.7	0.7			<0.1						44.0		<0.1
	PsS	130	30.1	3.8	1.3		2.8		2.6		46.8				<0.1		<0.1	0.1			12.1		0.3
	PsL	52	15.5		7.2		25.2		4.0	6.7	35.3										5.0		1.1
All	CrS	325	11.4	4.8			<0.1				45.0			0.3	28.9	1.0	6.9	0.6			0.2	0.2	0.8
months	CrM	362	10.7	3.4		5.0	6.2				40.3	<0.1	0.7	0.8	23.6	3.8	2.6	1.0			0.8	0.7	0.6
	CrL	77	1.1	0.6	19.8						69.2			0.5	0.1	0.7	0.5	0.2			5.9		1.3
	Ms	48	8.3	0.2	5.3	0.2	3.6		1.1	10.0	18.0	1.4	4.3	0.6		0.1	0.9	1.4	21.8		0.8	<0.1	0.1
	PdS	139		4.8		3.4	4.7		9.2		22.6	1.5	4.2	2.9	26.9	2.0	6.7	3.5	1.0		4.7		1.1
	PdM	447	7.8	3.6		16.8	3.2	4.3	2.6		29.7	8.3	1.8	1.5	10.9	0.4	1.0	1.4	0.1	<0.1	5.1	<0.1	1.4
	PdL	121	1.0	0.7		4.2	4.8	10.9	2.3		16.5	2.7	<0.1	0.2	0.3		0.2		<0.1		55.4		0.6
	PsS	400	33.5	8.7	0.9		3.8		1.9		41.7			<0.1	0.1	<0.1	0.1	0.1			9.0	<0.1	0.3
	PsL	78	17.0	0.1	6.4	0.4	22.2		3.7	6.0	33.3		<0.1		<0.1				2.6		4.8		1.0

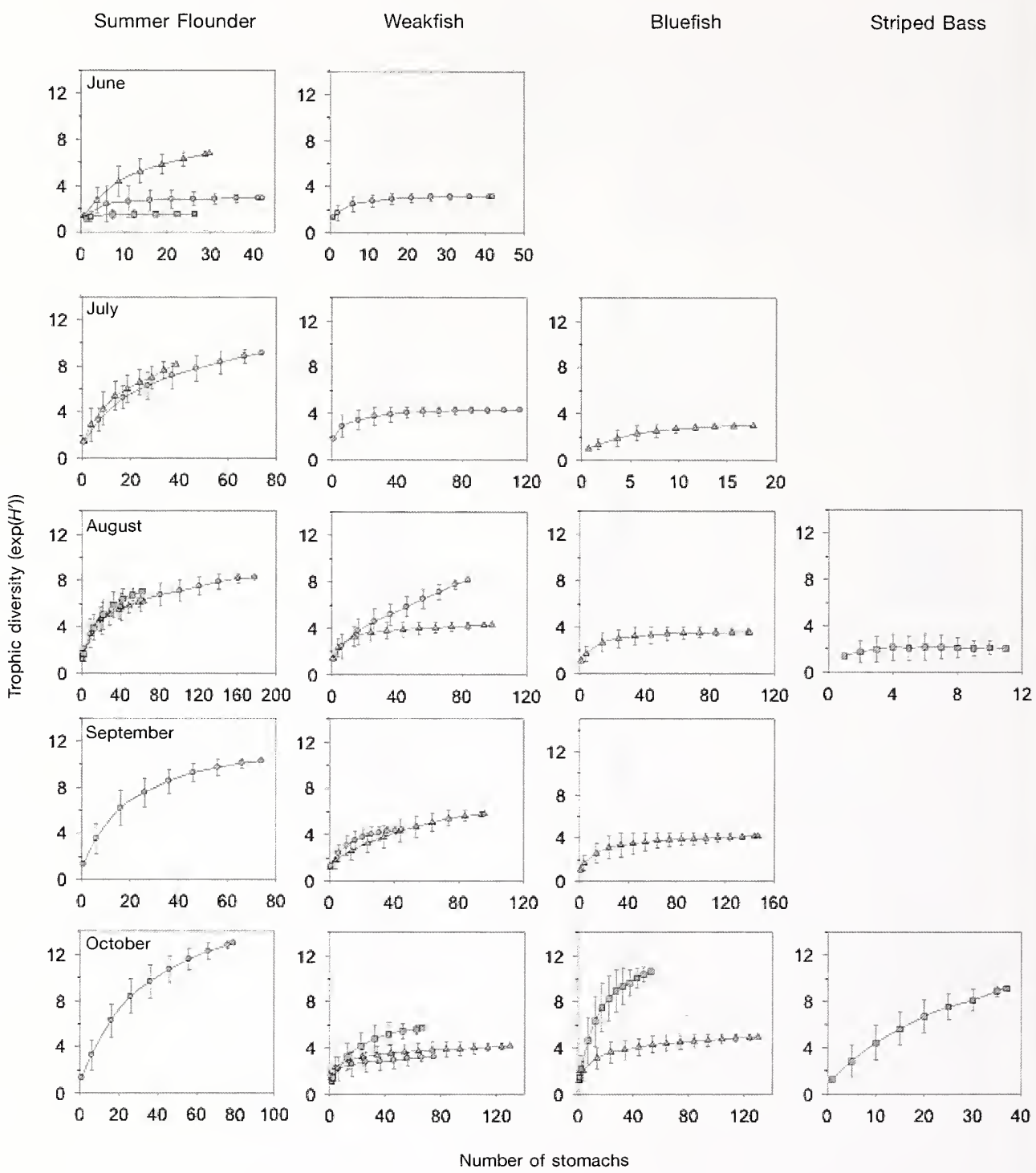

Figure 4

Trophic diversity (exp(H')) as a function of the number of stomachs analyzed for Summer Flounder (*Paralichthys dentatus*), Weakfish (*Cynoscion regalis*), Bluefish (*Pomatomus saltatrix*), and Striped Bass (*Morone saxatilis*), collected from June (top row) to October (bottom row) in 2005 off the coast of New Jersey. Plotted are the means of 100 randomizations for a selected number of stomachs (error bars indicate ±1 standard deviation). Lines with triangles, circles, or squares indicate results for small, medium, or large size classes, respectively. Note that the x-axis scales are different across species.

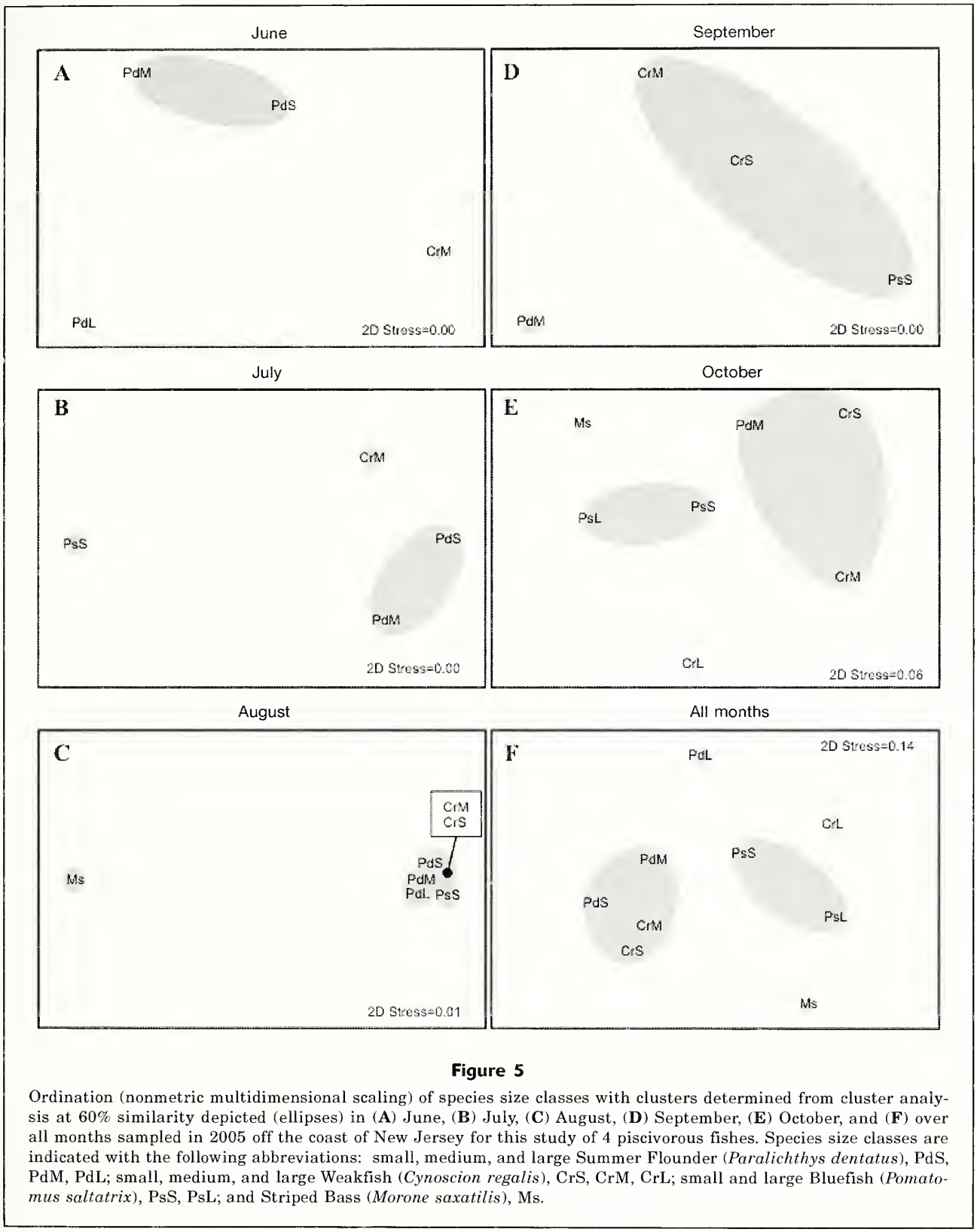

Figure 5

Ordination (nonmetric multidimensional scaling) of species size classes with clusters determined from cluster analysis at 60% similarity depicted (ellipses) in (**A**) June, (**B**) July, (**C**) August, (**D**) September, (**E**) October, and (**F**) over all months sampled in 2005 off the coast of New Jersey for this study of 4 piscivorous fishes. Species size classes are indicated with the following abbreviations: small, medium, and large Summer Flounder (*Paralichthys dentatus*), PdS, PdM, PdL; small, medium, and large Weakfish (*Cynoscion regalis*), CrS, CrM, CrL; small and large Bluefish (*Pomatomus saltatrix*), PsS, PsL; and Striped Bass (*Morone saxatilis*), Ms.

mysids (4.8–20.6%), rock crabs (2.7–23.8%), and large amounts of UID and other fishes (24.7–35.3%). About 10% of medium Summer Flounder diet in July was composed of pelagic Round Herring (*Etrumeus teres*), and small Summer Flounder consumed a substantial amount of Weakfish. Medium Weakfish formed their own group with a diet consisting largely of mysids (62.4%) and anchovies (Bay Anchovy and *Anchoa* spp.; 17.1%), and decapod crustaceans were also present (5.1%). Small Bluefish also formed their own group, feeding principally on 2 prey types: anchovies (61.2%) and UID and other fish species (38.8%).

Four groups were identified at 60% similarity by the cluster analysis in August, 2 with broad diets, 1 intense piscivore, and 1 bivalve consumer. The first broad diet group included medium and large Summer Flounder, which consumed varying amounts of UID fishes (29.7–41.0%), squids (3.5–28.0%), Round Herring (7.6–28.9%), mysids (0.7–19.7%), rock crabs (6.4–11.8%), and ocellate lady crab (*Ovalipes ocellatus;* 0.1–6.2%). The second broad diet group, consisting of medium and small Weakfish and small Summer Flounder, also consumed large amounts of UID and other fishes (21.5–42.1%). However, this group differed from the previous group in the consumption of mysids (16.3–37.9%), shrimps (3.2–8.0%), ocellate lady crab (0–7.9%), decapod crustaceans (0.8–7.0%), anchovies (9.9–17.6%), Weakfish (0–23.5%), and Butterfish (0–8.4%). Although cannibalism by medium Weakfish was substantial (23.5%) during this month, Weakfish were not detected in the diets of small Weakfish or small Summer Flounder. Small Bluefish, with a diet of anchovies (75.6%), Weakfish (9.5%), and UID and other fishes (12.3%), made up the piscivore group. Striped Bass, composing the fourth group in August, consumed mostly bivalves (45.3%) and some UID and other fish species were present (6.1%).

In September, the cluster analysis identified 2 groups at the 60% similarity level from the 4 species size classes with enough data. The first group, consisting of medium and small Weakfish and small Bluefish, consumed varying amounts of anchovies (29.3–35.4%), mysids (<1–34.5%), and UID and other fish species (25.3–64.2%). Medium Summer Flounder made up the second group and differed from the previous group by displaying a more diverse diet that included rock crabs (13.7%), mysids (13.2%), Round Herring (12.8%), and nondecapod crustaceans (7.2%) in addition to anchovies (28.2%).

In October, 4 groups were identified, along with UID and other fish species as the primary diet component for each of them. The first group, consisting of small and medium Weakfish and medium Summer Flounder, differed from the rest primarily in the amounts of prey consumed: anchovies (4.3–18.0%), mysids (2.8–23.2%), sand lances (0–13.3%), Weakfish (0–9.5%), UID and other fishes (43.1–71.7%), decapod crustaceans (0.3–9.4%), and squids (0–6.6%). The second group, composed of small and large Bluefish, preyed on a variety of fish species, including anchovies (15.5–33.9%), Atlantic Menhaden (*Brevoortia tyrannus*; 1.3–7.2%), Butterfish (2.6–4.0%), Northern Puffer (*Sphoeroides maculatus*; 0–6.7%), Weakfish (2.8–25.2%), UID and other fishes (35.3–46.8%), and squids (5.0–12.1%). Large Weakfish formed the third group and consumed primarily Atlantic Menhaden (20.7%), with large amounts of UID and other fishes (70.3%), and a lesser amount of squids (6.2%). Striped Bass, the final group, consumed ocellate lady crab (8.2%) and a variety of fish species: Atlantic Menhaden (10.1%), Bay Anchovy (16.0%), Northern Puffer (19.2%), Weakfish (6.9%), and UID and other fishes (29.0%). Cannibalism among Weakfish was not prevalent in this month, although all other species consumed Weakfish to some degree.

When the data are aggregated across months, 1 multispecies group, 1 single-species group, and 3 groups, each of a single-species and single-size, emerge. The multispecies group consisted of small and medium Weakfish and small and medium Summer Flounder, with large and small Bluefish composing the single species group. The multispecies group consumed anchovies (4.8–16.2%), sand lances (0–16.8%), Weakfish (<0.1–6.2%), butterfish (0–9.2%), UID and other fishes (22.6–45.0%), mysids (10.9–28.9%), rock crabs (0–8.3%), decapod crustaceans (1.0–6.9%), and squids (0.2–5.1%). Large and small Bluefish also consumed a variety of fishes—Atlantic Menhaden (0.9–6.4%), anchovies (17.1–42.2%), Northern Puffer (0–6.0%), Weakfish (3.8–22.2%), UID and other fish species (33.3–41.7%)—and squids (4.8–9.0%) but consumed less mysids, rock crabs, and decapod crustaceans than did the multispecies group. Large Summer Flounder, the third group, consumed a mix of squids (55.4%) and fishes, mostly Round Herring (10.9%) and UID and other fish species (16.5%). The fourth group, large Weakfish, preyed mainly upon Atlantic Menhaden (19.8%), UID and other fish species (69.2%), and squids (5.9%). Striped Bass formed the final group, with a diet of bivalves (21.8%) and fishes: Bay Anchovy (8.3%), Atlantic Menhaden (5.3%), Northern Puffer (10.0%), UID and other fish species (18.0%).

Habitat and diet overlap indices

Monthly overlap (α from Schoener's index) in habitat and diet for each pair of predators (species size classes) indicated shared use of resources ($\alpha>0$); however, α was below the biologically important level of 0.6 in most months (Fig. 6). Some groups had substantial overlap (>0.6) in habitat but not diet (e.g., large, medium, and small Summer Flounder). There also were instances of overlap (>0.6) in diet but not habitat (e.g., small Weakfish versus medium Weakfish and small Summer Flounder). There were no cases where substantial overlap (>0.6) in both habitat and diet occurred at the same time. For many of the pairwise comparisons, overlaps in both habitat and diet increased severalfold during the fall in this 5-month study, from levels of ~0.2 in

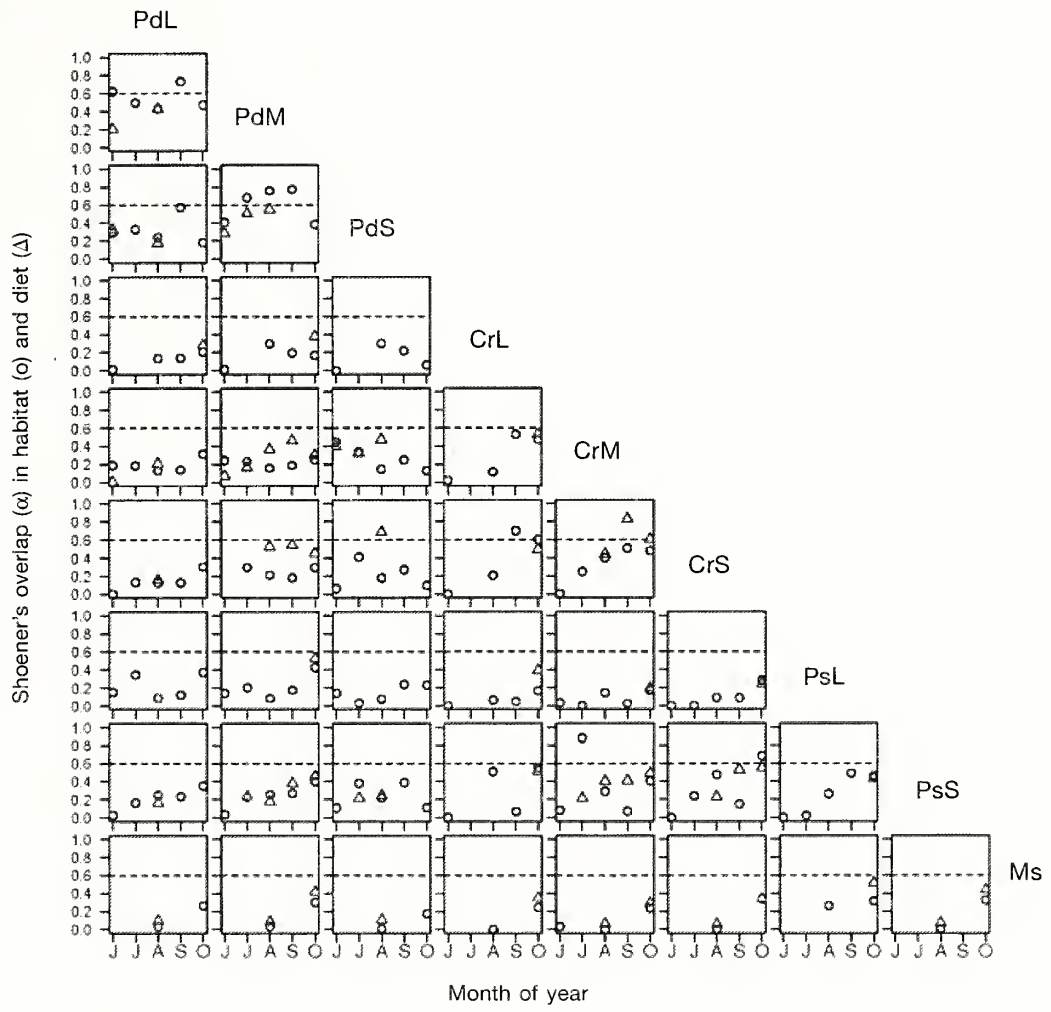

Figure 6

Pairwise monthly overlap (α), from Schoener's index, in habitat (open circles) and diet (triangles) between species size classes sampled from June to October in 2005 off the coast of New Jersey for this study. Habitat overlap is shown for all cases when both groups were captured in the same month. Diet overlap is shown only for groups with sufficient sample sizes (see main text). Horizontal dashed lines indicate biologically important overlap threshold (0.6). Species size classes are indicated in this manner: small, medium, and large Summer Flounder (*Paralichthys dentatus*), PdS, PdM, PdL; small, medium, and large Weakfish (*Cynoscion regalis*), CrS, CrM, CrL; small and large Bluefish (*Pomatomus saltatrix*), PsS, PsL; and Striped Bass (*Morone saxatilis*), Ms.

June and July to levels >0.4 in September and October. Small and medium Weakfish had relatively high overlap in diet, but lower overlap in habitat, with small and medium Summer Flounder from August to October. The limited spatial distribution of Striped Bass, in addition to their absence during some months, resulted in a low degree of overlap in habitat with groups of other species, but Striped Bass were most abundant in the fall and, therefore, overlapped with the other predators at that time.

Discussion

The degree of habitat and diet overlap among Summer Flounder, Weakfish, Bluefish, and Striped Bass varied with size and season. The size classes of these 4 predators examined in our study exhibited different patterns in spatial distribution, depth, and habitat use. Summer Flounder were most evenly distributed throughout our study area—a pattern also observed in a longer (1982–2003) time series of sampling at generally deep-

er depths (from 27 to >193 m) (Able and Fahay, 2010), with similar sizes present during our 5-month study on the inner continental shelf. Weakfish in our study occurred primarily inshore in shallow strata. Their abundance increased through the summer because of the appearance of YOY fish, and they dominated the catch by October—a trend also observed in composite collections over time on the deeper continental shelf (Able and Fahay, 2010).

The size structure of Bluefish was similarly variable with multiple YOY cohorts appearing during summer and eventually dominating the proportion of catch by October. Bluefish were concentrated at inshore, shallow stations, as had been documented previously (Able et al., 2003; Wiedenmann and Essington, 2006; Wuenschel et al., 2012). In October, the distribution of Bluefish was more uniform with depth, and they appeared to utilize a greater portion of the inner continental shelf during the period of southward migration, as was evident from other composite sampling at similar and deeper depths (Able and Fahay, 2010).

Bluefish and Weakfish distributions indicated a high degree of similarity in their use of the inshore shelf during the summer months. In contrast, the distribution of Striped Bass was limited to the northernmost stations during summer. Like Bluefish, Striped Bass were more abundant throughout the study area during their fall migration (October). The limited collections of Striped Bass, coupled with a priority to tag and release them during certain months, restricted our ability to describe Striped Bass diets. Nevertheless, Striped Bass showed little overlap in habitat use with the other predators studied.

The species-level distributions and monthly size frequencies tended to overestimate overlap because different sizes may have occupied different locations in a given month. When viewed at the size-class level, spatial (habitat) overlap was rarely above 0.6. Similarly, assessment of diet overlap at the species level (i.e., combining size classes and ignoring ontogenetic shifts in diet) would likely increase perceived overlap. For example, large and medium Summer Flounder diet overlap was moderate (α ~0.2–0.5) and overlap between medium and small sizes was similarly variable (α ~0.3–0.6), but overlap between large and small Summer Flounder was much lower (α ~0.2–0.3). This result supports the interpretation of gradual ontogenetic changes in diet and some similarity between adjacent size classes. Use of a single size group for Striped Bass because of limited sample sizes prevented the exploration of ontogenetic shifts for this species, which were significant in one study (Smith and Link, 2010) but not another (Walter et al., 2003). Regardless of potential ontogenetic differences, their extensive use of estuaries in New Jersey and throughout their range during many seasons (Able and Fahay, 2010) probably also contributes to the limited co-occurrence of this species with the other species size classes studied.

Unidentified fish remains were large components of the diet for many of the species size classes in our study—a common problem encountered in the analysis of stomach contents (Garrison and Link, 2000a; 2000b). The presence of large portions of UID fishes serves to increase the overlap in diet and decrease the number of distinct clusters from the groups analyzed. Assuming that identifiable and unidentifiable prey occur in similar relative proportions, we consider the separation of distinct groupings in our analysis to be conservative. Where diets between species size classes showed little overlap, we can conclude diets were indeed different.

The diets of Summer Flounder, Weakfish, Bluefish, and Striped Bass on the inner continental shelf of New Jersey during summer varied month to month—an observation that could not be obtained from previous studies conducted in the region across a greater portion of the shelf region over multiple years (Garrison and Link, 2000b; Link et al., 2002; Walter et al., 2003; Buckel et al., 2009; Smith and Link, 2010). The finer scale in our study accounts for the slightly different patterns of similarity among Summer Flounder, Weakfish, Bluefish, and Striped Bass diets in comparison with results that had been reported previously for the shelf ecosystem of the northeastern United States (Garrison and Link, 2000b). Although the size classes differed slightly, this previous study reported Summer Flounder (21–70 cm) and Bluefish (>31 cm) in a piscivore guild distinct from small Bluefish (10–30 cm) and Weakfish (10–50 cm).

On a much finer spatial scale, we observed greater overlap in diets, which varied through time, between Summer Flounder and Weakfish, particularly for the small and medium size classes. This similarity was driven by large amounts of mysids and other crustaceans in the diet. Both Summer Flounder and Weakfish incorporated more fishes and squids in their diet as they increased in size. The early onset of piscivory by Bluefish separated them from the smaller size classes of Summer Flounder and Weakfish. Together, these differences relative to earlier studies point out the advantages of the finer temporal, spatial, and size-class scales used in this study.

Of the 4 predators analyzed from the Mid-Atlantic region in our study, only Weakfish were consumed in appreciable numbers by the other species. Weakfish were consumed by small Summer Flounder (16.5%) in July and small Bluefish (9.5%) in August, and an appreciable amount of cannibalism by medium-size Weakfish (23.5%) was observed in August. In October, large Bluefish and Summer Flounder fed extensively on Weakfish (25.2–26.7%), with medium and small Summer Flounder and Striped Bass also consuming Weakfish but in lesser proportions. Similarly, in Long Island bays, YOY Bluefish and Summer Flounder consumed Weakfish (7.5% and 3.0% by weight, respectively); however, data were reported across sizes and seasons (spring, summer, and fall), and Weakfish diet was not investigated

(Sagarese et al., 2011). Predation on juvenile Weakfish has also been observed in Delaware Bay by adult Weakfish and Summer Flounder (Taylor, 1987).

A recent synopsis of diets documented across the continental shelf in the region indicated that Weakfish occurred at relatively low levels (~5%) in diets of Bluefish, Summer Flounder, and Weakfish (Smith and Link, 2010). Although direct predation on Weakfish by the 4 piscivores investigated was high at different times during our study, large numbers of Weakfish were also collected in our surveys, indicating high availability of this prey type. However, the possibility that the high degree of predation may influence the continuing low population levels of Weakfish (NEFSC[2]) needs further study, especially because some of these predators, such as Summer Flounder (Able et al., 2011) and Striped Bass, have reached high population levels in recent years (ASMFC[3]).

Another prey species, Atlantic Menhaden, has received increased attention because of its historical importance as the main prey of Striped Bass at other locations during other times (Nelson et al., 2003; Walter et al., 2003; Overton et al., 2008). Uphoff (2003) suggested that a shortage of Atlantic Menhaden as prey for Striped Bass in the Chesapeake Bay may have reduced the nutritional condition of those Striped Bass in the 1990s, making them susceptible to disease. In our study, there was little evidence of Atlantic Menhaden in the diets of any of these predators except in October when Striped Bass, Weakfish, and Bluefish consumed them to some degree, although Atlantic Menhaden are typically present in the area during the other months (Ahrenholz, 1991; Smith, 1999). Adult Atlantic Menhaden occur along the coast in summer (Smith, 1999), but YOY Atlantic Menhaden reside in estuaries in summer and are not plentiful in the ocean until October (Able and Fahay, 2010), when they appeared in the diets of the piscivores examined in our study. Adult Atlantic Menhaden exceed the gape limitation for most of the species size classes examined, except that for Striped Bass and large Bluefish; therefore, it is not surprising that little consumption of this species was documented in summer. Diet analyses for larger predator species and larger individuals of those species considered in our study are needed to fully evaluate consumption of large Atlantic Menhaden in the Middle Atlantic Bight.

As with our study, Woodland and Secor (2011) reported no clupeids in the diet of YOY Bluefish collected on the inner continental shelf off Maryland in August, although clupeids made up 9% of the diet of YOY Bluefish collected in Chesapeake Bay in the same month. However, Atlantic Menhaden contributed a large portion to Bluefish diets, but less so for Summer Flounder in Long Island bays (Sagarese et al., 2011), and large proportions to the diets of Weakfish, Bluefish, and Sandbar Shark (*Carcharhinus plumbeus*) in Delaware Bay (Taylor, 1987), underscoring the importance of Atlantic Menhaden as prey in estuaries during summer. Additionally, we acknowledge that the degree of consumption and overlap in diets may vary with the population size of the predators. At the time of our study, the populations of Striped Bass (ASMFC[3]) and Summer Flounder (Able et al., 2011; Terceiro, 2011) were relatively high and the populations of Bluefish (Shepherd and Nieland[4]) and Weakfish (NEFSC[2]) were relatively low. More detailed estimates of population-level consumption with more diet information from larger size classes would help to determine the direct effect of the predation of these piscivores on Weakfish and Atlantic Menhaden populations.

One behavioral attribute that may reduce resource overlap between these predators is their use of the water column. Recent studies have indicated that a presumed benthic species, Summer Flounder, may spend considerable time in the water column (Yergey, 2011; Henderson, 2012). This observation is consistent with the surprisingly large proportion of pelagic prey in their diets and their ability to feed in the water column in the laboratory (Olla et al., 1972). In addition, aggregation of diet data across the 24 h cycle may obscure some interactions with prey that undergo diel migrations (e.g., mysids and Summer Flounder; Buchheister and Latour, 2011). Although sampling was limited to daylight hours, given that gut evacuation rate generally decreases with fish size (Wuenschel and Werner, 2004) and with the relatively slow passage of food in carnivores (Smith, 1989; Adams and Breck, 1990), the results of our study capture much of the nighttime feeding habits of the predators examined.

Another caveat to consider when evaluating overlap in habitat between these species is that overlap may be confounded by the length of a tow with a relatively large net. Although the duration of tows was short in our study, the distance covered (~1.85 km) may have included multiple discrete habitats, inflating assessments of overlap. However, the overlap estimates were not systematically high and the area covered per tow was very small relative to the overall study area and to the distances that the species examined are known to move; therefore, analysis at the tow level is appropriate.

This study has described in fine spatial and temporal detail the degree of overlap in habitat and diet

[2] NEFSC (Northeast Fisheries Science Center). 2009. 48th Northeast Regional Stock Assessment Workshop (48th SAW) Assessment Report. U.S. Dept. Commer., Northeast Fish. Sci. Cent. Ref. Doc. 09-15, 834 p. [Available from National Marine Fisheries Service, 166 Water Street, Woods Hole, MA 02543-1026 or http://www.nefsc.noaa.gov/nefsc/publications/.]

[3] ASMFC (Atlantic States Marine Fisheries Commission). 2011. Striped Bass Stock Assessment Update 2011, 207 p. Prepared by the Striped Bass Stock Assessment Subcommittee and Striped Bass Tagging Subcommittee. [Available from http://www.asmfc.org/speciesDocuments/stripedBass/reports/stockassmts/2011StripedBassAssmtUpdate.pdf.]

[4] Shepherd, G. R., and J. Nieland. 2010. Bluefish 2010 stock assessment update. U.S. Dept. Commer., Northeast Fish. Sci. Cent. Ref. Doc. 10-15, 33 p. [Available from National Marine Fisheries Service, 166 Water Street, Woods Hole, MA 02543-1026 or http://www.nefsc.noaa.gov/nefsc/publications/.]

of 4 piscivores on the inner continental shelf off New Jersey from summer through fall. It does not consider these parameters on adjacent estuaries where these species can also be abundant (Able and Fahay, 2010). For example, Striped Bass are known to use estuaries in the region during the summer (Tupper and Able, 2000; Able and Grothues, 2007; Ferry and Mather, 2012). The same is true for Bluefish (Grothues and Able, 2007; Sagarese et al., 2011), Summer Flounder (Sackett et al., 2007; 2008; Sagarese et al., 2011), and Weakfish (Taylor, 1987; Turnure 2010). Therefore, our findings from the inner shelf should be viewed with this qualification in mind. As an example, the diets described here for inshore waters revealed differences in diets, compared with diets observed in studies carried out within estuaries (Gartland et al., 2006; Latour et al., 2008; Sagarese et al., 2011).

Although not necessarily unexpected given differences in prey availability between estuarine and ocean habitats, these differences in diets underscore the need to incorporate into ecosystem models both distribution and diet information from the inner shelf and adjacent estuaries because of connectivity between them, especially over seasonal scales (Able, 2005). These data have typically been lacking. Many prey categories were shared by the piscivores examined in our study on the inner continental shelf, but different patterns in habitat use (in time and space) seemed to alleviate overlap between these predators for prey. However, overlaps in fish distributions and diets increased during fall as species left estuaries and underwent coastal migrations. Therefore, the information on spatial distributions and food habits reported here at finer spatial and temporal scales, compared to results from previous studies, complements and provides a critical link between what is known about these mobile, seasonally migratory predators within estuaries and about these same piscivores across larger geographic scales (e.g., the northeastern shelf of the United States). It is reasonable to ask whether diet overlap may continue to increase during winter when many of these predators are concentrated farther south and likely co-occur in thermal refuges in the South Atlantic Bight.

Conclusions

Results from this study, at finer temporal, spatial, and size-class scales than have been attempted typically in other studies, indicate that overlap in distribution on the inner continental shelf for the 4 piscivores examined was not uniform through time and that they had moderate levels of overlap in diet. The exception was observed in the fall, when many of these species became concentrated as both larger individuals and smaller YOY fishes left estuaries, gathered with other individuals on the inner shelf, and began their southward migration as temperatures cooled. Given the high seasonal variability in water temperature and productivity in the system studied and the migratory nature of the species investigated, it is not surprising that habitat use and species interactions were variable.

Our understanding of species interactions on the inner continental shelf has been limited, in the past, by the gap between sampling programs within estuaries and bays and programs occurring farther offshore. The intensive monthly sampling of this study on the inner continental shelf revealed the dynamic nature of habitat and diet overlap for Summer Flounder, Weakfish, Bluefish, and Striped Bass. The use of inner shelf resources by these 4 important species had previously been poorly defined. The limited degree of resource overlap in summer and the increasing overlap in fall for the 4 piscivores indicate that this period of changeable overlap may be important for the population dynamics of these species and that information about it should be incorporated into not only species-specific models of population dynamics but also broader ecosystem-level models.

Acknowledgments

This study was funded through a grant from the collaborative Bluefish/Striped Bass Dynamics Research Program of Rutgers University and the National Marine Fisheries Service. The authors thank New Jersey Department of Environmental Protection personnel (L. Barry, A. Mazzarella and S. Reap), the staff at the Rutgers University Marine Field Station and Captain S. Cluett and crew of the RV *Seawolf* for assistance. The following individuals provided field and laboratory assistance: R. Nichols, M. Greaney, J. Conwell, J. Lamonaca, J. Eppenstiener, and J. Bunkiewicz. B. Smith, S. Rowe, and anonymous reviewers provided constructive comments on the manuscript. We are grateful to all of the above. This article is contribution no. 2013-3 from the Institute of Marine and Coastal Sciences, Rutgers University.

Literature cited

Able, K. W.
2005. A reexamination of fish estuarine dependence: evidence for connectivity between estuarine and ocean habitats. Estuar. Coast. Shelf Sci. 64:5–17

Able, K. W., and M. P. Fahay.
1998. The first year in the life of estuarine fishes in the Middle Atlantic Bight, 342 p. Rutgers Univ. Press, New Brunswick, NJ.
2010. Ecology of estuarine fishes: temperate waters of the western North Atlantic, 584 p. Johns Hopkins Univ. Press, Baltimore.

Able, K. W., and T. M. Grothues.
2007. Diversity of estuarine movements of striped bass (*Morone saxatilis*): a synoptic examination of an estuarine system in southern New Jersey. Fish. Bull. 105:426–435.

Able, K. W., P. Rowe, M. Burlas, and D. Byrne.
2003. Use of ocean and estuarine habitats by young-of-year bluefish (*Pomatomus saltatrix*) in the New York Bight. Fish. Bull. 101:201–214.

Able, K. W., M. C. Sullivan, J. A. Hare, G. Bath-Martin, J. C. Taylor, and R. Hagan.
2011. Larval abundance of summer flounder (*Paralichthys dentatus*) as a measure of recruitment and stock status. Fish. Bull. 109:68–78.

Adams, S. M., and J. E. Breck.
1990. Bioenergetics. *In* Methods for fish biology (C. B. Schreck, and P. B. Moyle, eds.), p. 389–415. Am. Fish. Soc., Bethesda, MD.

Ahrenholz, D. W.
1991. Population biology and life history of the North American menhadens, *Brevoortia* spp. Mar. Fish. Rev. 53:3–19.

Andrews, K. S., and C. J. Harvey.
2013. Ecosystem-level consequences of movement: seasonal variation in the trophic impact of a top predator. Mar. Ecol. Prog. Ser. 473:247–260.

Belleggia, M., E. Mabragana, D. E. Figueroa, L. B. Scenna, S. A. Barbini, and J. M. Diaz de Astarloa.
2008. Food habits of the broadnose skate, *Bathyraja brachyurops* (Chondrichthyes, Rajidae), in the southwest Atlantic. Sci. Mar. 72:701–710.

Bellgraph, B. J., C. S. Guy, W. M. Gardner, and S. A. Leathe.
2008. Competition between saugers and walleyes in nonnative sympatry. Trans. Am. Fish. Soc. 137:790–800.

Bethea, D. M., J. A. Buckel, and J. K. Carlson.
2004. Foraging ecology of the early life stages of four sympatric shark species. Mar. Ecol. Prog. Ser. 268:245–264.

Braga, R. R., H. Bornatowski, and J. R. S. Vitule.
2012. Feeding ecology of fishes: an overview of worldwide publications. Rev. Fish Biol. Fish. 22:915–929.

Braccini, J. M., B. M. Gillanders, and T. I. Walker.
2005. Sources of variation in the feeding ecology of the piked spurdog (*Squalus megalops*): implications for inferring predator–prey interactions from overall dietary composition. ICES J. Mar. Sci. 62:1076–1094.

Buchheister, A., and R. J. Latour.
2011. Trophic ecology of summer flounder in lower Chesapeake Bay inferred from stomach content and stable isotope analyses. Trans. Am. Fish. Soc. 140:1240–1254.

Buckel, J. A., and K. A. McKown.
2002. Competition between juvenile striped bass and bluefish: resource partitioning and growth rate. Mar. Ecol. Prog. Ser. 234:191–204.

Buckel, J. A., D. O. Conover, N. D. Steinberg, and K. A. McKown.
1999a. Impact of age-0 bluefish (*Pomatomus saltatrix*) predation on age-0 fishes in the Hudson River estuary: evidence for density-dependent loss of juvenile striped bass (*Morone saxatilis*). Can. J. Fish. Aquat. Sci. 56:275–287.

Buckel, J. A., M. J. Fogarty, and D. O. Conover.
1999b. Foraging habits of bluefish, *Pomatomus saltatrix*, on the U.S. east coast continental shelf. Fish. Bull. 97:758–775.
1999c. Mutual prey of fish and humans: a comparison of biomass consumed by bluefish, *Pomatomus saltatrix*, with that harvested by fisheries. Fish. Bull. 97:776–785.

Buckel, J. A., J. P. Pessutti, J. E. Rosendale, and J. S. Link.
2009. Interactions between bluefish and striped bass: behavior of bluefish under size- and number-impaired conditions and overlap in resource use. J. Exp. Mar. Biol. Ecol. 368:129–137.

Byrne, D.
1994. Stock assessment of New Jersey's nearshore recreational fisheries resources. *In* Proceedings of the workshop on the collection and use of trawl survey data for fisheries management; Charleston, SC, 15–17 August (T. Berger, ed.), p. 36–42. Atlantic States Mar. Fish. Comm., Washington, D.C.

Carr, W. E. S., and C. A. Adams.
1972. Food habits of juvenile marine fishes: evidence of the cleaning habit in the leatherjacket, *Oligoplites saurus*, and the spottail pinfish, *Diplodus holbrooki*. Fish. Bull. 70:1111–1120.

Clarke, K. R., and R. M. Warwick.
2001. Change in marine communities: an approach to statistical analysis and interpretation, 2nd ed., 172 p. PRIMER-E Ltd., Plymouth, UK.

Cortés, E.
1997. A critical review of methods of studying fish feeding based on analysis of stomach contents: application to elasmobranch fishes. Can. J. Fish. Aquat. Sci. 54:726–738.

Elliot, M., and K. L. Hemingway (eds.).
2002. Fishes in estuaries, 636 p. Blackwell Science Ltd., Oxford, UK.

Ferry, L. A., and G. M. Cailliet.
1996. Sample size and data analysis: are we characterizing and comparing diet properly? *In* "Gutshop '96:" feeding ecology and nutrition in fish symposium proceedings, International Congress on the Biology of Fishes; San Francisco, 14–18 July (D. MacKinley and K. Shearer, eds.), p. 71–80. Am. Fish. Soc., Bethesda, MD.

Ferry, K. H., and M. E. Mather.
2012. Spatial and temporal diet patterns of subadult and small adult striped bass in Massachusetts estuaries: data, a synthesis, and trends across scales. Mar. Coast. Fish. 4:30–45.

Garrison, L. P., and J. S. Link.
2000a. Diets of five hake species in the northeast United States continental shelf ecosystem. Mar. Ecol. Prog. Ser. 204:243–255.
2000b. Dietary guild structure of the fish community in the Northeast United States continental shelf ecosystem. Mar. Ecol. Prog. Ser. 202:231–240.

Gartland, J., R. J. Latour, A. D. Halvorson, and H. M. Austin.
2006. Diet composition of young-of-the-year bluefish in the lower Chesapeake Bay and the coastal ocean of Virginia. Trans. Am. Fish. Soc. 135:371–378.

Grothues, T. M., and K. W. Able.
2007. Scaling acoustic telemetry of bluefish in an estuarine observatory: detection and habitat use patterns. Trans. Am. Fish. Soc. 136:1511–1519.

Heithaus, M. R., A. Frid, A. J. Wirsing, and B. Worm.
2008. Predicting ecological consequences of marine top predator declines. Trends Ecol. Evol. 23:202–210.

Henderson, M. J.
2012. Movements, growth, and mortality of Chesapeake Bay summer flounder based on multiple tagging technologies. Ph.D. diss., 262 p. College of William & Mary, Williamsburg, VA.

Hyslop, E. J.
1980. Stomach contents analysis—a review of methods and their application. J. Fish Biol. 17:411–429.
Jaworski, A., and S. A. Ragnarsson
2006. Feeding habits of demersal fish in Icelandic waters: a multivariate approach. ICES J. Mar. Sci. 63:1682–1694.
Jost, L.
2006. Entropy and diversity. Oikos 113:363–375.
Latour, R. J., J. Gartland, C. F. Bonzek, and R. A. Johnson.
2008. The trophic dynamics of summer flounder (*Paralichthys dentatus*) in Chesapeake Bay. Fish. Bull. 106:47–57.
Link, J. S.
2002. Ecological considerations in fisheries management: when does it matter? Fisheries 27:10–17.
Link, J. S., K. Bolles, and C. G. Milliken.
2002. The feeding ecology of flatfish in the northwest Atlantic. J. Northwest Atl. Fish. Sci. 30:1–17.
Myers, R. A., and B. Worm.
2003. Rapid worldwide depletion of predatory fish communities. Nature 423:280–283.
Nelson, G. A., B. C. Chase, and J. Stockwell.
2003. Food habits of striped bass (*Morone saxatilis*) in coastal water of Massachusetts. J. Northwest Atl. Fish. Sci. 32:1–25.
Olla, B. L., C. E. Samet, and A. L. Studholme.
1972. Activity and feeding behavior of the summer flounder (*Paralichthys dentatus*) under controlled laboratory conditions. Fish. Bull. 70:1127–1136.
Overholtz, W. J., and J. S. Link.
2007. Consumption impacts by marine mammals, fish, and seabirds on the Gulf of Maine–Georges Bank Atlantic herring (*Clupea harengus*) complex during the years 1977–2002. ICES J. Mar. Sci. 64:83–96.
Overholtz, W. J., J. S. Link, and L. E. Suslowicz.
2000. Consumption of important pelagic fish and squid by predatory fish in the northeastern USA shelf ecosystem with some fishery comparisons. ICES J. Mar. Sci. 57:1147–1159.
Overton, A. S., C. S. I. Manooch, J. W. Smith, and K. Brennan.
2008. Interactions between adult migratory striped bass (*Morone saxatilis*) and their prey during winter off the Virginia and North Carolina Atlantic coast from 1994–2007. Fish. Bull. 106:174–182.
Persson, L., P. Bystrom, E. Wahlstrom, J. Andersson, and J. Hjelm.
1999. Interactions among size-structured populations in a whole-lake experiment: size- and scale-dependent processes. Oikos 87:139–156.
Rudershausen, P. J., J. A. Buckel, J. Edwards, D. P. Gannon, C. M. Butler, and T. W. Averett
2010. Feeding ecology of blue marlins, dolphinfish, yellowfin tuna, and wahoos from the North Atlantic Ocean and comparison with other oceans. Trans. Am. Fish. Soc. 139:1335–1359.
Sackett, D. K., K. W. Able, and T. M. Grothues.
2007. Dynamics of summer flounder, *Paralichthys dentatus*, seasonal migrations based on ultrasonic telemetry. Estuar. Coast. Shelf Sci. 74:119–130
2008. Habitat dynamics of summer flounder, *Paralichthys dentatus*, within a shallow USA estuary, based on multiple approaches using acoustic telemetry. Mar. Ecol. Prog. Ser. 364:199–212.
Sagarese, S. R., R. M. Cerrato, and M. G. Frisk.
2011. Diet composition and feeding habits of common fishes in Long Island bays, New York. Northeast. Nat. 18:291–314.
Schoener, T. W.
1970. Nonsynchronous spatial overlap of lizards in patchy habitats. Ecology 51:408–418.
Schmitz, O. J.
2007. Predator diversity and trophic interactions. Ecology 88:2415–2426.
Smith, B. E., and J. S. Link.
2010. The trophic dynamics of 50 finfish and 2 squid species on the northeast US continental shelf. NOAA Tech. Memo. NMFS-NE-216, 640 p.
Smith, J. E.
1999. Distribution of Atlantic menhaden, *Brevoortia tyrannus*, purse-seine sets and catches from southern New England to North Carolina, 1985–96. NOAA Tech. Rep. NMFS 144, 22 p.
Smith, L. S.
1989. Digestive functions in teleost fishes. *In* Fish nutrition, 2nd ed. (J. E. Halver, ed.), p. 332–423. Academic Press, San Diego, CA.
Sutton, T. M., and J. J. Ney.
2002. Trophic resource overlap between age-0 striped bass and largemouth bass in Smith Mountain Lake, Virginia. N. Am. J. Fish. Manage. 22:1250–1259.
Taylor, E. T.
1987. Food habits of dominant piscivorous fishes in Delaware Bay, with special reference to predation on juvenile weakfish. M.S. thesis, 82 p. Univ. Delaware, Graduate College of Marine Studies, Lewes, DE.
Terceiro, M.
2011. The summer flounder chronicles II: new science, new controversy, 2001–2010. Rev. Fish Biol. Fish. 21:681–712.
Tupper, M., and K. W. Able.
2000. Movements and food habits of striped bass (*Morone saxatilis*) in Delaware Bay (USA) salt marshes: comparison of a restored and a reference marsh. Mar. Biol. 137: 1049–1058.
Turnure, J. T.
2010. Estuarine habitat ecology of adult weakfish (*Cynoscion regalis*): a multi-scale approach. M.S. thesis, 125 p. Rutgers Univ., New Brunswick, NJ.
Uphoff, J. H., Jr.
2003. Predator–prey analysis of striped bass and Atlantic menhaden in upper Chesapeake Bay. Fish. Manage. Ecol. 10:313–322.
Wallace, R. K., Jr.
1981. An assessment of diet-overlap indexes. Trans. Am. Fish. Soc. 110:72–76.
Walter, J. F., III, A. S. Overton, K. G. Ferry, and M. E. Mather.
2003. Atlantic coast feeding habits of striped bass: a synthesis supporting a coast-wide understanding of trophic biology. Fish. Manage. Ecol. 10:349–360.
Weiss, H. M.
1995. Marine animals of southern New England and New York: identification keys to common nearshore and shallow water macrofauna. State Geological and Natural History Survey of Connecticut, Department of Environmental Protection. Bulletin 115, 344 p.
Wiedenmann, J., and T. E. Essington.
2006. Density-dependent overwinter survival in young-of-year bluefish (*Pomatomus saltatrix*)? A new approach for assessing stage-structured survival. Can. J. Fish. Aquat. Sci. 63:1934–1943.

Woodland, R. J., and D. H. Secor.
2011. Differences in juvenile trophic niche for two coastal fish species that use marine and estuarine nursery habitats. Mar. Ecol. Prog. Ser. 439:241–254.
Woodland, R. J., D. H. Secor, and M. A. Wedge.
2011. Trophic resource overlap between small elasmobranchs and sympatric teleosts in Mid-Atlantic Bight nearshore habitats. Estuaries Coasts 34: 391–04.
Wuenschel, M. J., K. W. Able, J. A. Buckel, J. W. Morley, T. Lankford, A. C. Branson, D. O. Conover, D. Drisco, A. Jordaan, K. Dunton, D. H. Secor, R. J. Woodland, F. Juanes, and D. Stormer.
2012. Recruitment patterns and habitat use of young-of-the-year bluefish along the United States east coast: insights from coordinated coastwide sampling. Rev. Fish. Sci. 20:80–102.
Wuenschel, M. J., and R. G. Werner.
2004. Consumption and gut evacuation rate of laboratory-reared spotted seatrout (Sciaenidae) larvae and juveniles. J. Fish Biol. 65:723–743.
Yergey, M. S.
2011. Movement of summer flounder (*Paralichthys dentatus*): application of telemetry to understanding ecology and bycatch discard mortality. M.S. thesis, 69 p. Rutgers Univ., New Brunswick, NJ.

Multiscale analysis of factors that affect the distribution of sharks throughout the northern Gulf of Mexico

J. Marcus Drymon (contact author)[1, 2]
Laure Carassou[3]
Sean P. Powers[1, 2]
Mark Grace[4]
John Dindo[2]
Brian Dzwonkowski[2]

Email address for contact author: mdrymon@disl.org

[1] Department of Marine Sciences
University of South Alabama, LSCB-25
Mobile, Alabama 36688

[2] Dauphin Island Sea Lab
101 Bienville Boulevard
Dauphin Island, Alabama 36528

[3] Department of Zoology and Entomology
Rhodes University
P.O. Box 94
Grahamstown 6140, South Africa

[4] Mississippi Laboratories
Southeast Fisheries Science Center
National Marine Fisheries Service, NOAA
3209 Frederic Street
Pascagoula, Mississippi 39567

Abstract—Identification of the spatial scale at which marine communities are organized is critical to proper management, yet this is particularly difficult to determine for highly migratory species like sharks. We used shark catch data collected during 2006–09 from fishery-independent bottom-longline surveys, as well as biotic and abiotic explanatory data to identify the factors that affect the distribution of coastal sharks at 2 spatial scales in the northern Gulf of Mexico. Centered principal component analyses (PCAs) were used to visualize the patterns that characterize shark distributions at small (Alabama and Mississippi coast) and large (northern Gulf of Mexico) spatial scales. Environmental data on temperature, salinity, dissolved oxygen (DO), depth, fish and crustacean biomass, and chlorophyll-*a* (chl-*a*) concentration were analyzed with normed PCAs at both spatial scales. The relationships between values of shark catch per unit of effort (CPUE) and environmental factors were then analyzed at each scale with co-inertia analysis (COIA). Results from COIA indicated that the degree of agreement between the structure of the environmental and shark data sets was relatively higher at the small spatial scale than at the large one. CPUE of Blacktip Shark (*Carcharhinus limbatus*) was related positively with crustacean biomass at both spatial scales. Similarly, CPUE of Atlantic Sharpnose Shark (*Rhizoprionodon terraenovae*) was related positively with chl-*a* concentration and negatively with DO at both spatial scales. Conversely, distribution of Blacknose Shark (*C. acronotus*) displayed a contrasting relationship with depth at the 2 scales considered. Our results indicate that the factors influencing the distribution of sharks in the northern Gulf of Mexico are species specific but generally transcend the spatial boundaries used in our analyses.

Manuscript submitted 25 October 2012.
Manuscript accepted 29 August 2013.
Fish. Bull. 111:370–380.
doi: 10.7755/FB.111.4.6

The views and opinions expressed or implied in this article are those of the author (or authors) and do not necesarily reflect the position of the National Marine Fisheries Service, NOAA.

Paramount to the conservation of marine resources and ecosystems is the identification of proper spatial scales for management plans. Although long recognized as a central, if not universal, concept in ecology, the notion of scale more recently has begun a transition from qualitative description to quantitative assessment (Schneider, 2001). For marine systems, this transition is particularly important because choice of spatial scale directly affects the identification of patterns (Perry and Ommer, 2003). As fisheries management plans transition to an ecosystem-based approach, the identification of suitable spatial scales becomes even more important (Hughes et al., 2005; Francis et al., 2007).

For sharks, many of which are considered top predators and play a central role in regulation of marine ecosystems (Heithaus et al., 2008), the identification of appropriate spatial scales for management is made more difficult than the identification of spatial scales for bony fishes because of their highly migratory nature and relative paucity. Traditional mark-and-recapture methods allow for examination of gross spatial-scale patterns in sharks, but these methods are limited by low recapture rates. Pop-up satellite archival tags circumvent this problem by exponentially increasing the odds of retrieving data from tagged sharks. Unfortunately, their use is often cost prohibitive, and the algorithms presently employed to estimate geographic locations are too coarse to provide reliable spatial pattern data on small scales (i.e., tens of kilometers) (Sims, 2010; Hammerschlag et al., 2011). Consequently, information

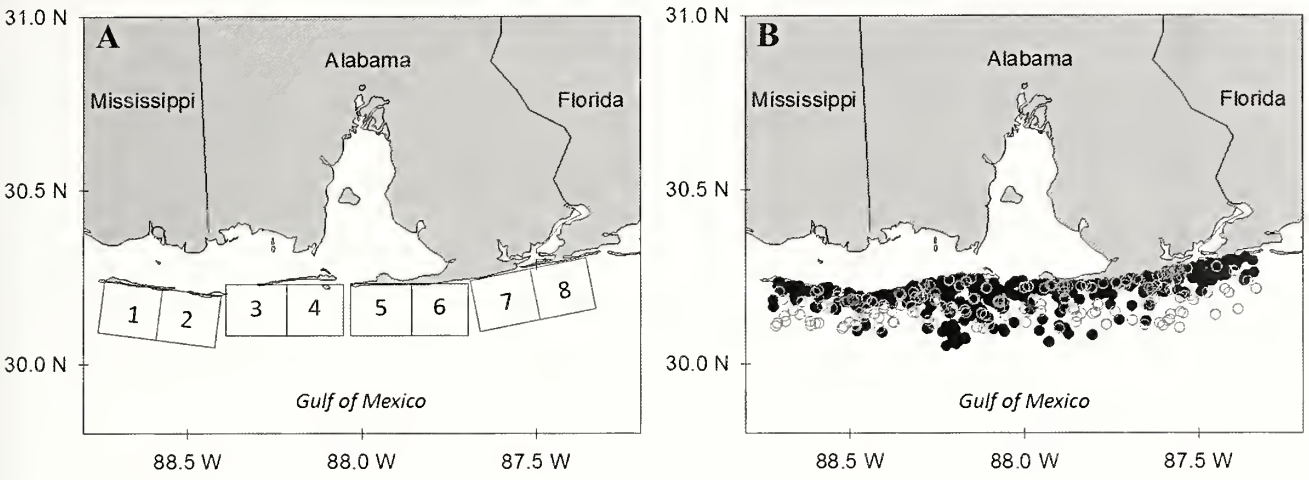

Figure 1

Spatial extent of the area used in our small-scale analysis of shark distribution in the northern Gulf of Mexico during 2006–09. (**A**) Eight blocks (1–8, west to east), which spanned depths from 1 to ~20 m, where the shark bottom-longline survey was conducted during all months by the Dauphin Island Sea Laboratory. (**B**) Sample locations for the small-scale bottom-longline data during 2006–09 (filled circles) and trawl data during 2007–09 from the Southeast Area Monitoring and Assessment Program database (http://seamap.gsmfc.org) (open circles).

concerning spatial patterns and distributions of shark communities in coastal marine systems is still needed before resource managers can successfully incorporate sharks into sustainable ecosystem management plans (Heithaus et al., 2007).

Long-term, fishery-independent monitoring programs are one of the most common ways to assess spatial patterns for marine vertebrates. The NOAA Southeast Fisheries Science Center (SEFSC) Mississippi Laboratories have been conducting annual bottom-longline surveys to assess patterns of shark distributions across the entire northern Gulf of Mexico since 1995, and the data from these surveys are incorporated into stock assessments that ultimately shape fishery management plans for these animals. Given the importance of merging biological scales with the scales of fisheries management, we sought to examine spatial patterns in assemblages of shark species on the scale of the northern Gulf of Mexico and to investigate to what extent those patterns in shark communities were present regionally, along the coasts of Mississippi and Alabama.

The goal of this investigation was to characterize the spatial distribution of shark communities in coastal waters of the northern Gulf of Mexico. Previous studies have examined the distributions of coastal sharks in the northern Gulf of Mexico (Drymon et al., 2010), and we sought to further the approach in these studies by relating spatial trends in shark species assemblages to abiotic and biotic data, including the degree to which these patterns were driven by the availability of potential prey items. Ultimately, we wanted to determine whether patterns in the structure of shark communities and the factors that drive them are independent of scale. We predict this multifaceted approach will allow for a more precise understanding of the determinants of the spatial distributions of these predators in nature and for a definition of appropriate management measures.

Materials and methods

Small-scale study site

A bottom-longline survey was initiated in May 2006 by the National Marine Fisheries Service (NMFS) and the Dauphin Island Sea Lab (DISL). During this survey sharks were sampled from waters at depths of 1–20 m along the Alabama and Mississippi coastlines (Fig.1). Sampling occurred during all months (January–December) on NMFS research vessels (all 20–30 m in length), such as the RV *HST*, RV *Gandy*, and RV *Caretta*. A stratified random block design was used and 8 blocks were established along the combined coast of Mississippi and Alabama. Each block was ~10 km east–west and extended from the shoreline to approximately the 20-m isobath. Blocks 1–4 were located west of 88°00 W (western blocks), and blocks 5–8 were located east of 88°00 W (eastern blocks) (Fig. 1A). Sampling was allocated evenly and replicated within each block. For this study, we analyzed data collected in 2006–09 as part of this survey.

Small-scale sampling methods

Between 12 and 16 stations were randomly selected and sampled each month using a stratified random

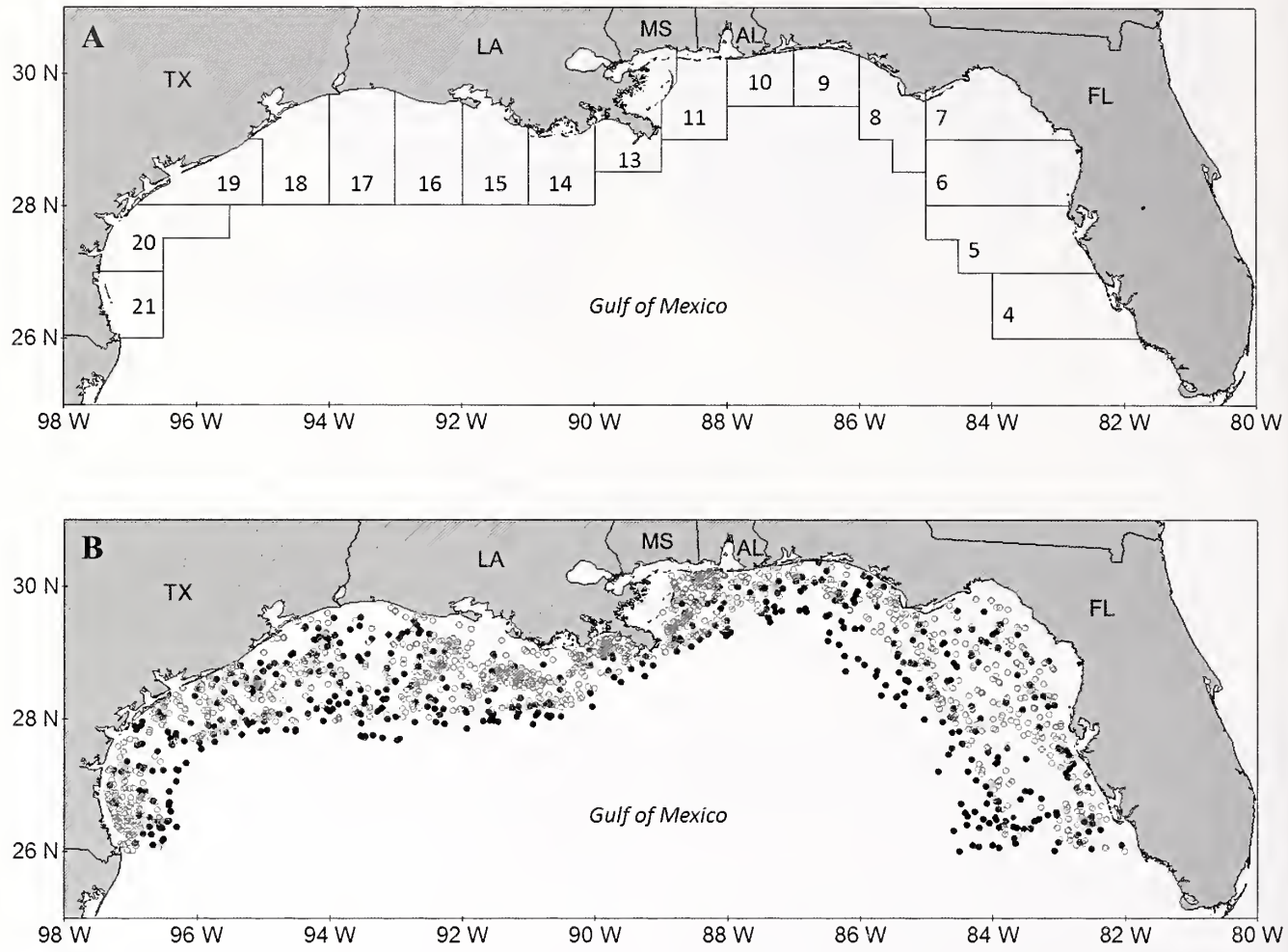

Figure 2

Spatial extent of the area used in the large-scale analysis of shark distribution in the northern Gulf of Mexico during 2006–09. (**A**) Seventeen National Marine Fisheries Service statistical zones (4–21 east to west, excluding zone 12), which spanned depths from 1 to ~250 m, where the bottom-longline sets were conducted by the NOAA Southeast Fisheries Science Center Mississippi Laboratories during the months of August and September. (**B**) Sampling locations for the large-scale bottom-longline data for 2006–09 are indicated by filled circles; trawl data for 2007–09 from the Southeast Area Monitoring and Assessment Program database (http://scamap.gsmfc.org) are indicated by open circles.

survey design that ensured equal effort across blocks 1–8 and the range of depths sampled (Fig. 1A). At each station, a single bottom-longline was set and soaked for 1 h. The main line consisted of 1.85 km (1 nmi) of 4-mm monofilament (545-kg test) that was set with 100 gangions. Gangions consisted of a longline snap and a 15/0 circle hook baited with Atlantic Mackerel (*Scomber scombrus*). Each gangion was made of 3.66 m of 3-mm monofilament (320-kg test).

Sharks that could be boated safely were removed from the main line, unhooked, and identified to species following Castro (2011). For each individual, sex, length (precaudal, fork, natural, and stretch total in centimeters), weight (in kilograms), and maturity stage (when possible) were recorded. All length measurements originated at the tip of the rostrum and terminated at the origin of the precaudal pit, the noticeable fork in the tail, the upper lobe of the caudal fin in a natural position, and the upper lobe of the caudal fin in a stretched position for precaudal, fork, natural, and stretch total lengths, respectively. Maturity in males was assessed according to Clark and von Schmidt (1965). Sharks were tagged either on the anterior dorsal fin with a plastic Rototag[1] (Dalton ID, Henley-on-Thames, UK) or just below the first dorsal fin with a metal dart tag. Which tag type was used depended both

[1] Mention of tradenames or commercial companies is for identification purposes only and does not imply endorsement by the National Marine Fisheries Service, NOAA.

on species and size of a shark at capture (Kohler and Turner, 2001).

Additional data sets

To determine whether the patterns that characterize the shark community assemblage in our study region (coasts of Alabama and Mississippi, hereafter referred to as *small scale*) were applicable across the northern Gulf of Mexico (hereafter called *large scale*), we obtained bottom-longline data from the SEFSC Mississippi Laboratories. This information included catch, fork length, and environmental data collected across Gulf of Mexico statistical zones 4–21 (Fig. 2A) in 2006–09. During that period bottom-longline sets were conducted by the Mississippi Laboratories in August and September. The methods used for the bottom-longline survey were identical at the small and large scales, and a complete description of these methods is provided in Driggers et al. (2008).

To examine factors that potentially influence the distribution of sharks on both small and large scales, we analyzed the relationships between longline shark data and a set of environmental factors, including trawl data and abiotic parameters. Biotic trawl data were obtained from the Southeast Area Monitoring and Assessment Program (SEAMAP) database (http://seamap.gsmfc.org, November 2010) of the Gulf States Marine Fisheries Commission. We restricted our analysis of SEAMAP data to those years for which trawling was conducted across the entire northern Gulf of Mexico (2007–09). The data from those years that were used in our analysis originated from both state (Louisiana, Alabama, Mississippi, and Florida) and federal (NOAA Fisheries) regulatory agencies. All data archived in the SEAMAP trawl database were collected according to standard SEAMAP trawl protocols (Rester, 2012). Two biotic variables, representative of the availability of potential prey for sharks, were selected for inclusion in our analysis of SEAMAP trawl data: fish biomass and crustacean biomass per station in kilograms. All biomass data from the trawl data set were standardized to kilogram per minute. The abiotic variables temperature (degrees Celsius), salinity (practical salinity unit), dissolved oxygen (milligrams per liter) and depth (meters) were collected with conductivity, temperature, and depth (CTD) instruments (SBE 911*plus* and SBE 25*plus* Sealogger, Sea-Bird Electronics, Inc., Bellevue, WA) during bottom-longline sampling at both the large and small scales.

To include a proxy for primary production in our analysis, we used data on chlorophyll-*a* (chl-*a*) concentration as a measure of phytoplankton biomass (Canion, 2008; Martinez-Lopez and Zavala-Hidalgo, 2009). The satellite-based ocean color data used in this study were derived from the moderate resolution imaging spectroradiometer (MODIS) on the Aqua satellite (for a detailed sensor description go to the MODIS mission website at http://modis.gsfc.nasa.gov). The data on chl-*a* concentration used for analyses in our study were downloaded from the Ocean Color website (http://oceancolor.gsfc.nasa.gov, accessed April 2012). For this study, annual binned level-3 chl-*a* data (Campbell et al., 1995) at a spatial resolution of 4 km were used from 2006 to 2009. The annual composites are produced by averaging all valid, cloud-free acquisitions for each ocean pixel. The valid pixels are determined by using an extensive quality control process that tests for numerous factors known to degrade data accuracy. Additional details for the level-3 chl-*a* data can be found at http://modis.gsfc.nasa.gov/data/atbd/index.php. Despite that extensive quality control process, the optically complex nature of the coastal zone can still present difficulties for ocean color algorithms. In the case of data on chl-*a* concentration, algorithms are known to overestimate concentrations in coastal zones, particularly in regions that are influenced by a river, because of estuarine materials, such as suspended sediment and concentrations of dissolved organic material. However, this phenomenon occurs primarily at depths <10 m (Martinez-Lopez and Zavala-Hidalgo, 2009); therefore, we obtained data on chl-*a* concentration from the 25-m isobath to limit the effect of these degrading influences.

Data analyses

Bottom-longline data sets were limited to those species observed in both the small- and large-scale bottom-longline surveys. Data of catch per unit of effort (CPUE), measured as sharks 100 hooks^{-1} h^{-1}, were log(x+1)-transformed to reduce the influence of the most common species and to standardize the data (Legendre and Legendre, 1998). All sets, including those with zero catches, were included in our analyses. Mean CPUE data were then analyzed as a function of block (blocks 1–8) across the small scale (Fig. 1A) and as a function of statistical zone (zones 4–21, minus zone 12) across the large scale (Fig. 2A).

A centered principal component analysis (PCA) was performed on mean transformed shark CPUE data for both small- and large-scale data. The data collected with the CTD instruments and the MODIS satellite data (collectively hereafter referred to as *environmental data*) at both small and large scales were analyzed with a normed PCA. At each spatial scale, centered (for shark CPUE data) and normed (for environmental data) PCAs allowed for the identification of the major spatial patterns that characterize shark assemblages and environmental conditions and for the visualization of covariances between shark species and of correlations between environmental factors (Legendre and Legendre, 1998).

The relationships between values of shark CPUE and environmental factors were then analyzed at each spatial scale with co-inertia analyses (COIA). Co-inertia analysis is a flexible, multivariate method that couples environmental and faunal data and measures the degree of agreement between them (Dolédec and

Chessel, 1994; Dray et al., 2003). This method has been used successfully on diverse ecological data sets and organisms, including fishes (e.g., Mellin et al., 2007; Carassou et al., 2011; Lecchini et al., 2012), zooplankton (e.g., Carassou et al., 2010), benthic invertebrates (e.g., Bremner et al., 2003), and bacteria (e.g., Jardillier et al., 2004). In our study, each COIA was based on the matching of a normed PCA of environmental data and a centered PCA of shark abundance data (PCA-PCA-COIA, Dray et al., 2003). Monte Carlo tests with 10,000 permutations between observations were used to confirm the significance of COIA results (fixed-D test; Dray et al., 2003), with significance assessed at $P \leq 0.05$. For each COIA, the vectorial correlation (RV) coefficient, a multivariate generalization of the squared Pearson's correlation coefficient, provided a quantitative measure of the co-structure between explanative (environmental) and explained (shark CPUE) variables, with a value of 1 indicating a perfect match between the 2 data sets (Dolédec and Chessel, 1994; Dray et al., 2003). The criterion of total inertia was used to compare the amount of agreement between environmental and shark data for the 2 spatial scales considered (Dray et al., 2003). All multivariate analyses were performed with the ADE-4 software (Thioulouse et al., 1997, 1995–2000).

Results

Small-scale sampling

During small-scale sampling, 353 stations were surveyed, spanning the months from March to November during 2006–09 (Fig. 1B). Winter months (December, January, and February) were excluded from subsequent analyses because of the complete absence of sharks in the small-scale survey area during this time (2100 hooks with no sharks). Over the course of this survey, 2417 individuals representing 12 shark species were encountered. Of these 12 species, 5 species met our criteria for inclusion in subsequent analyses (i.e., they also were abundant in the large-scale data set): Atlantic Sharpnose Shark (*Rhizoprionodon terraenovae*), Blacktip Shark (*Carcharhinus limbatus*), Blacknose Shark (*C. acronotus*), Spinner Shark (*C. brevipinna*), and Bull Shark (*C. leucas*). Mean CPUE (±standard error [SE]) ranged from 2.88 [0.28] sharks 100 hooks^{-1} h^{-1} for Atlantic Sharpnose Shark to 0.11 (0.02) sharks 100 hooks^{-1} h^{-1} for Bull Shark (Table 1). Wide size ranges, with size measured as fork length (FL) in centimeters, were found for Atlantic Sharpnose (36.0–96.3 cm FL), Blacktip (59.8–164.0 cm FL), Blacknose (40.9–136.0 cm FL), and Spinner (49.9–165.9 cm FL) Sharks. A smaller size range was seen for Bull Sharks (73.0–155.5 cm FL), the least commonly encountered of the 5 species (Table 1).

The centered PCA conducted with small-scale data on shark abundance explained 91.88% of the variability between observations (across blocks 1–8) on the first 2 principal components (PC1 and PC2) (Fig. 3A). Variation along PC1 was explained primarily by data for Atlantic Sharpnose Shark, which was most abundant in blocks 2, 3, and 4 (western blocks), less common in block 1, and relatively rare in blocks 5, 6, 7, and 8 (eastern blocks). Spinner Shark showed a similar but less marked spatial pattern (Fig. 3A). Variation along PC2 was explained primarily by data for Blacktip Shark, which was more abundant in block 1 (western block), and relatively rare in block 5 and 6 (eastern blocks) (Fig. 3A). Patterns were less clear for Blacknose and Bull Shark.

The normed PCA on small-scale environmental data explained 74.18% of the variability between observations (blocks) on the first 2 principle components (PC1 and PC2) (Fig. 4A). Temperature and crustacean biomass were positively correlated with each other and both of those variables had a high negative correlation with salinity. These 3 variables explained most of the variability along PC1. Fish biomass was negatively correlated with depth. Chl-*a* concentration and dissolved oxygen were negatively correlated, together explaining most of the variability along PC2. Blocks 7 and 8 (eastern blocks) were characterized by high dissolved oxygen and low concentration of chl-*a*, and the inverse was true for block 3 (a western block) (Fig. 4A).

The COIA that coupled small-scale shark abundance and environmental data was characterized by a total inertia of 0.22 and an RV coefficient of 0.65, indicating a relatively high degree of agreement between the structures of the 2 data sets. Axes 1 and 2 supported 99.17% of this common structure (Fig. 5A). Atlantic Sharpnose Shark abundance was positively related with chl-*a* concentration and negatively related with dissolved oxygen and salinity. Abundance of Blacktip Shark was more positively associated with crustacean biomass than with other environmental variables. Blacknose and Spinner Sharks had high negative associations with dissolved oxygen, and Blacknose Shark had a strong positive association with depth (Fig. 5A).

Large-scale sampling

Across the large-scale survey area, shark abundance data were obtained from 551 stations sampled during the months of August and September during 2006–09 (Fig. 2B). Over the course of this survey, 4493 sharks, comprising 26 species, were captured. Mean catch per unit of effort (±SE) ranged from 4.74 (0.41) sharks 100 hooks^{-1} h^{-1} for Atlantic Sharpnose Shark to 0.06 (0.01) sharks 100 hooks^{-1} h^{-1} for Bull Shark (Table 1). Wide size ranges were observed for Atlantic Sharpnose (33.0–115.5 cm FL), Blacktip (38.2–157.0 cm FL), Blacknose (40.0–104.9 cm FL), and Spinner (54.0–169.0 cm FL) Sharks. The smallest size range was seen in Bull Shark (131.4–176.0 cm FL), the least commonly encountered of the 5 species (Table 1).

Table 1

Data that we used in our analyses of shark distribution in the northern Gulf of Mexico during 2006–09. Number, mean size (measured as fork length [FL] in centimeters and standard error of the mean [SE]), size range, and mean catch per unit of effort (CPUE), measured as sharks 100 hooks^{-1} h^{-1}, are shown for the 5 shark species common to both of the 2 data sets: small (Alabama and Mississippi coasts) and large (across the northern Gulf of Mexico). The 5 species were Atlantic Sharpnose Shark (*Rhizoprionodon terraenovae*), Blacktip Shark (*Carcharhinus limbatus*), Blacknose Shark (*C. acronotus*), Spinner Shark (*C. brevipinna*), and Bull Shark (*C. leucas*). *n*=no. of sharks sampled.

Species	*n*	Mean size ±SE (cm FL)	Range (cm FL)	Mean CPUE ±SE (sharks 100 hooks^{-1} h^{-1})
Small scale				
Atlantic Sharpnose Shark	1016	68.8 (0.43)	36.0–96.3	2.88 (0.28)
Blacktip Shark	474	102.7 (0.93)	59.8–164.0	1.34 (0.14)
Blacknose Shark	600	91.1 (0.42)	40.9–136.0	1.70 (0.19)
Spinner Shark	147	70.1 (1.86)	49.9–165.9	0.42 (0.06)
Bull Shark	40	102.8 (6.09)	73.0–155.5	0.11 (0.02)
Large scale				
Atlantic Sharpnose Shark	2596	73.9 (0.20)	33.0–115.5	4.74 (0.41)
Blacktip Shark	254	111.7 (1.19)	38.2–157.0	0.51 (0.08)
Blacknose Shark	530	85.0 (0.52)	40.0–104.9	0.98 (0.11)
Spinner Shark	158	104.7 (2.17)	54.0–169.0	0.29 (0.08)
Bull Shark	21	155.0 (2.77)	131.4–176.0	0.06 (0.01)

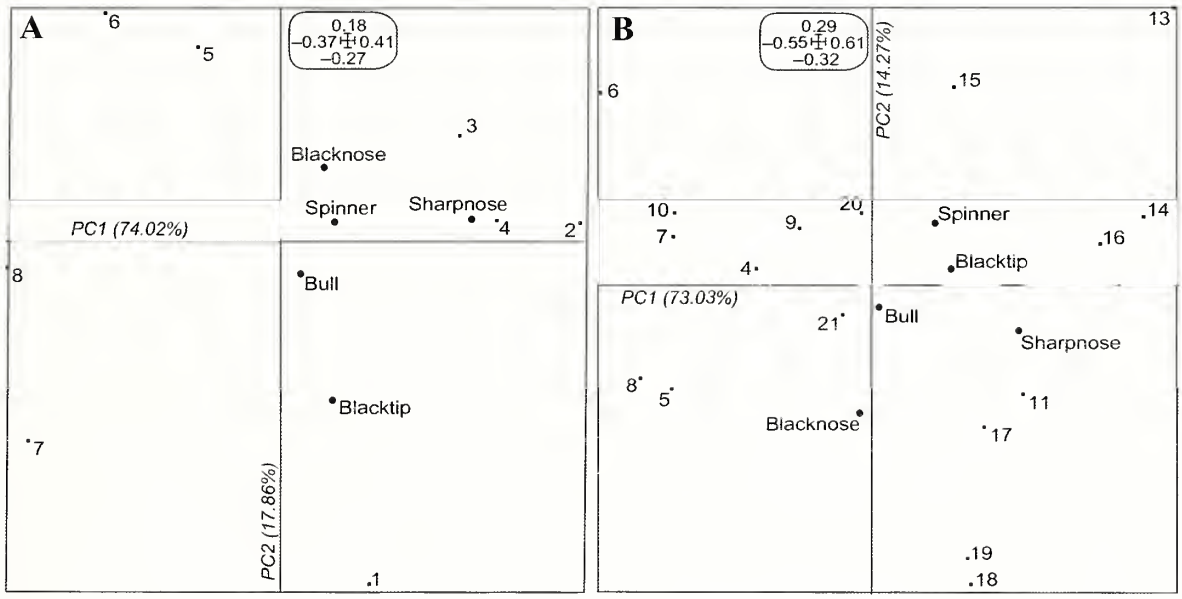

Figure 3

Results of the centered principal components analysis (PCA) on shark data from (**A**) small-scale and (**B**) large-scale bottom-longline surveys conducted in the northern Gulf of Mexico during 2006–09. Numbers within the panels correspond to the sampling blocks (1–8) and statistical zones (4–21, minus 12) of the small- and large-scale surveys, respectively, used in our analysis (blocks and zones are defined in Figs. 1 and 2). Filled circles represent shark species. The sum of the variation explained by the first (PC1) and second (PC2) principal components is 91.88% for small-scale survey and 87.30% for large-scale survey. The scale is shown in ovals at top of each panel.

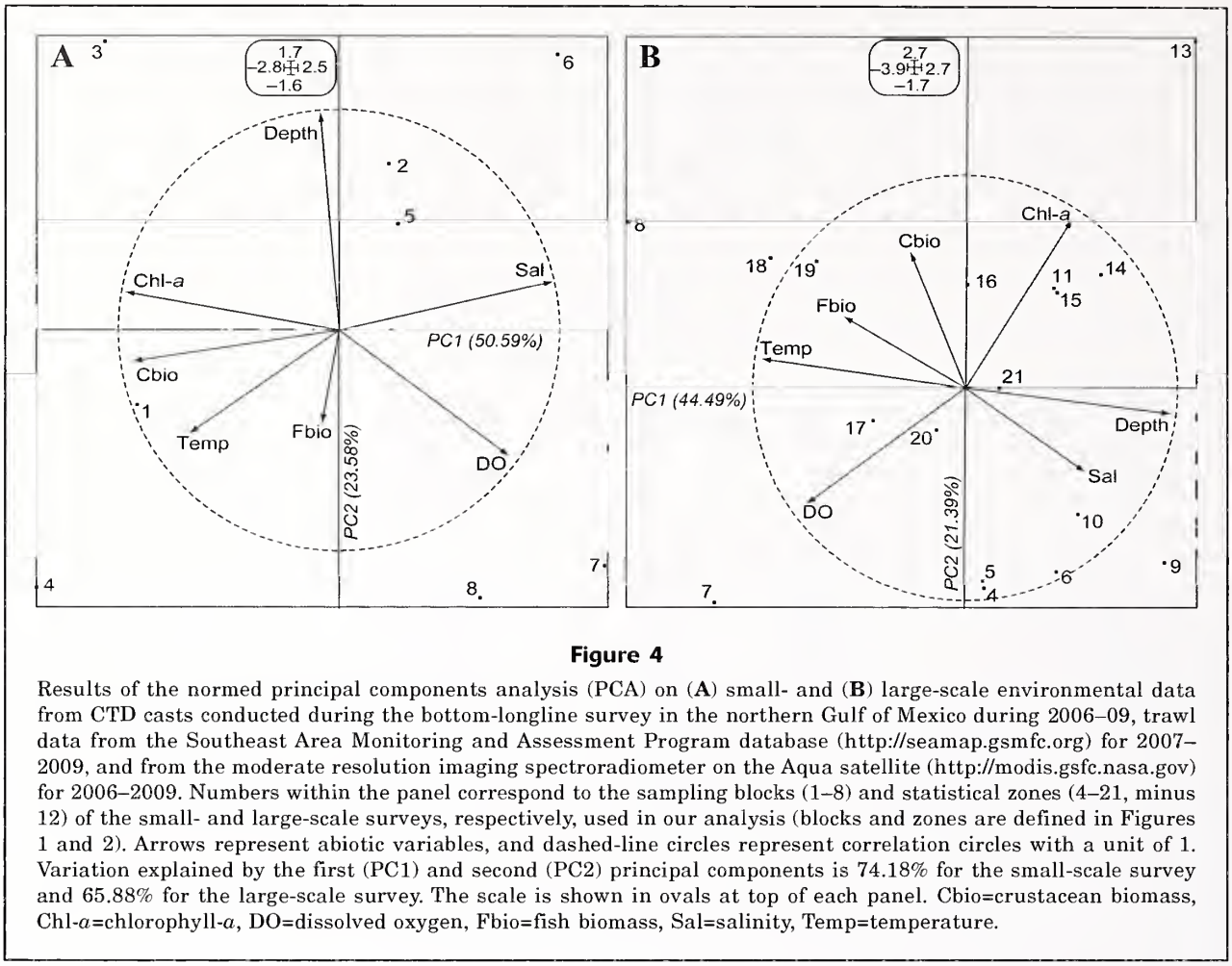

Figure 4

Results of the normed principal components analysis (PCA) on (**A**) small- and (**B**) large-scale environmental data from CTD casts conducted during the bottom-longline survey in the northern Gulf of Mexico during 2006–09, trawl data from the Southeast Area Monitoring and Assessment Program database (http://seamap.gsmfc.org) for 2007–2009, and from the moderate resolution imaging spectroradiometer on the Aqua satellite (http://modis.gsfc.nasa.gov) for 2006–2009. Numbers within the panel correspond to the sampling blocks (1–8) and statistical zones (4–21, minus 12) of the small- and large-scale surveys, respectively, used in our analysis (blocks and zones are defined in Figures 1 and 2). Arrows represent abiotic variables, and dashed-line circles represent correlation circles with a unit of 1. Variation explained by the first (PC1) and second (PC2) principal components is 74.18% for the small-scale survey and 65.88% for the large-scale survey. The scale is shown in ovals at top of each panel. Cbio=crustacean biomass, Chl-*a*=chlorophyll-*a*, DO=dissolved oxygen, Fbio=fish biomass, Sal=salinity, Temp=temperature.

The centered PCA conducted with large-scale data on shark abundance explained 87.30% of the variability between observations (across NMFS statistical zones) on the first 2 principal components (Fig. 3B). Variation along PC1 was mainly explained by data for Atlantic Sharpnose Shark, which was more abundant in zones 11, 14, and 16 (western zones), and variation along PC2 was mainly explained by data for Blacknose Shark, which was more abundant in zones 3 and 5 (eastern zones) (Fig. 3B). Compared with other species, Bull Shark displayed a weaker pattern because of their lower abundances (Fig. 3B).

The normed PCA on large-scale environmental data explained 65.88% of the variability between observations (NMFS statistical zones) on the first 2 principle components (Fig. 4B). Fish biomass and temperature were correlated, and both of these variables were negatively correlated with depth. These 3 variables explained most of the variability along PC1 (Fig. 4B). Chl-*a* concentration and crustacean biomass were positively correlated, and concentration of chl-*a* had a strong negative correlation with dissolved oxygen. Together, these 3 variables explained the majority of variability along PC2. NMFS statistical zones 11, 14, 15, and 16 were characterized by high chl-*a* concentration, and zones 18 and 19 were characterized by high fish biomass. Conversely, eastern zones 4–6 were characterized by low fish and crustacean biomass (Fig. 4B).

The COIA that coupled large-scale shark abundance and environmental data was characterized by a total inertia of 0.20 and a RV coefficient of 0.42, indicating good agreement between the 2 data sets. Axes 1 and 2 supported 97.32% of this common structure (Fig. 5B). Abundance of Atlantic Sharpnose Shark was strongly related to chl-*a* concentration and had a strong negative relation to dissolved oxygen. Spinner Shark showed a similar pattern. Blacktip Shark abundance was related to crustacean biomass and had a strong negative relation to salinity. Abundance of Blacknose Shark was strongly related to temperature and inversely related to depth (Fig. 5B)

Discussion

For comparison of the factors that affect the distribution of sharks across spatial scales, COIA provides a

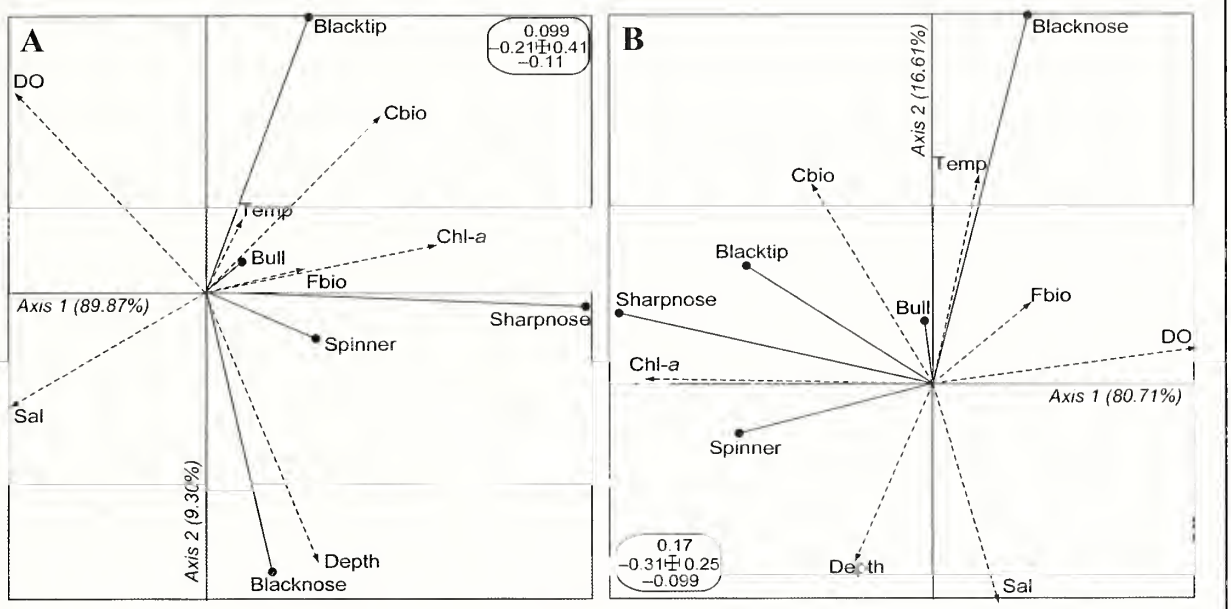

Figure 5

Results of the co-inertia analyses on (**A**) small- and (**B**) large-scale shark and environmental data from the northern Gulf of Mexico during 2006–09. Small-scale total inertia is 0.22, and axes 1 and 2 supported 99.17% of this structure. Large-scale total inertia is 0.20, and axes 1 and 2 supported 97.32% of this structure. The scale is shown in ovals at top of each panel. Arrows and dotted lines represent environmental variables. Filled circles and full lines represent shark species. Cbio=crustacean biomass, Chl-*a*=chlorophyll-*a*, DO=dissolved oxygen, Fbio=fish biomass, Sal=salinity, Temp=temperature.

robust tool. Examination of the results for total inertia indicates that analyses at both small and large scales were equally useful for identification of patterns between sharks and explanatory variables. However, the RV coefficients indicate that explanatory variables were better correlated with shark abundances at the small scale (RV=0.65) than at the large scale (RV=0.42). Given 1) the unique coupling of bottom-longline data sets collected through the use of identical methods across the same temporal scale and 2) the similarity in shark size and catch between the surveys at 2 spatial scales, our data are particularly well suited to COIA. Our results indicate that the factors affecting the distribution of sharks in the Gulf of Mexico are species specific but relatively well conserved across spatial scales.

The factors that affect the distribution of Blacktip Shark were similar at small and large scales, and the distribution of this species was best explained by crustacean biomass at both scales. However, it is unlikely that Blacktip Shark responded to crustaceans as potential prey. Although previous studies of feeding habits of Blacktip Shark in the northern Gulf of Mexico (Hoffmayer and Parsons, 2003; Barry et al., 2008) and Florida (Heupel and Hueter, 2002) have identified crustacean components, these same studies have revealed that Blacktip Sharks prey predominately on teleosts. That Blacktip Shark distributions may not be influenced by the distribution of their preferred prey is not surprising. In an acoustic telemetry study in Terra Ceia Bay, Florida, no correlation was found between juvenile Blacktip Shark and their prey (Heupel and Hueter, 2002). After examination of the influence of prey abundance on the distribution of sharks (including Blacktip Shark) at 2 spatial scales, Torres et al. (2006) showed no correlation between shark catch and teleost abundance at individual sampling locations, although a correlation was shown between shark catch and teleost abundance within a region. The strong relationship observed in our study between Blacktip Shark and crustacean biomass at both spatial scales indicates that perhaps the underlying mechanism that most influences the distribution of this species correlates with crustacean biomass.

Distribution of Atlantic Sharpnose Shark was best explained by chl-*a* concentration, a pattern that, like the one seen for Blacktip Shark, was independent of scale. However, although Blacktip Shark may have been influenced by factors other than prey, Atlantic Sharpnose Shark may have been indirectly responding to available prey as indicated by the observed relationship with concentration of chl-*a*. The contrast between Blacktip Shark and Atlantic Sharpnose Shark may illustrate basic differences in the ecology of these 2 species. As adults, Blacktip Sharks are a larger, more mo-

bile species than Atlantic Sharpnose Sharks, and they are capable of moving hundreds of kilometers on short time scales, as illustrated by traditional (Kohler et al., 1998) and pop-up satellite archival (senior author and S. Powers, unpubl. data) tagging data. In contrast, Atlantic Sharpnose Sharks have a relatively small home range (Carlson et al., 2008). Blacktip Sharks, compared with Atlantic Sharpnose Sharks, may show higher vagility when faced with a patchy prey environment. For example, Atlantic Sharpnose Sharks sampled in the small-scale survey showed relative trophic plasticity. Portunid crabs and shrimp contribute more to the diet of Atlantic Sharpnose Sharks sampled west (blocks 1-4 in the current study) than to the diet of this shark species east (blocks 5-8) of Mobile Bay, and therefore may reflect differences in the prey base between these 2 areas (Drymon et al., 2012). These findings indicate that the Atlantic Sharpnose Shark may have a wider dietary breadth than the Blacktip Shark and may, therefore, be responding to gradients in overall production as opposed to fish or crustacean biomass, specifically.

Distributions of Atlantic Sharpnose and Spinner Sharks at both large and small scales were negatively related to dissolved oxygen. This relationship has been previously identified for other species of juvenile sharks. In Chesapeake Bay, Virginia, tree-based regression models indicated the importance of dissolved oxygen as a factor that influences the distribution of juvenile Sandbar Shark (*Carcharhinus plumbeus*) (Grubbs and Musick, 2007). Similarly, researchers have noted that, although dissolved oxygen is not as widely considered as temperature or salinity, it may play an important role as an environmental influence that affects the distribution of top predators in coastal environments, as has been demonstrated for juvenile Bull Shark in Florida waters (Heithaus et al., 2009).

In our study, a wide size range of Spinner Shark was documented across both the small- and large-scale surveys. On the basis of age and growth data (Carlson and Baremore, 2005), the mean sizes of Spinner Shark captured in small- and large-scale surveys corresponded to the ages of approximately 1 and 4 years old, respectively. Conversely, across surveys at both spatial scales, the mean size of Atlantic Sharpnose Shark was indicative of mature, adult animals (Carlson and Baremore, 2003). Our findings, therefore, support previous work that indicated the importance of dissolved oxygen as an influence on the distribution of juvenile sharks (Grubbs and Musick, 2007; Heithaus et al., 2009) and indicates that dissolved oxygen may influence the distribution of adult sharks as well.

Distributions of Blacknose Shark were best explained by depth, the direction of which varied as a function of scale. On the small scale, Blacknose Shark distribution was strongly and positively associated with water depth (i.e., deeper water resulted in higher Blacknose Shark CPUE). Conversely, at the large scale, distribution of Blacknose Shark were strongly and negatively associated with deep water (i.e., the shallower the depth, the lower the observed CPUE Blacknose Shark). This apparent dichotomy highlights differences in the range of depths associated with each spatial scale and likely reflects a preferred depth range for this species. Small-scale sampling occurred at depths up to ~20 m, and large-scale sampling occurred primarily at depths >20 m. Discrete depth preferences for Blacknose Shark have previously been documented. Analyzing the same 2 bottom-longline data sets used in our analyses, Drymon et al. (2010) showed a discrete depth preference of 10–30 m for Blacknose Shark. Our data support these findings yet provide no additional insight into why Blacknose Shark occupy these depths.

Although our analyses identified factors that may influence the distribution of selected shark species at 2 different spatial scales, our approach has certain limitations. For instance, the faunal component of our analyses was based on catch data (CPUE). Bait loss can affect CPUE calculations (Torres et al., 2006). In areas where (or during times when) bait loss is high, CPUE may be artificially low. Recording the status of individual gangions (i.e., fish caught, bait present, bait absent) allows for hook-specific CPUE to be calculated, resulting in more accurate determination of CPUE and, hence, improving the power of this approach. In addition, the analyses we used are sensitive to the temporal alignment of the data sets used. Restriction of analyses to data collected with the same methods and during the same time period will facilitate the identification of reliable relationships between faunal and explanatory data.

Conclusions

Identification of the factors that affect the distribution of large predators is challenging. Our analysis encompasses physical parameters (salinity, temperature, dissolved oxygen, and depth), proxies for primary (chl-*a* concentration) and secondary (trawl) productivity, and predatory data sets across 2 spatial scales. Our results indicate that the factors that affect the distribution of sharks in the Gulf of Mexico are species dependent but may transcend the spatial boundaries that we examined. As physical and biological characteristics of ecosystems in the Gulf of Mexico change, species-specific knowledge of how these factors influence the distributions of top predators will be critical for the implementation of proactive management measures.

Acknowledgments

The authors wish to thank all members of the Fisheries Ecology Laboratory at Dauphin Island Sea Laboratory (DISL), as well as members of the NOAA Southeast Fisheries Science Center Mississippi Laboratories shark team for the countless hours they spent at sea collecting valuable data. Data from DISL's Fisheries

Oceanography of Coastal Alabama research program, which is funded by the Alabama Department of Conservation and Natural Resources, Marine Resources Division, were used to provide ground truth for remotely sensed data from NASA's Sea-viewing Wide Field-of-view Sensor (SeaWifs) Project. We wish to thank T. Henwood and E. Hoffmayer from the National Marine Fisheries Service for constructive comments that improved this manuscript.

Literature cited

Barry, K. P., R. E. Condrey, W. B. Driggers III, and C. M. Jones.
2008. Feeding ecology and growth of neonate and juvenile blacktip sharks *Carcharhinus limbatus* in the Timbalier-Terrebone Bay complex, LA, U.S.A. J. Fish Biol. 73:650–662.

Bremner, J., S. I. Rogers, and C. L. J. Frid.
2003. Assessing functional diversity in marine benthic ecosystems: a comparison of approaches. Mar. Ecol. Prog. Ser. 254:11–25.

Campbell, J. W., J. M. Blaisdell, and M. Darzi.
1995. Level-3 SeaWiFS data products: spatial and temporal binning algorithms. NASA Tech. Memo. 104566, vol. 32, 73 p.

Canion, A.K.
2008. Variability in productivity model inputs on multiple timescales: implications for productivity monitoring in Weeks Bay, Alabama. M.S. thesis, 99 p. Univ. South Alabama, Mobile, AL.

Carassou, L., R. LeBorgne, E. Rolland, and D. Ponton.
2010. Spatial and temporal distribution of zooplankton related to the environmental conditions in the coral reef lagoon of New Caledonia, Southwest Pacific. Mar. Pollut. Bull. 61:367–374.

Carassou, L., B. Dzwonkowski, F. J. Hernandez, S. P. Powers, K. Park, W. M. Graham, and J. Mareska.
2011. Environmental influences on juvenile fish abundances in a river-dominated coastal system. Mar. Coast. Fish. 3:411–427.

Carlson, J. K., and I. E. Baremore.
2003. Changes in biological parameters of Atlantic sharpnose shark *Rhizoprionodon terraenovae* in the Gulf of Mexico: evidence for density-dependent growth and maturity? Mar. Freshw. Res. 54:227–234.

Carlson, J. K., and I. E. Baremore.
2005. Growth dynamics of the spinner shark (*Carcharhinus brevipinna*) off the United States southeast and Gulf of Mexico coasts: a comparison of methods. Fish. Bull. 103:280–291.

Carlson, J. K., M. R. Heupel, D. M. Bethea, and L. D. Hollensead.
2008. Coastal habitat use and residency of juvenile Atlantic sharpnose sharks (*Rhizoprionodon terraenovae*). Estuaries Coasts 31:931–940.

Castro, J. I.
2011. The sharks of North America, 640 p. Oxford Univ. Press, Inc., New York.

Clark, E., and K. von Schmidt.
1965. Sharks of the central Gulf coast of Florida. Bull. Mar. Sci. 15:13–83.

Dolédec, S., and D. Chessel.
1994. Co-inertia analysis: an alternative method for studying species-environment relationships. Freshw. Biol. 31:277–294.

Dray, S. D., D. Chessel, and J. Thioulouse.
2003. Co-inertia analysis and the linking of ecological data tables. Ecology 84(11):3078–3089.

Driggers, W. B., G. W. Ingram, M. A. Grace, C. T. Gledhill, T. A. Henwood, C. N. Horton, and C. M. Jones.
2008. Pupping areas and mortality rates of young tiger sharks *Galeocerdo cuvier* in the western North Atlantic Ocean. Aquat. Biol. 2:161–170.

Drymon, J. M., S. P. Powers, J. Dindo, B. Dzwonkowski, and T. A. Henwood.
2010. Distributions of sharks across a continental shelf in the northern Gulf of Mexico. Mar. Coast. Fish. 2:440–250.

Drymon, J. M., S. P. Powers, and R. H. Carmichael.
2012. Trophic plasticity in the Atlantic sharpnose shark (*Rhizoprionodon terraenovae*) from the north central Gulf of Mexico. Environ. Biol. Fishes 95:21–35.

Francis, R. C., M. A. Hixon, M. E. Clarke, S. A. Murawski, and S. Ralston.
2007. Ten commandments for ecosystem-based fisheries scientists. Fisheries 32:217–233.

Grubbs, R. D., and J. A. Musick.
2007. Spatial delineation of summer nursery areas for juvenile sandbar sharks in Chesapeake Bay, Virginia. Am. Fish. Soc. Symp. 50:87–108.

Hammerschlag, N., A. J. Gallagher, and D. M. Lazarre.
2011. A review of shark satellite tagging studies. J. Exp. Mar. Biol. Ecol. 398(1–2):1–8.

Heithaus, M. R., D. Burkholder, R. E. Heuter, L. I. Heithaus, H. R. Pratt Jr., and J. C. Carrier.
2007. Spatial and temporal variation in shark communities of the lower Florida Keys and evidence for historical population declines. Can. J. Fish. Aquat. Sci. 64:1302–1313.

Heithaus, M. R., A. Frid, A.J. Wirsing, and B. Worm.
2008. Predicting ecological consequences of marine top predator declines. Trends Ecol. Evol. 23:202–210.

Heithaus, M. R., B. K. Delius, A. J. Wirsing, and M. M. Dunphy-Daly.
2009. Physical factors influencing the distribution of a top predator in a subtropical oligotrophic estuary. Limnol. Oceanogr. 54:472–482.

Heupel, M. R., and R. E. Hueter.
2002. Importance of prey density in relation to the movement patterns of juvenile blacktip sharks (*Carcharhinus limbatus*) within a coastal nursery area. Mar. Freshw. Res. 53:543–550.

Hoffmayer, E. R., and G. R. Parsons.
2003. Food habits of three shark species from the Mississippi Sound in the northern Gulf of Mexico. Southeast. Nat. 2:271–280.

Hughes, T. P., D. R. Bellwood, C. Folke, R. S. Steneck, and J. Wilson.
2005. New paradigms for supporting the resilience of marine ecosystems. Trends Ecol. Evol. 20:380–386.

Jardillier, L., M. Basset, I. Domaizon, A. Belan, C. Amblard, M. Richardot, and D. Debroas.
2004. Bottom-up and top-down control of bacterial community composition in the euphotic zone of a reservoir. Aquat. Microb. Ecol. 35:259–273.

Kohler, N. E., J. G. Casey, and P. A. Turner.
1998. NMFS cooperative shark tagging program, 1962–1993: an atlas of shark tag and recapture data. Mar. Fish. Rev. 60(2):1–87.

Kohler, N. E., and P. A. Turner.
2001. Shark tagging: a review of conventional methods and studies. Environ. Biol. Fishes. 60:191–223.

Lecchini, D., L. Carassou, B. Frédérich, Y. Nakamura, S. C. Mills, and R. Galzin.
2012. Effects of alternate reef states on coral reef fish habitat associations. Environ. Biol. Fishes 94:421–429.

Legendre, P., and L. Legendre.
1998. Numerical ecology, 2nd ed., 853 p. Elsevier Science, Amsterdam.

Martinez-Lopez, B., and J. Zavala-Hidalgo.
2009. Seasonal and interannual variability of cross-shelf transport of chlorophyll in the Gulf of Mexico. J. Mar. Syst.77:1–20.

Mellin, C., M. Kulbicki, and D. Ponton.
2007. Seasonal and ontogenetic patterns of habitat use in coral reef fish juveniles. Estuar. Coast. Shelf Sci. 75:481–491.

Perry, R. I., and R. E. Ommer.
2003. Scale issues in marine ecosystems and human interactions. Fish. Oceanogr. 12:513–522.

Schneider, D. C.
2001. The rise of the concept of scale in ecology. Bioscience 51:545–553.

Sims, D. W.
2010. Tracking and analysis techniques for understanding free-ranging shark movements and behavior. *In* Sharks and their relatives II: biodiversity, adaptive physiology, and conservation (J. C. Carrier, J. A. Musick, and M. R. Heithaus, eds.), p. 351–392. CRC Press, Boca Raton, FL.

Rester, J. K. (ed.).
2012. SEAMAP environmental and biological atlas of the Gulf of Mexico, 2010, 84 p. Gulf States Marine Fisheries Commission, Ocean Springs, MS.

Thioulouse, J., D. Chessel, S. Dolédec, and J-M. Olivier.
1997. ADE-4: a multivariate analysis and graphical display software. Stat. Comput. 7:75–83.

Thioulouse, J., D. Chessel, S. Dolédec, J-M. Oliver, F. Goreaud, and R. Pelissier.
1995–2000. ADE-4. Ecological data analysis: exploratory and euclidean methods in environmental sciences. Version 2001, CNRS, Lyon, France. [Available from http://pbil.univ-lyon1.fr/ADE-4-old/ADE-4.html.]

Torres, L. G., M. R. Heithaus, and B. Delius.
2006. Influence of teleost abundance on the distribution and abundance of sharks in Florida Bay, USA. Hydrobiologia 569:449–455.

Food habits of Sowerby's beaked whales (*Mesoplodon bidens*) taken in the pelagic drift gillnet fishery of the western North Atlantic

Frederick W. Wenzel (contact author)[1]
Pamela T. Polloni[2]
James E. Craddock[2] (deceased)
Damon P. Gannon[3]
John R. Nicolas[1] (deceased)
Andrew J. Read[4]
Patricia E. Rosel[5]

Email address for contact author: frederick.wenzel@noaa.gov

[1] Protected Species Branch
Northeast Fisheries Science Center
National Marine Fisheries Service, NOAA
166 Water Street
Woods Hole, Massachusetts 02543

[2] Biology Department
Woods Hole Oceanographic Institution
Woods Hole, Massachusetts 02543

[3] Department of Biology
Bowdoin College
6500 College Station
Brunswick, Maine 04011

[4] Division of Marine Science and Conservation
Nicholas School of the Environment
Duke University
Beaufort, North Carolina 28516

[5] Protected Resources and Biodiversity Division
Southeast Fisheries Science Center
National Marine Fisheries Service, NOAA
646 Cajundome Blvd.
Lafayette, Louisiana 70506

Abstract—We describe the food habits of the Sowerby's beaked whale (*Mesoplodon bidens*) from observations of 10 individuals taken as bycatch in the pelagic drift gillnet fishery for Swordfish (*Xiphias gladius*) in the western North Atlantic and 1 stranded individual from Kennebunk, Maine. The stomachs of 8 bycaught whales were intact and contained prey. The diet of these 8 whales was dominated by meso- and benthopelagic fishes that composed 98.5% of the prey items found in their stomachs and cephalopods that accounted for only 1.5% of the number of prey. Otoliths and jaws representing at least 31 fish taxa from 15 families were present in the stomach contents. Fishes, primarily from the families Moridae (37.9% of prey), Myctophidae (22.9%), Macrouridae (11.2%), and Phycidae (7.2%), were present in all 8 stomachs. Most prey were from 5 fish taxa: Shortbeard Codling (*Laemonema barbatulum*) accounted for 35.3% of otoliths, Cocco's Lanternfish (*Lobianchia gemellarii*) contributed 12.9%, Marlin-spike (*Nezumia bairdii*) composed 10.8%, lanternfishes (*Lampanyctus* spp.) accounted for 8.4%; and Longfin Hake (*Phycis chesteri*) contributed 6.7%. The mean number of otoliths per stomach was 1196 (range: 327–3452). Most of the fish prey found in the stomachs was quite small, ranging in length from 4.0 to 27.7 cm. We conclude that the Sowerby's beaked whales that we examined in this study fed on large numbers of relatively small meso- and benthopelagic fishes that are abundant along the slope and shelf break of the western North Atlantic.

Manuscript submitted 4 February 2013.
Manuscript accepted 30 August 2013.
Fish. Bull. 111:381–389.
doi: 10.7755/FB.111.4.7

The views and opinions expressed or implied in this article are those of the author (or authors) and do not necesarily reflect the position of the National Marine Fisheries Service, NOAA.

The Sowerby's beaked whale (*Mesoplodon bidens*) is 1 of 4 species of the genus *Mesoplodon* (Family Ziphiidae) in the western North Atlantic. The Sowerby's beaked whale is restricted to the North Atlantic and the most boreal species in its genus, with observations recorded as far north as 71°N (Carlstrom et al., 1997; Hooker and Baird, 1999; McAlpine and Rae, 1999; Lucas and Hooker, 2000; Waring et al., 2010). There is also a single record of a stranded Sowerby's beaked whale from the Gulf of Mexico (Bonde and O'Shea, 1989).

Most information on the distribution and abundance of beaked whales off the northeastern coast of the United States has been derived from vessel surveys conducted by NOAA Fisheries. It is difficult to identify *Mesoplodon* beaked whales to species level at sea; therefore estimates of abundance are often reported at the generic level in stock assessments (e.g., Waring et al., 2010). Waring et al. (2001) reported that off the northeastern coast of the United States, *Mesoplodon* beaked whales were encountered most frequently along the shelf break and north wall of the Gulf Stream. The habitat preferences of these animals overlap with the habitat preferences of the sperm whale (*Physeter macrocephalus*), but Sowerby's beaked whales were concentrated on the colder shelf edge (Griffin, 1999; Waring et al., 2001).

MacLeod et al. (2003) reviewed available information on the diet of beaked whales and concluded that fishes are important prey of 5 of the 10 (Family Ziphiidae) species for which diet information was available. This conclusion stands in contrast to earlier reviews of the diet of beaked whales where the importance of squids was emphasized (e.g., Clarke, 1986). Beaked whales are cryptic, deep-diving odontocetes, and,

as a result, direct observation of foraging is impossible. Most insight into their feeding behavior has come from digital acoustic tags, which record the 3-D movement and acoustic environment of tagged individuals (e.g., Madsen et al., 2005). Application of these tags to individuals of the Blainville's beaked whale (*Mesoplodon densirostris*) indicates that this species forages at depths of more than 1000 m in dives that may last for almost 1 h (Arranz et al., 2011). To date, however, no Sowerby's beaked whales have been studied with digital acoustic tags.

Given the challenges of studying live whales, all published information on the food habits of the Sowerby's beaked whale has been acquired from stranded specimens (Dix et al., 1986; Lien and Barry, 1990; Lien et al. 1990; Ostrom et al., 1993; Pereira et al., 2011; Spitz et al., 2011; Santos et al.[1,2]). Recent analysis of the stomach contents of 10 stranded Sowerby's beaked whales from the Azores in the eastern North Atlantic (Pereira et al., 2011) provided evidence that small meso- and bathypelagic fishes constitute an important part of the diet of this species in this area.

One largely untapped source of information on the biology of the Sowerby's beaked whale comes from a sample of animals taken as bycatch in a pelagic drift gillnet fishery for Swordfish (*Xiphias gladius*) that operated in the western North Atlantic between 1989 and 1998. The pelagic drift gillnet fishery was monitored by observers from the Northeast Fisheries Observer Program (NEFOP); these observers documented bycatch consisting of more than 1100 individuals of 14 marine mammal species (Waring et al., 2000). This bycatch included 46 beaked whales taken in the "northern or summer stratum" of the fishery that operated along the continental shelf break along the southern side of Georges Bank (Waring et al., 2009). Pelagic drift gillnets were prohibited after 1998 because of the large number of cetaceans taken during fishing operations that used them (Waring et al., 2000; 2002). Here, we describe the stomach contents of Sowerby's beaked whales taken in this pelagic drift net fishery, and we provide the first detailed account of the food habits of Sowerby's beaked whales from the western North Atlantic.

Materials and methods

We examined the stomach contents of 10 Sowerby's beaked whales taken incidentally in the pelagic drift gillnet fishery for Swordfish in the Atlantic between August 1989 and July 1996 and a single dead stranded individual from Kennebunk, Maine (Table 1 and Fig. 1). We obtained skin tissue from each bycaught specimen and conducted DNA analysis at the NOAA Southeast Fisheries Science Center to confirm that each animal was in fact a Sowerby's beaked whale. DNA was extracted from the tissue through the use of standard proteinase K digestion followed by organic extraction (Rosel and Block, 1996). The quality of the DNA was assessed through agarose gel electrophoresis, and DNA quantity was measured with a fluorometer (Amersham Biosciences[3], now GE Healthcare Life Sciences, Little Chalfont, UK).

To confirm field identifications on the basis of morphology, the 5'-end of the mitochondrial DNA control region was amplified and sequenced as described in Sellas et al. (2005). Resultant DNA sequences were identified to species through phylogenetic reconstruction with an alignment that contained the new control region sequences and the sequences obtained from the 5 species of beaked whales present in the western North Atlantic. Mesoplodont whales form strongly supported clades in phylogenetic analyses of control region sequences; therefore, this method is well suited to species identification of unknown samples (Henshaw et al., 1997; Dalebout et al., 2004).

The unusual stomach anatomy of beaked whales has been described in detail by Mead (1989, 1993, 2007). We examined the contents of the esophagus and upper digestive tract, including the fore stomach, main stomach, connecting chambers, and pyloric stomach. We followed a standard protocol for analysis of stomach contents (see Craddock et al., 2009), separating hard parts from the remaining digesta by elutriation and then decanting them through a sieve with a 0.5-mm mesh. We then sorted, dried, and identified all hard parts to the lowest possible taxonomic level. Certain diagnostic bones of fishes (e.g., otoliths, dentaries, premaxillaries, and maxillaries) were stored separately from other hard parts. Squid beaks and all parasites were counted and preserved in 70% ethanol. We archived the contents of each stomach separately.

We identified the hard parts of prey items through the use of published guides (Roper et al., 1984; Clarke, 1986; Harkonen, 1986; Vecchione et al., 1989; Campana, 2004) and the otolith and skeletal bone reference collection prepared by J. E. Craddock at the Woods Hole Oceanographic Institution (WHOI). This collection is now part of the ichthyology collection of the Museum of Comparative Zoology, Harvard University, Cambridge, Massachusetts (http://www.mcz.harvard.edu/Departments/Ichthyology/researchcoil.html, accessed May 2013).

We estimated the number of fish prey using half the number of otoliths when more than 50 otoliths were present. When fewer than 50 otoliths were present, we

[1] Santos, M. B., G. J. Pierce, H. M. Ross, R. J. Reid, and B. Wilson. 1994. Diets of small cetaceans from the Scottish coast. ICES Council Meeting (C.M.) document, 1994/N:11. [Presented as a poster.]

[2] Santos, M. B., G. J. Pierce, G. Wijnsma, H. M. Ross, and R. J. Reid. 1995. Diets of small cetaceans stranded in Scotland 1993–1995. ICES Council Meeting (C.M.) document, 1995/N:6.

[3] Mention of trade names or commercial companies is for identification purposes only and does not imply endorsement by the National Marine Fisheries Service, NOAA.

Table 1

Origin and description of Sowerby's beaked whales (*Mesoplodon bidens*) obtained in the western North Atlantic between August 1989 and October 2003. Most whales were retained as bycatch in the pelagic drift gillnet fishery for Swordfish (*Xiphias gladius*). One whale was collected stranded in Kennebunk, Maine. Latitudes and longitudes are given in decimal degrees. NA=not available; M=male; F=female.

Whale identification	Latitude	Longitude	Depth (m)	Year	Month	Day	Source	Sex	Length (cm)	Wt. of stomach contents (g)
D00253	40.23	67.90	1050	1989	10	10	Drift gillnet	M	491	1816
D00341	40.02	68.80	1200	1995	6	24	Drift gillnet	F	485	5830
D01369	40.87	66.42	1600	1994	6	10	Drift gillnet	M	462	5897
D01380	40.97	66.32	1900	1994	6	3	Drift gillnet	F	460	4082
D03070	40.03	68.77	1350	1996	7	4	Drift gillnet	F	476	2700
D03202	40.35	67.35	1350	1996	7	6	Drift gillnet	M	470	2650
D03458	40.03	68.63	1600	1996	7	4	Drift gillnet	F	471	NA
D03486	40.97	66.40	750	1994	7	10	Drift gillnet	F	495	4082
D06061	40.78	66.57	1250	1990	8	9	Drift gillnet	F	274	Empty
F00120	40.87	66.48	1150	1989	8	26	Drift gillnet	M	473	Partial
MH03-604	43.33	70.52	NA	2003	10	2	Stranding	M	442	Empty

counted the maximum number of either right or left otoliths for each fish species. We assessed relative prey importance by frequency of occurrence (FO) and proportion of numerical abundance (%N). FO is the proportion of stomachs that contained a particular type of prey, %N is the proportion that each prey type represented of the total number of prey items recovered, and the minimum number of fish, is determined by the number of paired otoliths found in each stomach, with any odd numbered otolith raising the minimum number of fish by one (Table 2). We measured whole undigested otoliths from abundant fish prey with a stage micrometer or vernier calipers and estimated prey sizes with linear regressions derived from the WHOI reference collection (Table 3). We estimated the number of individual cephalopod prey from the maximum number of either upper or lower beaks (Table 4).

Results

One of the 10 stomachs which we examined was from a calf and contained only mucous or milk, and the stomach of the stranded individual was completely empty. In addition to the 10 stomachs examined for this study, another stomach was dissected and examined at sea by a NEFOP observer who retained only 14 otoliths: 9 Marlin-spike (*Nezumia bairdii*) and 5 Cocco's Lanternfish (*Lobianchia gemellarii*). Because of the incomplete examination of the stomach contents of this individual, we did not include it in the quantitative analysis of food habits. The remaining 8 stomachs were intact and contained prey; therefore we used the contents of these stomachs in our quantitative analysis of the frequency, numerical abundance, and size of prey. Genetic analysis confirmed that these stomachs were all from Sowerby's beaked whales.

Fishes dominated the diet of these whales; in total, we recovered 9451 otoliths of fishes and jaws of 18 Sloan's Viperfish (*Chauliodus sloani*). The only prey represented by more jawbones than otoliths was Sloan's Viperfish. The mean number of otoliths per stomach was 1196 (range: 327–3452). The recovered otoliths represented at least 31 species from 15 families of deepwater fishes (Table 2). Fishes from the families Moridae (%N=37.9% of prey), Myctophidae (22.9%), Macrouridae (11.2%), and Phycidae (7.2%) were present in all 8 stomachs. Most (74.1%) prey were from the following 5 taxa, ordered by proportion of numerical abundance: 1) Shortbeard Codling (*Laemonema barbatulum*), Moridae, 35.3%; 2) Cocco's Lanternfish, Myctophidae, 12.9%; 3) Marlin-spike, Macrouridae, 10.8%; 4) lanternfishes (*Lampanyctus* spp.), Myctophidae, 8.4%; and 5) Longfin Hake (*Phycis chesteri*), Phycidae, 6.7%. In each stomach, 12–19 different fish taxa were present, with a mean of 15. The estimated standard lengths of fish prey ranged from 4.0 cm to 27.7 cm (Table 3). In its esophagus, whale D01380 had 13 whole Cocco's Lanternfish, ranging in length from 8.0 to 10.0 cm (mean: 9.2 cm), similar to lengths of fish estimated from otoliths of this species found in the other 7 stomachs examined (Table 3).

Squid remains were found in 7 of the 8 analyzed stomachs, but they were represented by only 123 beaks (minimum 73 individuals) of 3 identified taxa (Table 4); cephalopods accounted for only 1.5% of total prey. The mean number of squid beaks per stomach was 15.4 (range: 0.0–35.0).

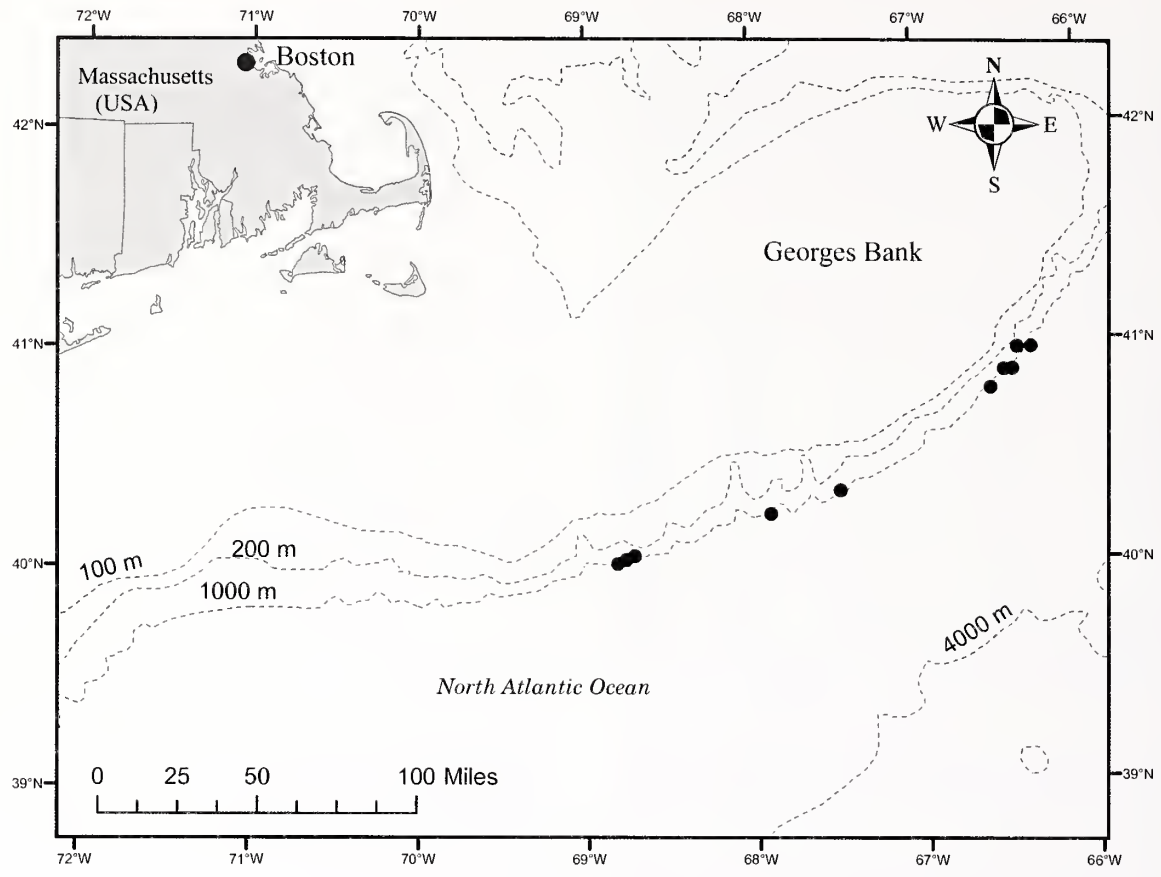

Figure 1

Map of locations where 10 specimens of the Sowerby's beaked whale (*Mesoplodon bidens*) were taken in the pelagic drift gillnet fishery for Swordfish (*Xiphias gladius*) in the western North Atlantic between August 1989 and July 1996. The stomach contents of 8 of these whales were examined to determine the food habits of this species.

Discussion

The Sowerby's beaked whales that we examined had been feeding primarily on large numbers of relatively small meso- and benthopelagic fishes before their death; cephalopod prey constituted a very minor part of the diet of these animals. Our findings are similar to those of Pereira et al. (2011), who examined the stomach contents of 10 stranded Sowerby's beaked whales from the Azores and found a predominance of small fish prey. It is important to note that all but one of the whales that we examined were killed at sea, and, with the exception of the single stranded animal, they were apparently healthy at the time of their death. The presence of intact prey in the esophagus of one specimen and the large numbers of prey items in the stomachs that we examined indicate that these animals had been foraging before death. The average minimum number of prey in the stomachs that we examined was more than 600 (4789 fishes, plus 73 squids, in all 8 stomachs combined), compared with 85 prey in the stranded specimens examined by Pereira et al. (2011).

We believe the stomach contents of the whales that we examined are representative of the summer diet of Sowerby's beaked whales along the continental shelf break off the northeastern coast of the United States. Nevertheless, biases from several sources could affect our conclusions. For example, our analysis of the stomach contents of these bycaught cetaceans could have been biased if these whales had been feeding in or around a fishing gear. Such behavior has not been reported for beaked whales, however, and the Sowerby's beaked whales that we examined were taken in pelagic drift gillnets that targeted large Swordfish and tunas in the top 10 m of the water column. These large-mesh gillnets could not have captured the prey we identified in stomachs of Sowerby's beaked whales; the only whole fish we recovered were 13 small (<10.0 cm) Cocco's Lanternfish found in one esophagus. Therefore, the Sowerby's beaked whales that we examined were not actively feeding in nets when captured.

Table 2

Analysis of fish prey identified in stomachs of Sowerby's beaked whales (*Mesoplodon bidens*) taken in the pelagic drift gillnet fishery for Swordfish (*Xiphias gladius*) in the western North Atlantic between August 1989 and July 1996. %FO= percentage of frequency of occurrence; %N=percentage of number of otoliths. *Unidentified* means that the structure of the otoliths was distinct for identification but the otoliths were not identified. *Unidentifiable* otoliths were worn or digested and not identifiable.

Family	Species	Common name	Occurrence (no. of stomachs)	%FO	Number of otoliths	%N	Minimum number of fish
Alepocephalidae	*Alepocephalus* cf. *agassizii*	Agassiz's Smoothhead	4	50	10	0.1	6
Diretmidae	*Diretmus argenteus*	Spinyfin	1	13	2	0.0	1
Gonostomatidae	*Gonostoma elongatum*	Longtooth Anglemouth	2	25	6	0.1	4
Macrouridae	*Coelorinchus* sp.	Grenadier	1	13	4	0.0	2
Macrouridae	*Coryphaenoides* sp.	Grenadier	3	38	39	0.4	21
Macrouridae	*Nezumia bairdii*	Marlin-spike	8	100	1019	10.8	515
Melamphaidae	*Poromitra capito*	Ridgehead	1	13	3	0.0	2
Melamphaidae	*Scopelogadus beanii*	Bean's Bigscale	7	88	344	3.6	178
Merlucciidae	*Merluccius albidus*	Offshore Hake	1	13	1	0.0	1
Merlucciidae	*Merluccius bilinearis*	Silver Hake	2	25	311	3.3	156
Moridae	*Gadella imberbis*	Beardless Codling	3	38	65	0.7	33
Moridae	*Laemonema barbatulum*	Shortbeard Codling	8	100	3332	35.3	1672
Moridae	Unidentified morid	Codling	1	13	178	1.9	89
Myctophidae	*Benthosema glaciale*	Glacier Lanternfish	3	38	5	0.1	3
Myctophidae	*Bolinichthys supralateralis*	Stubby Lanternfish	1	13	2	0.0	1
Myctophidae	*Ceratoscopelus maderensis*	Horned Lanternfish	7	88	75	0.8	40
Myctophidae	*Hygophum hygomii*	Bermuda Lanternfish	4	50	6	0.1	4
Myctophidae	*Lampadena speculigera*	Mirror Lanternfish	7	88	36	0.4	19
Myctophidae	*Lampanyctus* spp.	Lanternfishes	8	100	797	8.4	403
Myctophidae	*Lobianchia gemellarii*	Cocco's Lanternfish	8	100	1222	12.9	613
Myctophidae	*Nannobrachium* cf. *atrum*	Dusky Lanternfish	5	63	15	0.2	8
Paralepididae	*Arctozenus risso*	White Barracudina	8	100	90	1.0	49
Paralepididae	Unidentified paralepidid		2	25	4	0.0	2
Paralichthyidae	*Paralichthys oblongus*	Fourspot Flounder	1	13	1	0.0	1
Phycidae	*Phycis chesteri*	Longfin Hake	7	88	634	6.7	321
Phycidae	*Urophycis chuss*	Red Hake	2	25	30	0.3	15
Phycidae	*Urophycis tenuis*	White Hake	2	25	8	0.1	4
Scorpaenidae	*Helicolenus dactylopterus*	Blackbelly Rosefish	7	88	350	3.7	179
Serrivomeridae	*Serrivomer beanii*	Stout Sawpalate	1	13	3	0.0	2
Sternoptychidae	*Polyipnus clarus*	Slope Hatchetfish	1	13	2	0.0	1
Stomiidae	*Chauliodus* cf. *sloani*	Sloan's Viperfish	4	50	15	0.2	9
		Unidentified otoliths	8	100	215	2.3	114
		Unidentifiable otoliths	8	100	627	6.6	318
Total otoliths					9451		
Stomiidae	*Chauliodus* spp.	Viperfish jaws	2	25	18		3
Total fishes							4789

A second potential bias arises because hard parts of different prey may pass through the gastrointestinal tract at different rates. For example, squid beaks are resistant to digestion and often accumulate in stomachs of marine mammals, but the soft tissue and bones of fishes are more readily digested (Bigg and Fawcett, 1985). The complex structure of beaked whale stomachs (Mead 1989, 1993, 2007) makes it likely that relatively indigestible squid beaks are retained for prolonged periods. Therefore, the results reported here may overestimate the already low importance of cephalopods in the diet of the Sowerby's beaked whale.

A third possible bias arises from the secondary ingestion of prey, in which recovered hard parts enter whales in the stomachs of prey and are not consumed directly by whales themselves. It is difficult to evaluate this potential source of bias. It is possible, for example, that the Horned Lanternfish (*Ceratoscopelus maderensis*) we recovered could have been secondarily introduced into the stomachs of the Sowerby's beaked whales that we examined, given the small size of the

Table 3

Habitat and size of the most abundant prey species found in stomachs of Sowerby's beaked whales (*Mesoplodon bidens*) taken in the pelagic drift gillnet fishery for Swordfish (*Xiphias gladius*) in the western North Atlantic between August 1989 and July 1996. Habitat/depths are taken from Fishbase (http://www.fishbase.org/search.php, accessed June 2013). Standard length was used to measure fish lengths. R^2=coefficient of multiple determination; NA=not available

Prey species	Habitat	Diurnal migrant	Depth range (m)	Number measured	Mean otolith length (cm)	Otolith length range (cm)	Otolith length (OL) – fish length regression	Mean length of prey (cm) with range
Laemonema barbatulum	Benthopelagic	No	50–1620	136	0.4	0.2–0.6	NA	NA
Lobianchia gemellarii	Mesopelagic	Yes	200–800	140	0.7	0.6–0.8	Fish length = 0.0643OL + 1.0482 R^2=0.9799	9.7 (8–11)
Nezumia bairdii	Benthopelagic	No	90–700	198	0.8	0.5–1.0	Fish length = 0.035OL – 0.0961 R^2=0.9348	22 (13–28)
Lampanyctus spp.	Mesopelagic	Yes	40–1000	127	0.3	0.2–0.4	NA	NA
Phycis chesteri	Benthopelagic	No	90–1400	74	1	0.6–1.3	NA	NA
Helicolenus dactylopterus	Bathydemersal	No	50–1100	40	0.3	0.2–0.6	NA	NA
Scopelogadus beanii	Meso- to bathypelagic	Yes	400–1000	38	0.3	0.2–0.4	Fish length = 0.0169OL + 1.6267 R^2=0.5816	8.1 (5–11)
Arctozenus risso	Mesopelagic	No	200–1000	43	0.4	0.3–0.4	Fish length = 0.0086OL + 1.6552 R^2=0.8359	21.5 (10–27)
Ceratoscopelus maderensis	Mesopelagic	Yes	330–600	24	0.3	0.2–0.3	Fish length = 0.0511OL – 0.1393 R^2=0.9454	5.4 (4–6)

fish we recovered (4.0–6.3 cm) and their low numbers. This fish species is generally abundant and found in schools in the deep scattering layer (DSL) along the shelf break on the southern side of Georges Bank (Backus et al., 1968) where the Sowerby's beaked whales that we examined were taken.

The mechanisms by which the Sowerby's beaked whale locates and captures prey are largely unknown. All whales in the genus *Mesoplodon* have relatively small mouths and few teeth, and they are believed to employ suction while feeding (Mead et al. 1982; Heyning and Mead, 1996). The Sowerby's beaked whale has 2 teeth that erupt only in sexually mature males (Mead, 1989; Heyning and Mead, 1996). The relatively small mouth and 2 teeth of this species may explain why Sowerby's beaked whales typically are found to have only small prey items in their stomachs.

Studies that employed digital acoustic tags on other beaked whales in this genus have provided brief but exceptionally rich glimpses into the foraging behavior of these animals. For example, tagged Blainville's beaked whales in the Canary Islands have been reported to feed on prey in the lower part of the DSL and within the benthopelagic zone (Arranz et al., 2011). Almost half of the attempts at prey capture made by these whales in the Canary Islands occurred in the benthic boundary layer, reinforcing the importance of benthopelagic prey for them. In addition, these Blainville's beaked whales appeared to focus on the oxygen minimum layer just below the DSL in areas of steep topography. Johnson et al. (2008) described the behavior of a tagged Blainville's beaked whale in the Bahamas that appeared to provoke a schooling reaction in mesopelagic prey that resulted in a school of prey up to 4 m in diameter and created an opportunity for the whale to more easily capture those prey. Until a tag is deployed for the deep-diving Sowerby's beaked whale, we can only speculate about the foraging behavior of

Table 4

Cephalopod prey from the stomachs of Sowerby's beaked whales (*Mesoplodon bidens*) taken in the pelagic drift gillnet fishery for Swordfish (*Xiphias gladius*) in the western North Atlantic between August 1989 and July 1996. %N=percentage of number of total beaks. %FO=percentage of frequency of occurrence, on the basis of the number of stomachs studied.

Prey item	D00253	D00341	D01369	D01380	D03070	D03202	D03458	D03486	Total	%N	%FO
Unidentified upper beaks		0	2	2	4	10	19	12	49	39.8	87.5
Unidentified lower beaks		0			5	8	16		29	23.6	50.0
Histioteuthis spp.	4		13	7				9	33	26.8	50.0
Taonius pavo	9							2	11	8.9	25.0
Chiroteuthis veranyi	1								1	0.8	12.5
Total beaks	14	0	15	9	9	18	35	23	123	100.0	
Total cephalopods									73		

this species, but the results presented here indicate that their hunting strategies may be similar to those of their better-studied congener.

Therefore, on the basis of knowledge of the habitat preferences of prey recovered from the stomachs of Sowerby's beaked whales, we conclude that these animals feed in the meso- and benthopelagic environments along the shelf break, foraging in the water column and near the seafloor. Mesopelagic fishes in this region are important prey for several other cetacean species. Horned Lanternfish, in particular, is consumed by the Atlantic white-sided dolphin (*Lagenorhynchus acutus*) (Craddock et al., 2009) and by the common dolphin (*Delphinus delphis*), both of which are also caught incidentally in the pelagic drift gillnet fishery for Swordfish in the Atlantic (Craddock and Polloni[4]). The stomach of a harbor porpoise (*Phocoena phocoena*), captured in a pelagic drift net fishery off North Carolina was found to contain more than 1900 otoliths of Horned Lanternfish (Read et al., 1996).

Many marine organisms are concentrated in oceanographic frontal zones, as a result of increased production and advection (Jahn and Backus, 1976; Backus et al., 1977; Olson and Backus, 1985). As a consequence of these aggregations, predators (including swordfish) and fishermen exploit fronts. The mosaic of oceanic fronts associated with the Gulf Stream and its warm- and cold-core rings have long been targeted by fishermen of Swordfish, particularly along the shelf break (Smith et al., 1996). Swordfish have been reported to feed on some of the same prey items that we recovered from Sowerby's beaked whales (Scott and Tibbo, 1968; Stillwell and Kohler, 1985).

For example, barracudinas (Paralepididae) are important food items for Swordfish in the northwestern Atlantic (Scott and Tibbo, 1968) and were common prey of the Sowerby's beaked whales that we examined; White Barracudina (*Arctozenus risso*) is the most common barracudina in this region (Moore et al., 2003). Lanternfishes (Myctophidae) also are consumed by Swordfish in large numbers, but, because of their relatively small size, they do not contribute significantly to the mass ingested by these predators (Scott and Tibbo, 1968). The pelagic drift gillnet fishery in the Atlantic targeted Swordfish and tunas, and the fishing effort focused on thermal fronts along the shelf break, as described by Podesta et al. (1993). Therefore, the common prey fields and habitats of Swordfish and Sowerby's beaked whales may help to explain the relatively high bycatch rates of Sowerby's beaked whales in this fishery.

Conclusions

The diet of Sowerby's beaked whales in the western North Atlantic is dominated by meso- and benthopelagic fishes (98.5%), and cephalopods accounted for only 1.5% of their prey. Future research with digital acoustic tags would be helpful to examine the diving and echolocation behavior of Sowerby's beaked whales in relation to the vertical and horizontal distribution of prey. A study that combines both the tagging methods used by Arranz et al. (2011) and survey data of the prey field documented with the use of scientific echosounders and by direct capture of voucher specimens would be particularly profitable. The regular occurrence of Sowerby's beaked whales in and near the canyons on the southern margin of Georges Bank, where the whale specimens we studied were captured, offers a promising field opportunity for such research.

[4] Craddock J. E., and P. T. Polloni. 2005. Food habits of small marine mammals from the Gulf of Maine and from slope water off the northeast US coast. Year 3, Final Report, revised, 31 p. Request no. EA 133F-02-RQ-0081. Requisition no. NFFM7320-2-15375. [Available from Northeast Fisheries Science Center, National Marine Fisheries Service, NOAA, 166 Water St., Woods Hole, MA 02543 http://www.nefsc.noaa.gov/publications/reports/EA133F02RQ0081.pdf.]

Acknowledgments

We dedicate this paper to the memory of coauthors James Craddock and John Nicolas, who were instrumental in this study. We thank J. Galbraith, T. Sutton, and the Northeast Fisheries Science Center for providing fish specimens to add to the reference collection; E. Josephson and H. J. Foley for providing maps; B. Hayward and M. Moore for assistance with sorting stomach contents; K. Hartel and C. Kenaley of the Museum of Comparative Zoology, Harvard University, for reference material and additional otolith measurements. We also recognize K. Hartel, D. Waples, F. Serchuk, M. Simpkins, G. Waring, and T. Fenster and 3 anonymous reviewers for the useful comments that helped to improve this manuscript. Our work was made possible by the dedication of observers from NEFOP and the cooperation of pelagic drift net fishermen. We thank our colleagues aboard the *Abel-J* for their assistance in the field. This work was funded by the Northeast Fisheries Science Center, Woods Hole, Massachusetts.

Literature cited

Arranz, P., N. Aguilar de Soto, P. T. Madsen, A. Brito, F. Bordes, and M. P. Johnson.
2011. Following a foraging fish-finder: diel habitat use of Blainville's beaked whales revealed by echolocation. PLoS ONE 6(12):e28353. doi:10.1371/journal.pone.0028353.

Backus, R. H., J. E. Craddock, R. L. Haedrich, and B. H. Robison.
1977. Atlantic mesopelagic zoogeography. *In* Fishes of the Western North Atlantic, part 7. (R. H. Gibbs, ed.), p. 266–287. Foundation Mar. Res., Yale Univ., New Haven, CT.

Backus, R. H., J. E. Craddock, R. L. Haedrich, D. L. Shores, J. M. Teal, A. S. Wing, G. W. Mead, and W. D. Clarke.
1968. *Ceratoscopelus maderensis*: peculiar sound-scattering layer identified with this myctophid fish. Science 160:991–993.

Bigg, M. A., and I. Fawcett.
1985. Two biases in diet determination of northern fur seals (*Callorhinus ursinus*). *In* Marine mammals and fisheries. (J. R. Beddington, R. J. H. Beverton, and D. M. Lavigne, eds), p. 284–291. George Allen & Unwin, Ltd., London.

Bonde, R. K., and T. J. O'Shea.
1989. Sowerby's beaked whale (*Mesoplodon bidens*) in the Gulf of Mexico. J. Mammal. 70:447–449.

Campana, S.
2004. Photographic atlas of fish otoliths of the northwest Atlantic Ocean, 284 p. Can. Spec. Publ. Fish. Aquat. Sci. 133.

Carlstrom, J., J. Denkinger, P. Feddersen, and N. Oien.
1997. Record of a new northern range of Sowerby's beaked whale (*Mesoplodon bidens*). Polar Biol. 17:459–461.

Clarke, M. R.
1986. A handbook for the identification of cephalopod beaks, 273 p. Oxford Univ. Press, Oxford.

Craddock, J. E., P. T. Polloni, B. Hayward, and F. Wenzel.
2009. Fishes and cephalopods in the diet of Atlantic white-sided dolphins (*Lagenorhynchus acutus*) off the coast of New England. Fish. Bull. 107:384–394.

Dalebout, M. L., C. S. Baker, J. G. Mead, V. G. Cockcroft, and T. K. Yamada.
2004. A comprehensive and validated molecular taxonomy of beaked whales, family Ziphiidae. J. Hered. 95:459–473.

Dix, L., J. Lien, and D. E. Sergeant.
1986. A North Sea beaked whale, *Mesoplodon bidens*, in Conception Bay, Newfoundland. Can. Field-Nat. 100:389–391.

Griffin, R. B.
1999. Sperm whale distributions and community ecology associated with warm-core ring off Georges Bank. Mar. Mamm. Sci. 15:33–51.

Harkonen, T.
1986. Guide to the otoliths of the bony fishes of the Northeast Atlantic, 256 p. Danbiu ApS, Biological Consultants, Hellerup, Denmark.

Henshaw, M. D., R. G. LeDuc, S. J. Chivers, and A. E. Dizon.
1997. Identifying beaked whales (Family Ziphiidae) using mtDNA sequences. Mar. Mamm. Sci. 13:487–495.

Heyning, J. E., and J. G. Mead.
1996. Suction feeding in beaked whales: morphological and observational evidence. Nat. Hist. Mus. Los Ang. Cty. Contrib. Sci. 464, 12 p.

Hooker, S. K., and R. W. Baird.
1999. Observations of Sowerby's beaked whale, *Mesoplodon bidens* in the Gully, Nova Scotia. Can. Field-Nat. 113:273–277.

Jahn, A. E., and R. H. Backus.
1976. On the mesopelagic faunas of the Slope Water, Gulf Stream, and northern Sargasso Sea. Deep Sea Res. 23:223–234.

Johnson, M., L. S. Hickmott, N. Aguilar Soto, and P. T. Madsen.
2008. Echolocation behaviour adapted to prey in foraging Blainville's beaked whale (*Mesoplodon densirostris*). Proc. R. Soc. Lond., Ser. B: Biol. Sci. 275:133–139.

Lien, J., and F. Barry.
1990. Status of Sowerby's Beaked Whale, *Mesoplodon bidens*, in Canada. Can Field-Nat. 104:125–130.

Lien, J., F. Barry, K. Breeck, and U. Zuschlag.
1990. Multiple strandings of Sowerby's Beaked Whale, *Mesoplodon bidens*, in Newfoundland. Can. Field-Nat. 104:414–420.

Lucas, Z. N., and S. K. Hooker.
2000. Cetacean strandings on Sable Island, Nova Scotia, 1970–1998. Can. Field-Nat. 114:45–61.

MacLeod, C. D., M. B. Santos, and G. J. Pierce.
2003. Review of data on diets of beaked whales: evidence of niche separation and geographic separation. J. Mar. Biol. Assoc. U.K. 83:651–665.

Madsen, P. T., M. Johnson, N. Aguilar de Soto, W. M. X. Zimmer, and P. Tyack.
2005. Biosonar performance of foraging beaked whales (*Mesoplodon densirostris*). J. Exp. Biol. 208:181–194.

McAlpine, D. F., and M. Rae.
1999. First confirmed reports of beaked whales, cf. *Mesoplodon bidens* and *M. densirostris* (Ziphiidae), from New Brunswick. Can. Field-Nat. 113:293–295.

Mead, J. G.
1989. Beaked whales of the genus *Mesoplodon*. *In* Handbook of marine mammals, vol. 4: river dolphins and the larger toothed whales (S. H. Ridgway and R. Harrison, eds.), p. 349–430. Academic Press, San Diego, CA.
1993. The systematic importance of stomach anatomy in beaked whales. Int. Mar. Biol. Res. Inst. [Japan] IBI Reports 4:75–86.
2007. Stomach anatomy and use in defining systemic relationships of the Cetacean Family Ziphiidae (beaked whales). Anat. Rec. 290:581–595.

Mead, J. G., W. A. Walker and W. J. Houck.
1982. Biological observations on *Mesoplodon carlhubbsi* (Cetacea: Ziphiidae). Smithsonian Contributions to Zoology 344:iii + 1-25.

Moore, J. A., K. E. Hartel, J. E. Craddock, and J. K. Galbraith.
2003. An annotated list of deepwater fishes from off the New England Region with new area records. Northeast. Nat. 10:159–248.

Olson, D. B., and R. H. Backus.
1985. The concentrating of organisms at fronts: a cold-water fish and a warm-core Gulf Stream ring. J. Mar. Res. 43:113–137.

Ostrom, P. H., J. Lien, and S. A. Macko.
1993. Evaluation of the diet of the Sowerby's beaked whale, *Mesoplodon bidens*, based on isotopic comparisons among northwestern Atlantic cetaceans. Can. J. Zool. 71:858–861.

Pereira, J. N., V. C. Neves, R. Prieto, M. A. Silva, I. Cascao, C. Oliveira, M. J. Cruz, J. V. Medeiros, J. P. Barreiros, F. M. Porteiro, and D. Clarke.
2011. Diet of mid-Atlantic Sowerby's beaked whales, *Mesoplodon bidens*. Deep Sea Res. (I Oceanogr. Res. Pap.) 58:1084–1090.

Podestá, G. P., J. A. Browder, and J. J. Hoey.
1993. Exploring the association between swordfish catch rates and thermal fronts on U.S. longline grounds in the western North Atlantic. Cont. Shelf Res. 13:253–277.

Read, A. J., J. R. Nicolas, and J. E. Craddock.
1996. Winter capture of a harbor porpoise in a pelagic drift net off North Carolina. Fish. Bull. 94:381–383.

Roper, C. F. E., M. J. Sweeney, and C. E. Nauen.
1984. FAO species catalogue. Vol. 3. Cephalopods of the world. An annotated and illustrated catalogue of species of interest to fisheries. FAO Fish. Synop. 125, vol. 3, 277 p. FAO, Rome.

Rosel, P. E., and B. A. Block.
1996. Mitochondrial control region variability and global population structure in the swordfish, *Xiphias gladius*. Mar. Biol. 125:11–22.

Scott, W. B., and S. N. Tibbo.
1968. Food and feeding habits of swordfish, *Xiphias gladius*, in the western North Atlantic. J. Fish. Res. Board Can. 25:903–919.

Sellas, A. B., R. S. Wells, and P. E. Rosel.
2005. Mitochondrial and nuclear DNA analyses reveal fine scale geographic structure in bottlenose dolphins (*Tursiops truncatus*) in the Gulf of Mexico. Conserv. Genet. 6:715–728.

Smith, T. D., R. B. Griffin, G. T. Waring, and J. G. Casey.
1996. Multispecies approaches to management of large marine predators. *In* The Northeast Shelf ecosystem: assessment, sustainability, and management (K. Sherman, N. A. Jaworski and T. J. Smayda, eds.), p. 467–490. Blackwell Science, Cambridge, MA.

Spitz, J., Y. Cherel, S. Bertin, J. Kiszka, A. Dewez, and V. Ridoux.
2011. Prey preferences among the community of deep-diving odontocetes from the Bay of Biscay, Northeast Atlantic. Deep Sea Res. (I Oceanogr. Res. Pap.) 58:273–282.

Stillwell, C. E., and N. E. Kohler.
1985. Food and feeding ecology of the swordfish *Xiphias gladius* in the western North Atlantic Ocean with estimates of daily ration. Mar. Ecol. Prog. Ser. 22:239–241.

Vecchione, M., C. F. E. Roper, and M. J. Sweeney.
1989. Marine flora and fauna of the eastern United States: Mollusca: Cephalopoda. NOAA Tech. Rep. NMFS 73, 23 p.

Waring, G. T., T. Hamazaki, D. Sheehan, G. Wood, and S. Baker.
2001. Characterization of beaked whale (Ziphiidae) and sperm whale (*Physeter macrocephalus*) summer habitat in shelf-edge and deeper waters off the Northeast U.S. Mar. Mamm. Sci. 17:703–717.

Waring, G. T., E. Josephson, K. Maze-Foley, and P.E. Rosel (eds.).
2009. U.S. Atlantic and Gulf of Mexico marine mammal stock assessments—2009. NOAA Tech. Memo. NMFS-NE-213, 528 p.
2010. U.S. Atlantic and Gulf of Mexico marine mammal stock assessments—2010. NOAA Tech. Memo. NMFS-NE-219, 595 p.

Waring, G. T., J. M. Quintal, and C. P. Fairfield (eds.).
2002. U.S. Atlantic and Gulf of Mexico marine mammal stock assessments—2002. NOAA Tech. Memo. NMFS-NE-169, 318 p.

Waring G. T., J. M. Quintal, and S. L. Swartz (eds.).
2000. U.S. Atlantic and Gulf of Mexico marine mammal stock assessments—2000. NOAA Tech. Memo. NMFS-NE-162, 298p.

Reproductive biology of Black Anglerfish (*Lophius budegassa*) in the northwestern Mediterranean Sea

Ana I. Colmenero (contact author)
Víctor M. Tuset
Laura Recasens
Pilar Sánchez

Email address for contact author: colmenero@icm.csic.es

Institut de Ciències del Mar (ICM)
Consejo Superior de Investigaciones Científicas (CSIC)
Passeig Marítim de la Barceloneta 37-49
08003 Barcelona, Spain

Abstract—Gonadal morphology and reproductive biology of the Black Anglerfish (*Lophius budegassa*) were studied by examining 4410 specimens collected between June 2007 and December 2010 in the northwestern Mediterranean Sea. Ovaries and testes presented traits common among fishes of the order Lophiiformes. Spawning occurred between November and March. Size at first maturity (L_{50}) was 33.4 cm in total length (TL) for males and 48.2 cm TL for females. Black Anglerfish is a total spawner with group-synchronous oocyte development and determinate fecundity. Fecundity values ranged from 87,569 to 398,986 oocytes, and mean potential fecundity was estimated at 78,929 (standard error of the mean [SE] 13,648) oocytes per kilogram of mature female. This study provides the first description of the presence of 2–3 eggs sharing the same chamber and a semicystic type of spermatogenesis for Black Anglerfish. This new information allows for a better understanding of Black Anglerfish reproduction—knowledge that will be useful for the assessment and management of this species.

Manuscript submitted 19 October 2012.
Manuscript accepted 19 September 2013.
Fish. Bull. 111:390–401 (2013).
doi: 10.7755/FB.111.4.8

The views and opinions expressed or implied in this article are those of the author (or authors) and do not necesarily reflect the position of the National Marine Fisheries Service, NOAA.

Lophius, a genus commonly known as anglerfishes or monkfishes, includes 7 species broadly distributed and exploited worldwide. Most of these species inhabit the northwestern Atlantic, as do Goosefish (*Lophius americanus*) and Blackfin Goosefish (*L. gastrophysus*), or the northeastern Atlantic, as do Cape Monk (*L. vomerinus*), Shortspine African Angler (*L. vaillanti*), Black Anglerfish (*L. budegassa*), and White Anglerfish (*L. piscatorius*), although Black Anglerfish and White Anglerfish also live in the Mediterranean Sea and Yellow Goosefish (*L. litulon*) can be found only in the northwestern Pacific (Fariña et al., 2008). In the past, species of *Lophius* have been captured as bycatch in mixed fisheries, but an increase in their economic value, together with the overexploitation of other groundfish species, has led to the development of targeted anglerfish fisheries (Hislop et al., 2001). In the northwestern Mediterranean Sea, landings of Black Anglerfish and White Anglerfish have accumulated to just over 6000 metric tons during the last 10 years.[1] The scarce reproductive information available for these species does not allow for a proper assessment or informed management of anglerfish fisheries.

This study focuses on Black Anglerfish, a demersal fish distributed along the Mediterranean Sea, as well as the northeastern Atlantic from the British Isles to Senegal (Caruso, 1986). This species is found over the continental shelf and upper slope at depths of up to 800 m and inhabits sandy, muddy, and rocky bottoms (Carlucci et al., 2009). They occupy the water column as eggs and larvae, and then they shift to a benthic existence as juveniles and adults (Fariña et al., 2008). This species co-occurs with White Anglerfish over all its bathymetric range, although White Anglerfish has a deeper distribution that reaches to depths >1000 m (Afonso-Dias and Hislop, 1996). Despite the overlapping distributions of these species, Colmenero et al. (2010) concluded that no ecological competition exists between these species because of a temporal segregation in their biorhythms; Black Anglerfish is more active at nighttime, and White Anglerfish is more active during daytime.

Most studies of these species have been undertaken in northeastern Atlantic waters, and they often have dealt with age and growth (Dupouy et al., 1984; Landa et al., 2008a; Woodroffe et al., 2003), feeding habits (Crozier, 1985; Laurenson

[1] Tudó Vila, P. 2012. Unpubl. data. Directorate of Fishing and Maritime Affaires, Government of Catalonia, Avinguda Diagonal, 523-525, 08029 Barcelona, Spain.

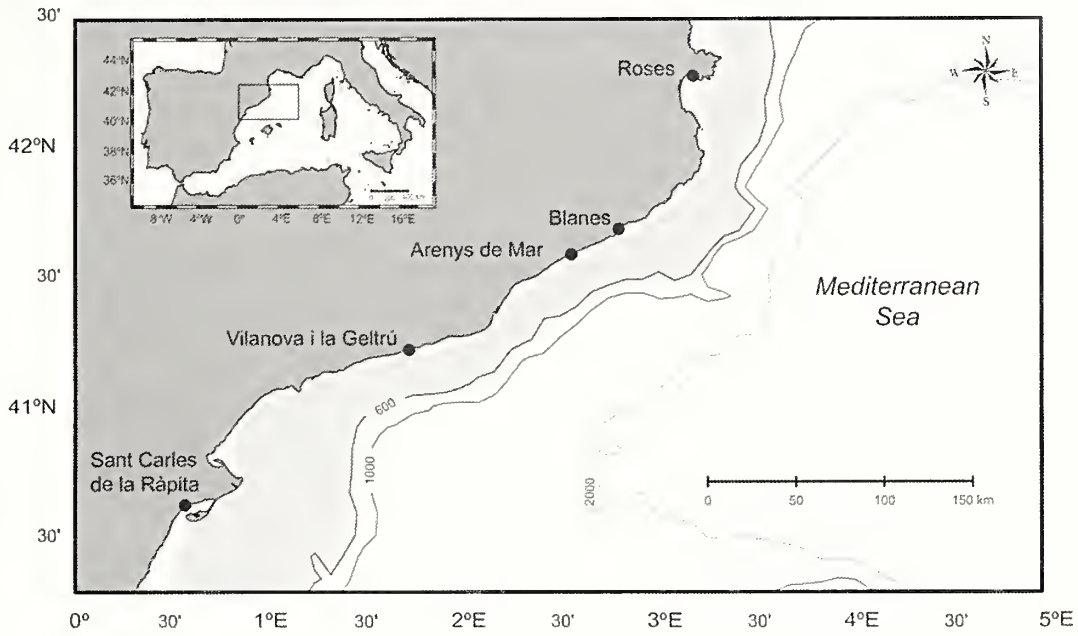

Figure 1

Map of study area where specimens of Black Anglerfish (*Lophius budegassa*) were collected in the northwestern Mediterranean Sea between June 2007 and December 2010 to examine the reproductive biology of this species. The zone shaded in light gray closest to the Catalan coast indicates the sampling area. The cities shown on the coast were the ports of commercial trawl fishery vessels from which specimens were collected.

and Priede, 2005; Preciado et al., 2006), geographical and depth distribution (Caruso, 1985; Landa et al., 2008b; Velasco et al., 2008), and reproduction (Afonso-Dias and Hislop, 1996; Duarte et al., 2001; Laurenson, 2006). In the Mediterranean Sea, studies have been less numerous and for the most part have focused on biological aspects similar to the ones examined in the studies just described (Carlucci et al., 2009; Colmenero et al., 2010; García-Rodríguez et al., 2005; La Mesa and De Rossi, 2008; Maravelias and Papaconstantinou, 2003; Negzaoui-Garali and Ben Salem, 2008; Negzaoui-Garali et al., 2008; Tsimenidis, 1984; Tsimenidis and Ondrias, 1980; Ungaro et al., 2002). However, only Tsimenidis (1980) and Carbonara et al. (2005) focused on reproductive traits of Black Anglerfish.

Information about the duration of the spawning season, fish size at first maturity, reproductive strategy, maturation of oocytes, and fecundity are very relevant for studies of the biology and population dynamics used in stock assessments for management of fishery resources. Of all these reproductive features, fecundity is the most difficult biological parameter to obtain, although it is critical for accurate stock assessments (Trippel et al., 1997). In the peculiar case of species of *Lophius*, studies on fecundity are scarce because of the difficulty of 1) acquisition of suitably mature individuals in the maturity phases of spawning capable or actively spawning and 2) the use of a proper method for fecundity estimation, which is especially complicated because of the morphological features of the gonads of these species. During reproduction, a gelatinous material is secreted into the lumen, and enumeration and measurement of eggs embedded in this mucus matrix is extremely difficult.

Although species of *Lophius* have similar traits throughout the world, some biological aspects and catch trends of fisheries present interspecific and spatial variations (Fariña et al., 2008). For that reason, reproductive parameters of the Atlantic stock of Black Anglerfish cannot be applied to the stock in the Mediterranean. In addition, knowledge of the reproductive biology of this species in the northwestern Mediterranean Sea is very limited. Therefore, our study is the first one to take a detailed approach to the examination of reproductive traits of Black Anglerfish in the Mediterranean Sea, and the results of this study can contribute to improvement of stock assessment and effective management of this species in this region.

Materials and methods

Sample collection

Monthly samples of Black Anglerfish were obtained from 467 sampling stations situated in the fishing grounds off the Catalan coast in the northwestern Mediterranean Sea from 40°5.980′N to 43°39.310′N

Table 1

Macroscopic and microscopic description of the 5 maturity phases in the reproductive cycle of male and female Black Anglerfish (*Lophius budegassa*) collected from the northwestern Mediterranean Sea between June 2007 and December 2010; adapted from Afonso-Dias and Hislop (1996) and Brown-Peterson et al. (2011).

Phase	Males	Females
Immature (I)	Testes are long, narrow, and tubular shaped. They are translucent with no visible vascularization. The medial seminiferous duct is distinct. Only spermatogonia and primary spermatocytes are present.	Ovaries are very narrow, thin, and flattened-tube shaped. They are translucent; no oocyte clusters visible and minimal vascularization. Only oogonia and primary growth oocytes are present.
Developing/ Regenerating (II)	Testes are small with visible blood vessels around the seminal duct. Spermatogonias, primary and secondary spermatocytes are predominant. Spermatids are scarce.	Ovaries are small. Still no noticeable individual oocyte clusters. They acquire a cream color and vascularization is visible. Only oogonia and primary growth oocytes are present.
Spawning capable (III)	Testes increase in length and width. They have a firm texture and cream color. Seminal duct is highly vascularized. Germ cells at all stages of spermatogenesis are present. Spermatids are predominant with a lot of spermatozoa in the lumen of the sperm duct.	Ovaries increase in width and length. They have a light orange color, and blood vessels are prominent. The edges of the ovaries start to curl and they occupy a larger proportion of the body cavity. A mucus matrix starts to develop. Primary growth, cortical alveolar, and primary and secondary vitellogenic oocytes are present.
Actively spawning (IV)	Testes are large and firm and have a creamy coloration. Large amounts of sperm produced when testes are dissected. Abundant quantities of spermatozoa are present in the seminiferous tubules.	Ovaries are extremely long and wide and occupy most of the body cavity. The color of the oocytes is orange, and they are visible macroscopically. Ovaries are characterized by the presence of large hyaline oocyte clusters enclosed in a transparent gelatinous matrix that is completely developed. High vascularization is present. Oocytes are in tertiary vitellogenesis, migratory nucleus and hydration.
Regressing (V)	Testes are small, flaccid, and have brown or red areas in their beige surface. They are still highly vascularized. Sperm and residual spermatozoa can be found in the lumina of the sperm duct. Spermatogonia are present in the testes cortex.	Ovaries are flaccid and highly vascularized and often have longitudinal striations. Their color is dark pink or red. Atresia and postovulatory follicles, together with primary growth stages, are present. Cortical alveolar, primary and secondary vitellogenesis can be found.

and from 0°32.922′E to 3°35.718′E between June 2007 and December 2010. Specimens were collected onboard commercial trawl fishery vessels at depths of 20–600 m and identified according to Caruso (1986). The trawl fleet belonged to the ports of Roses, Blanes, Arenys de Mar, Vilanova i la Geltrú, and Sant Carles de la Ràpita (Fig. 1). For this study, 4410 specimens were measured to the nearest centimeter in total length (TL), weighed to the nearest gram in total weight (TW) and gutted weight (GW), and measured with an accuracy of 0.01 g in gonad weight (GNW) and liver weight (LW).

Macroscopic and histological description of gonads

Of the total number of specimens, 3562 fish had gonads removed and their sex was determined, and they were assigned macroscopically to a gonadal stage on the basis of a scale with 5 maturity phases that were described in previous studies: immature (phase I), developing or regenerating (phase II), spawning capable (phase III), actively spawning (phase IV), and regressing (phase V) (Afonso-Dias and Hislop, 1996; Brown-Peterson et al., 2011) (Table 1). Sex was easily assessed macroscopically in mature individuals. However, gonads from small individuals (approximately <20 cm TL) were indistinguishable macroscopically because ovaries and testes were small, translucent, and string-like. Fish that were too small to determine their sex or assign to a gonadal phase were classified as indeterminate.

To corroborate the macroscopic classification of some unclear and undetermined gonads, 372 specimens were histologically examined. They were fixed in 10% buffered formalin solution before they were dehydrated and embedded in a methacrylate polymer resin.

Cross sections, each 3–4 µm thick, were made with a manual microtome Leica Reichert-Jung 2040 (Leica Microsystems,[2] Wetzlar, Germany), stained with Lee's stain (methylene blue and basic fuchsin), and mounted in a synthetic resin of dibutyl phthalate xylene (DPX) on microscope slides. Gonads were classified according to the morphological features and the presence of specific inclusions (oil droplets, yolk granules, yolk vesicles, or postovulatory follicles) (Wallace and Selman, 1981). The ovarian and testicular phases were defined by the developmental stage of the most advanced cell within the gonad (Yoneda et al., 1998b).

Spawning season and size at first maturity

The spawning season was established from the analysis of the monthly variation of the maturity phases and the changes in gonadosomatic (GSI) and hepatosomatic (HSI) indices for each sex (Afonso-Dias and Hislop, 1996). Because immature specimens were not considered, 1437 males and 1167 females were used to determine both indices, which were calculated according to Yoneda et al. (2001) with the following equations:

$$GSI = (GNW / GW) \times 100. \quad (1)$$

$$HSI = (LW / GW) \times 100. \quad (2)$$

Size at first maturity (L_{50}) was determined through the examination of males and females in mature phases (phase III, phase IV, or phase V) and immature individuals collected during the spawning period (Duarte et al., 2001). Total length of all individuals was used to estimate L_{50}, defined as the size at which 50% of all fish sampled were at sexually mature phases. Maturity curves were determined with a logistic curve (Pope et al., 1975):

$$P = 100 / (1 + \exp [a + b\mathrm{TL}]), \quad (3)$$

where P = the percentage of mature individuals as a function of size class (TL); and
a and b = specific parameters that can change during the life cycle.

A logarithmic transformation was applied to this equation to calculate the parameters a and b by means of linear regression.

Reproductive strategy and fecundity

Patterns of ovarian organization and fecundity were tested by oocyte size-frequency distributions (West, 1990). For our analysis, 36 fish, with lengths between 20.0 and 72.5 cm TL, were randomly selected from all maturity phases. From these fish, 4428 oocytes—with more than 300 oocytes from each maturity phase (I=961; II=1106; III=1046; IV=381; V=934)—were measured for their diameter with an image analysis program (Image-Pro Plus, vers. 5.0, Media Cybernetics, Inc., Rockville, MD) in combination with an Axioskop 2 Plus microscope (Carl Zeiss Microscopy, LLC, Thornwood, NY) and a ProgRes C14 digital microscope camera (Jenoptik AG, Jena, Germany). Diameters were measured to the nearest 0.01 µm. The mean oocyte diameter by developmental stage was determined by calculating the diameter of all oocytes encountered in each subsample. Measurements were taken only of oocytes that were sectioned through the nucleus (Afonso-Dias and Hislop, 1996).

Before fecundity was estimated, the gonads of 7 individuals were divided into 3 sections (anterior, middle, and posterior) to test differences in mean oocyte density within the ovary by using a one-way analysis of variance (ANOVA). This use of 3 sections ensured that the analyzed subsample represented the entire ovary (Murua et al., 2003). Batch fecundity (BF), the total number of mature eggs produced in a single spawning batch by an individual female, was estimated by using the gravimetric method on the basis of the relation between ovary weight and the density of oocytes in the ovary (Hunter and Goldberg, 1980). Three ovarian tissue samples of known weight, representing 10% of the total ovarian weight, were extracted from different areas of the same ovary (anterior, middle, and posterior ovarian lobe). These subsamples were collected from 15 specimens with ovaries in phases III and IV with neither postovulatory follicles nor atretic oocytes present. Because the oocytes could not be extracted from their mucogelatinous matrix without destroying them, whole tissue subsamples were mounted on several slides for analysis and covered with a cover slip.

Images of each ovarian tissue sample were taken with a Canon Powershot SD870 IS digital camera (Canon USA, Melville, NY), and oocytes were counted manually with Image-Pro Plus software. Fecundity values were obtained by examining Black Anglerfish with total lengths of 46–65 cm, TW of 1096–5592 g, GW of 986–3600 g, and GNW of 88.70–2300 g. Batch fecundity for each female was calculated as a product of the number of secondary vitellogenic oocytes per unit of weight multiplied by the total ovarian weight (Yoneda et al., 2001). Relative batch fecundity (RBF), the total number of mature eggs released by a female during the spawning batch per gram of body weight of gutted fish, was calculated as BF divided by GW (Pavlov et al., 2009):

$$BF = (\textit{oocyte number} / \textit{sampled GNW}) \times \textit{total GNW}. \quad (4)$$

$$RBF = BF / GW. \quad (5)$$

Linear regression analysis was used to examine the relationships between BF and fish TL, TW, and GW (Armstrong et al., 1992). Linear regression analysis also was applied to analyze the relationship between RBF and TL. Mean potential fecundity was

[2] Mention of trade names or commercial companies is for identification purposes only and does not imply endorsement by the National Marine Fisheries Service, NOAA.

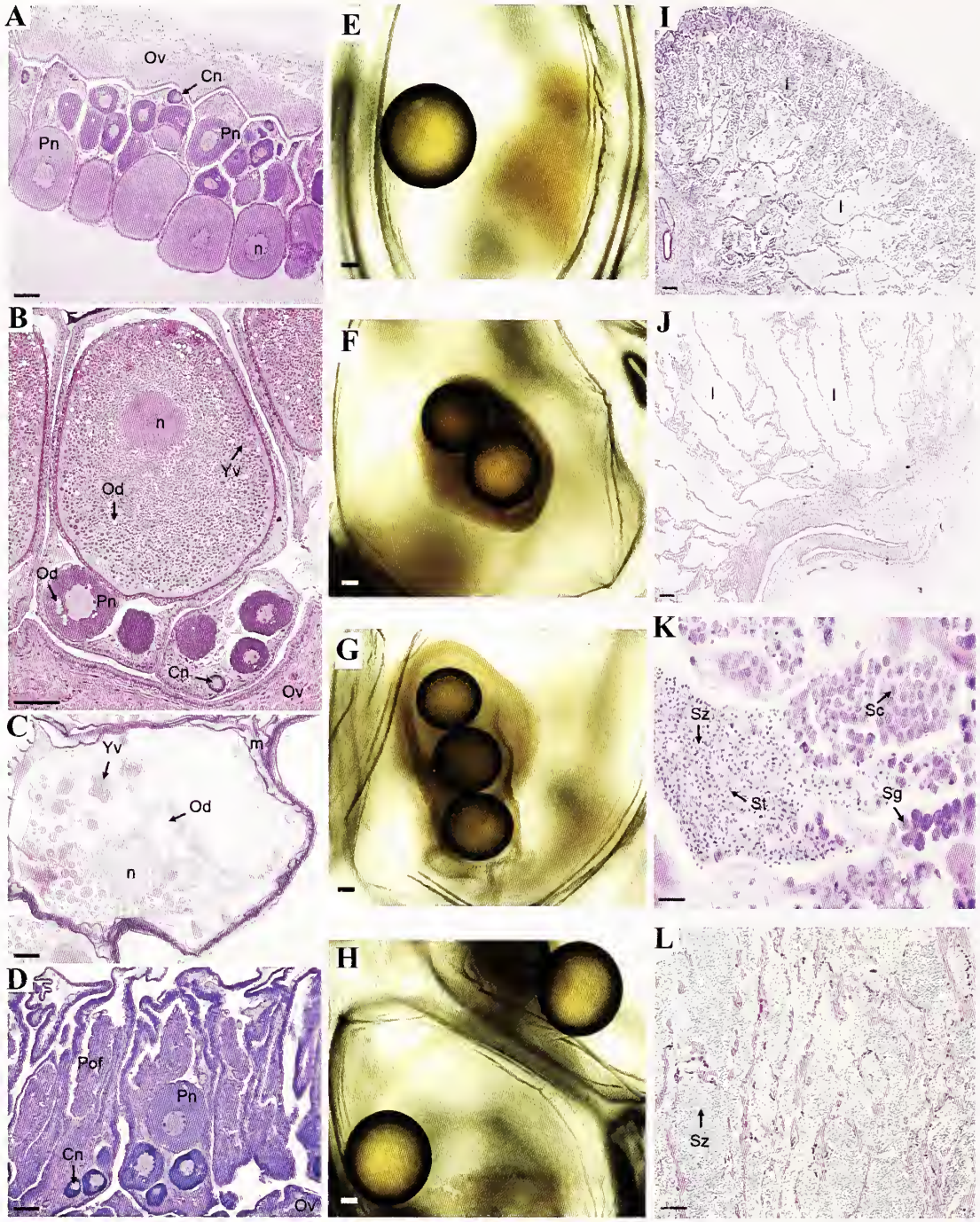

Figure 2

Micrographs of transverse sections of ovaries, oocytes inside the gelatinous matrix, and testes of Black Anglerfish (*Lophius budegassa*) collected in the northwestern Mediterranean Sea between June 2007 and December 2010. The final 4 stages of ovary development are shown in the left column: (**A**) Phase II: developing or regenerating; (**B**) Phase III: spawning capable; (**C**) Phase IV: actively spawning; (**D**) Phase V: regressing. Oocytes are featured in the middle column: (**E**) 1 oocyte in a chamber (486 µm in diameter), (**F**) 2 oocytes floating in a chamber (427 µm and 359 µm in diameter), (**G**) 3 oocytes in a chamber (341 µm, 330 µm, and 322 µm in diameter), and (**H**) closed-up division between chambers. In the right column, transverse sections of testes show (**I**) its lobular organization, (**J**) empty lobules, (**K**) seminal lobule during spermatogenesis, and (**L**) spermatozoa in the lumen of the seminal lobule. Ov=ovigerous membrane; n=nucleus; Od=oil droplet; Yv=yolk vesicle; m=mucus matrix; Cn=chromatin nucleolar; Pn=perinucleolar; Pof=postovulatory follicle; l=seminal lobule; Sg=spermatogonia; Sc=spermatocyte; St=spermatid; Sz=spermatozoa. Scale bars=100 µm.

also calculated as the number of vitellogenic oocytes divided by kilogram of mature female (Murua et al., 2003).

Results

Gonadal morphology

Ovarian structure consists of a flattened band with 2 distinctive lobes that are folded up and connected to each other at their posterior end. The lobes form a single organ attached to the abdominal cavity by a black mesenteric tissue called the mesovarium. One side of the ovarian wall is made of an ovigerous membrane and connective tissue. The nonovigerous side is made of epithelial cells. A single layer of oocyte clusters projects from the ovigerous membrane to the lumen (Fig. 2A). Inside each gonad, the clusters can be in different development stages. Only the oocytes situated closest to the tip of the clusters have progressed through all maturity stages, and the other oocytes are only oogonia or in the primary growth stage (Fig. 2B).

A gelatinous material is secreted into the lumen during the late phases of gonad maturation, producing the mucus matrix characteristic of the reproduction of *Lophius* species (Fig. 2C). Hydration of the oocytes occurs just before spawning, and postovulatory follicles (Fig. 2D) are found during the regression phase of the reproductive cycle. Ripe eggs, which are usually situated on the tip of the oocyte cluster, rupture the follicles and are pressed into the layer of mucus. In this study, every chamber examined contained at least 1 egg in the gelatinous matrix (Fig. 2E), although the presence of 2 (Fig. 2F) or 3 eggs (Fig. 2G) floating in separate chambers was also noted (Fig. 2H).

Oocyte diameter appeared to differ depending on the quantity of oocytes present in each chamber; the oocytes that were isolated in their chambers were found to be larger in size than other oocytes. A diameter of 486 µm was obtained for the oocyte that was the single oocyte in its chamber. Diameters of 427 µm and 359 µm were found for the 2 oocytes floating together in a chamber, and diameters of 341 µm, 330 µm, and 322 µm were observed for the 3 oocytes that shared the same chamber. Measurements of more oocyte diameters are needed to confirm these preliminary observations.

The testes are a pair of elongated and tubular structures located in the dorsal portion of the abdominal cavity, and they are bean-shaped in transverse section. The organization of the testes is lobular: the connective tissue extends from the testicular capsule to form lobules that have their blind ends on the surface of the gonads, converging ventrally towards the sperm duct (Fig. 2I). These lobules are fused to the posterior end of each testicular lobe to form a common sperm duct that leads to a genital pore (Fig. 2J). Spermatogenesis takes place in a capsule-like sac called a cyst, but it is not completed within the cyst. Each cyst contains spermatogonia or developing spermatocytes (Fig. 2K). Before the end of the spermatogenesis, the cyst breaks up and spermatids are released into the lumina of the lobules, where spermatogenesis is then completed and spermatids transform into spermatozoa (Fig. 2L). The cysts appear to be arranged in order of maturation, with a gradient of germ cells of increasing maturation from the cortex to the sperm duct. The shape of the spermatozoa head seems to be elongated.

Spawning season and size at first maturity

Monthly distribution of macroscopic classification of the maturity phases (Fig. 3, A and B) revealed that the period of maximum occurrence of females in the spawning capable phase (III) was from November to January. The presence of females in the actively spawning phase (IV) was observed from November to March, with a maximum peak in January. Females in the immature, regressing, and developing and regenerating phases (I, V, and II, respectively) were found throughout the year, with the highest percentage of immature individuals seen in May. A slight increase in phase-III females was observed in August, and that increase would likely result in spawning activity in September, indicating the possibility of a secondary breeding season. Males in all maturity phases were observed throughout the year, with 2 maxima of mature males occurring in December and July.

For mature males and females, GSI and HSI indices were calculated. In males, GSI was fairly constant throughout the year and a maximum index value of 1.06 was reached in January (Fig. 3C). The mean GSI for females was highest from December to March, with a peak of maximum activity in January (4.94) and February (2.43) (Fig. 3D). The mean HSI for females and males followed the same pattern. The highest value for males was found in September (2.50), and the lowest value in February (1.65) (Fig. 3C). In females, HSI values ranged from 3.19 in January to 1.86 in March (Fig. 3D). The highest HSI values were found just at the beginning of the main spawning season. GSI and HSI results, together with observations of maturity phases throughout the year, indicate that there is one main spawning season from November to March.

Comparison of L_{50} curves showed a clear difference between males and females. The size at 50% sexual maturity was 33.4 cm TL for males (Fig. 4A) and 48.2 cm TL for females (Fig. 4B).

Reproductive strategy and fecundity

The size-frequency distributions of oocyte diameters in each of the 5 maturity phases indicate that oocytes in different stages of development were found in each maturity phase (Table 2; Fig. 5). During phase I, only oocytes in the primary growth stage (chromatin nucleolar and perinucleolar) with a narrow range of diameters were present (Fig. 5A). In phase II, cortical alveolar

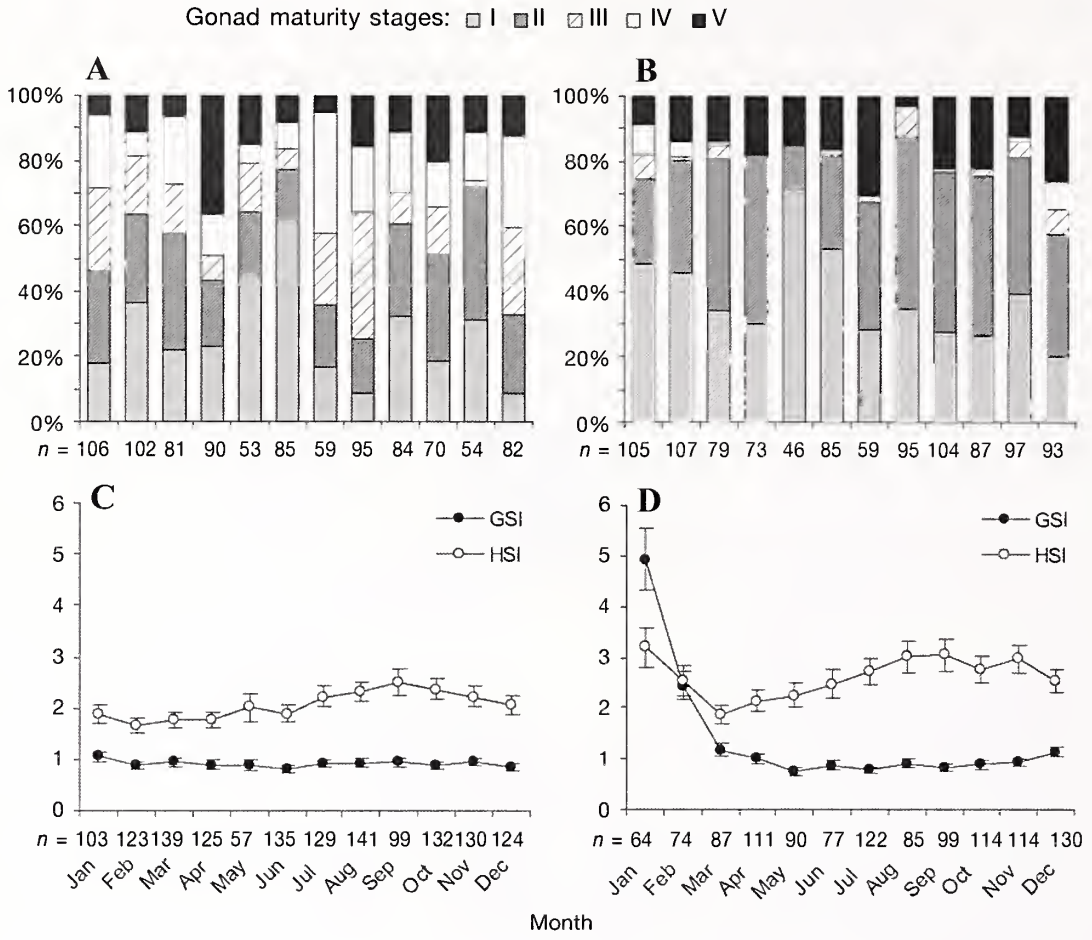

Figure 3

Monthly distributions of (**A**) males and (**B**) females in the 5 phases of gonad maturity of Black Anglerfish (*Lophius budegassa*) collected from the northwestern Mediterranean Sea between June 2007 and December 2010 and monthly changes in the mean gonadosomatic index (GSI) and hepatosomatic index (HSI) for (**C**) males and (**D**) females. On the basis of macroscopic examination, specimens were assigned to the following phases: immature (phase I), developing or regenerating (phase II), spawning capable (phase III), actively spawning (phase IV), and regressing (phase V). Error bars indicate ±1 standard error of the mean.

vesicles were found in the cytoplasm together with oocytes in the stage of primary growth with diameters that had increased notably (Fig. 5B). In phase III, yolk granule stages (Murua et al., 2003) were present along with the previous 2 types of oocytes. The oocytes increased in size as the yolk accumulated, and a wider oocyte diameter range distribution was observed during this phase (Fig. 5C). In phase IV, oocytes were observed in different stages (primary growth, vitellogenesis, migratory nucleus, and hydration). Two populations of oocytes were recognized in phase IV: a population of larger oocytes (defined as a clutch) and a population of smaller oocytes from which the clutch was recruited (Fig. 5D). In phase V, oocytes in the primary growth stage were found along with postovulatory follicles and atretic oocytes (Fig. 5E).

The presence of oocytes in different developmental stages within the same cluster and the frequency distribution of oocyte diameter along all maturity phases indicate that oocyte development in Black Anglerfish is group-synchronous. The existence of a gap that separates the yolked oocyte stock, the ones to be spawned during the current breeding season, from the unyolked oocytes, the ones to be spawned in the coming breeding season, together with the increase of the mean diameter of the advanced vitellogenic oocytes, indicates that annual fecundity is determinate.

Significant differences in oocyte densities among

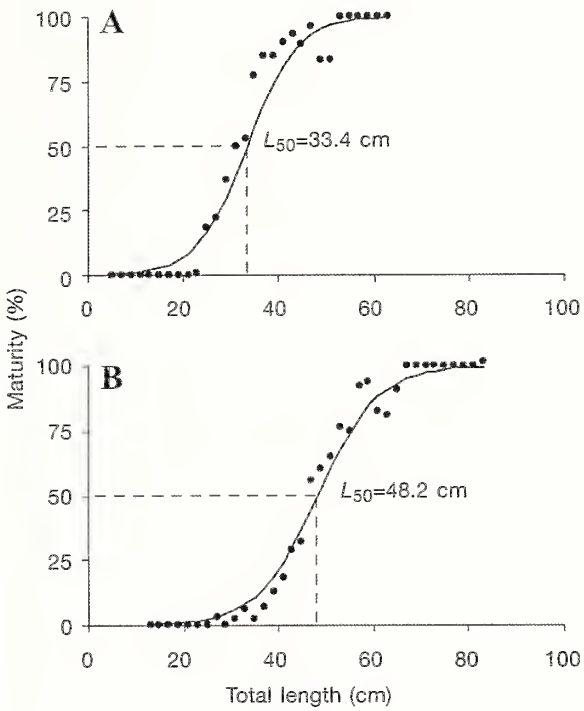

Figure 4

Maturity ogives used to estimate length at maturity (L_{50}) for (**A**) male and (**B**) female Black Anglerfish (*Lophius budegassa*) collected from the northwestern Mediterranean Sea between June 2007 and December 2010.

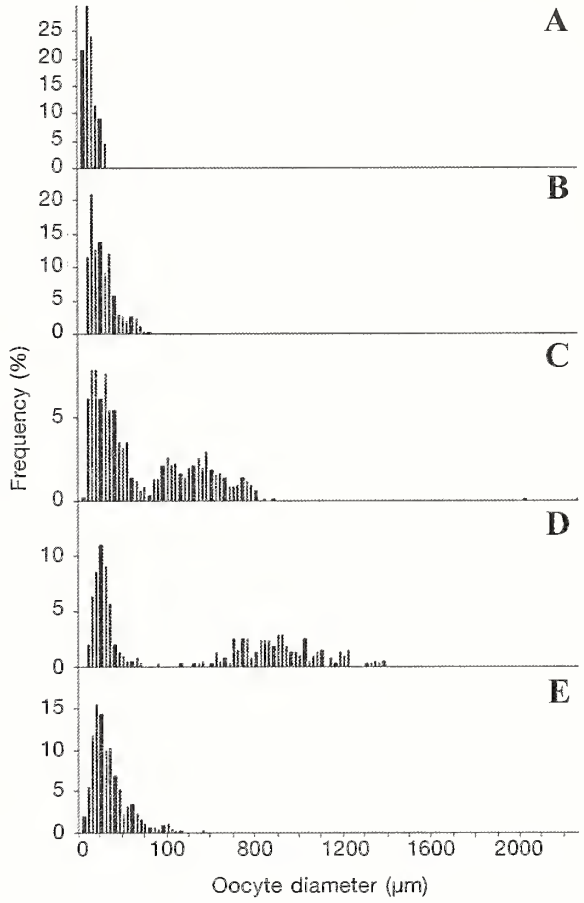

Figure 5

Size-frequency distributions of oocyte diameters at each phase of gonad maturity of Black Anglerfish (*Lophius budegassa*) collected from the northwestern Mediterranean Sea between June 2007 and December 2010. The 5 maturity phases are (**A**) phase I, immature, n=961; (**B**) phase II, developing or regenerating, n=1106; (**C**) phase III, spawning capable, n=1046; (**D**) phase IV, actively spawning, n=381; (**E**) phase V, regressing, n=934.

ovary sections were not observed (ANOVA, $F_{(2,42)}$=0.002, P=0.998). Batch fecundity ranged between 87,569 and 398,986 oocytes, and mean BF was 218,020 oocytes (standard error of the mean [SE] 90,018). Relative batch fecundity was estimated at 102 (SE 20) oocytes per gram of female (GW), and mean potential fecundity was 78,929 (SE 13,648) oocytes per kilogram of mature female.

Batch fecundity tended to increase linearly with TL (linear regression, coefficient of determination [r^2]=0.89, $F_{1,13}$=106.57, P<0.001), TW (linear regression, r^2=0.82, $F_{1,13}$=60.79, P<0.001), and GW (linear regression, r^2=0.82, $F_{1,13}$=59.31, P<0.001), indicating that fecundity is dependent on size and body weight (Fig. 6). No significant correlation was found between RBF and TL, indicating that RBF is not size dependent (linear regression, r^2=0.16, $F_{1,13}$=2.50, P=0.138).

Discussion

This study indicates that oocyte development and the fecundity pattern of Black Anglerfish are similar to findings for other species of *Lophius*: White Anglerfish (e.g., Fulton, 1898), Cape Monk (Leslie and Grant, 1990), Goosefish (Armstrong et al., 1992) and Yellow Goosefish (Yoneda et al., 2001). The eggs of Black Anglerfish appear to be shed as a part of a single event and are likely released only once during the spawning season—the pattern of a total spawner. This type of spawning has been observed also in Goosefish (e.g., Feinberg, 1984) and White Anglerfish (Afonso-Dias and Hislop, 1996), although the possibility of spawning several batches over the spawning season is not unfeasible because this behavior has been described for Yellow Goosefish (Yoneda et al., 2001).

Batch fecundity estimates for Black Anglerfish reveal a positive relationship between number of oocytes

Table 2

Oocyte histological characteristics of Black Anglerfish (*Lophius budegassa*) collected between June 2007 and December 2010 in the northwestern Mediterranean Sea; descriptions follow those of Wallace and Selman (1981). Mean oocyte diameters, which were measured to the nearest 0.01 µm, are provided by developmental stage with standard errors of the mean (SE).

Oocyte developmental stage	Oocyte diameter (µm)	Histological characteristics
Chromatin nucleolar	36.55 (SE 21.27)	Nucleus contains a large nucleolus and some small peripheral nucleoli. Yolk granules are not present in the cytoplasm.
Perinucleolar	110.78 (SE 62.54)	Nucleus grows and several big peripheral nucleoli and vacuoles are present. No yolk granules are present in the cytoplasm.
Cortical alveolar	256.35 (SE 80.81)	Nucleus is central. Cortical alveolar vesicles and oil droplets appear in the cytoplasm. Yolk granules are still not present in the cytoplasm.
Primary vitellogenic	364.54 (SE 37.31)	Yolk granules appear between cortical alveolar vesicles. Nucleus remains central.
Secondary vitellogenic	406.20 (SE 39.60)	Yolk granules fill the cytoplasm. Nucleus is still central.
Tertiary vitellogenic	544.55 (SE 185.49)	Yolk granules are in contact with the nucleus, which is still central, and the oocyte size has increased from size at previous stages.
Migratory nucleus	883.42 (SE 153.33)	Yolk granules and oil droplets start to fuse. Nucleus migrates to one pole of the oocyte.
Hydration	1125.09 (SE 176.93)	Yolk granules form a single mass. Nucleus is not present in the cytoplasm.

and fish length and weight; therefore, large spawners have a higher contribution to egg production than do smaller ones. Previous authors have found lower fecundity values than the ones observed in this study. In the Tyrrhenian Sea, Carbonara et al. (2005) determined mean potential fecundity as 54,057 oocytes per kilogram of mature female and total fecundity as 211,687 oocytes from data obtained from a single individual (59 cm TL). In the case of the Aegean Sea, where fecundity values varied from 105,800 to 284,200 oocytes, fecundity was determined from an undefined number of individuals and size range (Tsimenidis, 1980).

Another relevant feature of the reproduction of Black Anglerfish is the presence of a gelatinous matrix, which has been noted for other *Lophius* species (Armstrong et al., 1992; Fulton, 1898; Leslie and Grant, 1990; Yoneda et al., 2001). The matrix consists of individual chambers where hydrated oocytes are released. In our study, we detected the presence of 2 or 3 eggs in some chambers (Fig. 2). This phenomenon also has been described for Goosefish, and it has been assumed that such eggs in that species may have been fertilized (Armstrong et al., 1992; Everly, 2002). Trippel et al. (1997) concluded that for the same species, larger eggs have a higher probability of hatching and of subsequent larval survival than do smaller ones. It is unknown whether the smaller eggs of Black Anglerfish that share a chamber hatch at a different rate or produce less viable larvae than the larger eggs that are alone in a chamber. Finally, the semicystic kind of spermatogenesis has been described only once before in the family Lophiidae, for Blackmouth Angler (*Lophiomus setigerus*) (Yoneda et al., 1998a). Muñoz et al. (2002) reported that semicystic spermatogenesis may be related to the secretion of abundant, thick seminal fluid, the function of which is to keep the spermatozoa together to enable fertilization of the entire egg mass.

The variation in spawning seasonality of Black Anglerfish between spring (La Mesa and De Rossi, 2008) and winter (Carbonara et al., 2005; Duarte et al., 2001; Tsimenidis, 1980) may be associated with local oceanographic features. Eddies and fronts enhance productivity, often function as physical barriers that retain larvae and juveniles, and provide favorable conditions for the feeding behavior of recruits and their subsequent transport toward the main nursery areas (Sánchez and Gil, 2000). During spring and summer, temporary eddies are generated in the Adriatic Sea (Mediterranean Sea) and in the Bay of Biscay (Atlantic) (Artegiani et al., 1997a, 1997b). In contrast, in wintertime eddies are generated in the Aegean and the Tyrrhenian seas, and the northern component of the outflow water from the Mediterranean Sea influences the Atlantic Iberian coast (Iorga and Lozier, 1999).

Finally, maturity sizes between individuals off the Atlantic Iberian coast, 53.6 cm TL in females and 38.6 cm TL in males (Duarte et al., 2001), and individuals in the northwestern Mediterranean Sea, 48.2 cm TL

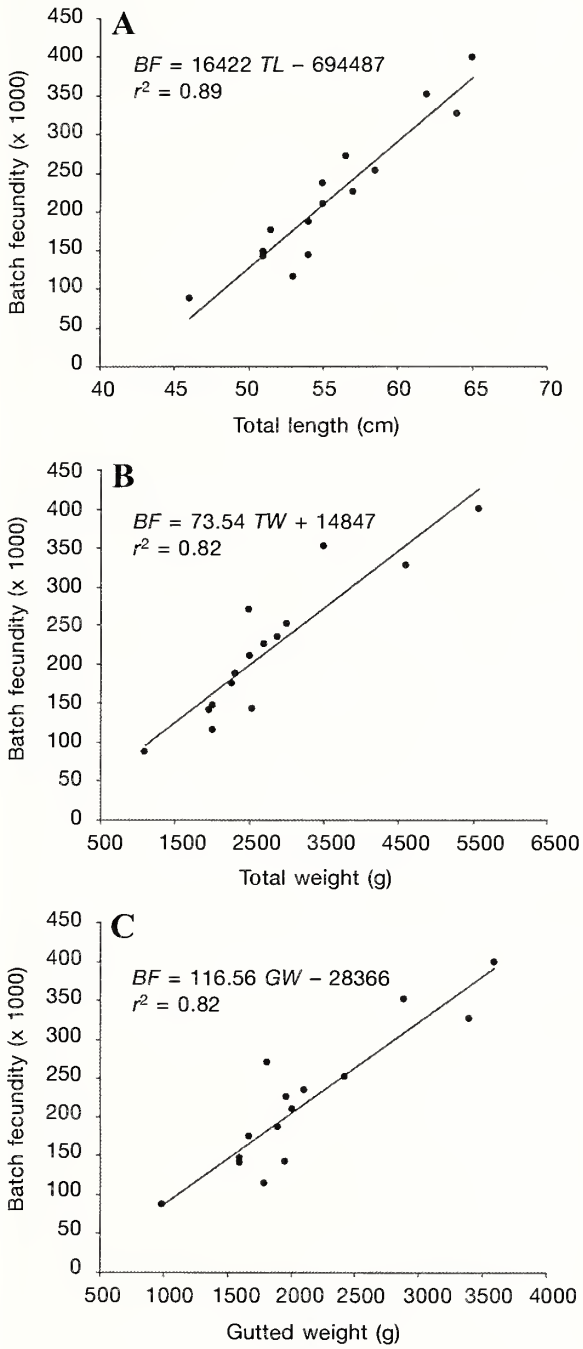

Figure 6

Relationships between batch fecundity (BF) and (**A**) total length (TL), (**B**) total weight (TW), and (**C**) gutted weight (GW) for Black Anglerfish (*Lophius budegassa*) collected from the northwestern Mediterranean Sea between June 2007 and December 2010. r^2=coefficient of determination.

in females and 33.4 cm TL in males in our study, were very similar, in contrast to the sizes observed for individuals in the Aegean Sea, 34 cm TL in females and 24 cm TL in males (Tsimenidis, 1980). These variations in L_{50} could be related to environmental and anthropogenic factors (e.g., temperature, food availability, or fishing pressure) (Trippel et al., 1997).

Conclusions

Black Anglerfish is a bycatch species in commercial fisheries off the Catalan coast of Spain. Despite not being a target species for these fisheries, the rise of its economic value has led to an increase of captures in the northwestern Mediterranean Sea. The lack of information about reproduction and fecundity of the Black Anglerfish off the Catalan coast has been a problem for management of the fishery for Black Anglerfish. The results of our study improve the current understanding of the reproductive dynamics of this species. From the morphological point of view, the structure and the development of ovaries and testes do not differ from the development of gonads in other Lophiiformes, although Black Anglerfish presents variation in its spawning season—a variation that is linked to its geographic area.

Our most important results are for L_{50}. Males and females both reach L_{50} at large sizes: 33.4 cm TL for males and 48.2 cm TL for females. As a consequence, the large catch and retention of individuals below the L_{50}, 57% of males and 83% of females landed, indicate that overfishing of this species could be a concern in the northwestern Mediterranean Sea. Therefore, our study provides new data that are needed for a better understanding of the biology and ecology of Black Anglerfish; this knowledge will be useful in assessment and management of the stock that is exploited by the fisheries of the northwestern Mediterranean Sea.

Acknowledgments

We thank the crews of the fishing vessels *Avi Pau*, *Estel. lada*, *Germans Félix*, *San Benito*, and *Port de Roses* for their collaboration during sampling. We also recognize M. Baeta and L. Martínez for their help with data collection; S. Torres, R. Sánchez, and I. Salvo for their assistance with histological and fecundity analyses; and A. Ospina for development of the study area map. We appreciate M. Casadevall and M. Muñoz for their valuable comments about male reproduction. Special thanks go to C. Vestfals for editorial help. This study was conducted within the project, Monitoratge dels recursos pesquers i marisquers al litoral català (Direcció General de Pesca i Afers Marítims, Generalitat de Catalunya). V. Tuset is a scientist of CSIC within the modality JAE-Postdoc of Programme Junta para la Ampliación de Estudios cofunded by the European Social Foundation.

Literature cited

Afonso-Dias, I. P., and J. R. G. Hislop.
1996. The reproduction of anglerfish *Lophius piscatorius* Linnaeus from the north-west coast of Scotland. J. Fish Biol. 49:18–39.

Armstrong, M. P., J. A. Musick, and J. A. Colvocoresses.
1992. Age, growth, and reproduction of the goosefish *Lophius americanus* (Pisces: Lophiiformes). Fish. Bull. 90:217–230.

Artegiani, A., D. Bregant, E. Paschini, N. Pinardi, F. Raicich, and A. Russo.
1997a. The Adriatic Sea general circulation. Part I: Air-sea interactions and water mass structure. J. Phys. Oceanogr. 14:1492–1514.
1997b. The Adriatic Sea general circulation. Part II: baroclinic circulation structure. J. Phys. Oceanogr. 14:1515–1532.

Brown-Peterson, N. J., D. M. Wyanski, F. Saborido-Rey, B. J. Macewicz, and S. K. Lowerre-Barbieri.
2011. A standardized terminology for describing reproductive development in fishes. Mar. Coast. Fish. 3:52–70.

Carbonara, P., R. Zupa, and M. T. Spedicato.
2005. Occurrence of a spawning female of *Lophius budegassa* Spinola, 1807 in the Salerno Gulf. Biol. Mar. Mediterr. 12:488–491.

Carlucci, R., F. Capezzuto, P. Maiorano, L. Sion, and G. D'onghia.
2009. Distribution, population structure and dynamics of the black anglerfish (*Lophius budegassa*) (Spinola, 1987) in the Eastern Mediterranean Sea. Fish. Res. 95:76–87.

Caruso, J. H.
1985. The systematics and distribution of the lophiid anglerfishes: III. Intergeneric relationships. Copeia 1985:870–875.
1986. Lophiidae. *In* Fishes of the North-eastern Atlantic and the Mediterranean (P. J. P. Whitehead, M.-L. Bauchot, J.-C. Hureau, J. Nielsen, and E. Tortonese, eds.), p. 1362–1363. UNESCO, Paris.

Colmenero, A. I., J. Aguzzi, A. Lombarte, and A. Bozzano.
2010. Sensory constraints in temporal segregation in two species of anglerfish, *Lophius budegassa* and *L. piscatorius*. Mar. Ecol. Prog. Ser. 416:255–265.

Crozier, W. W.
1985. Observations on the food and feeding of the anglerfish, *Lophius piscatorius* L., in the northern Irish Sea. J. Fish Biol. 27:655–665.

Duarte, R., M. Azevedo, J. Landa, and P. Pereda.
2001. Reproduction of anglerfish (*Lophius budegassa* Spinola and *Lophius piscatorius* Linnaeus) from the Atlantic Iberian coast. Fish. Res. 51:349–361.

Dupouy, H., R. Pajot, and B. Kergoat.
1984. Study on age and growth of the anglerfishes, *Lophius piscatorius* and *L. budegassa*, from nord-east Atlantic using illicium. Rev. Trav. Inst. Pech. Marit. 48:107–131.

Everly, A. W.
2002. Stages of development of the goosefish, *Lophius americanus*, and comments on the phylogenetic significance of the development of the luring apparatus in Lophiiformes. Environ. Biol. Fishes 64:393–417.

Fariña, A. C., M. Azevedo, J. Landa, R. Duarte, P. Sampedro, G. Costas, M. A. Torres, and L. Cañás.
2008. *Lophius* in the world: a synthesis on the common features and life strategies. ICES J. Mar. Sci. 1272–1280.

Feinberg, M. N.
1984. All head and mouth. Nat. Hist. 93:28–33.

Fulton, T. W.
1898. The ovaries and ovarian eggs of the angler or frog-fish (*Lophius piscatorius*), and of the John Dory (*Zeus faber*). Sixteenth Annual Report of the Fishery Board for Scotland Part III:125–134.

García-Rodríguez, M., P. Pereda, J. Landa, and A. Esteban.
2005. On the biology and growth of the anglerfish *Lophius budegassa* Spinola, 1807 in the Spanish Mediterranean: a preliminary approach. Fish. Res. 71:197–208.

Hislop, J. R. G., A. Gallego, M. R. Heath, F. M. Kennedy, S. A. Reeves, and P. J. Wright.
2001. A synthesis of the early life history of the anglerfish, *Lophius piscatorius* (Linnaeus, 1758) in northern British waters. ICES J. Mar. Sci. 58:70–86.

Hunter, J. R., and S. R. Goldberg.
1980. Spawning incidence and batch fecundity in northern anchovy, *Engraulis mordax*. Fish. Bull. 77:641–652.

Iorga, M. C., and M. S. Lozier.
1999. Signatures of the Mediterranean outflow from a North Atlantic climatology: 1. Salinity and density fields. J. Geophys. Res. 104:25985–26009.

La Mesa, M., and F. De Rossi.
2008. Early life history of the black anglerfish *Lophius budegassa* Spinola, 1807 in the Mediterranean Sea using otolith microstructure. Fish. Res. 93:234–239.

Landa, J., R. Duarte, and I. Quincoces.
2008a. Growth of white anglerfish (*Lophius piscatorius*) tagged in the Northeast Atlantic, and a review of age studies on anglerfish. ICES J. Mar. Sci. 65:72–80.

Landa, J., I. Quincoces, R. Duarte, A. Fariña, and H. Dupouy.
2008b. Movements of black and white anglerfish (*Lophius budegassa* and *L. piscatorius*) in the northeast Atlantic. Fish. Res. 94:1–12.

Laurenson, C. H.
2006. A note on the development of the embryos of anglerfish *Lophius piscatorius*. J. Fish Biol. 68:1287–1290.

Laurenson, C. H., and I. G. Priede.
2005. The diet and trophic ecology of anglerfish *Lophius piscatorius* at the Shetland Islands, UK. J. Mar. Biol. Assoc. U.K. 85:419–424.

Leslie, R. W., and W. S. Grant.
1990. Lack of congruence between genetic and morphological stock structure of the southern African anglerfish *Lophius vomerinus*. S. Afr. J. Mar. Sci. 9:379–389.

Maravelias, C. D., and C. Papaconstantinou.
2003. Size-related habitat use, aggregation patterns and abundance of anglerfish (*Lophius budegassa*) in the Mediterranean Sea determined by generalized additive modelling. J. Mar. Biol. Assoc. U.K. 83:1171–1178.

Muñoz, M., M. Casadevall, and S. Bonet.
2002. Testicular structure and semicystic spermatogenesis in a specialized ovuliparous species: *Scorpaena notata* (Pisces, Scorpaenidae). Acta Zool. 83:213–219.

Murua, H., G. Kraus, F. Saborido-Rey, P. R. Witthames, A. Thorsen, and S. Junquera.
2003. Procedures to estimate fecundity of marine fish species in relation to their reproductive strategy. J. Northwest Atl. Fish. Sci. 33:33–54.

Negzaoui-Garali, N., and M. Ben Salem.
2008. Morphological characters and meristic counts in two anglerfishes, *Lophius budegassa* and *L. piscatorius* (Osteichthyes: Lophiidae) from Tunisian coastal waters (central Mediterranean). Ann. Ser. Hist. Nat. 18:17–26.
Negzaoui-Garali, N., M. Ben Salem, and C. Capapé.
2008. Feeding habits of the black anglerfish, *Lophius budegassa* (Osteichthyes: Lophiidae), off the Tunisian coast (central Mediterranean). Cah. Biol. Mar. 49:113–122.
Pavlov, D. A., N. G. Emel'yanova, and G. G. Novikov.
2009. Reproductive dynamics. *In* Fish reproductive biology: implications for assessment and management (T. Jakobsen, M. J. Fogarty, B. A. Megrey, and E. Moksness, eds.), p. 48–90. Blackwell Publ. Ltd., West Sussex, UK.
Pope, J. A., A. R. Margetts, J. M. Hamley, and E. F. Akyuz.
1975. Manual of methods for fish stock assessment. Part III. Selectivity of fishing gear, 46 p. FAO Fisheries Technical Paper No. 41, Revision 1. FAO, Rome.
Preciado, I., F. Velasco, I. Olaso, and J. Landa.
2006. Feeding ecology of black anglerfish *Lophius budegassa*: seasonal, bathymetric and ontogenetic shifts. J. Mar. Biol. Assoc. U.K. 86:877–884.
Sánchez, F., and J. Gil.
2000. Hydrographic mesoscale structures and Poleward Current as a determinant of hake (*Merluccius merluccius*) recruitment in southern Bay of Biscay. ICES J. Mar. Sci. 57:152–170.
Trippel, E. A., O. S. Kjesbu, and P. Solemdal.
1997. Effects of adult age and size structure on reproductive output in marine fishes. *In* Early life history and recruitment in fish populations. Fish and Fisheries Series 21 (R. C. Chambers, and E. A. Trippel, eds.), p. 31–62. Chapman & Hall, London.
Tsimenidis, N. C.
1980. Contribution to the study of the angler-fishes *Lophius budegassa* Spinola, 1807 and *L. piscatorius* L., 1758 in Greek seas. Inst. Oceanogr. Fish. Res. (Athens) Spec. Publ. 4:180–190.
1984. The growth pattern of otoliths of *Lophius piscatorius* L., 1758 and *Lophius budegassa* Spinola, 1807 in the Aegean Sea. Cybium 8:35–42.
Tsimenidis, N. C., and J. C. Ondrias.
1980. Growth studies on the angler-fishes *Lophius piscatorius* L., 1758 and *Lophius budegassa* Spinola, 1807 in Greek waters. Thalassografika 3:63–94.
Ungaro, N., G. Marano, R. Auteri, A. Voliani, E. Massutí, M. García-Rodríguez, and K. Osmani.
2002. Distribution, abundance and biological features of anglerfish (*Lophius piscatorius* and *Lophius budegassa*) (Osteichthyes: Lophiiformes) in the Mediterranean Sea. Sci. Mar. 66:55–63.
Velasco, F., J. Landa, J. Barrado, and M. Blanco.
2008. Distribution, abundance, and growth of anglerfish (*Lophius piscatorius*) on the Porcupine Bank (west of Ireland). ICES J. Mar. Sci. 65:1316–1325.
Wallace, R., and K. Selman.
1981. Cellular and dynamic aspects of oocyte growth in teleosts. Am. Zool. 343:325–343.
West, G.
1990. Methods of assessing ovarian development in fishes: a review. Mar. Freshw. Res. 41:199–222.
Woodroffe, D. A., P. J. Wright, and J. D. M. Gordon.
2003. Verification of annual increment formation in the white anglerfish, *Lophius piscatorius* using the illicia and sagitta otoliths. Fish. Res. 60:345–356.
Yoneda, M., M. Tokimura, H. Fujita, N. Takeshita, K. Takeshita, M. Matsuyama, and S. Matsuura.
1998a. Ovarian structure and batch fecundity in *Lophiomus setigerus*. J. Fish Biol. 52:94–106.
1998b. Reproductive cycle and sexual maturity of the anglerfish *Lophiomus setigerus* in the East China Sea with a note on specialized spermatogenesis. J. Fish Biol. 53:164–178.
2001. Reproductive cycle, fecundity, and seasonal distribution of the anglerfish *Lophius litulon* in the East China and Yellow seas. Fish. Bull. 99:356–370.

Errata

Fishery Bulletin 109:394–401 (2011).
O'Connell, Craig P., Daniel C. Abel, Eric M. Stroud, and Patrick H. Rice
Analysis of permanent magnets as elasmobranch bycatch reduction devices in hook-and-line and longline trials

Corrections

Page 397. Last paragraph of left column

Please note that the original article included typographical errors in the catch statistics between the control and procedural control (i.e., sham magnet) treatments for 4 species of elasmobranch (i.e., *S. acanthias*, *M. canis*, *R. eglanteria*, and *C. limbatus*). These values are corrected here; however, these errors did not influence the associated conclusions made in this article. The paragraph that begins at the bottom of the left column should read as follows:

For all species combined, no statistical significance in capture was found between control and procedural control hooks: *R. terraenovae* (χ^2=0.419, P=0.518); *S. acanthias* (χ^2=0.000, P=1.000); *M. canis* (χ^2=0.000, P=1.000); *R. eglanteria* (χ^2=0.077, P=0.719); *C. limbatus* (χ^2=0.143, P=0.706); and *S. lewini* (χ^2=0.000, P=1.000). Therefore, direct comparison between combined control and magnetic treatments was statistically warranted.

Page 397. Table 2 caption

Please note that the original caption for this table contained an error in the accepted P-value that denotes significance (i.e., P<0.005). This value was a typographical error for P<0.05. All text in this manuscript was prepared originally with a P-value of P<0.05; therefore, this typographical error had no effect on the text of this article. The caption for Table 2 should read:

Table 2. Elasmobranch catch composition from longline gear with barium-ferrite magnets in 54 sets. Asterisks indicate significant (P<0.05) differences between control and magnetic treatments in chi-square analyses.

Page 397, Table 3

Please note that this table contained 2 errors. The first error was the accepted P-value that was used to denote significance (i.e., P<0.005). This was a typographical error for P<0.05; however, the manuscript was prepared originally with a P-value of P<0.05, and, therefore, this typographical error had no effect on the text of this article. The second error pertained to the number of "Total elasmobranchs" captured. The value entered, "147," was a typographical error and should have been "300." The corrected Table 3 is presented below:

Table 3. Elasmobranch catch composition from hook-and-line gear with neodymium-iron-boron magnets in 660 trials. Procedural control data were not included because no significant difference in catch for control and procedural control was observed. Asterisks indicate significant (P<0.05) differences between control and magnetic treatments in chi-square analyses.

Table 3

Species	*n*	Control	Magnets
*Rhizoprionodon terraenovae**	169	67	30
*Mustelus canis**	21	10	1
Squalus acanthias	85	31	23
Raja eglanteria	16	6	3
Carcharhinus limbatus	7	4	0
Sphyrna lewini	2	1	0
Total elasmobranchs*	300	119	57
Total teleosts	16	6	5

Acknowledgement of reviewers

The editorial staff of *Fishery Bulletin* would like to acknowledge the scientists who reviewed manuscripts during 2012–13. Their contributions have helped ensure the publication of quality science.

Alexandre Alonso-Fernandez
Allen Andrews
Michael Armstrong
Julian Ashford
Amelie Auge
Peter Auster

Susanne Baden
Carolyn Belcher
Mark Benfield
Kevin Boswell
John Bower
Karine Briand
Richard Brodeur
Andre Buchheister
Michael Burton
Morgan Busby

John Carlson
Yong Chen
M. Alexandra Chícharo
J. Howard Choat
Rui Coelho
Kevin Craig

David Die
David Demer
Jose Domingos
Rafael Duarte

Billy Ernst
Alan Everson

Thomas Farrugia
Gary Fitzhugh
Joel Fodrie
Arild Folkvord
Alain Fonteneau
Brian Fry

Gilbert Carter
Larissa Graham
Churchill Grimes
John Goff
Gwen Goodmanlowe

Owen Hamel
John Hampton
Juliana Harding
Julianne Harris
Euan Harvey
Pingguo He
Michael Heithaus
Scott Heppell
Hsuan-Ching Ho
Chien-Chung Hsu
Hua Hsun Hsu
Reid Hyle

David Itano
Sara Iverson

Brenda Jensen
Andrea Johnson

Shawna Karpovich
Christopher Kelley
Jessie Knapp
John Kraeuter

Mauricio Landaeta
Timothy Loher

Stephen MacAvoy
Juan Madrid-Vera
Ann Matarese
Martha Mather
Camilla McCandless
Samuel McClatchie
Susanne McDermott
Andrew McDougall
Rick Methot
Gary Melvin
Frederic Menard
Robert Moffitt
Jeffrey Moore
Frank Morado
Robert Muller

Mikko Olin
Victoria Ortiz de Zárate

Steven Parker
Will Patterson
Hudson Pinheiro
Beth Phillips
Beth Phelan
Charles Potter
Ian Potter
Sean Powers
André Punt

Susan Riemer
Cara Rodgveller
Janette Roletto
Christopher Rooper
Kevin Rowling
Barry Russell
Alexander Rzhavsky

Kurt Schaefer
Bernard Sainte-Marie
Skylar Sagarese
Rochelle Seitz
Yasuko Semba
M. Shareef M. Siddeek
John Smith
David Somerton
Liming Song
Andi Stephens
Kevin Stierhoff
Gabriele Stowasser
S. Kersey Sturdivant
Stephen Szedlmayer

Toshiyuki Tanabe
Jason Toft
Ed Trippel
Troy Tuckey

Michael Vecchione
Pedro Veiga
Francesca Vitale

John Walter, III
Diana Watters
Toshie Wakabayashi
Randal Walker
Kristi West
Michael Wilberg
Gregory Williams
Richard Wong
Ryan Woodland

Jeannette Zamon

Fishery Bulletin

Guidelines for authors

Manuscript preparation

Contributions published in *Fishery Bulletin* describe original research in marine fishery science, fishery engineering and economics, as well as the areas of marine environmental and ecological sciences (including modeling). Preference will be given to manuscripts that examine processes and underlying patterns. Descriptive reports, surveys, and observational papers may occasionally be published but should appeal to an audience outside the locale in which the study was conducted. Although all contributions are subject to peer review, responsibility for the contents of papers rests upon the authors and not on the editor or publisher. *Submission of an article implies that the article is original and is not being considered for publication elsewhere.* **Articles** may range from relatively short contributions (10–15 typed, double-spaced pages [tables and figures not included]) to extensive contributions (20–30 typed pages). Manuscripts must be written in English; authors whose native language is not English are strongly advised to have their manuscripts checked by English-speaking colleagues before submission.

Title page should include authors' full names and mailing addresses and the senior author's telephone, fax number, and e-mail address. **Abstract** should be limited to 250 words (one-half typed page), state the main scope of the research, and emphasize the authors conclusions and relevant findings. Do not review the methods of the study or list the contents of the paper. Because abstracts are circulated by abstracting agencies, it is important that they represent the research clearly and concisely.

General text must be typed in 12-point Times New Roman font throughout. A brief introduction should convey the broad significance of the paper; the remainder of the paper should be divided into the following sections: **Materials and methods, Results, Discussion, Conclusions,** and **Acknowledgments.** Headings within each section must be short, reflect a logical sequence, and follow the rules of subdivision (i.e., there can be no subdivision without at least two subheadings). The entire text should be intelligible to interdisciplinary readers; therefore, all acronyms, abbreviations, and technical terms should be written out in full the first time they are mentioned.

For general style, follow the U.S. *Government Printing Office Style Manual* (2008) [available at http://www.gpoaccess.gov/stylemanual/index.html] and *Scientific Style and Format: the CSE Manual for Authors, Editors, and Publishers* (2006, 7th ed.) published by the Council of Science Editors. For scientific nomenclature, use the current edition of the American Fisheries Society's *Common and Scientific Names of Fishes from the United States, Canada, and Mexico* and its companion volumes (*Decapod Crustaceans, Mollusks, Cnidaria and Ctenophora*, and *World Fishes Important to North Americans*). For species not found in the above mentioned AFS publications and for more recent changes in nomenclature, use the Integrated Taxonomic Information System (ITIS) (available at http://itis.gov/), or, secondarily, the California Academy of Sciences *Catalog* of *Fishes* (available at http://researcharchive.calacademy.org/research/ichthyology/catalog/fishcatmain.asp) for species names not included in ITIS. Citations must be given of taxonomic references used for the identification of specimens. For example, "Fishes were identified by using Collette and Klein-MacPhee (2002); sponges were identified by using Stone et al. (2011)."

Dates should be written as follows: 11 November 2000. Measurements should be expressed in metric units, e.g., 58 metric tons (t); if other units of measurement are used, please make this fact explicit to the reader. Use numerals, not words, to express whole and decimal numbers in the general text, tables, and figure captions (except at the beginning of a sentence). For example: We considered 3 hypotheses. We collected 7 samples in this location. Use American spelling. Refrain from using the shorthand slash (/), an ambiguous symbol, in the general text.

Word usage and grammar that may be useful are the following:

Aging For our journal the word *aging* is used to mean both age determination and the aging process (senescence). The author should make clear which meaning is intended where ambiguity may arise.

Fish and fishes For papers on taxonomy and biodiversity, the plural of *fish* is *fishes,* by convention. In all other instances, the plural is *fish.*

Examples: The fishes of Puget Sound [biodiversity is indicated];
The number of fish caught that season [no emphasis on biodiversity];
The fish were caught in trawl nets [no emphasis on biodiversity].

The same logic applies to the use of the words *crab* and *crabs, squid* and *squids,* etc.

Sex For the meaning of male and female, use the word *sex*, not *gender.*

Participles As adjectives, participles must modify a specific noun or pronoun and make sense with that noun or pronoun.

Incorrect: *Using the recruitment model, estimates of age-1 recruitment were determined.* [Estimates did not use the recruitment model.]

Correct: *Using the recruitment model, we determined age-1 estimates of recruitment.* [The participle now modifies the word *we,* those who were using the model.]

Incorrect: *Based on the collected data, we concluded that the mortality rate for these fish had increased.* [We were not based on the collected data.]

Correct: *We concluded on the basis of the collected data that the mortality rate for these fish had increased.* [Eliminate the participle and replace it with an adverbial phrase.]

Equations and mathematical symbols should be set from a standard mathematical program (MathType) or tool (Equation Editor in MS Word). LaTex is acceptable for more advanced computations. For mathematical symbols in the general text (α, χ^2, π, $\pm$, etc.), use the symbols provided by the MS Word program and italicize all variables. Do not use photo mode when creating these symbols in the general text.

Number equations (if there are more than 1) for future reference by scientists; place the number within parentheses at the end of the first line of the equation. Round all values to 2 decimal points.

Literature cited section comprises published works and those accepted for publication in peer-reviewed journals (in press). Follow the name and year system for citation format in the "Literature cited" section (that is to say, citations should be listed alphabetically by the authors' last names, and then by year if there is more than one citation with the same authorship. Abbreviations of serials should conform to abbreviations given in Cambridge Scientific Abstracts (http://www.csa.com/ids70/serials_source_list.php?db=aquclust-set-c).

Authors are responsible for the accuracy and completeness of all citations. Literature citation format: Author (last name, followed by first-name initials). Year. Title of article. Abbreviated title of the journal in which it was published. Always include number of pages. If there is a sequence of citations in the text, list chronologically: (Smith, 1932: Green. 1947; Smith and Jones, 1985).

Digital object identifier (doi) code ensures that a publication has a permanent location online. Doi code should be included at the end of citations of published literature. Cite all software and special equipment or chemical solutions used in the study within parentheses in the text (e.g., SAS, vers. 6.03, SAS Inst., Inc., Cary, NC).

Footnotes are used for all documents that have not been formally peer reviewed and for observations and communications. These types of references should he cited sparingly in manuscripts submitted to the journal. All reference documents, administrative reports, internal reports, progress reports, project reports, contract reports, personal observations, personal communications, unpublished data, manuscripts in review, and council meeting notes are footnoted in 9 pt font and placed at the bottom of the page on which they are first cited. Footnote format is the same as that for formal literature citations. A link to the online source (e.g., [http://www/..... , accessed July 2007.]), or the mailing address of the agency or department holding the document, should be provided so that readers may obtain a copy of the document.

Tables are often overused in scientific papers; it is seldom necessary or even desirable to present all the data associated with a study. Tables should not be excessive in size and must be cited in numerical order in the text. Headings should be short but ample enough to allow the table to be intelligible on its own. All unusual symbols must be explained in the table legend. Other incidental comments may be footnoted with italic numeral footnote markers. Use asterisks only to indicate significance in statistical data. Do not type table legends on a separate page; place them above the table data. *Do not submit tables in photo mode.*

Figures must be cited in numerical order in the text. Graphics should aid in the comprehension of the text, but they should be limited to presenting patterns rather than raw data. Figures should not exceed one figure for every four pages of text. Figures must be labeled with the number of the figure. Place labels **A**, **B**, **C**, etc. within the upper left area of graphs and photos. Avoid placing labels vertically (except for the y axis). Figure legends should explain all symbols and abbreviations seen in the figure and should be double-spaced on a separate page at the end of the manuscript. Color is allowed in figures to show morphological differences among species (for species identification), to show stain reactions, and to show gradations in temperature contours within maps. Color is discouraged in graphs, and for the few instances where color may be allowed, the use of color will be determined by the Managing Editor.

- Notate probability with a capital, italic *P*.
- Provide a zero before all decimal points for values less than one (e.g., 0.07).
- Capitalize the first letter of the first word in all labels within figures.
- Do not use overly large font sizes in maps and for units of measurements along axes in figures.
- Do not use bold fonts or bold lines in figures.
- Do not place outline rules around graphs.
- Use a comma in numbers of five digits or more (e.g., 13,000 but 3000).
- Place a North arrow and label degrees latitude and longitude (e.g., 170°E) in maps.
- Use symbols, shadings, or patterns (not clip art) in maps and graphs.

Failure to follow these guidelines and failure to correspond with editors in a timely manner will delay publication of a manuscript.

Copyright law does not apply to *Fishery Bulletin,* which falls within the public domain. However, if an author reproduces any part of an article from *Fishery Bulletin* in his or her work, reference to source is considered correct form (e.g., Source: Fish. Bull. 97:105).

Submission

Submit manuscript online at http://mc.manuscriptcentral.com/fisherybulletin. Commerce Department authors should submit papers under a completed NOAA Form 25-700. For further details on electronic submission, please contact the Associate Editor, Kathryn Dennis, at

kathryn.dennis@noaa.gov

When requested, the text and tables should be submitted in Word format. Figures should be sent as PDF files (preferred), Windows metafiles, TIFF files, or EPS files. Send a copy of figures in the original software if conversion to any of these formats yields a degraded version of the figure

Questions? If you have questions regarding these guidelines, please contact the Managing Editor, Sharyn Matriotti, at

sharyn.matriotti@noaa.gov

Questions regarding manuscripts under review should be addressed to Kathryn Dennis, Associate Editor.

Fishery Bulletin

Subscription form

Superintendent of Documents **Publications** Order Form

*5178

☐ YES, please send me the following publications:

____ Subscriptions to *Fishery Bulletin*
for $32.00 per year ($44.80 foreign)

The total cost of my order is $ _____ . Prices include regular domestic postage and handling and are subject to change.

_____
(Company or Personal Name) (Please type or print)

_____
(Additional address/attention line)

_____
(Street address)

_____
(City, State, ZIP Code)

_____
(Daytime phone including area code)

_____
(Purchase Order No.)

Charge your order. IT'S EASY!

VISA

MasterCard

Please Choose Method of Payment:

☐ Check Payable to the Superintendent of Documents
☐ GPO Deposit Account ☐☐☐☐☐☐☐☐–☐
☐ VISA or MasterCard Account
☐☐☐☐☐☐☐☐☐☐☐☐☐☐☐☐
☐☐☐☐ (Credit card expiration date)

To fax your orders (202) 512-2104

_____
(Authorizing Signature)

Mail To: U.S. Government Printing Office
P.O. Box 979050, St. Louis, MO 63197-9000

Thank you for your order!

Also available online at
http://bookstore.gpo.gov/actions/GetPublication.do?stocknumber=703-023-00000-2

SMITHSONIAN INSTITUTION LIBRARIES
3 9088 01750 9191